Laboratoire
Léon Brillouin

SCIENTIFIC REPORT

1999-2000

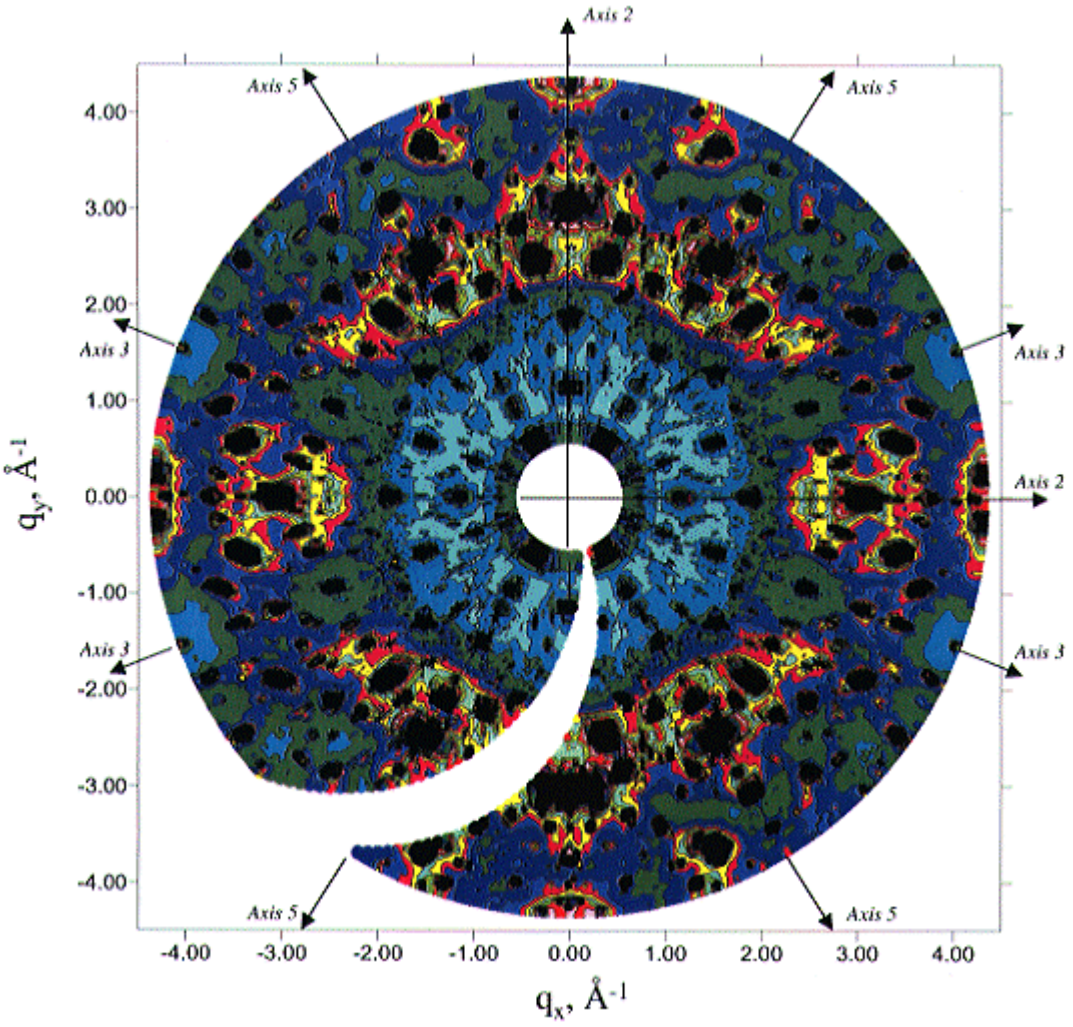

Contents

FOREWORD

This report presents an overview of the activities of the Laboratoire Léon Brillouin (LLB) during the years 1999 and 2000.
The LLB is funded and depends both on the Centre National de la Recherche Scientifique (CNRS) and the Commissariat à l'Energie Atomique (CEA). These two institutions have recently (in march 2001) signed a new agreement for running the LLB laboratory and its associated neutron source, the reactor Orphée.
The LLB has been created with a triple purpose :
to be a large national facility where neutron scattering experiments proposed by external users, including industrials, can be realised in the best conditions,
to train young researchers, in particular giving the opportunity of preparing PhD thesis essentially based on neutron scattering techniques and instrumentation,
to have its own research activity based on the work of permanent or semi-permanent groups, centred on the use of LLB facilities.
Certainly, the three types of activities largely overlap each other, and the scientific evolution of the laboratory since its creation shows that the LLB is continuously adapting to recent developments both in research and in technology. Such an overlap favours original studies based, for example, in new instruments or in extended researches less compatible with short time periodic applications.
It is worth mentioning in this context the various relations established with several partners in France and in many European countries. In particular, the participation of the LLB to the Access to Research Infrastructures Programme of the European Union increased substantially the number of European users since 1993. As a consequence, the LLB is recognized as one of the best neutron scattering facilities in Europe.
The following pages illustrate the activities of the LLB in 1999-2000. For each domain of research (magnetism and superconductivity, structures and phase transitions, disordered systems and materials science, chemical physics, biology), a synthesis of the scientific activity of the laboratory (mainly internal research and strong collaborations with external groups) is presented. Each of these synthesis is followed by a few selected recent highlights, which are mainly issued from the work performed on LLB instruments by external users. The report contains also a chapter on "Instrumental and Technical Developments", a presentation of the LLB with statistics, a summary of the user activities, and the list of publications for 1999-2000.
The LLB, the only French national neutron scattering facility, benefits of the quality of one of the best neutron sources in the world, the reactor Orphée, almost exclusively dedicated to research and run in a remarkable way by the Direction of Nuclear Energy of the Commissariat à l'Energie Atomique. In this way, the LLB, as well as ILL, can ensure the important responsibility of keeping alive and active a large community of researchers in many different domains (Physics, Chemistry, Biology, Geophysics and Material Sciences), for whom neutron scattering represents an essential tool of research.
We are convinced, with many members of the scientific community, that neutron scattering will still develop more in France and in Europe as one of the major techniques of fundamental and applied research and that the LLB will continue to occupy, in the future, a central role in this development.

José Teixeira Charles-Henri de Novion

PRESENTATION of LLB

The Laboratoire Léon Brillouin (LLB) is a facility that depends on both the Commissariat à l'Energie Atomique (CEA) and the Centre National de la Recherche Scientifique (CNRS). Its aim is to carry out fundamental and applied research in the field of condensed matter using neutron beams supplied by the reactor Orphée.
As a national laboratory, the LLB facility is opened to external users (via a written proposal and Selection Panel procedure), coming in priority from french laboratories, but also to some extent from foreign countries (mainly of European Union and Central and Eastern Europe).
The LLB both carries its own scientific research programme covering different fields of condensed matter physics, and collaborates closely with many scientists of the french and foreign communities, coming mainly from fundamental research laboratories, but also from applied research and industry. The synthesis of activities and the highlights presented in this Report, as well as the list of publications (more than 260 per year), show that the ensemble of research performed at LLB encompasses a very large scientific domain, in physics, chemistry, biology, materials science and earth sciences.

The Reactor Orphée and the LLB instruments
Orphée (which operates since december 1980) is the most recent and the highest flux medium size reactor, especially designed to produce thermal neutron beams for fundamental research. It is managed by the Direction of Nuclear Energy of CEA.
Orphée has a very compact highly enriched ^{235}U - 34% Al core, a heavy water reflector and a light water swimming pool.
The variety of problems studied by neutron scattering requires a neutron wavelength (and energy) distribution as broad as possible : small wavelength to explore a large volume of the reciprocal space for atomic structure resolution, large wavelength (and therefore low energy) to study large scale structures up to a fraction of μm and to perform high resolution energy spectroscopy (neV to meV scale). This is solved by local thermalization of 3 neutron beams by a hot source (heated graphite, 1400 K), of 8 others by two cold sources (liquid hydrogen, 20 K), the 6 remaining («thermal» beams) being thermalized at the temperature of the D_20 moderator (300 K). This makes available incident neutrons of any wavelength ranging from 0.5 to 15 Å. 6 cold neutron beams are distributed in a guide hall via neutron guides. The design of the 9 horizontal neutron beam tubes (which point tangentially towards the core) and of the 6 curved neutron guides, has allowed to considerably reduce the background due to fast neutrons and γ-rays coming from the reactor, and to optimize the signal-to-background ratio measured on the spectrometers.
The Orphée reactor is maintained at the best possible working order and safety requirements : in 1997, the zircaloy housing core has been replaced; the safety authority undertook a detailed examination of the reactor, and declared itself quite satisfied with it.
A layout of the reactor hall and the neutron guide hall instrumentation is shown in the joined figure. The characteristics of the 25 neutron scattering instruments opened to external users are given in Table 1. Two other new instruments (a small-angle diffractometer with polarized neutrons «PAPOL», and a neutron resonance spin-echo spectrometer «MUSES») have been opened to users at the beginning of year 2000.
In addition to neutron scattering, a part of Orphée reactor activity is devoted to other utilizations : non-destructive testing of industrial components by neutron radiography, chemical analysis by neutron activation, irradiation of silicon for the industry and elaboration of isotopes for medical use. These activities are not described in the present Report. But it is worth to mention that the Orphée neutron radiography facility allowed recently a german-french team to develop a new technique for the measurement of the viscosity of silicate melts at high temperature *(highlight)*.

Collaborations
Several collaborations with other countries, particularly European, have been developed, and the international character of the laboratory appears clearly in the large number of publications where many researchers from external laboratories (worldwide) appear either as first authors or as co-authors. The LLB is consequently an ideal place for the exchange of scientific ideas and for the establishment of collaborations.

Presentation of LLB

Among the international collaborations, it is worth mentioning some particularly intense and fruitful ones.
1) Germany. An agreement exists since 1979 with the Kernforschungszentrum of Karlsruhe, following the CRG principle. It concerns two spectrometers : the triple-axis 2T and the 4-circles 5C2. The latter is supervised by the University of Aachen (prof. G. Heger). Two german physicists and one technician work on a permanent basis at LLB.
The Technical University of Munich has built the resonant spin-echo spectrometer MUSES, and supports the physicist responsible of this instrument.
2) Austria. Since 1980, a 3-axis spectrometer (G4.3) works also in the conditions of a CRG. This collaboration was initiated by Prof.O. Blaschko, who unfortunately deceased in 1997, and the austrian authorities decided recently to end the collaboration with LLB (formally at the end of year 2002).
3) Italy. One of the largest users, Italy (INFM) has a general collaboration agreement with LLB, and participates to the renewal and utilisation of the diffractometer DIANE (G5.2), that studies residual stresses in the field of materials science. Negociations are presently in progress to reinforce this collaboration, in particular around the small-angle instrument PAXE.
4) Russia. Three agreements of scientific collaboration have been signed in 1994 by the CNRS and the CEA with the Petersburg Nuclear Physics Institute of the Russian Academy of Sciences, the Kurchatov Institute at Moscow, and the Joint Institute of Nuclear Research at Dubna.
A diffractometer for the study of the structure of powders at high resolution, built at Gatchina, operates at LLB (G4.2) as a CRG since 1997.
5) Hungary. A collaboration has been established with the Neutron Physics Department of the Research Institute for Solid State Physics at Budapest (Prof. L. Rosta).
6) Other international operations concern Morocco, and to a less extent Korea and China.

The LLB continues also a very fruitful collaboration with the Institut Laue-Langevin (ILL), namely in the domain of instrumentation, in particular on the elaboration of polarizing Heusler single crystals.
It participates also (since July 1998) in the pool that uses as a CRG the backscattering spectrometer IN 13 at ILL, mostly for biological studies.

Finally, in the international domain, the LLB benefits since 1993 from the funds of the «Large Research Infrastructures» access programmes («Human Capital and Mobility» (1993-96), «Training and Mobility of Researchers» (1997- 2000) and «Improving Human Potential» (2000-2004)) for the countries of the European Union and associated states. Within this frame, the LLB participates in the networks TECHNI (Technology for Neutron Instrumentation) and ENPI (European Neutron Polarization Initiative).

Undertaking an important role in the training of young scientists, the LLB participates in the european course HERCULES, and since the year 2000 organises at Saclay a one-week training course, with practicals on spectrometers, "les FAN du LLB" (see advertisement on following page). For this first year, 28 trainers were selected among 55 candidates ; most of them were PhD’s or post-docs from french laboratories. They were distributed into 9 thematic groups, each assigned to one or two instruments, with an experiment proposed either by LLB or the participant.

LLB researchers have organized in september 1999 the DYPROSO (Dynamical Properties of Solids) XXVII workshop in Tours, and in spring 2000 an advanced school on neutron scattering in Les Houches. LLB organises visits of its installations : some of the visits, during specific days, are adressed to a more general public.

The tables and statistics shown at the end of this Introduction (list of LLB staff, of long-term visitors and post-docs, and of PhD students) and in the chapter «Experimental Programme and User Activities» give a numerical idea of the ensemble of the activities. Even non exhaustive, they show how much the LLB is a tool used by several hundreds of researchers and students coming from many different places and disciplines. More than the numbers, the scientific production, as mirrored by the list of publications, shows the richness of the research activity, and the devotion of all the staff : permanent researchers, engineers and technicians of LLB and Orphée, administrative staff, associated researchers, post-docs and PhD's. It is due to their work and competence that the LLB can be considered among the most recognised places for neutron scattering research.

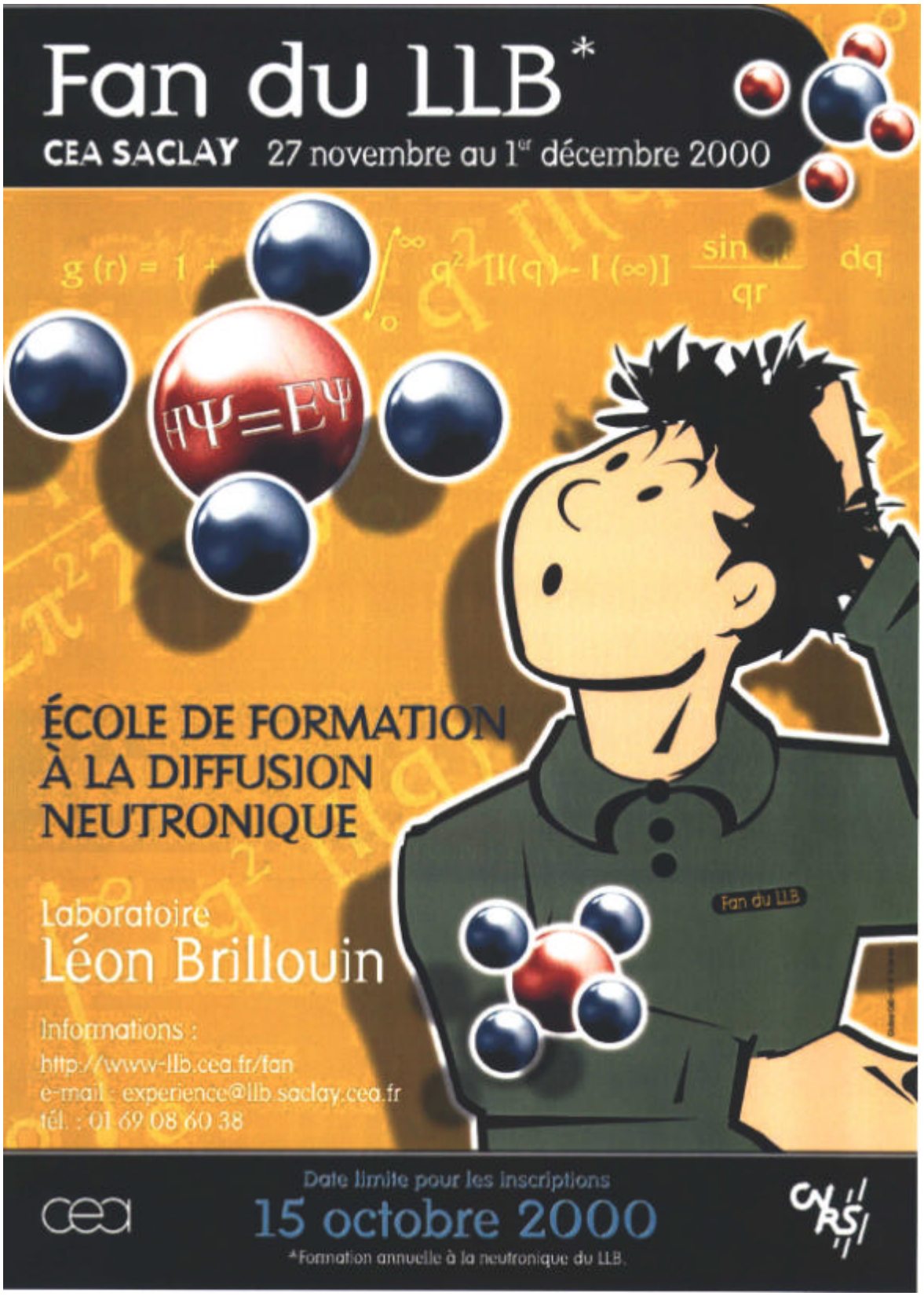
Fan du LLB*
CEA SACLAY 27 novembre au 1er décembre 2000
g (r) = 1 +
dq
qr
HΨ=EΨ
ÉCOLE DE FORMATION
À LA DIFFUSION
NEUTRONIQUE
Laboratoire
Léon Brillouin
Informations :
http://www-llb.cea.fr/fan
e-mail : experience@llb.saclay.cea.fr
tél. : 01 69 08 60 38
Fan du LLB
Date limite pour les inscriptions
15 octobre 2000
*Formation annuelle à la neutronique du LLB.
cea
CNRS

GENERAL IMPLANTATION OF LLB INSTRUMENTS

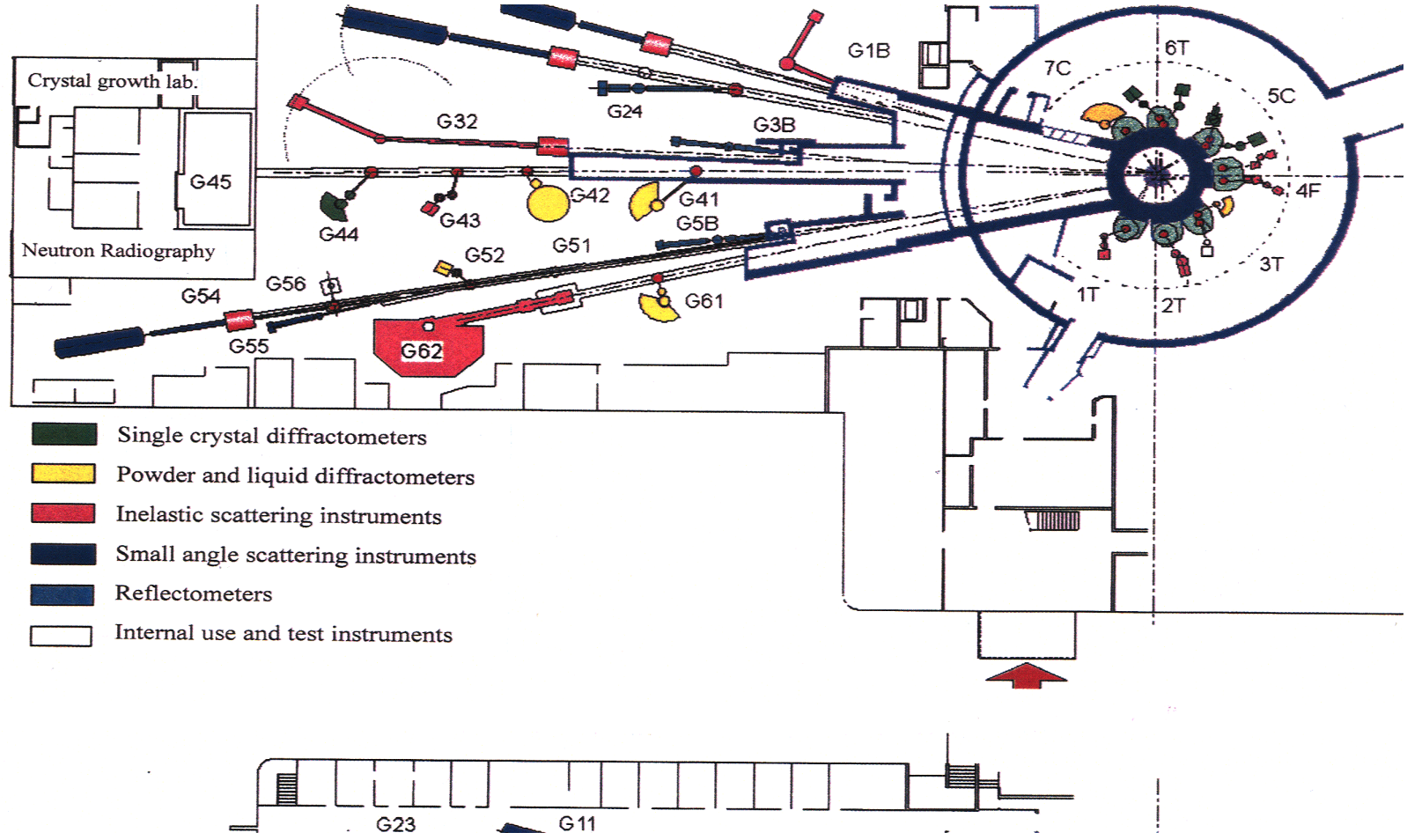

List of LLB instruments scheduled for external users

	Powder diffractometers
3T2	"Thermal neutrons" 2-axis (20 detectors) high resolution, mainly for nuclear structure determination
G4.1	"Cold neutrons" 2-axis (multidetector 800 cells) high flux, mainly for magnetic structure determination
G4.2	"Cold neutrons" 2-axis (7x10 detectors) high resolution, for structure determination on polycrystalline samples with large unit cell.
MICRO (G6.1)	"Cold neutrons" 2-axis (multidetector 400 cells) with long wavelength (-5A) and high flux, for the study of very small powder samples (<1 mm'). Very high pressure cell available (40 GPa).
	Diffractometers for material science studies
6T1	"Thermal neutrons" 4-circle for texture determination
DIANE (G5.2)	"Cold neutrons" 2-axis for internal strain mapping in bulk samples with spatial resolution ~1 mm^3.
	Single crystal diffractometers
5C1	"Hot neutrons" 2-axis with lifting arm, polarised neutrons, magnetic field (8 Tesla) for spin-density maps determination
5C2	"Hot neutrons" 4-circle for nuclear structure determination.
6T2	"Thermal neutrons" 2-axis, lifting arm and 4-circle, mainly for magnetic structure determination. 12 Tesla magnetic field available
	Diffuse scattering instruments
7C2	"Hot neutrons" 2-axis (multidetector 640 cells) for local order studies in liquid or amorphous systems. Cryostat and furnace available (1.2K 1300°C).
G4.4	"Cold neutrons" 2-axis (48 detectors, elastic/inelastic discrimination by Time-of-flight technique) for local order studies in single crystals. Furnace available (1400°C).
	Small-angle scattering instruments
PACE (G1.1)	"Cold neutrons" (annular detector, 30 rings) for study of large scale structures in isotropic systems (mainly polymers and colloids).
PAXY (G2.3)	"Cold neutrons" (X-Y detector, 128×128 cells) for study of large-scale structures (10 to 500 Å) in anisotropic systems (polymers under stress, metallurgical samples, vortex in superconductors ..).
PAXE (G5.4)	"Cold neutrons" (X-Y detector, 64x64 cells) for multipurpose studies of large scale structures
PAPOL (G.5.5)	“Cold polarized neutrons” with dynamic nuclear polarisation facility

	Reflectometers
EROS (G3bis)	"Cold neutrons" reflectometer operating in time-of-flight mode for multipurpose surface studies.
PRISM (G2.4)	"Cold neutrons" reflectometer with polarised neutrons and polarisation analysis for the study of magnetic layers.
	Triple-axis instruments
1T	"Thermal neutrons" high-flux 3-axis instrument with focusing monochromator and analyser, mainly devoted to phonon dispersion curves measurements. Very high pressure cell (100 Kbar) available.
2T	"Thermal neutrons" high-flux 3-axis instrument with focusing monochromator and analyser, mainly devoted to spin-waves and magnetic excitations studies (1.5 to 80 meV).
4F1	"Cold neutrons" high flux 3-axis instrument with double monochromator and analyser, mainly devoted to the study of low-energy (15µeV to 4meV) magnetic excitations. Polarised neutrons and polarisation analysis option available.
4F2	"Cold neutrons" high-flux 3-axis instrument for the study of low-energy excitations (e.g. soft modes) or modulated structural studies in single crystals.
G4.3	"Cold neutrons" high resolution and low background 3-axis instrument, mainly devoted to elastic diffuse scattering studies.
	Quasi-elastic instruments
MIBEMOL G6.2	"Cold neutrons" high resolution (~15 µeV at 10Å) time-of-flight instrument for the study of low energy excitations, mainly in disordered systems.
MESS (G3.2)	"Cold neutrons" small-angle high resolution spin-echo instrument, for the study of slow dynamics (Fourier time ~40 ns) of disordered matter (movements of large molecules in biology or physical chemistry, relaxation of magnetic moments).
MUSES (G1bis)	"Cold neutrons" large-angle high flux spin-echo instrument for the studies of biological or colloid systems

SCIENTIFIC HIGHLIGHTS

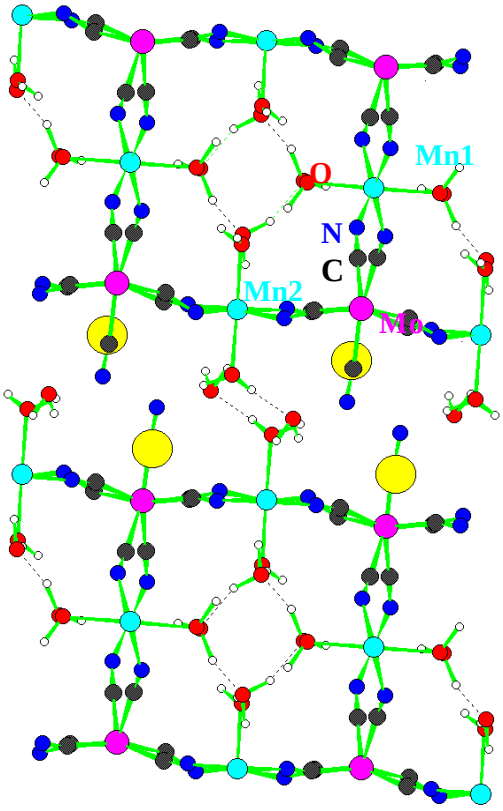

Hydrogen bonding in $K_2Mn_3(H_2O)_6[Mo(CN)_7]_2.6H_2O$: projection of the structure at 50K along the b-axis. All interactions shown up to $r_{O...H} < 2$ Å.

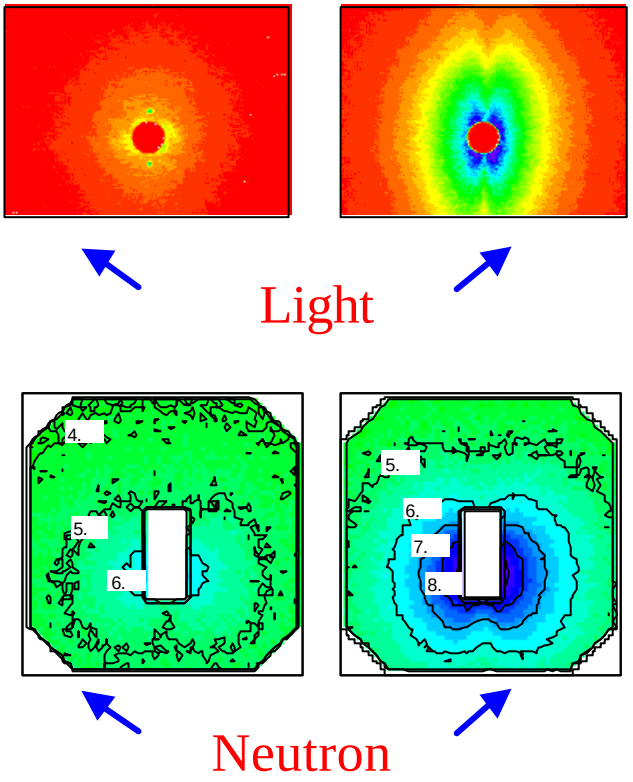

Small Angle Light and Neutron scattering of shear-induced structures in a polymer semi dilute solution in a Couette flow (**v,z** plane)**.** Right side : high shear. Left side : low shear ; neutrons are more sensitive than light.

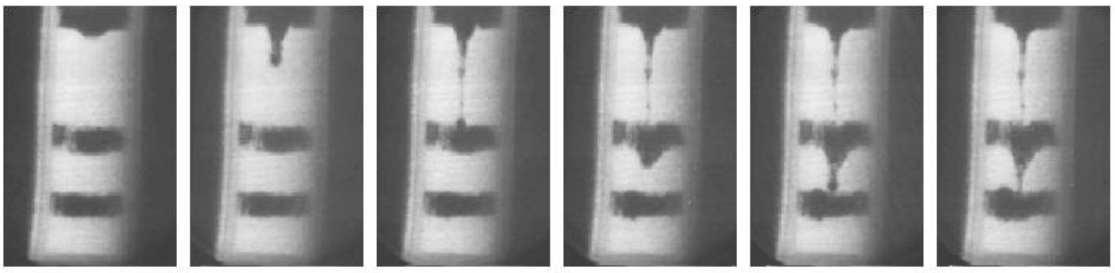

Real-time observation of a sphere falling through a silicate melt at 1050°C. The black and white layers are of equal density but the black ones are doped with gadolinium oxide. The boundaries between the layers stay sharp, indicating the absence of convection.

MAGNETISM AND SUPERCONDUCTIVITY

Magnetism and superconductivity represents a large part of the activity of LLB (8 thesis students present at LLB in 1999 and/or 2000). We have seen the emergence during the last years of several new subjects: topologically frustrated magnetic systems,the first study of a spin flop magnetic quantum tricritical point in Pr_2CuO_4, magnetic ordering in confined media,coexistence of magnetism and superconductivity in high Tc cuprates,the inelastic study of the spinwave spectrum in a thin film of MnTe.

The activities can be grouped into several subfields:
The first one, the largest one, concerns Complex Electronic Systems. It includes ruthenates, high Tc cuprates, manganites, mixed valence and Kondo systems particularly 1D magnetism in the charge ordered mixed valence system Yb_4As_3, non collinear antiferromagnetism and quantum critical effects in Pr_2CuO_4.

This field needs long term tenacious experimental efforts coupled to new theoretical developments to unravel intricate effects due to the interplay between numerous degrees of freedom (charge, spin, lattice). New concepts are emerging: competition between several ordered ground states and the presence of quantum critical points, importance of charge ordering and charge segregation phenomena, low dimensional effects.

The second one concerns Nanomagnetism, a rapidly progressing theme (under pressure from the technology oriented "Spintronics"), with new results such as: the inelastic study of thin films of magnetic semiconductors, the magnetism in confined media and the study of proximity effects in magnetic trilayer systems.

The third one is Molecular Magnetism developed in collaboration with several chemistry groups (Bordeaux, Montpellier, Florence).
The activity concerning the Topologically Frustrated Magnetic Systems constitutes now a new subfield.
Finally, magnetic ordered structure determination in various families of d and f intermetallic compounds constitutes a basic activity in collaboration with several Solid State Chemistry Laboratories.

The activity of LLB on Magnetism and Superconductivity is at the International level and benefits from tight collaborations mainly with Russia, Japan, Germany, Poland and Italy. There is also a close connection with Grenoble (ILL+CENG).

1. COMPLEX ELECTRONIC SYSTEMS

1.a. Ruthenates (see highlight)

(M.Braden, O.Friedt (thesis), Y.Sidis, P.Bourges, P.Pfeuty and Y.Maeno (Kyoto University))

Ruthenate Sr_2RuO_4 is the only superconducting layered perovskite isostructural with the cuprates. There is evidence that the superconducting pairing is unconventional (triplet symmetry) and the coupling mechanism is still subject of debate. A pairing mechanism via ferromagnetic fluctuations has not been confirmed by the inelastic neutron scattering studies developed at LLB. Instead it was found that the magnetic spectrum above Tc is dominated by incommensurate fluctuations which may arise from the quasi one dimensional nature of two of the Fermi surface sheets associated with the orbitals dxz and dyz of Ru. The change of the fluctuation spectrum when the superconducting phase is reached is actually under intense study at LLB.

The temperature dependence of the incommensurate dynamic excitations shows that a characteristic energy scale goes down with decreasing temperature which is the signature of closeness to a magnetic instability, in agreement with the recent finding of static incommensurate order (with the same incommensurability vector) in a compound with a slight Ti doping (x=.09 Ti replacing Sr)

Superconductivity in Sr_2RuO_4 is very sensitive to doping and disappears as soon as Sr is replaced by some doping element. Replacement of Sr by Ca (with smaller size) leads to a very rich phase diagram with a great variety of structural distortions and several magnetic phases (Thesis of O.Friedt). There is a close coupling between structural and magnetic anomalies due possibly to a change of the Fermi surface induced by structural modifications. For instance in $Sr_{1.5}Ca_{.5}RuO_4$ the magnetic susceptibility is enhanced and magnetic dynamical fluctuations have been seen at LLB for a q vector (.2,0,0) close to ferromagnetic q=(0,0,0), which is certainly revealing a change of the Fermi surface.

1.b High T_c cuprates

LLB Inelastic Neutron group (P.Bourges, Y.Sidis), B.Keimer+collaborators (MPI, Stuttgart), L.P.Regnault (CENG), A.S.Ivanov (ILL), LLB Crystallogenesis group (G.Collin), LLB Theory group (F.Onufrieva, P.Pfeuty))

The resonance mode

Recent studies have shown that the "resonance" magnetic exciton bound state dispersive mode, characteristic of the superconducting state and first seen by J.Rossat-Mignot et al ten years ago, is a generic feature in d-wave superconducting cuprates. This mode had been extensively studied in underdoped and optimally doped YBCO. It has been also found recently in optimally doped BiSCO. The dispersion of this mode, which is rather peculiar and which had been predicted by LLB theorists (Onufrieva, Pfeuty), has been shown experimentally in underdoped YBCO. Very recently, the resonance mode has been observed at 38 meV in overdoped bilayer BiSCO (T_c=83K). Its energy position is smaller than in optimally doped BiSCO (T_c=91K, E_{res}=43meV).

Very recent measurements performed at LLB provide evidence of the magnetic resonance E_{res} =47.5mev at (π,π) in the superconducting state of $Tl_2Ba_2CuO_{6+x}$ (T_c=92K), a single layer system without structural complexity such as copper oxide chains, incommensurate superstructure, or CuO_2 buckling distortions. This is the first evidence of a resonance mode for a single layer system, which rules out that the resonance mode is due to the strong interaction of two closely spaced oxide layers. All the experiments on the resonance mode are made in collaboration with B.Keimer's group (Max Planck Institute, Stuttgart). The sample which was used for this experiment is made of 300 aligned small single very pure crystals prepared in Russia and with a total volume of 100 mm^3.

Coexistence of antiferromagnetism and superconductivity

Commensurate antiferromagnetic ordering has been observed in the very underdoped high T_c cuprate $YBa_2Cu_3O_{6.5}$ (T_c =55K) by polarized and unpolarized elastic neutron scattering (see Figure 1). The form factor decreasing faster at large Q is consistent with more delocalized magnetic states. This could be a spin density wave state which coexists at lower temperature with d-wave superconductivity as shown by theoretical studies (F.Onufrieva, P.Pfeuty, M.Kisselev, F.Bouis (thesis)). This surprising observation of the coexistence of antiferromagnetism and superconductivity had been already made in 1988 (D.Petitgrand, published in J.Phys. (Paris) 49, 1815 (1988)) but not considered seriously at that time. The origin of this antiferromagnetic phase could be associated with impurities or defects acting as a revelator of an intrinsic situation, and more detailed studies are certainly needed. Similar coexistence of magnetism and superconductivity has also been observed in optimally doped YBCO in the presence of a small concentration of Co (with J.A Hodges).

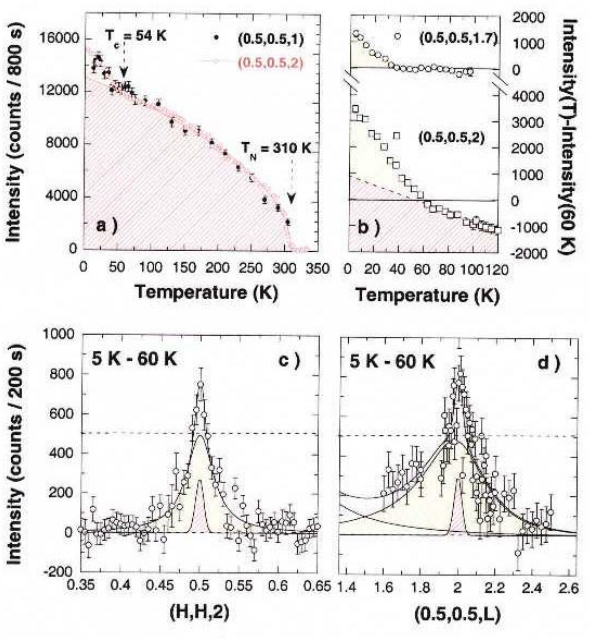

Figure 1. a, b) Temperature dependence of antiferromagnetic superlattice reflexion intensity in $YBa_2Cu_3O_{6.5}$ showing a kink at the superconductivity transition temperature T_c = 54K. c,d) The excess intensity below T_c.

1.c. Manganites

Inhomogeneities and magnetic excitations in $La_{1-x}Ca_xMnO_3$ at low doping
(M.Hennion, F.Moussa, G.Biotteau [thesis])

The study of manganites $La_{1-x}Ba_xMnO_3$ 0<x<.2 (insulator regime) B=Ca and Sr, has been pursued in two directions.
1.The spin dynamics in the low doping regime 0<x<.1 has been studied in the presence of a magnetic field and the picture emerging from the evolution of the different excitation branches with the magnetic field is a picture of ferromagnetic clusters enriched with holes coupled together ferromagnetically through an antiferromagnetically ordered matrix poor in holes.
2. At higher concentration, x>.1 close to the metallic ferromagnetic phase, the magnetic excitation spectrum changes drastically and acquires a magnetovibrational character. For x>.125, diffuse scattering experiments show that the charge segregation changes from a 3D cluster to a 2D lamellar organisation.

Charge orbital spin ordering phenomena
(J.Rodriguez-Carvajal, A.Daoud-Aladine [thesis])

The proposed orbital ordering which explains the complex antiferromagnetic order in half doped $R_{.5}D_{.5}MnO_3$ manganites is concomitant to a charge ordering. New neutron diffraction experiments on $Pr_{.6}Ca_{.4}MnO_3$ allows to discriminate previous proposed models based on a mixed valence charged ordered model with a stacking of small $Mn^{4+}O_6$ and large $Mn^{3+}O_6$ octahedra. A non centro-symmetric structure is obtained having Mn sites in two types of octahedra of very similar size, characteristic of an intermediate valence state.

Structural and magnetic properties of CMR manganites
(C.Autret (thesis CRISMAT-LLB), C.Martin (CRISMAT), G.André, F.Bourée)

Manganites are prepared and their physical properties are studied in Caen; their structural and magnetic properties are obtained in LLB. Three families have been studied.

1. The system $Pr_{.5}Sr_{.5-x}(Ca/Ba)_xMnO_3$ with x=.05,.2, has been first studied with a ratio $Mn^{3+}/Mn^{4+} \approx 1$. As function of decreasing temperature there is a succession of phases from paramagnetic metallic (PM) to ferromagnetic metallic (FM) and finally to antiferromagnetic metallic (AFM).
2. In another family, Mn is substituted by another d element and two systems have been studied: $Sm_{.2}Ca_{.8}(Mn_{1-x}Ru_x)O_3$ and $Ca(Mn_{1-x}Co_x)O_3$. In both cases for x=.1 a drastic change appears with CMR properties and the coexistence of both a ferromagnetic and an antiferromagnetic phase is observed.
3. The properties of the layered 2D manganite $Pr_{2-x}Ca_xMnO_4$ with 1.5<x<2. have been compared with those of a similar (also rich in Mn^{4+}) 2D manganite and in both cases there is a coexistence of a ferromagnetic and an antiferromagnetic phase.

1.d. Mixed valence and Kondo systems (J.M.Mignot, A.Gukasov)

Mixed valence semiconductors/Kondo insulators
(with P.A. Alekseev "Kurchatov Institute")

The spin gap behavior previously observed in the low temperature (T<50K) magnetic spectra of the Kondo insulator YB_{12} was confirmed by new high resolution time-of-flight experiments performed on IN6 (ILL). Above 50K, a broad quasielastic component reappears gradually. Lutetium substitution experiments show that up to x_{Lu}=.25 the gap structure remains similar to that of pure YB_{12}.

The inelastic response of $Sm_{.83}Y_{.17}S$ has been obtained. There are two different excitation branches with comparable dispersions, which appear to exchange their intensities about half way to the zone boundary. The lower branch is ascribed to the extended part of the Sm mixed valence wave function, in line with previous results obtained in SmB_6.

Valence instabilities in Tm monochalcogenides: novel magnetic phases at high pressure
(with I.N. Goncharenko and J.M. Mignot)

Previous measurements on TmTe have been extended to 6 GPa showing a new type I antiferromagnetic phase identical to that occurring at ambient pressure in TmSe.

TmSe is already in a mixed-valence state at P=0, but pressure changes the magnetic structure from type I to type II near P=3GPa. Recent measurements indicate that the AF I phase can be restored by applying a magnetic field in the direction <001> of about 2 Tesla at P=4.1GPa.

TmS is a metallic Kondo system with a complex incommensurate magnetic structure at low temperature. By applying a pressure of 5.7 GPa, the propagation vector is locked in at the commensurate vector (.5,.5,.5).

All these experiments have been realized in LLB on the spectrometer 6T2

Staggered field effect on the one dimensional S=1/2 antiferromagnet in the mixed valence system Yb_4As_3 (see highlight) (J.M.Mignot and A.Gukasov)

(this theme is under the leadership of M. Kohgi from the Tokyo Metropolitan University with K.Isawa et al)

The study of the mixed valence system Yb_4As_3, which is now pursued for several years, reveals a great richness of unexpected phenomena related to the physics of one dimensional spin chains which are formed at low temperature, when charge ordering takes place with the building of one dimensional arrays of Yb^{3+} carrying spin 1/2.

Recent experiments have shown that by applying a magnetic field perpendicular to the [111] direction, a gap opens in the normally gapless excitation spectrum. This effect has been explained (H.Shiba et al) as due to a "staggered field" on Yb^{3+} induced by the uniform magnetic field perpendicular to the chains in the presence of a Dzyaloshinsky-Moriya interaction.

1.e. A new quantum critical point induced by a magnetic field in Pr_2CuO_4 (see highlight)
(D.Petitgrand with A.S.Ivanov (ILL), theory made by S.V.Maleyev (Gatchina))

In Pr_2CuO_4, the pseudodipolar interaction is responsible for the non collinear antiferromagnetic structure. In the presence of a uniform magnetic field applied parallel to the CuO_2 plane, the directions of the spins in the two adjacent CuO_2 planes rotate and a spin-flop transition takes place. Such a spin-flop transition extends up to T=0 where the order of the transition depends on the angle ψ that the field makes with the direction <100>. This transition is first order when ψ is different of $\pi/4$ and becomes second order when ψ is equal to $\pi/4$. The point ($\psi = \pi/4$,H = Hc,T =0) is a Quantum Tricritical point of much interest (the first example) which is actually studied in great details from static and inelastic neutron measurements. The theory is developed by S.V. Maleev (Gatchina) and the quantum critical aspect is discussed by P.Pfeuty. Furthermore, the two relevant fields: temperature (a few K) and magnetic field (a few Tesla), are quite easily accessible experimentally, and a good single crystal of reasonable size is available. Results are already obtained and more experiments are programmed.

2. NANOMAGNETISM

Molecular nanomagnets (B.Gillon, D.Petitgrand)
"Giant spin" clusters (Mn+Mo, Co+Mo, Ni+Tu) prepared by J.Larionova (Montpellier) are actually studied by different neutron techniques (polarised neutrons, inelastic scattering...). This constitutes the beginning of a long term program.

Magnetic ordering and phase transitions in confined media (I.V.Golosovsky (Gatchina), I.Mirebeau, G.André (LLB), D.A.Kurdyukov, Yu.A.Kumzerov, S.B.Vakrushev (St Petersburg))

Antiferromagnetic MnO embedded in a porous SiO_2 glass has been studied by neutron diffraction. The type of magnetic ordering and the structural distortion are similar to those of the bulk, but the ordered magnetic moment is strongly reduced (from 4.89 to 3.84 μ_B per ion) and the Neel temperature is enhanced (from 118K to 124K). The magnetic transition is **second order** in contrast to the first order transition in the bulk. These results are not well understood. The MnO samples were prepared in situ (Russian collaboration) from a manganese nitrate solution by chemical bath deposition method. The glass matrix has a random interconnected network of elongated pores with a narrow distribution of pore diameters of 7 nm (see Figure 2).

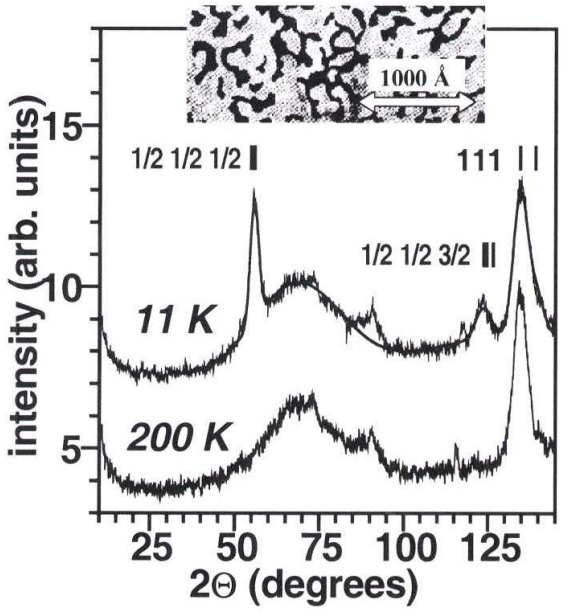

Figure 2. Neutron diffraction pattern of MnO embedded in a porous glass, measured at 11K and 200K on the G6.1spectrometer (λ=4.732 Å). The solid line corresponds to the calculated profile. In the top insert, a typical fragment of the pores network (in dark) viewed by electron microscopy.

Spin dynamics in thin film and multilayers of a magnetic semiconductor (B.Hennion and W.Szuszkiewicz (Poland))

This is the first inelastic neutron study of very thin 2D magnetic samples (thickness of a few microns, volume of the order of 1mm^3). The rapid development of spin electronics or "spintronics" with potential technological applications, pushes the study of magnetic semiconducting films. In this perpective, the MnTe films and MnTe+ZnTe multilayers have been studied by inelastic neutron scattering. Spin wave dispersion spectra have been obtained which give access to the magnetic interaction microscopic parameters.

Magnetization measurements in thin films and multilayers from neutron reflectivity (C.Fermon and F.Ott)

Neutron reflectivity allows the study of the surface and interface magnetism in magnetic multilayer systems. In artificial structures of very thin magnetic films (of the order of few nanometers) one can observe magnetic behaviors not observed in bulk materials. Non collinear magnetic coupling has been observed in $Fe_{1-x}Co_x$ Mn $Fe_{1-x}Co_x$ trilayer systems (see highlight, E.Kentzinger, S.Nerger, U.Rücker (Jülich)). There is also a great industrial interest in these magnetic multilayer systems because of the giant magneto-resistance effect which appears in these structures. Last year a collaboration has began with On-Stream, a company which develops high density magnetic tape storage. Reflectivity has allowed to characterize the magnetic switching behaviour of the GMR structures used in the read-heads of theses systems.

Another field of interest is the surface magnetism. These last three years, great hopes have been put into half-metallic ferromagnets which have an almost fully polarized conduction band. These materials would be especially suitable for spin injection in electronic devices (such as Magnetic-Rams or spin-transistors). These materials are mainly ferromagnetic oxides (Fe_3O_4, $La_{.7}Sr_{.3}MnO_3$). However, problems have arised related to the surface magnetism of these oxide thin films. They present a magnetic order which departs from the behaviour of bulk materials. Among these, are the finite size effects (which appear to be especially important in superexchange or double-exchange ferromagnets), the surface strains or epitaxial strains in the films or the proper control of the oxides stoichiometry at the interfaces. A lot of reflectivity work has been devoted to the study of these oxide surfaces to be able to distinguish between these different effects.

3. MOLECULAR MAGNETISM

(B.Gillon with J.Stride (post doctorate))

Magnetic structure of cyano-bridged (Mn^{II}, Mo^{III}) molecular-based compound (see highlight) (J.Stride, B.Gillon, A.Gukasov, O.Kahn (Bordeaux), J. Larionova (Montpellier))

The spin density in the ordered magnetic phase of the compound $K_2Mn_3(H_2O)_6[Mo(CN)_7]_26H_2O$ (T_c = 40K) was determined from polarised neutron diffraction data at 4K with an applied field of 3 Teslas. The spin densities upon the two metals were found of opposite sign which reflects an antiferromagnetic Mn^{II}-$M0^{III}$ interaction through the cyanobridge. This shows that this compound actually orders ferrimagnetically (and not ferromagnetically as it was previously proposed). There is a theoretical support from S.Alvarez (Barcelona).

Intramolecular ferromagnetic coupling between organic radicals (D.Gatteschi, A.Caneschi, L.Sorrace (University of Firenze) and B.Gillon)

The intramolecular ferromagnetic coupling between two semiquinonate radicals in the triplet ground state of the complex formed by the non magnetic Ti^{4+} ion and two semiquinonate ligands, may be due to direct overlap between the ligand magnetic orbitals or/and to superexchange mediated by the metal empty orbitals. From the determination of the spin distribution it has been demonstrated that the ferromagnetic interaction between the semiquinonate radicals is due to a superexchange mechanism via the d-orbitals of the Ti^{4+} diamagnetic ion.

In another system containing a rare earth (Gd) together with semiquinonate radicals, a study focusing on the nature of the interaction between the rare earth and the organic radical is under way in collaboration with the Italian group and with C.Lecomte (Nancy) for charge density measurements.

4. TOPOLOGICALLY FRUSTRATED MAGNETIC SYSTEMS

In regular magnetic lattices showing "topological frustration" (which is different from disordered spin-glass-like frustrated systems), no long range ordered spin arrangement is able to minimize the energy. This pecularity results in original magnetic behaviors such as spin "liquid", spin "glass", or even the recently discovered spin "ice" state. The most common "topologically frustrated lattices" are the hexagonal (triangular) and Kagome lattices in 2D and the FCC and the pyrochlore lattices in 3D. Two examples of pyrochlore lattices are discussed.

Magnetic properties of paramelaconite (Cu_4O_3) (A.Gukasov, J.Rodriguez-Carvajal, L.Pinsart-Gaudart (Orsay))

Paramelaconite is the first S = 1/2 pyrochlore lattice to be studied from the magnetic point of view. The sample studied is a natural single crystal of Cu_4O_3 ($5mm^3$) provided by the Smithonian Institute of Washington DC. It is a magnetic insulator with a magnetic transition at 40K. Magnetic order is characterized by magnetic reflections at k=(1/2,1/2,1/2). The critical exponent for the appearance of magnetic order is low (β=.23). The magnetic moment carried by Cu^{2+} is small (.14 μ_B). More work is needed to a better understanding of this interesting new system, with the development of synthesis of paramelaconite.

Magnetic instabilities in Laves Hydrides RMn_2D_x: New ordered magnetic phases induced by pressure and hydrogen order} (I.Goncharenko, I.Mirebeau, P.Cadavez-Peres (thesis),O.Makarova (Kurchatov Institute thesis))

1. Effect of hydrogen order

In the hexagonal Laves hydride $ErMn_2H_x$, different hydrogen superstructures (with hydrogen content x=3, 4.2, and 4.6) release the topological frustration (Mn moments being located on a pyrochlore lattice, a lattice of corner sharing tetrahedra) and impose different types of long range or short range magnetic orders.

2. Effect of applied pressure

Applying pressure allows one to modify the energy balance between the different types of magnetic interactions. In the H disordered hydride $Tb(Mn_{.9}Al_{.1})_2D$, Mn magnetism disappears above a pressure of 6 GPa and the compound recovers a long range ferromagnetic state between rare earth moments.

5. MAGNETIC STRUCTURES IN SYSTEMS WITH D AND F ELECTRONS

Magnetic structures in the Ce-Ni-Ge system

(L.Durivault (thesis LLB-ICMCB), F.Bourée, B.Chevalier (ICMCB), G.André)

Neutron powder diffraction studies have been performed in the Ce-Ni-Ge system in order to establish correlations between chemical composition, crystal structures, magnetic properties and Cerium valence state.

Ternary germanides containing more than 50% atomic percentage of germanium are antiferromagnetic and when the percentage in germanium diminishes, the ordering temperature also diminishes together with the value of the ordered magnetic moment.

Magnetic ground states of the tetragonal UFe_2Sn-type structure from anisotropic RKKY exchange
(S.Bordère, B.Chevalier, J.Etourneau (ICMCB), F.Bourée)

Magnetic structures observed in $(Ce_{1-x}U_x)_2Pd_{2.05}Sn_{.95}$, $U_2Pd_{2+x}Sn_{1-x}$ and $U_2(Ni_{1-x}Pd_x)_2Sn$ have been explained on the basis of a general RKKY model based on a non-spherical Fermi surface to account for the magnetic interactions involved in these systems.

Crystal and magnetic structures, and superexchange interactions in condensed phosphates
(G.André, N.Blanchard, F.Bourée, G.Collin, J.Rodriguez-Carvajal, T.Roisnel, A.Boukhari, R.Cherkaoui, El Moursli (Rabat),N.El Khayati (thesis LLB-Rabat))

Phosphate materials are quite close to oxides but there is a stronger trend towards charge localisation. Two families of magnetic insulator phosphates have been selected: $CuFe_2(P_2O_7)_2$ and $MFePO_5$ (M=divalent transition metal). Information on the super and the supersuperexchange through phosphate groups $(PO_4)_n$ has been obtained from the determination of the magnetic structures by neutron diffraction on powder samples.

Applications of polarized neutrons (A.Gukasov)

1. Magnetic anisotropy in UNiGa and UCoGa determined by polarized neutrons (K.Prokes, V. Sechovsky (Prague), A.Gukasov)

As proposed by G.Lander et al, magnetic anisotropy can be determined by measuring flipping ratios of **polarized neutrons** on the sample oriented with the easy-magnetization direction making some angle with the applied field. Such an experiment has been performed recently in LLB on 5f isostructural antiferromagnets UNiGa and UCoGa. The results of neutron-scattering studies give extremely high magnetic anisotropy in UNiGa and UCoGa, an anisotropy which is comparable to those of the strongest rare-earth-based permanent magnet materials.

2. Spin and orbital moments in Uranium pnictides. (P.Wisniewski, Z.Henkie (Poland), A.Gukasov)

Polarized neutron diffraction technique allows to determine the ratio of orbital and spin components of magnetic moments. This ratio in uranium compounds is usually considered as a measure of the degree of hybridization (the smaller the ratio, the stronger the hybridization). A systematic study of a series of U_3X_4 pnictides (X=N,P,As and Bi) was performed which demonstrated an important hybridization of 5f-electron states with the conduction band for all four compounds. The hybridization plays a significant role in the appearance of local anisotropy in U_3X_4 pnictides, which in turn has a strong influence on the magnetic structure in these compounds. For another ferromagnetic uranium compound UAsSe, where the strong anisotropy of the hybridization has been predicted, the value of L/S ratio obtained from the polarized neutron data favours nearly free ion U^{4+} state, which indicates rather weak hybridization of 5f-electrons.

3. Spin density on ligands O^{2-} and covalency of Fe^{3+} ions in antiferromagnets garnets. (V.Plakhty, O.P.Smirnov (Gatchina), A.Gukasov, R.Papoular)

Magnetism in ionic crystals appears owing to covalency, a partial redistribution of electrons between the magnetic cation and surrounding anions-ligands. All the mechanisms of superexchange between magnetic ions via the ligands can be expressed in terms of covalency. Usually the covalency parameter is estimated from the comparison of the magnetic ion moment determined from the Bragg intensities with that of the free-ion for the zero- point spin fluctuations. However, the covalent moment transfer can be obtained directly using polarized neutron diffraction. The measurement consists in the determination of the magnetic moment induced on the ligand itself in an antiferromagnet subjected to an external magnetic field. In this method no corrections for the zero-point spin fluctuations are needed and, which is more important, the corrections for the moment reduction caused by frustration due to magnetic impurities is avoided. This method evidenced unambiguously significant (.025) positive spin density transfer on the ligand ion O^{2-}, this value being consistent with the theory prediction for the covalent reduction of moment in Fe^{3+}.

MAGNETISM IN PURE AND DOPED Sr_2RuO_4.

O. Friedt[1], Y. Sidis[1], M. Braden[1,2] P. Bourges[1], G. André[1], P. Pfeuty[1], B. Hennion[1], Z.Q. Mao[3], M. Minakata[3], S. Nakatsuji, S. NishiZaki[3] and Y. Maeno[3,4].

[1] Laboratoire Leon Brillouin , CEA/CNRS , F.-91191, Gif sur Yvette CEDEX France.
[2] Forschungszentrum Karlsruhe, INFP, Postfach 3640, D-76021, Germany.
[3] Department of Physics, Kyoto University 606-8502, Japan.
[4] CREST, Japan Science and Technology Corporation, Kawaguchi, Saitima 332-0012, Japan.

After the discovery of High-T_c superconductivity in cuprates many groups looked for superconductivity in other transition metal oxides. The only success came in Sr_2RuO_4 [1], which is isostructural to $(La,Sr)_2CuO_4$. However, in marked contrast to cuprates, superconductivity appears in Sr_2RuO_4 only at low temperature (~1.5 K) and out of a normal state that is a well-formed Landau Fermi liquid. Nevertheless, the superconductivity in Sr_2RuO_4 is rather unconventional. In particular, there is growing evidence that the pairing exhibits triplet symmetry [2] in agreement with the early proposal that superconductivity in Sr_2RuO_4 is mediated by ferromagnetic fluctuations [3].

The Fermi-surface in Sr_2RuO_4 separates into two distinct regions : (i) the α, β sheets are derived from the $4d_{xz}$ and $4d_{yz}$ orbitals, (ii) the γ sheet is derived from the $4d_{xy}$ orbital. The quasi-1D α,β sheets give rise to strong nesting effects peaking the bare spin susceptibility at incommensurate positions $(\pm 2\pi/3a, \pm 2\pi/3a, 0)$ [4], where a stands for the RuO_2 plane lattice parameter. Our inelastic neutron scattering (INS) studies confirmed this analysis perfectly. The imaginary part of the dynamical magnetic susceptibility seems to be dominated by incommensurate fluctuations at $\mathbf{q}_0=(\pm 0.6\pi/a, \pm 0.6\pi/a, 0)$ [5]. Analyzed within Stoner theory, Sr_2RuO_4 appears very close to a magnetic transition at the wave vector $\mathbf{q}_0$. Furthermore, incommensurate spin fluctuations should favor a d-wave spin singlet superconducting order parameter [4], as in High-T_c cuprates. Finally, the direct observation of ferromagnetic fluctuations being still missing, our INS studies cast some doubt about the predominant role of ferromagnetic fluctuations in the superconductivity of Sr_2RuO_4.
Substitution of nonmagnetic Ti^{4+} ions ($4d^0$) for Ru^{4+} ions ($4d^4$) quickly suppresses superconductivity. Our neutron diffraction measurements in a sample with 9% Ti demonstrate that Ti impurities trigger a short range magnetic ordering at $\mathbf{q}_0$ below 25K [6].

The condensation of the incommensurate fluctuations observed in pure Sr_2RuO_4 through Ti substitution strongly suggests that Sr_2RuO_4 lies close to a quantum critical point and this close quantum critical point should be taken into account in the superconducting compound. Likewise, the magnetic moment in the Ti-compound (0.3 μ_B) points along the c axis, revealing a weak out-of-plane anisotropy, which is likely due to spin-orbit coupling [7]. Considering an incommensurate spin fluctuation driven pairing mechanism, the persistence of such an anisotropy in pure Sr_2RuO_4 has been proposed to tune the superconducting order parameter from a spin singlet even parity to a spin triplet odd parity [8].

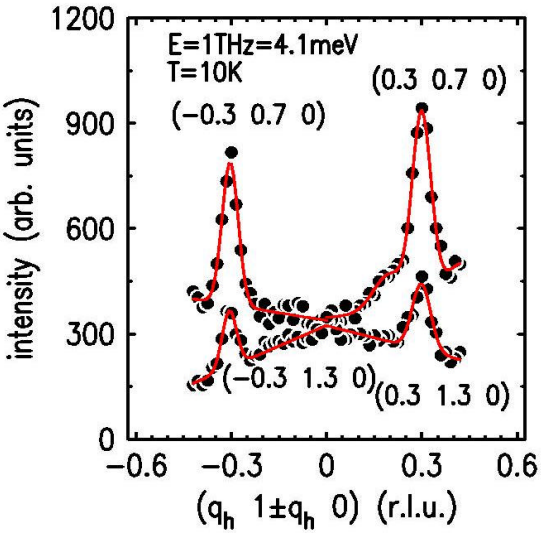

Figure 1: Constant energy scan at 4.1 meV along (110) and (-110) directions around the wave vector (0,1,0). Incommensurate spin fluctuations are located at wave vectors $Q_0=q_0+G$, where $q_0=(\pm 0.3, \pm 0.3, 0) = (\pm 0.6\pi/a, \pm 0.6\pi/a, 0)$ and G correspond to a zone center or a Z point in the (HK0) planes.

Besides, the substitution of Sr by isovalent Ca allows one to explore an astonishingly rich phase diagram [9,10], see Fig. 2. The smaller ionic radius

of the Ca drives a series of structural phase transitions characterized by rotations of the RuO_6-octahedra around distinct axes [9]. These structural distortions are coupled with anomalous magnetic and electronic phenomena. The most interesting behavior is observed for the end-member Ca_2RuO_4 which exhibits a transition from a paramagnetic metallic to an antiferromagnetic insulating state. This transition is accompanied by a prominent change in its crystal structure and has to be interpreted as a Mott-metal insulator transition. Due to its well defined crystal structure, Ca_2RuO_4 appears a very promising material for the study of such transitions.

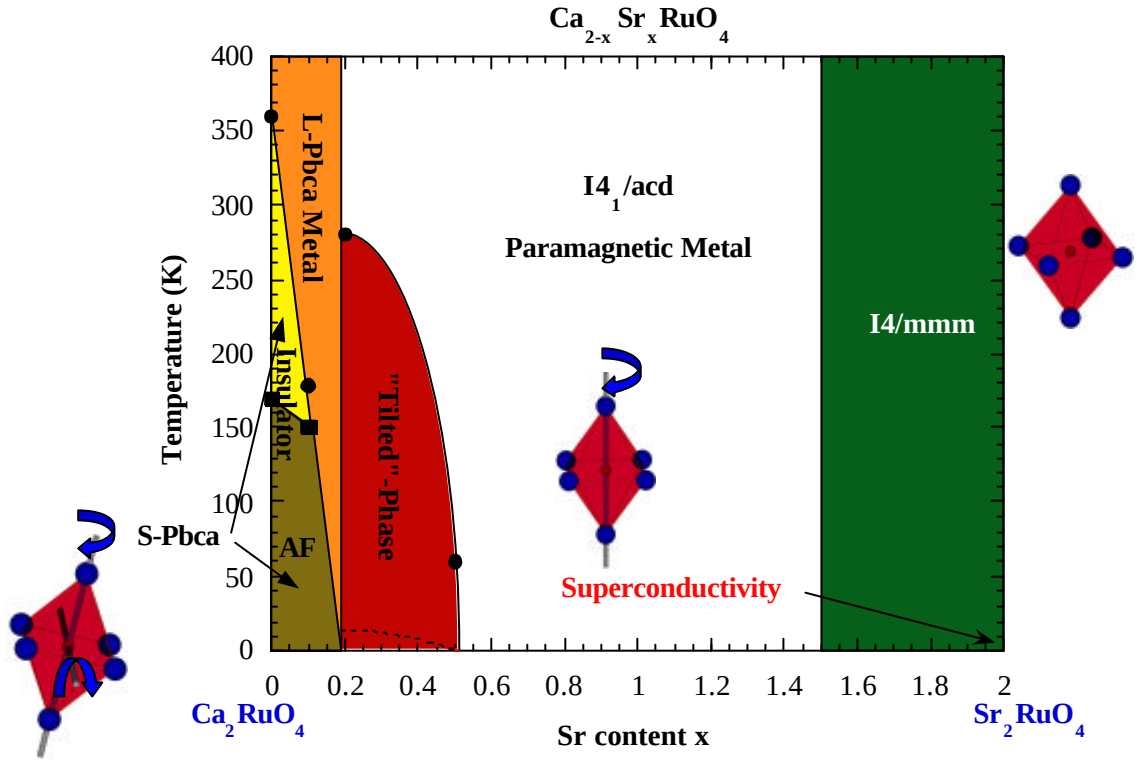

Figure 2. Phase diagram of $Ca_{2-x}Sr_xRuO_4$ [9] presenting the different structural and magnetic phases. Note that all phases are metallic except for S-Pbca. The drawings illustrate the different tilt and rotation schemes of the octahedra.

[1] Y. Maeno et al., *Nature* **372**, 532 (1994).
[2] K. Ishida et al., *Nature* **396**, 698 (1998); G. Luke et al., *Nature* **394**, 558 (1998).
[3] T.M. Rice and M. Sigrist, *J. Phys. Condens. Matter* **7**, L643 (1995).
[4] I.I Mazin et al., *Phys. Rev. Lett.* **82**, 4324 (1999).
[5] Y. Sidis et al., *Phys. Rev. Lett.* **83** , 3320 (1999).
[6] M. Braden et al., submitted to *Phys. Rev. Lett.* (2001).
[7] K.K Ng and M. Sigrist, *J. Phys. Soc. Jpn* **69**, 3764 (2000).
[8] M. Sato and M. Komoto, *J. Phys. Soc. Jpn* **69**, 3505 (2000), T. Kuwabara and M. Ogata, *Phys. Rev. Lett.* **85**, 4586 (2001).
[9] O. Friedt et al., Phys. Rev. B**63,** 174432 (2001), M. Braden et al. Phys. Rev. B**58**, 847 (1998).
[10] S. Nakatsuji et al., Phys. Rev. Lett. **84**, 2666 (2000).

STAGGERED FIELD EFFECT ON THE ONE-DIMENSIONAL S=1/2 ANTIFERROMAGNET Yb_4As_3

M. Kohgi[1], K. Iwasa[1], J.-M. Mignot[2], A. Gukasov[2], B. Gillon[2], H. Aoki[3], A. Ochiai[4] and T. Suzuki[5]

[1]Department of Physics, Tokyo Metropolitan University, Tokyo 192-0397, Japan
[2]Laboratoire Léon Brillouin, CEA-CNRS, CEA/Saclay, 91191 Gif sur Yvette, France
[3]Max-Planck Institute for Chemical Physics of Solids, D-01187 Dresden, Germany
[4]Center for Low Temperature Science, Tohoku University, Sendai 980-8578, Japan
[5]Tsukuba Institute of Science and Technology, Tsukuba, Ibaraki 300-819, Japan

Polarized neutron diffraction and inelastic neutron scattering experiments on Yb_4As_3 revealed that it exhibits typical behaviors of a one-dimensional S=1/2 Heisenberg-type antiferromagnet at low temperatures due to the formation of one-dimensional arrays of Yb^{3+} ions by the charge ordering transition. Staggered field effects on the Yb^{3+} chains induced by applying a magnetic field were also detected by the neutron scattering experiments.

Yb_4As_3 has an anti-Th_3P_4 type cubic crystal structure at temperatures above 290 K, below which it shrinks slightly along a [111] direction giving a trigonal structure. From several experimental observations, the phase transition was suggested to be accompanied by a charge ordering as shown in Fig. 1. The existence of charge ordering in the low temperature phase of Yb_4As_3 was directly proved by experiments performed at the polarized neutron diffractometer 5C1 at LLB [1], where flipping ratios of about 20 Bragg peaks were measured by applying a magnetic field H perpendicular to the [111] direction, using an incident neutron beam with wavelength of 0.84 Å.

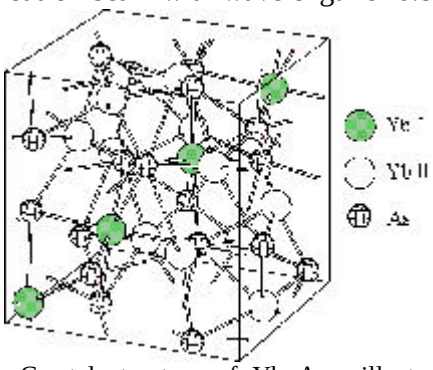

Figure 1. Crystal structure of Yb_4As_3, illustrating the expected charge ordering in the trigonal phase (T < 290 K). In the cubic phase, Yb_I and Yb_{II} are equivalent.

From the least squares fit analysis of the data, it was found that the induced moment of the four Yb ions aligned along the [111] direction (Yb_I) is much larger than that of the rest of 12 Yb ions (Yb_{II}); for example, the induced moments of Yb_I and Yb_{II} are m_I = (0.33 ± 0.01) m_B and m_{II} = (0.009 ± 0.006) m_B, respectively, at 1.5 K and H = 7 T. This clearly indicates that Yb_I is mainly trivalent whereas Yb_{II} is almost divalent.
The charge ordering gives rise to the formation of one-dimensional arrays of Yb^{3+} ions as seen in Fig. 1. In order to investigate the spin dynamics of the system, inelastic neutron scattering experiments on a single crystal (single domain) sample of Yb_4As_3 were performed at the triple axis spectrometers 4F2 at LLB, 6G and C11 at JAERI and IN14 at ILL [2].

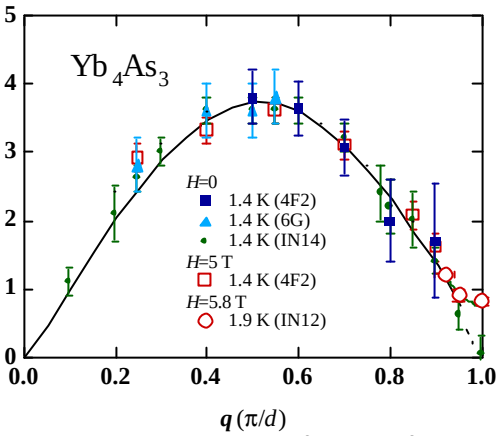

Figure 2. Dispersion relation of peaks of spin excitation spectra of Yb_4As_3 in the one-dimensional representation.

The observed spectra are well explained by the calculation based on the Müller ansatz for a one-dimensional spin 1/2 Heisenberg system with a nearest-neighbor antiferromagnetic coupling (1D-HAF) [3]. Fig. 2 depicts the dispersion relations of the peak positions of the observed spectra at 1.4 K against the 1D wave vector q in the unit of π/d for the Yb_I chains along the [111] direction, where d (=3.8 Å) is the atomic distance in the chain. The dashed curve in Fig. 2 shows the peak position of the resolution convoluted spectra of a 1D-HAF system which corresponds to the so-called des Cloizeaux-Pearson spin-wave mode $E_1(q) = \pi J/2|\sin(dq)|$ with the exchange interaction value of J = 2.23 meV. Since the observed crystal field excited levels (14, 21, 29 meV) are well above the J value [2], can be the 1D-HAF properties ascribed to the ground state doublet of the Yb^{3+} ions,
Thus, it becomes clear that the low-energy properties of the 1D chains of Yb^{3+} ions caused by the charge ordering are explained well by the 1D-HAF model when there is no magnetic field. However, experimental results of specific heat under magnetic field exhibit unusual properties which indicate the opening of a gap in the low energy excitations of Yb_4As_3 by applying a magnetic field [4]. This is not

consistent with the simple Zeeman effect on the 1D-HAF model which does not cause any energy gap [3]. The gap opening phenomenon was directly observed by the inelastic neutron scattering experiments under magnetic field performed on the spectrometers 4F2 at LLB and IN12 at ILL [5]. We found that, by applying a magnetic field perpendicular to the [111] direction, the spectrum at the 1D wave vector around q = 1 [π/d] changes drastically from the gap-less one with the spinon excitation continuum of the 1D-HAF system to the spin-wave-like sharp one at a finite excitation energy. The peak positions of the spectra at H = 5.8 T (IN12) and 5 T (4F2) are shown in Fig. 2 by open circles and squares, respectively. The magnetic field dependence of the peak position at q = 1 was found to be well proportional to $H^{2/3}$. This is in good agreement with the theory presented by Oshikawa et al. [6] which argues that the gap is opened by the staggered field on Yb^{3+} ions induced by the uniform magnetic field perpendicular to the chains due to existence of Dzyaloshinsky-Moriya interaction in the Yb^{3+} chains.

In order to check the staggered field model, we have also performed a polarized neutron diffraction experiment at 5C1 diffractometer under a magnetic field parallel to the [111] direction. Flipping ratios were measured at several temperatures under the same conditions as in the case of the perpendicular field as described above. Fig. 3 shows the obtained temperature dependence of the induced moment of Yb_I under the magnetic field of 7 T for both parallel and perpendicular field cases. As seen in Fig. 3(a), m_I under magnetic field parallel to the chain direction exhibits a broad maximum around 20 K as is expected for the 1D-HAF model, whereas that for perpendicular field, see Fig.3(b), does not show such a pronounced peak and instead shows an unusual enhancement below about 10 K. The difference of the magnetic field dependence of m_I is actually explained well by the staggered field model[7]. The solid lines in the figures are the sum of the calculated magnetization due to the crystal field ground state doublet

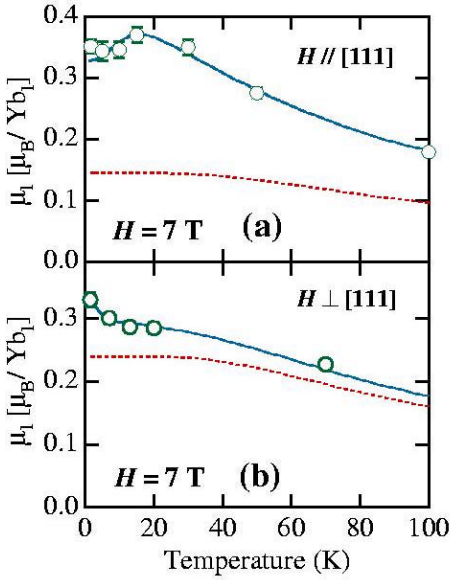

Figure 3. Temperature dependence of induced moment μ_I for *(a) H // [111] and (b) H ^ [111]*. See text .

and Van Vleck-type one due to the excited states (dashed lines in Fig. 3), where the former is calculated by the density matrix renormalization group method (DMRG) for the 1D-HAF system with and without the staggered field and only the first excited state contribution was taken into account in the calculation of the Van Vleck term. The effective g-value of the ground state doublet and the scaling factor of the Van Vleck term were determined by using least squares fit procedures, where the anisotropy of the g-factor determined from the scattering vector dependence of the spin excitation spectra was taken into account. The nice fit between the observation and calculation strongly supports the staggered field model.

The experimental results described above revealed that Yb_4As_3 is an ideal quantum spin system providing the new interesting problem of the staggered field. However, it is metallic, and its electrical resistivity shows a heavy-electron-like anomaly though the carrier density is extremely low (~10^{-3}/formula) at low temperatures [8]. Further study on this material is necessary.

[1] M. Kohgi et al., Physica B **230-232** (1997) 638; K. Iwasa et al., Physica B, **281&282** (2000) 460.
[2] M. Kohgi et al., Phys. Rev. B **56** (1997) R11388; M. Kohgi et al., Physica B **259-261** (1999) 269.
[3] G. Müller, H. Thomas, H. Beck and J.C. Bonner, Phys. Rev. B **24** (1981) 1429.
[4] R. Helfrich, M. Köppen M. Lang, R. Helfrich et al., J. Magn. Magn. Mater. **177-181** (1998) 309.
[5] M. Kohgi, K. Iwasa, J.-M. Mignot, B. Fåk, P. Gegenwart et al., Phys. Rev. Lett., **86** (2001) 2439.
[6] M. Oshikawa, K. Ueda, H. Aoki, A. Ochiai and M. Kohgi, J. Phys. Soc. Jpn. **68** (1999) 3181.
[7] K. Iwasa, M. Kohgi, A. Gukasov, J.-M. Mignot, N. Shibata et al., submitted to Phys. Rev. Lett.
[8] A. Ochiai, T. Suzuki and T. Kasuya, J. Phys. Soc. Jpn. **59** (1990) 4129.

SPIN DYNAMICS AND MAGNETIC ORDER NEAR THE FIELD-INDUCED QUANTUM CRITICAL POINT IN Pr_2CuO_4

D. Petitgrand [1] and A.S. Ivanov [2]

[1] Laboratoire Léon Brillouin (CEA-CNRS)
[2] Institut Laue-Langevin

Most of the cuprate compounds become high-T_c superconductors when they are doped by an appropriate substitution. Among them, the family of tetragonal R_2CuO_4 (R = Nd, Pr) cuprates has shown n-type superconductivity upon Ce doping. This has led to an increasing effort to understand the magnetic properties of the pure compounds. For the investigation of the Cu magnetic properties, Pr_2CuO_4 gets advantage of the non magnetic state of Pr, on the contrary to Nd_2CuO_4.

Pr_2CuO_4 is a non-collinear antiferromagnet made of strongly coupled CuO_2 AF planes with spin direction at right angle in adjacent planes.
The main magnetic properties of Pr_2CuO_4 can be described within a simple model of a planar antiferromagnet with a very large (J = 1400 K) [1] and slightly anisotropic Heisenberg interaction between in-plane neighbouring Cu ions on a square lattice. However the 3D magnetic structure as well as the low energy magnetic excitations have revealed that some subtle additional interactions are involved.

- Neighbouring planes are loosely coupled along the c-axis through a weak pseudo-dipolar exchange interaction [2].
- Due to quantum effects in the 2D S=1/2 antiferromagnet, the intraplane exchange interactions also acquire pseudo-dipolar terms which open a small gap in the excitation spectrum [2,3] and stabilise the spin direction along (100) [4].

Using a triple-axis spectrometer, we have studied the magnetic order and the spin dynamics of Pr_2CuO_4 under a magnetic field. The experiments have been performed with cold neutrons (k_i = 1.3 $Å^{-1}$), the sample being oriented with (110) and (001) in the scattering plane. The applied field produced by a superconducting coil, was vertical along (1 –1 0).
When a magnetic field is applied along (1 1 0), the direction of the staggered magnetisation of both types of planes gradually moves towards the direction perpendicular to the field, up to a second order transition line $H_c(T)$, which ends at the quantum critical point (H_c, T=0).

We have measured the magnetic Bragg intensity with k_1=(1/2 1/2 1) as a function of field at several temperatures. Figure 1 shows the experimental results at T=1.5 K together with a classical mean-field calculation (β=1/2, doted curve). Our results suggest that the magnetic order parameter vanishes at the quantum critical point (H_c,0) with a non-classical critical exponent.

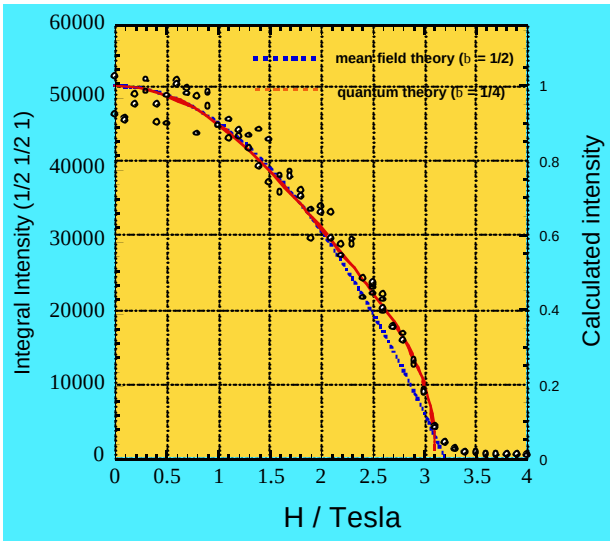

Figure 1 Intensity of the magnetic Bragg peak (1/2 1/2 1)) as a function of the applied field. Lines are fits with theoretical calculations of ref [2].

Full line of Figure 1 shows that our results can be accounted for by the theoretical curve exhibiting a critical exponent β=1/4 as recently suggested [2].

Another prediction associated with this phase transition is a softening of the magnetic excitation small gap as H approaches H_c (Figure 2).

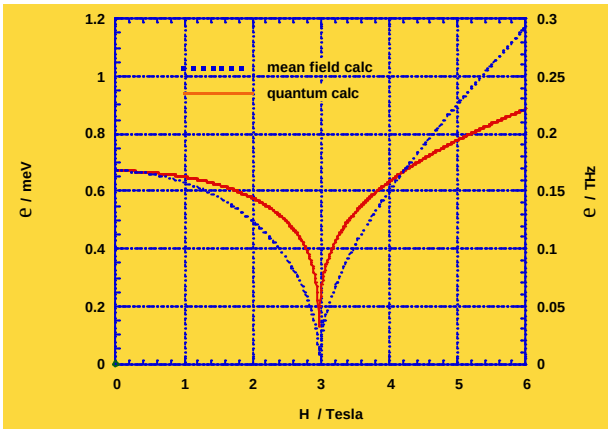

Figure 2 Theoretical field dependence of the small magnetic gap according theoretical calculations of ref [2].

To investigate this prediction, we have measured the magnetic inelastic scattering at Q=(1/2 1/2 1) for energy transfers of ε = 0.08 and 0.12 THz, which are below the zero field spin-wave gap, as a function of field.

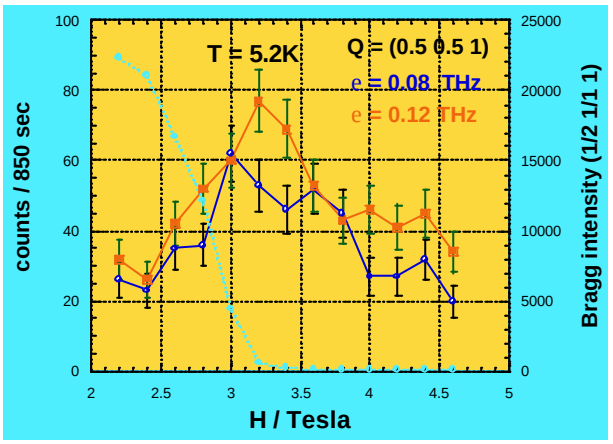

Figure 3 Inelastic intensities within the zero-field gap as a function of the applied field. Blue points show the decrease of the magnetic Bragg intensity towards the transition field. The maximum of the inelastic signalthus coincides with the transition field.

The results (Figure 3) show that, as the field approaches H_c , an additional intensity comes into the energy window, as a consequence of the softening of the gap. This gives an experimental evidence that, the gap Δ_0 of the in-plane acoustic magnetic excitation also vanishes at H_c.

Finally we have measured the interplane magnetic correlations along the (1/2 1/2 q_z) line. Results obtained at T = 1.5 K for H = 4 Teslas, compared to H = 0 show the persistence of mid-range correlations well above the transition field H_c = 3 Tesla (Figure 4). The lineshape is well accounted for by a Lorentzian convoluted by the resolution function, with a correlation along c of ξ = 12 Å which corresponds to two interplane spacings. In the direction perpendicular to the rod, the magnetic scattering appears resolution limited. Thus the point (H_c, T=0) appears as a 3D-2D quantum critical point for this component of the order parameter.

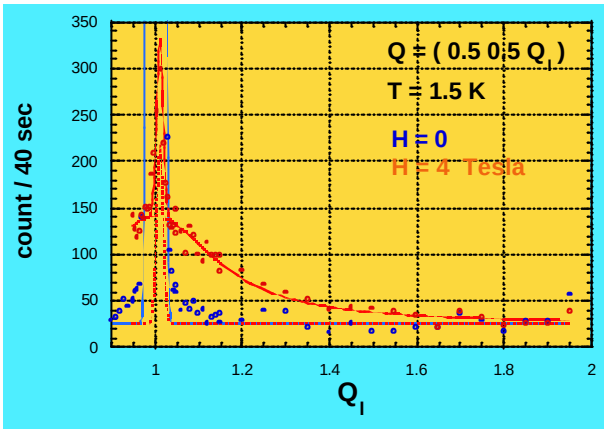

Figure 4 Magnetic elastic intensities along the (1/2 1/2 q_z) rod at T = 1.5 K for H = 0 and 4 Tesla.
The full line is a resolution-convoluted Lorentzian fit with a correlation length ξ = 12 Å, corresponding to 2 interplane spacings

Our experiments on magnetic order, magnetic correlations and magnetic excitations in Pr_2CuO_4 strongly suggest that this system shows a field-induced quantum critical point at (H_c = 3 Tesla, T=0) with unusual critical exponent, soft mode and short range 2D correlations extending far from the critical point.

[1] Ph. Bourges, H. Casalta, A.S. Ivanov and D. Petitgrand, Physical Review Letters, **79** (1997) 4906
[2] D. Petitgrand, S.V. Maleyev, Ph Bourges and A. S. Ivanov, Physical Review B **59** (1999) 1079
[3] A. S. Ivanov, P. Bourges and D. Petitgrand, Physica B **259** (1999) 879
[4] S. V. Maleyev, D. Petitgrand, Ph. Bourges and A.S. Ivanov, Physica B **259** (1999) 870

PROXIMITY EFFECTS IN $Fe_{1-x}Co_x$/Mn/$Fe_{1-x}Co_x$ TRILAYERS

E. Kentzinger, S. Nerger, U. Rücker

Institut für Festkörperforschung, Forschungszentrum Jülich, Germany.

In the last decade much effort has been dedicated to the study of the magnetic coupling in multilayer systems such as Dy/Y, Fe/Cr, Co/Cu because ultra-thin magnetic films exhibit unusual magnetic configurations and coupling not found in bulk systems. Among these, we can cite magnetic helicoidal ordering in Dy propagating through non magnetic rare-earth (Y, Lu), or oscillating coupling as a function of the spacer layer thickness in transition metal (e.g. Fe/Cr/Fe); the coupling changes from antiferromagnetic to quadratic and ferromagnetic depending on the Cr layer thickness. These structures have found practical applications as magnetic field sensors in magnetic read heads because of the large magneto-resistive effect observed when the relative orientation of the two magnetic layers is changed.

The purpose of this work has been to investigate the structure and magnetism of $Fe_{1-x}Co_x$/Mn/ $Fe_{1-x}Co_x$ trilayers, and especially to study the magnetic structure of δ-Mn (bcc with 2 atoms per cell) which can be stabilised in the form of thin films by molecular beam epitaxy on the (001) surface of bcc $Fe_{1-x}Co_x$ (x = 0-0.75) up to thicknesses of 3 nm.

Very recently, ab initio calculations of the magnetic structure of bcc Mn in the bulk and in $Fe_{1-x}Co_x$ /Mn multilayers have been presented, considering non collinear magnetic order [1]. It is shown that, in the bulk, the (001) anti-ferromagnetic structure can be almost degenerate in energy with a canted anti-ferromagnetic order and that, in $Fe_{1-x}Co_x$ /Mn multilayers. Fe atoms at the interfaces with the Mn layers favour the collinear state whereas Co atoms favour the non-collinear one. Our aim was to study the magnetic structure of the Mn in the $Fe_{1-x}Co_x$ /Mn/$Fe_{1-x}Co_x$ trilayers and to correlate it with its crystallographic structure, the interface morphology and the magnetic coupling. Results on the Fe/Mn/Fe system have been published in [2].

Sample preparation

The $Fe_{1-x}Co_x$/Mn/ $Fe_{1-x}Co_x$ trilayers are deposited in UHV by thermal evaporation onto a GaAs/Fe(1nm)/Ag(150nm) substrate-buffer system. The first layer is deposited at room temperature on Ag. The Mn atoms are deposited epitaxially on the $Fe_{1-x}Co_x$ at a temperature of 360 K. The Mn layer remains monocrystalline for thicknesses up to 3 nm. The figure 1 shows a description of the final system.

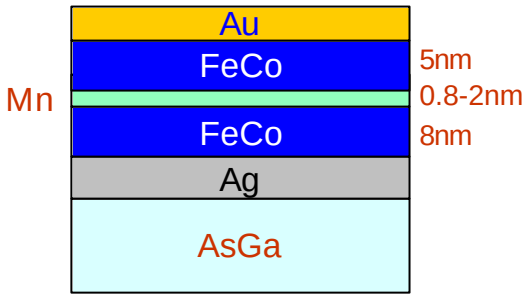

Figure 1. typical trilayer structure.

The structure of the interfaces was investigated using X-ray reflectivity. These measurements show that the interfaces are sharp. They also show that two lateral coherence length coexist in the height-height correlation functions, a long range (400 nm) and a short range one (4 nm). The long-range height-height correlation function evolves in phase from one interface to the other and corresponds to a long range correlated roughness between the layers (of the order of 0.45 nm). The short range correlation length corresponds to a very small roughness of 0.15 nm linked to local atomic disorder.

Magnetic measurements

From magneto-optical Kerr effect (MOKE) measurements, we found non-collinear coupling between the FeCo layers for Mn thicknesses up to 1.3 nm. The easy axis of magnetisation in the $Fe_{1-x}Co_x$ layers is the [110] crystallographic axis (whereas the easy axis in Fe layers is [100]).

The angle between the magnetisation vectors of the FeCo layers at remanence start from about 180° for a Mn layer between 0.5 and 0.85 nm and gradually decreases between 0.85 and 1.3 nm. Above 1.3 nm, perfectly square hysteresis is observed, meaning a ferromagnetic coupling between the FeCo layers. The non ferromagnetic

coupling strength shows a maximum around 0.85 nm.

In figure 2, we show polarised neutron reflectometry (PNR) performed on a $Fe_{0.5}Co_{0.5}$/ Mn(0.8nm)/ $Fe_{0.5}Co_{0.5}$ sample on the polarised reflectometer PRISM under a saturating field of 0.5 T.

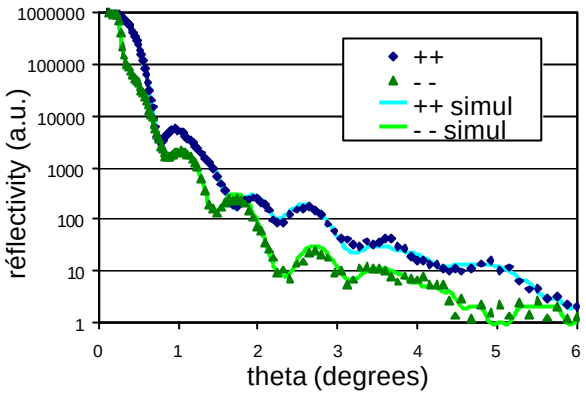

Figure 2. reflectivity of a $Fe_{0.5}Co_{0.5}$ (8nm)/ Mn(0.8nm)/ $Fe_{0.5}Co_{0.5}$(5nm)/ Au(5nm) trilayer in a saturation field of 0.5 T.

From a fit of the non-spin-flip channels (up-up) and (down-down), we obtain a net magnetisation of 0.8 ± 0.3 μ_B/at in the Mn layer. A net magnetisation in Mn has been predicted from ab-initio calculations on (bcc Co_{5ML})/bct Mn_{4ML}) multilayers [1], parallel to the total magnetisation and varying from 0.85 to 0.25μ_B/at when the angle between the net magnetisation of two successive layers is increased from 0 to 180°. Figure 3 shows the reflectivity measured at remanence (1.2 mT). In this case, a large spin-flip signal (yellow) is observed which indicates a strong non colinear magnetic coupling between the FeCo layers.

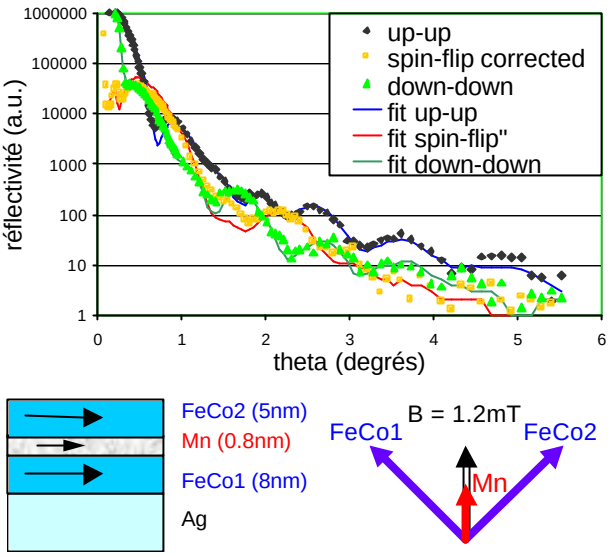

Figure 3. (a) reflectivity of a trilayer system in a low magnetic field (1.2 mT). (b) magnetic configuration deduced from the fit.

For the fit (solid lines), only the three angles of magnetisation have been varied, the other parameters being fixed at their values obtained at saturation (measurement in fig. 2). A good fit is obtained for the Mn magnetisation parallel to the applied field and an angle between the $Fe_{0.5}Co_{0.5}$ layers magnetisations of $90 \pm 5°$, both being tilted at 45° with respect to the applied field. Another fit was performed letting also the magnetisation inside the Mn layer free to vary. It stayed at the same value as at saturation.

Conclusion

We proved that monocrystalline δ-Mn can be efficiently stabilised on $Fe_{1-x}Co_x$ alloys and that the interfaces are sharp. PNR performed at room temperature indicate a net magnetisation of 0.8 ± 0.3 μ_B/at. to be present in the Mn layers in $Fe_{0.5}Co_{0.5}$/Mn/$Fe_{0.5}Co_{0.5}$ sample but no net magnetisation could be found in the Fe/Mn/Fe trilayers.

[1] C. Cornea and D. Stoeffler, J.M.M.M. **198-199** (1999) 282.
[2] E. Kentzinger, U. Rücker, W. Caliebe et al, Physica B **276-278** (2000) 586.
[3] S. Nerger, E. Kentzinger, U. Rücker et al, Physica B **297** (2001) 185-188.

SPIN DENSITY IN A CYANO-BRIDGED MOLECULAR-BASED ORDERED MAGNETIC COMPOUND

John Stride[1], Béatrice Gillon[1], Arsen Goukassov[1], Joulia Larionova[2], Rodolphe Clérac[3], Olivier Kahn[4]

1 Laboratoire Léon Brillouin, CEA-CNRS
2 Laboratoire de Chimie Moléculaire et Organisation du Solide, UMR 5637, Univ. Montpellier II
3 Centre de Recherche Paul Pascal (CRPP), UPR CNRS No. 8641, 33600 Pessac.
4 Intitut de Chimie de la Matière Condensée de Bordeaux (ICMCB), UPR CNRS No. 9048, 33608 Pessac.

Over the past few years, few molecular-based compounds that display magnetic ordering above room temperature have been reported[1]. These materials, related to Prussian Blue, have a faced-centred cubic structure, with A-NC-B linear linkages, where A and B are both 3d metal ions, A being a high spin ion and B a low spin ion, i. e. V^{II} and Cr^{III} ions. Compounds display either three-dimensional ferro- or ferri-magnetism, depending of the nature of the A-B interactions through the cyano-bridge. However, a major drawback of this class of materials is that no magnetic anisotropy (which is essential for future practical applications) can be expected because of the cubic nature of the structure. In this respect, the recent synthesis of cyano-bridged bimetallic analogues to Prussian Blue but with a lower symmetry, from a 4d ion Mo^{III}–molecular precursor $K_4[Mo^{III}(CN)_7]\cdot 2H_2O$, yielded promising results[2]. A strong magnetic anisotropy in the ordered state has thus been achieved for the compound $(K_2Mn^{II}_3(H_2O)_6[Mo^{III}(CN)_7]_2\cdot 6H_2O)$, for which a relatively high ferromagnetic ordering temperature T_C (39K) has been reported[3].

In order to investigate the origin of the ferromagnetic coupling between the Mn^{2+} and Mo^{3+} ions through the cyano bridge in this type of compound, we have performed a spin density study on the $(K_2Mn_3(H_2O)_6[Mo(CN)_7]_2\cdot 6H_2O)$ compound[4]. As a matter of fact, the determination of the spin density provides crucial information about phenomena such as spin delocalization and spin polarization that play a role in magnetic interactions between metallic ions through organic bridges.

This compound presents a two-dimensional structure with double-sheet layers stacked up along the direction of the b-axis. Each sheet, parallel to the (a, b) plane, is built upon cyano-bridged Mn_2Mo_2 lozenges. The nuclear structure at 50K, just above the ordering temperature, has been determined with help of unpolarised neutron diffraction measurements on the four-circle diffractometer 6T2. The title compound is air sensitive and so the crystal was kept in an inert atmosphere throughout the whole experimental procedure. This material is extensively hydrogen-bonded: three water molecules of crystallisation form small water clusters within the voids between the bi-layers and the three others are H-bonded to coordinated water molecules within the inter-bi-layer regions (Figure 1).

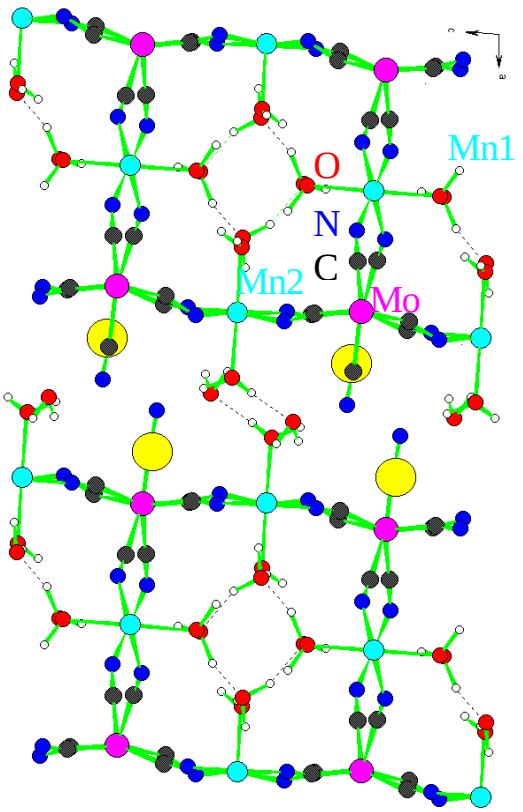

Figure 1: Hydrogen bonding in $K_2Mn_3(H_2O)_6[Mo(CN)_7]_2.6H_2O$: projection of the structure at 50K along the b-axis. All interactions shown up to $r_{O\ldots H} < 2$ Å.

The spin density in the ordered magnetic phase was determined from polarised neutron diffraction data at 4K with an applied field of 3 Teslas in order to achieve almost complete magnetic saturation.

The spin density maps displayed in Figure 2 have been reconstructed by a model refinement of the spin density on the set of flipping ratios according to the data treatment for a non-centrosymmetric space group. Surprisingly, opposite signs of the spin densities were observed upon the metal ions, reflecting an antiferromagnetic Mn^{II}–Mo^{III} interaction through the cyano-bridge.

The spin populations on the manganese (Mn1 and Mn2) and molybdenum sites were determined as being 4.34(16), 4.93(15) and -0.68(6) μ_B, respectively. The spin populations on the Mn sites are close to the spin-only values for the free ions. In contrast, by considering the deviation of the Mo^{III} spin population from -1 μ_B, the degree of spin delocalisation of the Mo^{III} ions is evident. This is manifested by the negative spin density upon the nitrogen atoms of each of the four CN bridging ligands situated in the *bc*-plane. This delocalisation of negative spin density only in the *bc*-plane, is consistent with the occupation of the dx^2-y^2 orbital (that lies in the *bc*-plane) by the unpaired electron of the Mo^{3+} ion. This is consistant with the orbital energy diagram for a Mo^{III} ion in a capped trigonal prism environment, with C_{2n} site symmetry.

The contradiction with the previously reported magnetisation measurements on this material which suggested predominantly ferromagnetic interactions, may be due to the uncertainty on the sample mass due to the special conditioning. The low temperature magnetic measurements are currently being completed in order to clarify this point

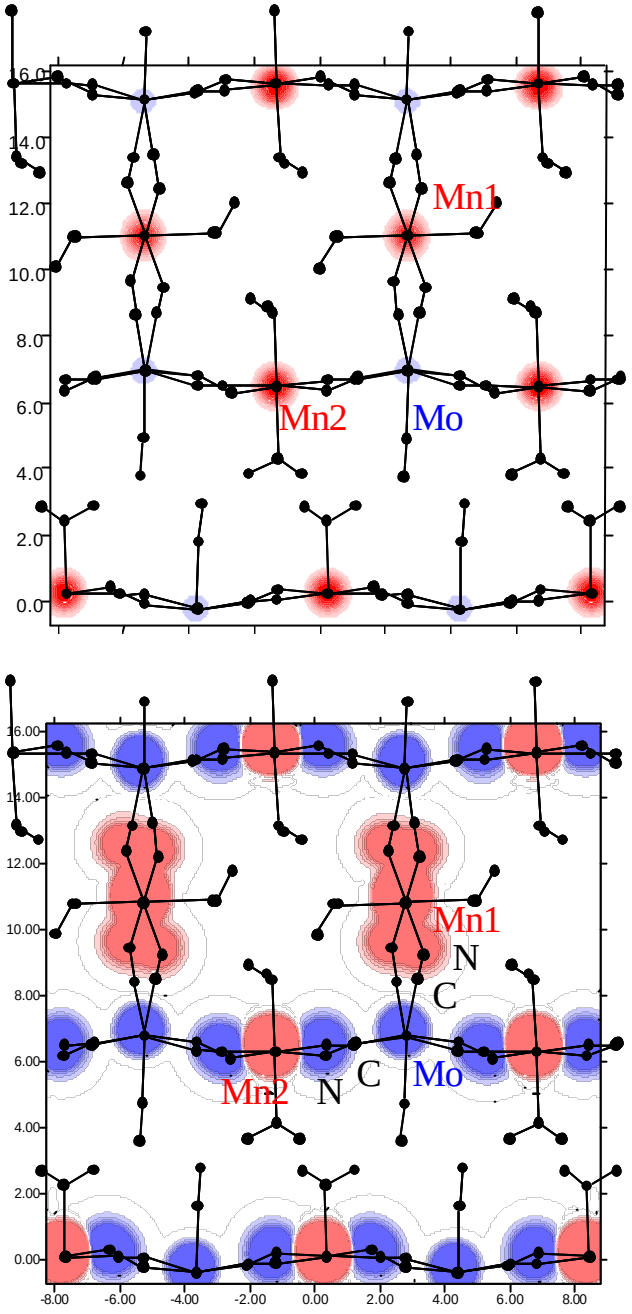

Figure 2: Projection of the spin density in $K_2Mn_3(H_2O)_6[Mo(CN)_7]_2.6H_2O$ along the b-axis. Positive spin density is in red and negative density in blue.
Top: High levels from -0.5 $\mu_B/Å^2$ to 5 $\mu_B/Å^2$ by step of 0.5$\mu_B/Å^2$). Bottom: Low levels from –0.1 to 0.1 $\mu_B/Å^2$ with intervals of 0.02$\mu_B/Å^2$. The zero line is not drawn.

Acknowledgments
This work is dedicated to the late Professor O. Kahn, from the Institut de Chimie de la Matière Condensée de Bordeaux (I.C.M.C.B.), who initiated this work. The authors thank A.Cousson (L.L.B.) for his help in the structural refinement.

[1] Ferlay S., Mallah T., Ouahès R., Veillet P., Verdaguer M., Nature 378 (1995) 701.
[2] Kahn O., Larionova J., Ouahab L., J. Chem. Soc., Chem. Commun. (1999) 945.
[3] Larionova J., Kahn O., Gohlen S., Ouahab L., Clérac R., J. Am. Chem. Soc. 121 (1999) 3349.
[4] Stride J., Gillon B., Larionova J., Clérac R., Kahn O., C. R. Acad. Sci. Paris, Chimie 4 (2001) 105.

STRUCTURES AND PHASE TRANSITIONS

Both crystallographic and magnetic structural phase transitions are an important component of Laboratoire Léon Brillouin's scientific activity. Neutron studies, either diffraction and/or inelastic scattering, are performed as a function of external parameters, namely temperature and pressure. Many different physical problems, both fundamental and applied, are in connection with phase transitions and the present summary intends to show the main results of the research in the field in 1999 and 2000, from perovskites to molecular crystals, from superalloys to hydrides, from carbon nanotubes to ice surfaces, from incommensurate to quasicrystalline materials, with an important LLB contribution in solid state's theory. Let us note however that magnetic phase transitions are dealt with in a different chapter of this report.

PEROVSKITES : CHARGE/ORBITAL/SPIN ORDERING IN MANGANESE OXIDES

In manganese perovskites with giant magnetoresistance behaviour, correlations between Charge, Orbital and Spin orders is still a puzzling problem. In these compounds, insulating antiferromagnetism is usually understood within superexchange theory and an underlying ionic picture of charge and orbital ordering. This picture was recently "revisited" by a careful analysis of the crystal structure of a half-doped manganite (single crystal X-ray and neutron diffraction) [M. Daoud-Aladine, PhD, J. Rodriguez-Carvajal, LLB; in collaboration with L. Pinsard-Gaudart, A. Revcolevschi, Laboratoire de Physico-Chimie des Solides, Université Paris-Sud; M.T. Fernandez-Diaz, ILL]. A more complete description of the obtained results is given in the chapter "Magnetism and Superconductivity".

PEROVSKITES WITH ULTRA-HIGH ELECTRIC RESPONSES

Materials with ultra high piezoelectric, dielectric and electromechanical responses are widely used for technological applications such as capacitors, sensors, actuators… in the form of ceramics or thin films; they are mainly relaxor lead Pb(B,B')O3 oxides or belong to strontium titanate based compounds ($SrTiO_3$) in which a A-cation is substituted to strontium. They are extensively studied at LLB by the Laboratoire "Structures, Propriétés, Modélisation du Solide", UMR 8580, Ecole Centrale Paris (J.M. Kiat et al.; PhD: C. Ménoret). Physical properties are crucially dependent of the local polar order which drastically changes with the amount, size and charge of A, B, B' cations as well as the grain or film sizes, the electrical field and the thermal history. The combination of neutron scattering with high resolution X-ray diffraction is the only way to get information on the structural properties at nano- and meso-scales in order to understand and tailor the useful properties of these materials. In particular the structural evolutions within the phase diagrams of $PbMg_{1/3}Nb_{2/3}O_3/PbTiO_3$ (PMN/PT) and $SrTiO_3/BaTiO_3$ (SBT) have been determined and extensively studied using neutron diffraction (single crystal and high resolution powder studies, on 6T2 and 3T2 diffractometers respectively). In PMN/PT, a new monoclinic ferroelectric phase in the morphotropic concentrations was discovered, which allows the rotation of the polarisation between the rhombohedral and tetragonal adjacent ferroelectric phases: this new phase is clearly associated to the high piezoelectric response of these materials. In SBT, the $SrTiO_3$-like ferroelastic non ferroelectric distortion continuously decreases and vanishes with Ba concentration: above a critical concentration of 10% [Ba], $BaTiO_3$-like distortions appear and a long range ferroelectric order is recovered.

SUPERALLOYS

NiCr-based superalloys are of considerable interest because of their excellent mechanical behaviour up to high temperatures making them a key material in the construction of e.g. aircraft turbines. Their structure consists of an *fcc* γ–matrix containing cuboid-shaped precipitates of a $L1_2$-type ordered γ'-phase. While the contribution of the γ'-phase to the mechanical properties is quite well understood, much less is presently known about the influence of atomic ordering phenomena in the matrix. Aiming at an improved understanding of these ordering processes, which are important for the design of the next generation of NiCr-based high-performance materials, several modifications of the matrix of a presently used industrial superalloy were investigated with diffuse neutron scattering. The evolution of $D0_{22}$-type short-range order up to 1000°C was examined and interpreted in the context of complementary results obtained from electron

microscopy and mechanical testing. [Collaboration: M. Prem (LLB); G. Krexner, Institut für Experimentalphysik, Universität Wien, Austria; N. Clément and F. Pettinari, CEMES, Toulouse].
See F.Pettinari et al., Acta Mater. 49 (2001) 2549

LITHIUM OXIDE

Owing to its highly unusual properties, lithium oxide (Li_2O) has increasingly stimulated both fundamental and applied research. On the one hand, Li_2O being a superionic conductor, potential applications are seen in the field of solid state batteries. On the other hand, it is discussed as a first-wall material in future fusion reactors due to the tritium breeding properties of the lithium nucleus. In this context structural changes coming about under various conditions of irradiation are of particular interest. Indirect evidence of earlier investigations (using ESR, NMR, DSC) has suggested the formation of two populations of large and small metallic colloids as well as bubbles of molecular oxygen during MeV-electron irradiation. Elastic diffuse and small-angle neutron experiments were performed to confirm the existence of lithium colloids and to determine their structure, size and shape as well as their orientation relations to the oxide matrix. In particular, a detailed investigation of the distortion scattering around Bragg peaks of the Li_2O matrix has permitted to characterize also the small colloids whose study is complicated by their low concentration [Collaboration: M. Prem (LLB); G. Krexner, Institut für Experimentalphysik, Universität Wien, Austria; P.Vajda and F. Beuneu, Laboratoire des solides irradiés, Ecole Polytechnique, Palaiseau] .
See P.Vajda et al., Characterisation of Li-colloids in electron-irradiated Li_2O-crystals by neutron scattering, Nucl. Instr. Meth. B 166/7 (2000) 275.

TRITIUM STORAGE: Pd AND Pd-ALLOYS

Helium damage during tritium storage, forming an indispensable part of future fusion reactor technology, is considered a major problem since it may entail leakage and mechanical failure. Due to continuous radioactive decay of tritium into helium ($T \rightarrow {}^3He + e^- + \nu_e^- + 18.6$ keV) with a half-life of $T_{1/2} = 12.3$ years, an increasing amount of helium atoms is created inside the storage material leading to the formation of helium clusters. Such bubbles give rise to the punching of dislocation loops finally resulting in a dense network of dislocations in the course of time. Agglomeration of helium atoms at grain boundaries induces macroscopic fracture and eventual decomposition of the material. Pd and Pd-alloys are candidate materials for long-term tritium storage. Alloys of various compositions (Pd, $Pd_{95}Pt_{05}$, $Pd_{90}Pt_{10}$, $Pd_{85}Pt_{15}$; $Pd_{95}Rh_{05}$, $Pd_{90}Rh_{10}$ and $Pd_{90}Pt_{05}Rh_{05}$) were loaded with tritium at the site of CEA-Valduc and aged for 15 days, 3 months and 1 year, respectively. Elastic neutron scattering experiments at the three-axis spectrometer VALSE (G4.3) show lattice parameter shifts due to lattice expansion induced by interstitial helium atoms and tritium as well as a decrease of Bragg intensities, up to several orders of magnitude in comparison with the unloaded samples. In addition, changes in the shapes of the Bragg peaks are observed depending on sample composition and aging time. The results of these experiments provide better insight into the specific defect structure induced by helium damage in different alloys and thus allow to assess their potential performance and storage capacities [Collaboration: M. Prem (LLB); G. Krexner, Institut für Experimentalphysik, Universität Wien, Austria; I. Moysan and S. Thiébaut, CEA Valduc ; V. Paul-Boncour, Laboratoire de Chimie Métallurgique des Terres Rares, CNRS, Thiais]

HYDROGEN/DEUTERIUM : STRUCTURAL STUDIES

The determination of crystal structure of compounds including hydrogen (either hydrides or molecular crystals) is an important problem that can "easily" be solved by neutron diffraction. Neutron diffraction is in fact particularly suitable as the neutron scattering amplitudes of the different constituents (light and heavy atoms) are of the same order of magnitude, in contrast with the situation of X-ray scattering. Moreover, in the particular case of hydrogen, the isotopes hydrogen and deuterium have very different coherent scattering lengths, one being positive and the other negative. Two such studies are described below.

RM_5-hydrides

Most of the intermetallic alloys of general formula RM_n (R : rare earth or transition metal ; M : transition metal ; n = 5, 2 or 1) are able to store large amounts of hydrogen to form metallic hydrides. The absorption/desorption reaction is reversible in a large domain of temperature and pressure. Therefore these compounds have been developed for energy storage applications. Among the hydride forming compounds,

$LaNi_5$ is able to store more than 6H/formula unit at room temperature. Neutron diffraction is crucial for the determination of the structural properties of these phases: symmetry, nature of occupied insertion sites and occupation factor. Moreover, due to the neutron penetration depth, structural studies can be performed in closed cell under hydrogen pressure up to 100 bar allowing accurate control of the hydrogen composition. Different substitutions of nickel by other elements (Sn, Co, Al, Mn) have been studied. The crystal structures of three $LaNi_{5-x}Sn_x$ compounds (x=0.2, x=0.4 and x=0.5) and their deuterides have been investigated, for instance. The structural properties of $CeNi_{3.55}Mn_{0.4}Al_{0.3}Co_{0.75}$ and $LaNi_{3.55}Mn_{0.4}Al_{0.3}Co_{0.75}$, two potential materials for nickel-metal hydride batteries, as well as their hydrides have been studied and compared. Finally, the influence of superstoichiometry ($LaNi_{5+x}D_y$) on the structural properties has been considered [see Highlight: 'Influence of substitution and stoechiometry on the structural properties of RM_5-type hydride forming compounds", J.-M. Joubert & al, Laboratoire de Chimie Métallurgique des Terres Rares, CNRS, Thiais].

Molecular crystals

Determination of the crystal structure of molecular crystals is usually accessed via single crystal neutron diffraction. A first study, in connection with biology [Collaboration: Laboratoire de Chimie et Spectroscopie Biomoléculaire, Université Paris XIII, A. Navaza; LLB, G. Chevrier], allowed to localise all the deuterium atoms in $Y_2V_{10}O_{28}.24D_20$. The positions of the water molecules, and consequently the characteristics of hydrogen bonds, were analysed as a function of temperature (T = 60K, T = 300K). Let us note that such structural determinations are important for biology, but that they are rather rare due to the difficulty in obtaining crystals for "neutrons" (size…) of a sufficient quality.

The other studies in LLB are linked to the physics of methyl groups. A systematic study on methodology (comparison of neutron single crystal diffraction data, obtained either on a steady state reactor, or a pulsed reactor) was performed, via data obtained at ISIS on hexamine Nickel Chloride, Ni $(NH_3)_6Cl_2$ at T = 300K and T = 100K [Collaboration: LLB, R. Papoular; ISIS/RAL, C.C. Wilson; Tübingen University, W. Prandl].

The roles of H and/or D on methyl rotation was evidenced in $LiCH_3COO,2H_2O$ comparing the neutron diffraction obtained with either fully hydrogenated, either fully deuterated, either "mixed" systems [Collaboration: LADIR, Thiais, F. Fillaux; LLB: B. Nicolaï (PostDoc), A Cousson]. Whatever the temperature, the crystal structure of $LiCH_3COO,2H_2O$ or Liac(H_7) is orthorhombic, with *Cmmm* symmetry, and free rotation observed for methyl groups at any temperature above ~ 1K. As a powder neutron diffraction study of the totally deuterated analogue, $LiCD_3COO,2D_2O$ or Liac(D_7) has evidenced a crystal phase transition from *Cmmm* to *Pman*, with CD_3 groups ordered at low temperature, the crystal structure of $LiCD_3COO$, $2H_2O$ or Liac(D_3H_4), was investigated on 5C2 at 300K, 40K and 14 K. In that "mixed" sytem, the *Cmmm* to *Pman* transition is observed at T = 17.5±0.5K. The Fourier maps below provide a graphic view of temperature effects on the localisation of the deuterium atoms of the methyl groups CD_3.

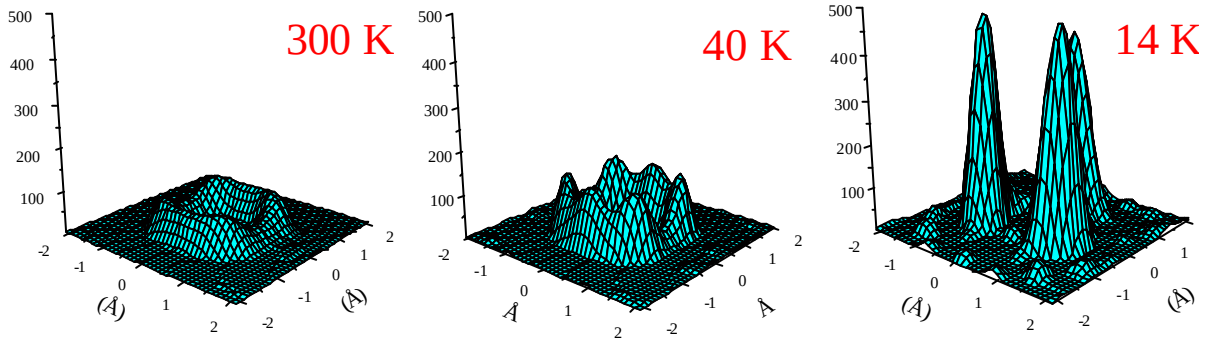

At 300 K free rotation occurs and the threefold symmetry of the methyl group is totally lost. At 14K the deuterium atoms are quite localised in a rather high potential barrier with threefold symmetry. At 40K, as compared to 300K, the methyl rotation is hindered and 6 maxima of density are distinguished, interpreted as a superposition of methyl groups in threefold potentials with two different and equally probable orientations rotated by 180°.

Structures and Phase Transitions

CARBON NANOTUBES

Since 1991, **carbon nanotubes** were extensively studied, due to their unique anisotropic structure and outstanding mechanical and electronic properties. Among all the techniques used for these studies, neutron and X-ray scattering were essential to obtain the structure over very large volumes: single-wall carbon nanotubes (SWNT) self assemblate into a two-dimensional hexagonal close packed lattice (SWNT bundles). The most common assumption as regards SWNT bundles' section is circular, but several theoretical models predict an elliptical deformation and/or a six-fold symmetry faceting of the tubes' section when the Van der Waals interaction between the tubes in the bundles is increased. Such an increase can be obtained via application of a pressure perpendicular to the tubes' surface. For the first time, this six-fold symmetry faceting of the tubes' section is clearly demonstrated when an external pressure is applied [see Highlight: "Structural changes in single-wall carbon nanotube bundles under pressure", S. Rols & al, Groupe de Dynamique des Phases Condensées, Université de Montpellier].

NEUTRAL-TO-IONIC PHASE TRANSITION

The "**neutral-to-ionic**" transition is an unusual type of transition associated to a change of electronic structure between two solid states. This transition is a consequence of the condensation and ordering (crystallisation) of charge transfer excitations. It has been observed in molecular materials of peculiar structures, when donor (D) and acceptor (A) molecules alternate in a linear chain. It is characterised by a cooperative modification of the electronic states of the molecules, accompanied by a significant increase of the level of charge transfer between the neutral and ionic states and by a dimerisation process taking place in the ionic state with formation of ionic pairs $D^{+}A^{-}$ along the stacking axis. The prototype of such compounds is TTF-CA. Neutron scattering results, combined with complementary techniques like X-ray diffraction (conventional or synchrotron sources), dielectric response or nuclear quadrupolar measurements, have provided determinant insights necessary for the understanding of the cascade of cooperative phenomena, responsible for the peculiar electronic-structural instability of these one-dimensional materials. In that frame, the quality of the high pressure (up to 10kbar) experiments carried out at low temperature played a key role. This scientific axis is developed by the University of Rennes, Groupe Matière Condensée et Matériaux, in collaboration with LLB [see Highlight: "Neutral-ionic transitions as the condensation and ordering of charge-transfer exciton-strings", E. Collet & al].

PHASE TRANSITIONS : INFLUENCE OF HCl ON THE STRUCTURE AND DYNAMICS OF ICE SURFACE

The interaction of HCl with crystalline water ice has attracted much attention since the mid'80s owing to its importance in heterogeneous reactions occurring on the surface of polar stratospheric clouds involved in the annual depletion of both Antarctic and Arctic ozone. The LLB experiment on "HCl and ice", as described in [Highlight: "Influence of pollutant gases on the structure and dynamics of ice surface. Implications for the environment", B. Demirdjian & al, CRMC2-Université de Marseille, LPM-Université de Franche-Comté] is a two-step experiment: structural and dynamical studies on pure ice films as a first step, influence of HCl on the structure and dynamics of the ice films in the HCl monolayer coverage range as a second step, with ice films condensed on the (001) MgO surfaces. The obtained results are original, and clearly demonstrate the mechanism of HCl adsorption.

PHASE TRANSITIONS : LATTICE DYNAMICS

The study of phonons is one of the main domains accessible to inelastic neutron scattering. In this field, the results obtained at LLB by the Karlsruhe Research group (M. Braden & al) and their comparison with *ab initio* calculations are essential. Recently, in collaboration with S. Klotz (LPMC, Université Pierre et Marie Curie, Paris), a common programme to measure **phonon and magnon spectra under very high pressure**, has been developed. Phonon and magnon dispersion curves of bcc iron up to 10GPa (world's highest available pressure for inelastic scattering experiments on a triple-axis machine) have been determined (see Highlight). These measurements have established that, in bcc iron, a regular hardening of acoustic phonons occurs. But no softening is observed as precursor effect of the bcc-hcp phase transition which takes place at 11GPa. In the same way, no pressure effect on the spin wave stiffness constant has been detected.

INCOMMENSURATE MATERIALS AND QUASICRYSTALS

Another important domain of research at LLB concerns incommensurate materials both in their structural and dynamical aspects. Here, incommensurate must be understood both in its strict meaning and in relation to the physics of quasi-crystals and composites.

Incommensurate BCCD

Betaine Calcium Chloride Dihydrate (**BCCD**) has been in recent years one of the most intensively studied dielectric compounds with an uniaxially modulated structure [Collaboration: M. Quilichini (LLB), O. Hernandez (Université de Rennes), J.M. Perez-Mato (Universidad del Pais Vasco, Bilbao), G. Schaak (Würzburg University) and L. Vieira (Minho University, Braga)]. Its rich phase diagram of incommensurate (*IC*) and commensurate (*C*) phases between T_I = 164 K and T_0 = 46 K is a textbook example of an incomplete devil's staircase behavior and neutron scattering has had a major contribution in establishing this fascinating phase diagram. Above T_I, BCCD is paraelectric and the neutron studies have allowed to show that the instability mechanism is of displacive type with a clear soft-phonon branch ($T \geq T_I$) and a phason branch ($T \leq T_I$). Below T_I, the modulation wavevector is $\mathbf{q} = \delta(T)\times\mathbf{c}^*$, $c^* = 2\pi/c_O$ with c_O lattice constant of the orthorhombic room temperature phase: up to fifteen phases have been observed at atmospheric pressure. For $T_I \geq T \geq T_C$ = 115 K, δ varies continuously, this *IC* region being interrupted by isolated narrow *C* phases (δ = 2/7, 3/11, 4/15…). Below T_C too, neutron scattering has been the unique technique allowing to show that the modulation was no more harmonic but square-waved: it has been clearly demonstrated that BCCD can then be considered to consist of microdomains of parallel Ising pseudospins separated by domain walls oriented normal to **c**: thus the phases with δ = 1/4 and δ = 1/5 have respective spin sequences (4 up, 4 down) (<4>) and (5 up, 5 down) (<5>), and phases $\delta = n/m$ with *n* even and *m* odd can be polar. Anomalies of the scattering intensity have been observed at *C*-*C* transitions and interpreted as due to critical scattering. To our knowledge, this phase diagram is unique and not encountered in any other 3-D system. Elastic neutron scattering experiments have also been performed at elevated hydrostatic pressure and high electric field respectively. The electric field experiments have shown a polarization spin-flip phase transition between phases with δ = 1/5, (<5>) and δ = 2/10 (<4,6>) ; the pressure experiments gave the pressure dependence of the critical scattering at T_0.

Incommensurate composite crystals

Aperiodic crystals can be subdivided into three classes: modulated incommensurate phases, incommensurate composite systems and quasicrystals. Composite crystals, which are usually classified between incommensurate systems and quasicrystals, consist of two ore more interpenetrating modulated sublattices. The sublattices are generally incommensurate in at least one direction, which implies that they are nonstoichiometric. The main difference from the modulated structure case is that one cannot define an average structure for the full crystal. Due to the lack of a single Brillouin zone, the elementary vibrational excitations should be qualitatively different. Experimental studies about the lattice dynamics in composite crystals are actually very scarce: intergrowth (inclusion) compounds [alkane/urea, Groupe Matière Condensée et Matériaux, Université de Rennes] and layer structures [BISCO and spin ladder systems, J. Etrillard & al , LLB and GMCM].

Interest in the dynamics of composite structures has been recently revived with the discovery of new materials for which large single crystals of good quality can now be synthetized. The high-temperature superconductors $\mathbf{Bi_2Sr_2Ca_{n-1}Cu_nO_{2n+4+d}}$ are generally known to have incommensurate modulated structures. Numerous refinements using the superspace formalism have given some discrepancies in the description of the BiO layers. According to recent neutron diffraction investigations of a member of the series, Bi-2212 (n=2), J. Etrillard, P. Bourges, LLB, in collaboration with B. Keimer, C.T. Lin, H.F. He and B. Liang, MPI, Stuttgart, suggested the composite approach. The assumed sublattices, BiO layer (rocksalt-type) and CuO_2 blocks (perovskite-type), seem to play equally important roles and such a description is introduced in new structural refinements, using a complete neutron data collection [J.M. Kiat]. In contrast, each (modulated/composite) model has distinct lattice dynamics properties. Recent inelastic neutron scattering experiments revealed the existence of two acoustic-like longitudinal branches along the incommensurate direction (Figure). This observed collective dynamics is more likely interpreted within the composite model .

$Bi_2Sr_2CaCu_2O_{8+d}$; room temperature

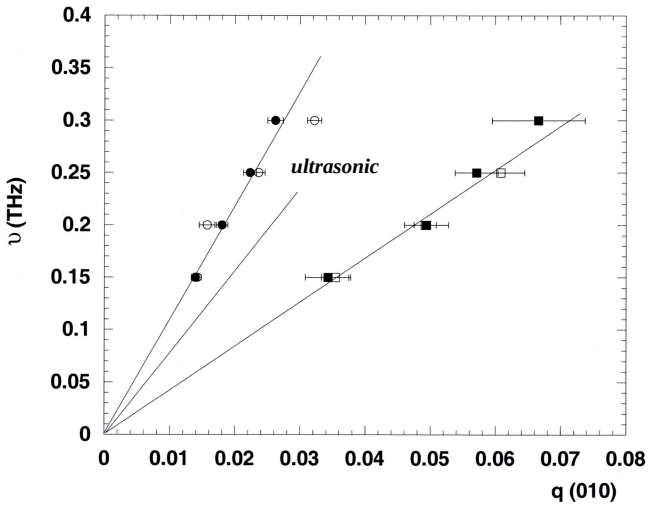

Bi-2212: dispersion curves of the two longitudinal acoustic phonons originating from Q= (0 2 0) (full symbols) and Q = (0 2.21 1) (open symbols) reflections. Q = (0 2 0) and Q = (0 2.21 1) are the main reflections originating from each subsystem. Straight lines correspond to linear fits: the slopes v_1 and v_2, $v_1<v_2$, are respectively associated to each of the subsystems (respective masses m_1 and m_2). The intermediate slope comes from ultrasonic measurements and obeys the law: $v = Sqrt\ \{(m_1v_1^2+m_2v_2^2)/(m_1+m_2)\}$.

The composite character of the **spin ladder** compound, $Sr_{14-x}Ca_xCu_{24}O_{41}$ [M. Braden, in collaboration with U. Ammerahl and A. Revcolevschi, Laboratoire de Chimie des Solides, Orsay] has been already established. One sublattice [$(Sr,Ca)_2Cu_2O_3$] contains two-leg ladders with (Sr,Ca) atoms on both sides, while the other sublattice consists of one-dimensional [CuO_2] chains. New inelastic neutron scattering studies have given two acoustic (transverse and longitudinal) dispersion curves with different velocities arising from each sublattice. At low frequencies, an additional optic-like branch has been detected and is explained by a relative displacement of both subsystems. Special attention is given to characterise this branch which may be attributed to the sliding mode.

Quasicrystals

The structure of **quasi-crystals** and the nature of their dynamic phasons are two main problems which have been solved.

The structural model of icosahedral Al-Pd-Mn quasicrystal has been studied by N. Shramchenko (LLB, PhD) in collaboration with D. Gratias and M. Quiquandon (LEM-CNRS/ONERA). The atomic structure of icosahedral Al-Pd-Mn quasicrystal, which can be obtained as large "single quasicrystal", has been the subject of intensive research during these last ten years. So far, two basic structural models have emerged, both based on the « cut and projection method » from 6D to 3D: (i) M. Boudard & al [*Philos. Mag. Lett. 64, 197 (1991)*] proposed atoms obtained by the 3D cut of 6D lattice with three family of spheres (called atomic surfaces) perpendicular to the physical space; (ii) Yamamoto & al [*Mater. Sci. Forum 150/151, 211 (1994)*] proposed a refined model where the previous spheres are replaced by complex polyhedra. Although these two models are satisfactory from a diffraction point of view, they both generate a non-negligible fraction of short interatomic distances that burdens their physical plausibility. The present contribution to that field had a double goal: first, to collect a fresh new set of neutron diffraction data measured on a well-characterized icosahedral Al-Pd-Mn sample (Y. Calvayrac, CECM, Vitry); secondly, to build out of this data set a physically acceptable atomic structure model with no small interatomic distances and simple chemical order. The neutron diffraction measurements were made using a 4-circle diffractometer (5C2, λ = 0.830Å): a total of 1025 reflections were measured, out of which only 217 independent reflections with $I>3\sigma$ were chosen for the modeling. The chemistry ordering of the model was done using the clusters description (M. Boudard & al [*Philos. Mag. Lett. 64, 197 (1991)*], C. Janot & al [*Phys. Rev. Lett. 72, 1674 (1994)*]) for which recent studies (see for instance: D. Gratias & al [*Phys. Rev. B, Vol 63, 1-16 (2000)*] have shown that using two types of

clusters, similar to Bergman and Mackay clusters, allows to describe 95% of the structure. The final model has the composition $Al_{69.92}Pd_{21.72}Mn_{8.36}$ and density 4.98 g/cm^3. In conclusion, this neutron diffraction study has shown that it is possible to construct an atomic model of Al-Pd-Mn structure presenting a relatively simple chemical order with physically acceptable composition, density and atomic distribution. This model agrees well with STM high resolution images of surface perpendicular to the 5-fold axis of i-Al-Pd-Mn, recently done by L. Barbier (DRECAM).

In contrast with the case of crystalline incommensurate materials, phasons in quasicrystals are not propagative modes but atomic jumps. An extensive triple-axis neutron scattering study of phason hopping in a single-domain of a perfect icosahedral $Al_{70.4}Mn_{8.6}Pd_{21.0}$ quasicrystal has been performed at LLB by G. Coddens (LSI, Ecole Polytechnique), S. Lyonnard (SCM, DRECAM) and B. Hennion (LLB). The quasielastic intensities exhibit important anisotropies. They are compared with theoretical models at various level of sophistication. This comparison strongly suggests the occurrence of **simultaneous correlated jumps**. They behave like a wave of collective jumps, as an elastic response of the quasiperiodic medium to a periodic external source of deformation. This elastic response is governed by the **phason** elastic constants. These surprising results represent an important contribution to the understanding of atomic mobility in quasi-crystals.

« DISCRETE BREATHERS » , FROM THEORY TO APPLICATIONS

Finally, one important activity of LLB is theory, with S. Aubry and co-workers: A.M. Morgante, LLB, PhD; M. Latkovic, Zagreb University, PhD; M. Johansson, LLB, PostDoc; G. Kopidakis (University of Crete). The main topic of these studies is "Discrete Breathers" (DB), or intrinsic localised modes, that are time-periodic spatially localised solutions of discrete classical non-linear hamiltonian systems. This self-localisation is the consequence of non-linearity and discreteness, independent of possible disorder. Discrete Breathers are non-linear modes, which are rather universal and can be found in many finite and infinite systems, of arbitrary dimension, which can be spatially periodic, random, and highly complex. Different problems have been studied by the LLB theoretical group. One of the most recent is the study of existence and stability properties of non-linear spatially periodic or quasiperiodic standing waves in one-dimensional lattices of coupled anharmonic oscillators [A.M. Morgante, M. Johansson, G. Kopidakis, S. Aubry, Physica D, 2001]. Another example is DB in hydrocarbon structures. The authors focus on carbon-hydrogen stretch vibrations, the frequencies of which are well separated from the rest of the vibrational modes. In the anharmonic region of the interaction potential, these spatially localized solutions persist for time scales which are orders of magnitude longer than the period of the atomic vibrations and with frequencies that are different from the normal mode frequencies. The conditions under which these DB solutions are created, the implications on energy relaxation fairly compare with experiments [G. Kopidakis, S. Aubry, Physica B].

Another recent work concerns the formulation of a new existence proof of DB (S. Aubry, G. Kopidakis). This new approach is purely variational. The method holds for systems either with optical phonons or with acoustic phonons (non-vanishing sound velocity), and does not use the concept of anticontinuous limit. Discrete breathers are obtained as loops in the phase space which maximize a certain energy function for a fixed pseudoaction appropriately defined. As a straightforward application of the method, DB are proven to exist at any energy in the quartic one-dimensional model, which up to now was lacking a rigorous existence proof. The method can also work for piezoactive DBs in one or more dimensions and in many more complex models.

The interest of the group is also focused on the problem of targeted energy transfer by DB. As a matter of fact, an interesting property of DBs is that in some cases they can transport energy beetween two anharmonic oscillators, in a highly selective way. Models for energy transfer, and recently for catalysis mechanism, have been formulated.

CONCLUSION

If we had to have a short summary of the above results, the first characteristics to be pointed out would be the wide diversity of the subjects needing neutron scattering. These span both above fundamental and applied research. Some are more or less classical goals for neutron scattering, but some new domains of investigations are emerging, such as environment physics. As for experimental conditions, non "ambient" temperatures, with electric or magnetic fields, and samples under controlled atmospheres are easily available

with neutron scattering. A "new" parameter is also more and more used in neutron experiments: "high pressure". And, in the recent years, neutron diffraction experiments under very high hydrostatic or quasi-hydrostatic pressures became available at the LLB. At the present moment, the LLB disposes of higher pressures (up to 500 kbar) than any other neutron source in the world. The development is based on a combination of a high-intensity neutron diffraction and compact pressure cells with sapphire (pressures up to 100 kbar) or diamond (pressures up to 500 kbar) anvils. New high pressure version of the G6.1 diffractometer ("MICRO"), equipped by a special focusing system, allows to study samples as small as 0.1-0.001 mm^3 in the wide range of pressures and temperatures. The technique is especially adopted to study magnetic orders and structural transformations in "mesoscopic" systems like, for example, nanomaterials. The advantages of neutron diffraction in measurements of structural properties of the "mesoscopic" systems have been recently demonstrated in the study of single-wall carbon nanotubes under applied pressures. The long-wavelength neutron diffraction provided a detailed information about the low-Q part of the diffraction spectra, hardly accessible for the conventional high pressure X-ray diffraction. Possibility to use different orientations of the pressure cell regarding to the incident and scattering beams allowed to study effects of pressure and unaxial stress on facetisation of the nanotubes.

INFLUENCE OF SUBSTITUTION AND STOICHIOMETRY ON THE STRUCTURAL PROPERTIES OF RM_5-TYPE HYDRIDE FORMING COMPOUNDS

J.-M. Joubert, M. Latroche and A. Percheron-Guégan
Laboratoire de Chimie Métallurgique des Terres Rares, ISCSA, CNRS, 2 rue Henri Dunant, 94320 Thiais.

Introduction

Neutron powder diffraction is a very useful tool for the characterisation of intermetallic compounds and metallic hydrides. For the intermetallic compounds, substitution on the metal sublattice is commonly used to tune their thermodynamic properties. Substituting elements are generally neighbours in the periodic table and show poor contrast using classical X-ray powder diffraction. This problem can be overcome by neutron diffraction since neighbouring elements can have quite different Fermi lengths allowing determination of the substitution rates on the different available crystallographic sites within the structure. Concerning the hydrides (or deuterides since deuterium is usually preferred to hydrogen according to its lower background contribution), neutron diffraction is crucial for the determination of the structural properties of the hydrogenated phase: symmetry, nature of occupied insertion sites and occupation factor. Moreover, due to the large neutron penetration depth, structural studies can be performed in closed cell under hydrogen pressure up to 100 bar allowing accurate control of the hydrogen composition

Scientific background

Most of the intermetallic alloys of general formula RM_n (R : rare earth or transition metal ; M : transition metal ; n=5, 2 or 1) are able to store large amounts of hydrogen to form metallic hydrides. The absorption/desorption reaction is reversible in a large domain of temperature and pressure. Therefore those compounds have been developed for energy storage applications. Among them, electrochemical storage of hydrogen leads to large capacity negative electrodes in $NiOOH/Ni(OH)_2|KOH|RM_n/RM_nH_x$ type batteries [1]. Among the hydride forming compounds, $LaNi_5$ is able to store more than 7H per formula unit at room temperature.

The reaction occurs following the reversible equation: $LaNi_5 + {}^{x}/_{2}\ H_2 \Leftrightarrow LaNi_5H_x$. This reaction implies a transition between the intermetallic compound (α phase) and its hydride (β phase) at a constant hydrogen pressure. This plateau pressure is related to the enthalpy of formation of the hydride by the Van't Hoff's law following the relation $Ln(P_{eq}) = \Delta H/RT - \Delta S/R$. However, this equilibrium pressure, above the atmospheric one for $LaNi_5$, is not suitable for electrochemical applications. It can be modified by convenient substitutions on R and/or M sublattice. Keeping the hexagonal $CaCu_5$-type structure (figure 1) of the parent intermetallic compound, substitutions involve cell volume variations and it has been shown that a linear correlation exists between the cell volume deviations and the plateau pressure logarithm [2].

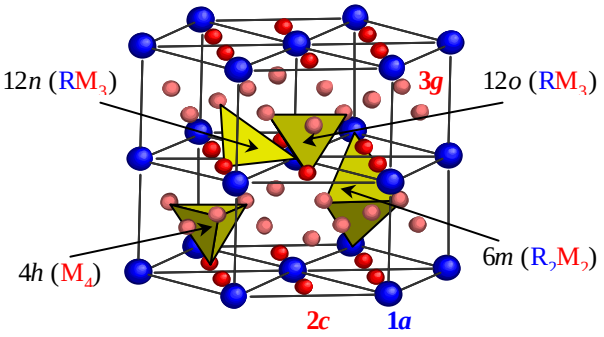

Figure 1 - $CaCu_5$-type structure for intermetallic compounds RM_5 : Space group *P6/mmm*, R (1*a*), M (2*c*), M' (3*g*). Nature and symmetry of the H/D occupied sites are shown as tetrahedra. For sake of clarity, the cell has been doubled along the c axis.

This behaviour is attributed to the correlation existing between the geometrical size and the energy well of the hydrogen occupied sites. It can be directly related to the enthalpy of formation of the hydride. By substitution on the Ni sites by elements such as Mn, Al or Co, it is then possible to decrease the plateau pressure and to improve the cycle life of battery materials without significant loss of the storage properties [3]. The capacity decrease on cycling is commonly attributed to the decomposition of the alloy and to the formation of lanthanum hydroxide **[**4**]**. It was shown that the corrosion process was directly related to the cycling effect and explained by the cell volume expansion observed during hydrogen absorption. By adequate substitution, reduced volume expansion is obtained

involving less internal stresses, less decrepitation and thus less new surfaces in contact with the highly oxidizing electrolyte.
Beside the substitution effects, reduced cell volume variations can also be achieved by preparing superstoichiometric compounds. These RM_{5+x} compounds, which contain an excess of chosen M-type elements (Ni, Mn, Cu or Sn), are obtained by substituting part of the R atoms in the crystal by dumb-bells of M atoms [5]. Such effect is of interest since electrode materials made from over-stoichiometric alloys present in addition better cycle life than stoichiometric ones [6]. Again, this is related to the discrete lattice expansion between the α and the β phases. This has been proved on overstoichiometric compounds $La(Ni_{1-y}Cu_y)_{5+x}$ and $La(Ni_{1-y}Mn_y)_{5+x}$ **[7-9]** for which excellent cycle life was connected to the low decrepitation and the small discrete lattice expansion upon cycling.

Results

Different substitutions of nickel by other elements (Co, Al, Mn) have been studied so far and substitution rates between the two available Ni sites have been achieved taking advantage of the better contrast provided by means of neutron diffraction analysis for these elements. In the case of tin, substituted compounds possess exceptional long term stability as regard to hydrogen cycling in gas storage applications. The crystal structures of three $LaNi_{5-x}Sn_x$ compounds (x=0.2, 0.4 and 0.5) and their deuterides have been investigated [10]. For each composition of the intermetallic compounds, it has been shown by neutron diffraction that tin substitutes only for nickel and is located on site 3*g*.
Concerning the deuterides, for x=0.5 and x=0.4, deuterium occupies four interstitial sites of space group P6/*mmm*: 4*h* (1/3, 2/3, z≈0.38), 6*m* (x≈0.14, 2x, 1/2), 12*n* (x≈0.47, 0, z≈0.11), 12*o* (x≈0.21, 2x, z≈0.33). On the contrary, for $LaNi_{4.8}Sn_{0.2}D_{6.1}$, a decrease of symmetry from P6/*mmm* to P6*mm* (keeping the same cell) is observed. It is due to ordering of deuterium atoms: site 4*h* splits into two sites 2*b*, 12*n* into two 6*d*, 12*o* into two 6*e*, 6*m* is conserved in 6*e*. This behaviour is summarised on figure 2 that shows the evolution of the site occupancy as a function of tin content x. The deuterium ordering is attributed to the higher capacity observed for this compound (6.1 D per formula unit) compared to 5.8 and 5.2 for x=0.4 and 0.5 respectively. Indeed, due to electrostatic interaction between protons, high concentration leads to exclusion rules between adjacent sites and involves hydrogen ordering [11,12].

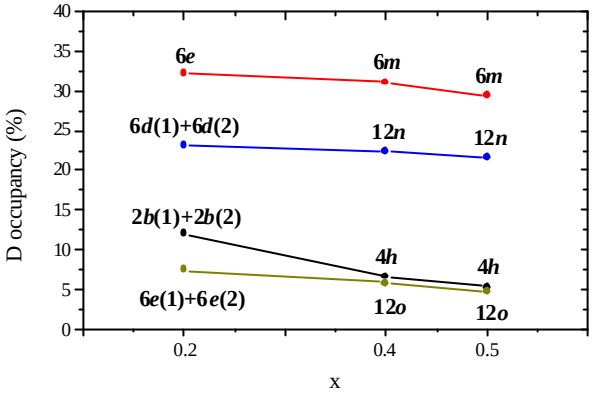

Figure 2 - Deuterium occupancy factors as a function of tin composition in $LaNi_{5-x}Sn_x$ deuterides. For low tin concentration, a symmetry lowering from *P/6mmm* into *P6mm* and a splitting of the deuterium sites is observed.

In battery applications, for cost reasons, lanthanum can be replaced by mishmetal (Mm), a mixture of rare earths essentially composed of La, Ce, Nd and Pr. However, cerium can play a significant role in the behaviour of these materials. Substitution of lanthanum by cerium has therefore been investigated [13]. The thermodynamic properties of hydrogen absorption by $CeNi_{3.55}Mn_{0.4}Al_{0.3}Co_{0.75}$ and $LaNi_{3.55}Mn_{0.4}Al_{0.3}Co_{0.75}$, two potential materials for nickel-metal hydride batteries, as well as the structural properties of their hydrides, have been studied and compared.

The cerium compound has a smaller cell volume and consequently higher equilibrium pressure. The α phase region is more extended in this latter compound and the plateau, keeping the same width, is shifted towards higher hydrogen compositions. This is attributed to a better occupancy of hydrogen sites 6*m* in both α and β phases as it has been determined by neutron diffraction analysis (figure 3). It can be related to an increased site size in the intermetallic compound. Anomalous behaviour of both cell volume expansion and 6*m* site filling was also observed (figure 3). Such behaviour has been interpreted by a valence change of cerium upon hydrogenation, later confirmed by X-ray absorption near edge spectroscopy [14].

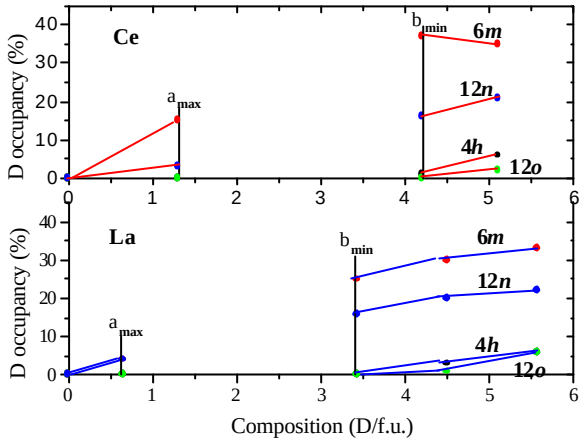

Figure 3 - Occupancies of the deuterium sites as a function of the deuteride composition for $LaNi_{3.55}Mn_{0.4}Al_{0.3}Co_{0.75}$ and Ce $Ni_{3.55}Mn_{0.4}Al_{0.3}Co_{0.75}$.

Finally, the influence of superstoichiometry on the structural properties has been considered. Several hydrides belonging to the $LaNi_{5+x}D_y$ system have been studied. For x=0.2 and y=6, superstructure lines involving a doubling of the c axis are observed. These results have to be compared to the crystal structure of stoichiometric $LaNi_5D_7$ [15] for which the same ordering effect is observed. For x=0.4 and y=5.7 D per formula unit, this superstructure is no longer observed and a possible decrease of the symmetry to *P*6*mm* space group is considered. This structural change is probably due to the lower capacity (5.7 D) observed for this overstoichiometric compounds but the influence of dumb-bells has also to be taken into account. According to these results, overstoichiometry can provide similar effects on both structural and thermodynamic properties than metallic substitution. Therefore it can be an alternative to substitution by costly elements like cobalt for instance.

Better knowledge of the structural properties of metallic hydrides as a function of substitution and stoichiometry remains very important for the optimisation of these energy storage materials. Substituants localisation, nature and rate of the occupied hydrogen sites can be achieved by neutron diffraction analysis. This technique allows data collection in closed cell under controlled deuterium gas pressure leading to accurate and unambiguous structural determination at various D concentration.

[1] Percheron-Guégan, A., Achard, J.-C., Sarradin, J. and Bronoël, G. *Electrode Material based on Lanthanum and Nickel, Electrochemical uses of such materials.* US patent 688537 (1978).

[2] Achard, J.-C., Percheron-Guégan, A., Diaz, H., Briaucourt, F. and Demany, F. 2nd Int. Congr. on Hydrogen in Metals. Paris (1977) 1E12.

[3] Percheron-Guégan, A., Latroche, M., Achard, J. C., Chabre, Y. and Bouet, J. Hydrogen and Metal Hydride Batteries, Pennington, NJ, USA. The Electrochemical Society Proceedings Series (1994) 196-219.

[4] Willems, J. J. G., *Suppl. Philips J. Res.*, **39** (1984) 1.

[5] Latroche, M., Joubert, J.-M., Percheron-Guégan, A. N. and Notten, P. H. L., *J. Solid State Chem.*, **146** (1999) 313-321.

[6] Latroche, M., Chabre, Y., Percheron-Guégan, A., Isnard, O. and Knosp, B., *J. Alloys Compd.*, **in press** (2001).

[7] Notten, P. H. L., Daams, J. L. C. and Einerhand, R. E. F., *J. Alloys Comp.*, **210** (1994) 233.

[8] Notten, P. H. L., Einerhand, R. E. F. and Daams, J. L. C., *J. Alloys Compd.*, **210** (1994) 221.

[9] Notten, P. H. L., Latroche, M. and Percheron-Guégan, A., *J. Electrochem. Soc.*, **146** (1999) 3181-3189.

[10] Joubert, J.-M., Latroche, M., Cerný, R., Bowman, R. C. J., Percheron-Guégan, A. and Yvon, K., *J. Alloys Compd.*, **293-295** (1999) 124-129.

[11] Percheron-Guégan, A., Lartigue, C. and Achard, J.-C., *J. Less-Common Met.*, **109** (1985) 287.

[12] Latroche, M., Rodriguez-Carvajal, J., Percheron-Guégan, A. and Bourée-Vigneron, F., *J. Alloys Compd.*, **218,** 1 (1995) 64-72.

[13] Joubert, J.-M., Latroche, M., Percheron-Guégan, A. and Bourée-Vigneron, F., *J. Alloys Compd.*, **275-277** (1998) 118-122.

[14] Paul-Boncour, V., Joubert, J.-M., Latroche, M. and Percheron-Guégan, A., *J. Alloys Compd.*, **in press** (2001).

[15] Lartigue, C., Le Bail, A. and Percheron-Guégan, A., *J. Less-Common Met.*, **129** (1987) 65.

STRUCTURAL CHANGES IN SINGLE-WALL CARBON NANOTUBE BUNDLES UNDER PRESSURE

S. Rols[1,2], I. N. Gontcharenko[3,4], R. Almairac[1], J.-L. Sauvajol[1], and I. Mirebeau[4]

[1]Groupe de Dynamique des Phases Condensées (UMR CNRS 5581), Université Montpellier II, 34095 Montpellier Cedex 5, France.
[2]Institut Laue-Langevin, 38042 Grenoble Cedex, France.
[3]Russian Research center "Kurtchatov Institut", 123182 Moscow, Russia.
[4]Laboratoire Léon Brillouin (CEA/CNRS), CE Saclay, 91191 Gif-sur-Yvette Cedex, France.

The physics of single-wall carbon nanotubes (SWNT) is of great interest because of their unique anisotropic structure and outstanding mechanical and electronic properties. SWNT usually self assemblate into a two-dimensional hexagonal close packed lattice (SWNT bundles or ropes) as schematically illustrated in the inset of Fig. 1, with the d(100) inter-tube spacing 3.2 Å typical of van der Waals interaction. A SWNT sample is a collection of such bundles. In a bundle, all the tube diameters range around the same average diameter and the average diameter can vary from a bundle to another (defining the diameter polydispersity). Even though it is usually assumed that SWNT's cross section is circular, several theoretical models have predicted a progressive elliptical deformation and/or six-fold symmetry faceting of the tubes' section when the van der Waals interaction between the tubes in the bundles is increased. This enhancement is effective when the diameter of the tubes is large or when an external strain is applied as it is the case when an external pressure is applied perpendicular to the tubes' surface (radial compression). The objective of the present study was to evidence the tube faceting under pressure. In this aim, the structural changes of SWNT ropes were investigated using neutron diffraction experiments in an extended pressure range (up to 50 kbars). For the SWNT samples used in this study, the mean diameter of the tubes is 1.32 nm with a dispersion of about 0.2 nm, and the (10) Bragg peak (the most intense peak) which is characteristic of the SWNT organization into bundle-like 2D hexagonal lattice of finite size is expected to occur around Q ≈ 0.45 $Å^{-1}$. The neutron diffraction measurements were performed on the G6-1 diffractometer, using the 4.734 Å incident wavelength and the investigated Q range: 0.1, 2.5 $Å^{-1}$, perfectly matches that of the 2D organization response for nanotube bundles. Samples were placed into the cylindrical hole of a gasketed saphir anvil cell. In order to test a possible anisotropy of the diffraction response of SWNT samples under pressure, two different orientations of the anvil cell with respect to the neutron beam were used : in the V configuration, the axis of the anvil cell is perpendicular to the diffraction plane ; in the H configuration, the axis of the anvil cell lies in the diffraction plane and along the direction of the Q(10) scattering vector.

Figure 1 shows the raw experimental diffraction patterns recorded at 0, 18, 28 and 47 kbars in the V and H configurations. The signal is normalized to the incoming neutron flux and the diffraction intensities measured in the two configurations are therefore comparable both qualitatively and quantitatively. The peak in Fig. 1 is the (10) Bragg peak. It is a direct probe of the bundle organization and it allows an indirect estimation of the tube shape. The position of the (10) Bragg peak is derived from a Lorentzian fit of the (10) peak profile in the background subtracted data. Then, the lattice parameter a(P) is derived from the modulus Q(10) using the expression : $a(P)=4\pi/Q(10)\ 3^{0.5}$. For each anvil cell configuration we observe an upshift of the (10) Bragg peak assigned to a contraction of the lattice under pressure. More striking, the intensity of that contraction is found to be higly configuration dependent. Qualitatively, at low and intermediate pressures, the (10) Bragg peak position is more upshifted, its width sharper and its intensity stronger in the H configuration than in the V configuration. In figure 2, the a(P) experimental data are compared with the pressure dependence of the lattice parameter due to the van der Waals compression of bundle of circular (model I, Fig. 2, dashed line) and hexagonal (model II, Fig. 2, dot-dashed line) tubes respectively. For **the V configuration** and in the [0, 20 kbars] range we observe a small dependence of the lattice parameter with pressure. Above 20 kbars, a significant softening of the lattice parameter occurs. At the highest pressure the lattice parameter takes the value calculated using model II. In **the H configuration**, the lattice parameter

exhibits an immediate and strong decrease as soon as the pressure is applied. At 30 kbars and above, its value is in good agreement with that expected from model II. All these results suggest that the tubes undergo a progressive faceting, from a cylindrical to a hexagonal tube section and this process is complete for high pressure around 50 kbars. The key to explain the significant anisotropy in the behavior of the lattice parameter under pressure, is to consider the presence of an uniaxial component along the axis of the anvil cell acting on the nanotube bundles. The effect of the uniaxial component is enhanced by the strong anisotropy of the nanotube bundles. The diffraction signal is due to bundles having their long axis in a plane perpendicular to the Q(10) scattering vector. In the V configuration, the strength of the uniaxial component which acts perpendicular to the bundles surface depends on the orientation of the axis of the bundle with respect to the axis of the anvil cell. Consequently, the profile of (10) Bragg peak results from the sum of signals due to bundles compressed in different ways (distribution of the applied pressure). In consequence the peak is expected to be broad. The experimental data are in agreement with this prediction (fig. 1). Above 20 kbars the significant decrease of the lattice parameter is assigned to an important deformation in the tubes section under pressure, from a circular to an hexagonal shape. By contrast to the V configuration, all the bundles involved in the diffraction process for the H configuration are bundles perpendicular to the axis of the anvil cell. Consequently, the uniaxial pressure component felt by the radial surface of the bundle is maximum and it is the same for all the bundles (no distribution of the applied pressure in this configuration). Consequently, a sharper peak is expected in the H configuration than in the V configuration in agreement with the experimental data (Fig. 1). On the other hand, the high pressure leads to an immediate and concomitant radial compression of the bundles and tubes deformation which explains the significant pressure dependence of the lattice parameter observed as soon as the pressure is applied (Fig. 2).

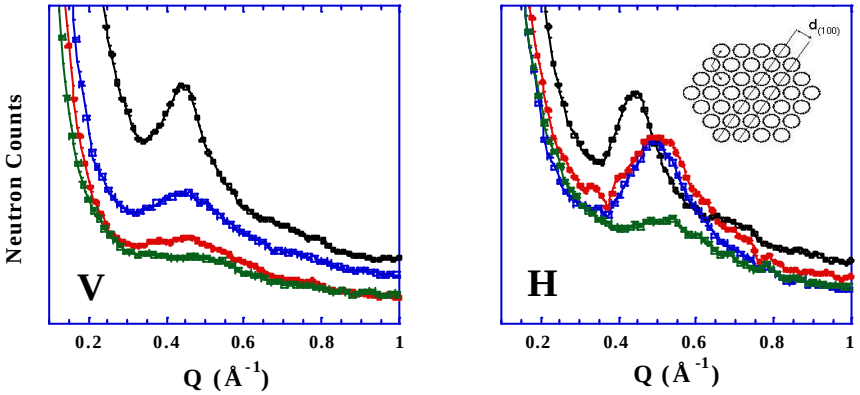

Figure 1. Raw experimental diagrams in the V and H configurations. black: 0 kbar, blue: 18 kbars , red: 28 kbars and green : 47 kbars. Inset: schematic view of a bundle

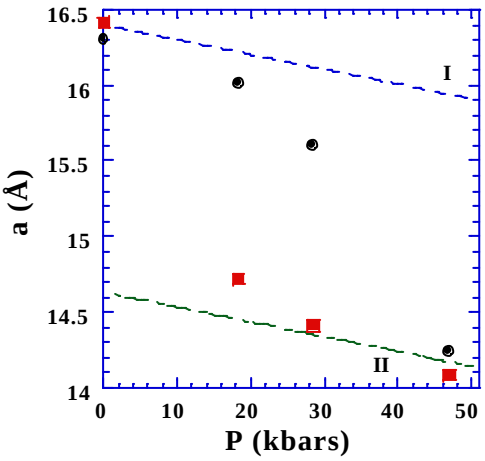

In conclusion, we have stated that under pressure the tubes section develops facets which optimise the van der Waals intertube bonding and a complete faceting is achieved at high pressure in agreement with the dependence of a(P) observed in both configurations. The results confirm theoretical predictions, and also allow one to interpret previous high pressure experiments by Raman scattering

Figure 2 Experimental pressure dependence of the lattice parameter a(P) measured in the V (circle) and H (square) configurations. Calculated pressure dependence of a(P) in model I (circular tubes, blue dashed line) and model II (hexagonal tubes, green dot-dashed line), see text .

NEUTRAL-IONIC TRANSITIONS AS THE CONDENSATION AND ORDERING OF CHARGE-TRANSFER EXCITON-STRINGS.

E. Collet,[1,2] M. Buron-Le Cointe,[1] M.H. Lemée-Cailleau,[1] H. Cailleau,[1] F. Moussa[2]
[1]Groupe Matière Condensée et Matériaux,UMR CNRS 6626, Université Rennes 1, F-35042 Rennes Cedex
[2]Laboratoire Léon Brillouin,C.E.A./C.N.R.S., F-91191 Gif-sur-Yvette Cedex

Many novel low-dimensional electronic materials, organic and inorganic, exhibit a high tunability between competing ground states. Interactions between charge, spin and lattice degrees of freedom are enhanced in the low-dimensional systems and cause cooperative phenomena and broken symmetries. The structure-function relationships are thus determined by self-trapped non-linear excitations, which induce intrinsic multiscale spatial structures and associate multiple timescales. Besides well-known examples such as high-Tc superconductors, manganite oxide perovskites, conducting polymers or mixed-valence chains, the mixed-stack charge-transfer (CT) organic compounds appear as other promising materials, in particular with the possibility of a neutral-ionic (N-I) transition, and can serve as model systems to study the physics of non-linear excitations. In those quasi one-dimensional systems, the alternation of electron donor (*D*) and acceptor (*A*) molecules along stacks (Fig. 1) gives rise to chain multistability between a regular neutral (N) state ...D^0 A^0 D^0 A^0... and two degenerate dimerized polar ionic (I_+ and I) states ...$(D^+A^-)(D^+A^-)$... and ...(A^-D^+) (A^-D+)... Compared with the N state, different intra- and inter-molecular structural distortions take place in the I states and the loss of inversion symmetry leads to the formation of ferroelectric chains. This unusual electronic-structural transition may be induced by temperature and pressure and is governed by the formation of lattice-relaxed (LR) CT exciton-strings, sequences of I dimers within N chains, ... D^0 A^0 $D^+A^-)(D^+A^-)$ D^0 A^0... [1], only recently directly evidenced by diffuse scattering [2].

New physical properties originate from these non-linear excitations, such as photo-induced phase transformations [3], new type of ferroelectric phenomena [4] or negative resistance effects [5]. The N-I transition may be analysed as a cascade of cooperative phenomena\,: formation of CT strings, their one-dimensional (1D) lattice relaxation which can be followed by their three-dimensional (3D) condensation and ordering, as it is the case in the singular (*P*,*T*) phase diagram of the prototype compound TTF-CA, similar to the solid-liquid-gas one [6] (Fig. 2). It was evidenced by different techniques with He pressure cells environment and especially the neutron scattering one available at LLB. The phase diagram can be described with two order parameters : the concentration *c* in *I* species (D^+A^-) (analogous to the density for the liquid-gas transition) and the symmetry breaking order parameter η (associated with the ferroelectric ordering between the dimerized *I* species). The first phase is the *N* one (N_{para}) with a low concentration in fluctuating *I* LR-CT excitations so that it is a disordered high symmetry phase ($c < 0.5$, $\eta = 0$). There is another disordered high symmetry phase which is the *I* paraelectric one (I_{para}) with a high concentration of I fluctuating excitations ($c > 0.5$, $\eta = 0$).

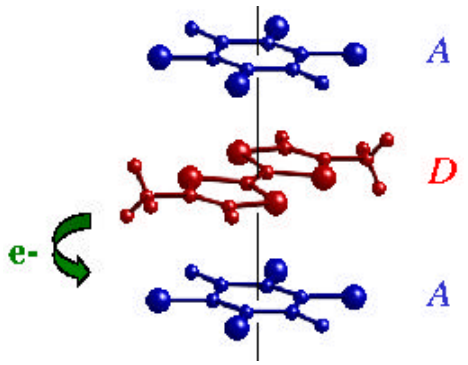

Figure 1. The mixed stack structure (here DMTTF-CA)

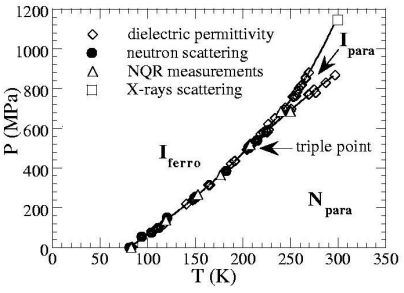

Figure 2 Phase diagram of TTF-CA described with gas-like CT excitation phase (N_{para}), a liquid-like one (I_{para}) and an ordered one (I_{ferro})

Between these two phases is the condensation line above the triple point, characterized by a discontinuous change of *c*, ending at a critical point. The last phase is the *I* ferroelectric one (I_{ferro}) with a ferroelectric ordering of the dimerized DA pairs ($c \approx 1$, $\eta \neq 0$). Above the triple point, located around 500 MPa, anomalies on the lattice parameters are observed for both the condensation and the crystallisation transitions [7]. The ferroelectric order associated with the last one is also characterized by the appearence of (0 2k+1 0) Bragg peaks.

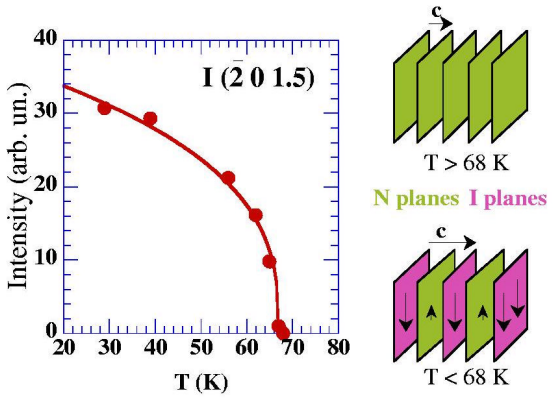

Figure 3. Cell doubling along c in DMTTF-CA, observed at $(\bar{2}01.5)$, associated with the N/I layering of the lattice. Below 68 K, both the stacks inside N and I planes are dimerized.

From one compound to another, different behaviours are observed. For example, we have recently reported that the DMTTF-CA compound undergoes a N-I transition of an unusual type, associated with a N/I ferrielectric layering of the lattice [8] below $T_c \cong 68$ *K*, with the regular alternation of antiparallel dimerized N and I (**a**,**b**) planes (**a** is the stacking axis). As characteristics for the transition, there are charge ordering and dimerization ordering. The transition between the N and N/I layered phases is then characterized by the appearance of superlattice reflections at **c***/2, as observed by neutron scattering measurements (Fig. 3).

A new mixed-stack CT compound, (BEDT-TTF)(ClMeTCNQ), has recently been synthesized [9]. The use of larger molecules than in the case of TTF-CA is supposed to suppress dimerization processes by an increase of inter-stack interactions, and so to induce the formation of paramagnetic I species. At high pressure, an I state is reached as it was observed by optical studies and electric measurements. The magnetic response observed by RPE increases with pressure on approaching the transition and no sign of dimerization is observed with IR spectroscopy. Recently a high resolution neutron diffraction experiment at constant pressure (400 and 540 MPa) on the triple axis spectrometer 4F1 at LLB has revealed clear anomalies on unit-cell parameters at the transition (Fig. 4), where a coexistence of the N and I phases is associated with the first order nature of the transition. The study of the symmetry breaking is now under investigations. One of the most interesting features of this compound is that it undergoes the N-I transition at 0 K under the only effect of pressure. Therefore it may be the good candidate to investigate quantum fluctuations at low temperature.

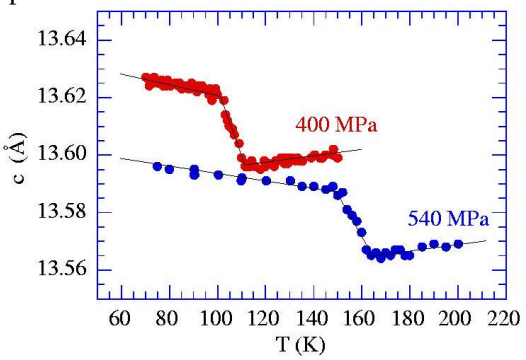

Figure 4. Jump of the lattice parameter c vs temperature at 540 and 400 MPa observed in (BEDT-TTF)(ClMeTCNQ).}

The N-I transformation in quasi-one-dimensional CT solids is an example of extreme electronic and structural cooperativity in molecular organic materials, where one can trigger under the effect of pressure and/or temperature the size, but also the concentration of electronic excitations, and so the physical properties. It may serve as model for thermo- and photo-chromic transformations in solids where cooperativity plays an important role. The existence of fast photo-induced transformations in this systems opens up the prospect of new applications.

[1] N. Nagaosa, J. Phys. Soc. Jap. **55,** 3488 (1986).
[2] E. Collet et al, submitted to Europhysics Letters.
[3] S. Koshihara et al, J. Phys. Chem. **103**, 2592 (1999).
[4] Y. Tokura et al, Phys. Rev. lett. **63**, 2409 (1989).
[5] Y. Tokura et al, Phys. Rev. B **38**, 2215 (1988).
[6] M.H. Lemée-Cailleau et al, Phys. Rev. lett. **79**, 1690 (1997).
[7] T. Luty et al, submitted.
[8] E. Collet et al, Phys. Rev. B **63**, 054105 (2001).
[9] T. Hasegawa et al, submitted.

INFLUENCE OF POLLUTANT GASES ON THE STRUCTURE AND DYNAMICS OF THE ICE SURFACE - IMPLICATIONS FOR THE ENVIRONMENT

B. Demirdjian, D. Ferry and J. Suzanne
CRMC2-CNRS, Campus de Luminy, case 913, F-13288 Marseille cedex 9, France
C. Toubin, S. Picaud, P.N.M. Hoang and C. Girardet
LPM , Faculté des Sciences, Université de Franche Comté F-25030 Besançon cedex, France

The interaction of HCl with crystalline water ice has attracted much attention since the mid 80's owing to its importance in heterogeneous reactions occurring on the surface of polar stratospheric clouds (PSC) involved in the annual depletion of both Antarctic and Arctic ozone [1,2]. Nowadays, the impact of ice in atmospheric chemistry remains a major uncertainty, owing to the fact that snow covers more than 50% of the northern hemisphere ground during winter, and that about half of the water mass condensed in clouds is made out of ice.

Numerous experimental studies of HCl-ice interactions have been undertaken since the mid 90's which have suggested that HCl uptake on ice is limited to about one monolayer surface coverage, probably because of the weak solubility of HCl in bulk ice [1]. However, most of the experiments were done at much lower temperatures than those currently considered in the stratosphere. Possible explanations are still uncertain and there is still a debate on the precise role of the ice surface with respect to HCl adsorption, solvation and incorporation into ice crystals. It is not perfectly known how HCl is incorporated into the ice lattice and how the ice lattice responds to the presence of HCl on structural and dynamical points of view. Among the relevant questions is whether the formation of a quasi-liquid layer (QLL) is required or not to explain the large HCl uptake by ice under stratospheric conditions, that is around 190-200 K. The existence of a QLL at the surface of ice in presence of HCl has been proposed by Molina [3] and Abbatt et al [1] to explain the solvation of HCl and the observed large HCl uptake by ice crystals.

The aim of the experiments we have undertaken at LLB is to contribute to this debate in order to understand the basic mechanisms of trace gases-ice interactions, their impact on the atmospheric chemistry and by consequences on the climate.

In a first step, we have characterized pure ice films on a structural and dynamical point of view. In a second step, we have studied the influence of HCl on the structure and dynamics of the ice films in the HCl monolayer coverage range. For that purpose, we have condensed ice films on the (100) MgO surfaces. This substrate allows the formation of an ice I_h crystalline film on top of a stable (3x2) water monolayer [3]. In order to have a good signal/noise ratio, we have used very uniform MgO powders featuring micro-cubes exposing (100) facets only. These powders have been used many times for monolayer adsorption studies showing properties very close to those of single crystal surfaces. The specific area of the powders is 10 m^2/g. We have limited the ice film thickness to 5 monolayers (ML) in order to avoid capillary condensation which would obscure the analysis of the neutron results. Furthermore, such a film thickness is comparable to the size of the simulation boxes used in our molecular dynamics calculations.

The neutron experiments have been performed on the G6.1 diffractometer for the structure determination and on the Time of Flight (TOF) spectrometer G6.2 (Mibemol) for the dynamical studies.

I. Structure and dynamics of pure ice films [3]

The neutron diffraction spectrum performed at 190 K on a 5 ML thick D_2O ice film indicates the formation of hexagonal ice I_h. The (002) peak is broadened when compared to bulk ice, indicating the formation of a thin film with large (0001) planes. From the quasi-elastic neutron scattering spectra (QENS) we have determined, via diffusion models, the translational and orientational mobilities. No translational mobility (less than the detection limit D_t @ 10^{-6} cm^2 /s) has been detected below 250 K. Our QENS measurements indicate that a mobile layer showing a translational diffusion coefficient close to that of liquid water appears between 250 K and 265 K. Hence, one may reasonably infer that a surface melting transition occurs within this temperature range at about 10 K below that of the bulk melting point.

The experimental results are in qualitative agreement with molecular dynamics (MD)

simulations. Fig. 1 shows a snapshot of the supported ice film at T=220 K. One sees that the surface is perturbed : the QLL is observed with a shift of 30-40 K in the simulations compared to the experiments. This shift comes from the inaccuracy of the potential used in the simulations.

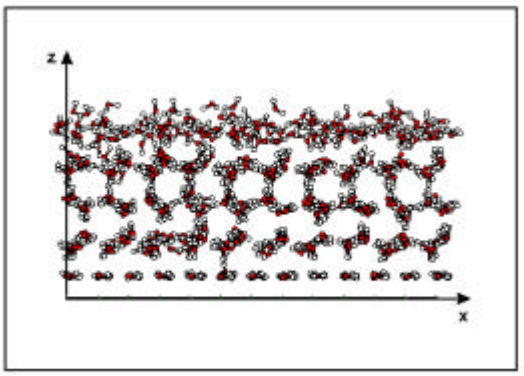

Figure 1. Snapshot of the supported ice film at T=220 K showing the MgO surface (z=0), the flat ice monolayer, and the hexagonal ice bilayers. One can see that the surface suffers strong disorder at this Temperature. Red and white circles represent oxygen and hydrogen atoms respectively

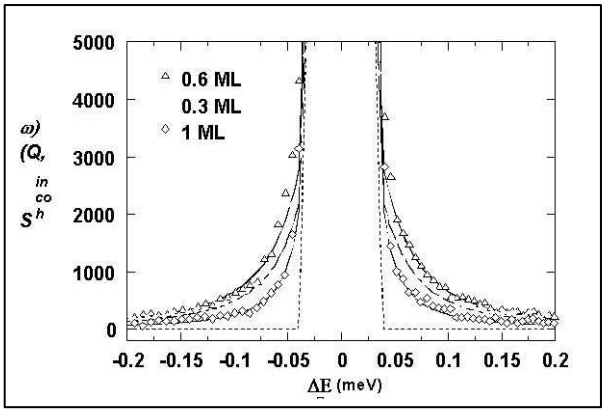

Figure 2. QENS spectra of the ice-HCl film at T=250 K showing broadening due to translational motion of water molecules in the ice film versus HCl coverage ($D_t = 0.8.10^{-5} cm^2/s$ for all coverages)

II. Influence of HCl adsorption [4,5]

The neutron-diffraction experiments conducted at T = 190K show clearly that, whatever the HCl coverage is, the structure I_h of the ice film appears to be unaffected by HCl adsorption, suggesting that HCl is mainly located at the surface and does not penetrate the film. This experimental result is in very good agreement with our MD calculations [5] showing that, at 190 K, 75% of the HCl molecules are trapped at the surface of the ice film, while the remaining 25% lie inside the outermost bilayer.

For an HCl coverage of 1 ML, hydrogen chloride dihydrate coexists with the hexagonal ice at T = 220 K. However, the absence of the (002) peak characteristic of bulk ice suggests that the ice I_h film is very thin. We interpret this feature by the fact that only one part of the film corresponds to the hydrate phase, while the other part corresponds to the ice I_h phase. As suggested by the MD calculations, at T ≥ 210K, HCl easily diffuses inside the ice film and destroys the ice I_h structure, except close to the MgO support where some order persists. At *T* = 250 K and 1 ML HCl, the diffractogram indicates that the ice/HCl film becomes an amorphous solid phase, which coexists with a small amount of liquid phase. As indicated by the QENS analysis (Fig. 2), the liquid proportion is weak under these conditions (≤ 9 %). For q_{HCl} = 0.3 and 0.6 ML, the liquid proportion found at *T* = 250 K (Fig. 2) corresponds to a film thickness of about one or two layers (namely, 30 and 45 % of the ice film thickness). MD calculations show that this mobility concerns preferentially the outermost layers, i.e. the occurrence of the surface premelting. *Hence, at submonolayer coverage, HCl is lowering the ice surface melting temperature by ~15 K compared to pure ice. Our experiments indicate that, at the lowest stratospheric temperature (T » 190 K), there is no quasi-liquid layer* having a translational mobility of a normal liquid at the ice surface. *Finally, the neutron experiments as well as the MD simulations are clearly showing that HCl is strongly perturbing the ice film in the temperature range of the troposphere, that is 230-260 K. That could be the case for other pollutants as well. Models of atmospheric chemistry will have to include these effects in order to explain the "in field" observations*, particularly in the upper troposphere and lower stratosphere where temperatures lie in the 220 K-260 K range.

[1] J.P. Abbatt, K.D. Beyer, A.F. Fucaloro, J.R. McMahon, P.J. Wooldridge, R.Zhang and M.J. Molina, J. Geophys. Research, **97** (1992) 15819
[2] M.J. Molina et al., Science, **261** (1993) 1418
[3] C. Toubin, S. Picaud, P. N. M. Hoang, C. Girardet, B. Demirdjian, D. Ferry, and J. Suzanne, J. Chem. Phys. **114** (2001) 6371
[4] B. Demirdjian, D. Ferry, J. Suzanne, C. Toubin, S. Picaud, P.N.M. Hoang and C. Girardet, submitted to J. Chem. Phys.
[5] C. Toubin, S. Picaud, P.N.M. Hoang, C. Girardet, B. Demirdjian, D. Ferry, J. Suzanne, submitted to J. Chem. Phys.

PHONON AND MAGNON DISPERSION OF BCC IRON TO 10 GPA

S. Klotz[1] and M. Braden[2]

[1]Physique des Milieux Condensés, CNRS UMR 7602, Université P&M Curie, B77, 75252 Paris

[2]Laboratoire Léon Brillouin (CEA-CNRS) and Forschungszentrum Karlsruhe, IFP, 76021 Karslruhe (Germany)

The properties of iron under extreme conditions are intensively studied [1] due to its relevance for geophysical models of the earth's interior. From a more general point of view, the behaviour of bcc iron under compression is interesting since almost half of the elements contain the bcc structure in their phase diagram. The phonon dispersion of bcc elements was studied in the past in search of dynamical precursor effects of lattice instabilities. Phonon dispersion curves exist for example for alkaline metals (Li, Na and K [2]) at low temperature as well as for transition metals (Zr, Ti, Hf and Sc) at high temperatures [3]. The lattice dynamics of bcc metals under reduced volume, however, is almost completely unknown. Similarly, the behaviour of the magnon dispersion under pressure is unknown for any of the ferromagnetic transition metals.

We have measured both the phonon and magnon dispersion of Fe at room temperature up to 10 GPa, i.e. over almost the entire stability range of the bcc-phase (which transforms to hcp iron at ~11 GPa) [4]. The measurements were carried out at the 1T1 spectrometer similar to previous experiments on Ge and Zn [5]. Typical scans through phonon and magnon branches are shown in Fig. 1. The position of the frequencies could be determined with a statistical error of < 1% in almost all cases and the ambient pressure frequencies agree within ~ 2% with those of published values.

Figure 2 shows the phonon dispersion along high-symmetry directions, 55 phonon mode frequencies have been determined at 0 and 9.8 GPa. All measured frequencies increase by 5-10% for a volume reduction corresponding to 5%. Of particular interest is the T_1-mode with wave vector along [110] and [1-10] polarisation which increases completely regularly at the zone boundary (N-point). This observation is important for the transition mechanism to the hcp-phase at ~10 GPa. The latter can be obtained from the bcc-phase by displacements which involve the $T_1(N)$ phonon (Burgers-mechanism). *Ab initio* calculations on the bcc-hcp transition in Ba predict a substantial softening of the $T_1(N)$ phonon on approaching the transition pressure [6]. In iron, such dynamical precursor effects due to the Burgers mechanism seem to be absent. Our results are in agreement with spin-polarised full-potential total energy calculations [7] which predict a slight increase of the $T_1(N)$ phonon frequency in the 0-10 GPa range. This scenario of the bcc-hcp transition is therefore different from that in Ba under pressure [6], and different from the situation found in all group 3 and 4 transition elements where there is a pronounced softening of the $T_1(N)$ frequency at ambient pressure and elevated temperature as the hcp phase is approached [3]. Iron seems to be an exceptional case in the sense that no dynamical precursor effects are visible on the $T_1(N)$ mode. The critical ingredient for this behaviour is the presence of ferromagnetism which stabilises the bcc-phase with respect to the non-magnetic fcc-phase. The effect of pressure is essentially to broaden the flat d-bands and thereby to decrease the density of states at the Fermi level $D(E_F)$ below the stability limit for ferromagnetism [7]. The bcc-hcp instability is hence not primarily due to phonon softening but due to the effect of pressure on the magnetism of iron.

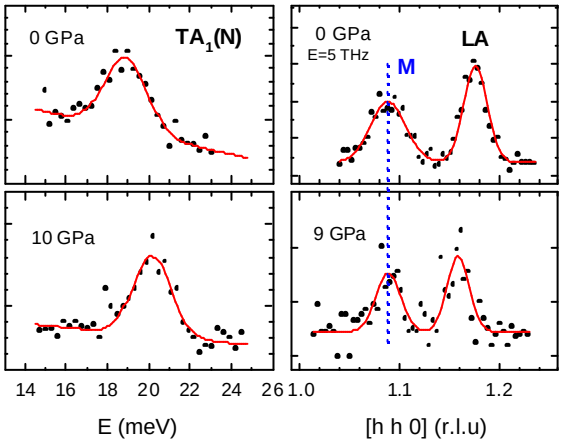

Figure 1 Constant-Q scans through the $TA_1(N)$ phonon branch (left) and constant-E scans through the magnon (M) and LA-phonon branches (right), at

ambient and maximal pressure. Note the insensitivity of the magnon energy to high pressure.

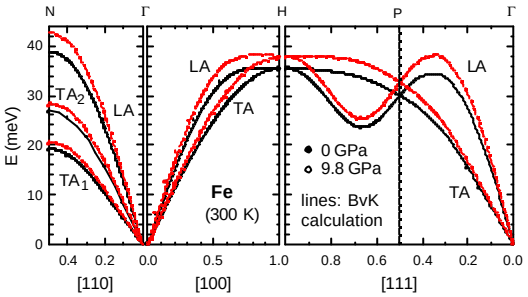

Figure 2. Phonon dispersion along high-symmetry directions at 0 and 9.8 GPa.

We performed lattice dynamical calculations using a general force constant model similar to previous ambient pressure investigations on iron and other bcc elements (Fig. 2). This model contains 13 force constants, seven of which were allowed to vary with pressure. It enables us to calculate the pressure dependence of the elastic constants to high accuracy. It also allows to extract the density of phonon states (Fig. 3) which gives thermodynamic parameters such as the specific heat at constant volume or the equivalent Debye temperature θ_D. Such results are difficult or impossible to obtain by other techniques.

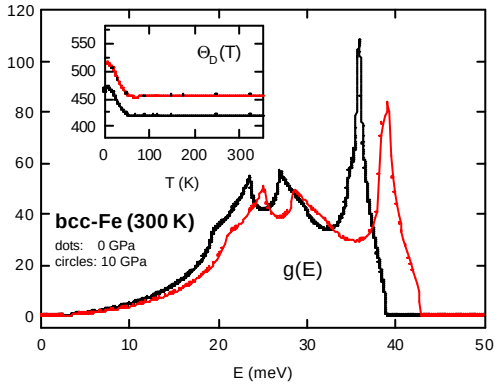

Figure 3. Phonon density of states and Debye temperature $\theta_D(T)$ (inset) at 0 and 9.8 GPa.

In view of the important role of Fe in stabilising the bcc-phase we decided to study also the magnetic excitations as a function of pressure. As for the spin-wave dispersion of bcc-iron and other ferromagnetic transition elements, it is known to be isotropic and follows for small $\mathbf{q}$ the dispersion law $E = D|\mathbf{q}|^2$, where $D = 2 J S a^2$ is the spin wave stiffness constant, S the spin, a the lattice parameter and J the coupling constant. Consequently, a measurement of the magnon dispersion under pressure allows us to determine the dependence of the magnetic interaction on the interatomic distance, providing $\partial S/\partial P$ is known. Fortunately, $\partial S/\partial P$ is well constrained by both experiments and theory to be ~ -3% between 0 and 10 GPa. Most surprisingly, no variation in the magnon energies is observed in our measurements up to 10 GPa (see Fig. 1). This unusual weak pressure dependence of the magnetic excitation spectrum is unexpected and hitherto unexplained by first-principle calculations. Hower, it appears to be in excellent quantitative agreement with Wohlfarth's itinerant electron model for ferromagnetism [8]. Within this theory, the weak pressure coefficient of D can be related to the pressure *in*dependence of the Curie temperature ($\partial T_C/\partial P=0\pm0.3$ K/GPa) and the elevated bulk modulus of Fe (164 GPa).

[1] R. Lübbers et al., Science **287**, 1250 (2000); G. Fiquet et al., Science **291**, 5503 (2001).
[2] O. Blaschko et al., Phys. Rev. B **37**, 4258 (1988), and refs. therein.
[3] W. Petry, J. de Physique (Paris) **C2**, 15 (1995).
[4] S. Klotz and M. Braden, Phys. Rev. Lett. **85**, 3209 (2000).
[5] S. Klotz et al., Phys. Rev. Lett. **79**, 1313 (1997); S. Klotz, M. Braden, J.M. Besson, Phys. Rev. Lett. **81**, 1239 (1998).
[6] Y. Chen, K.M. Ho, and B.N. Harmon, Phys. Rev. B **37**, 283 (1988).
[7] M. Ekman et al., Phys. Rev. B **58**, 5296 (1998).
[8] E.P. Wohlfarth, in: Physics of Solids under High Pressure (edts. J.S. Schilling and R.N. Shelton), North-Holland Publishers (1981).

54

DISORDERED SYSTEMS AND MATERIALS SCIENCE

In the domain of metallurgy and ceramics, the properties of technological interest depend on the defect properties and on the defect structure of the material at the atomic (vacancies, impurities,…) or at the mesoscopic (dislocations, porosities, …) level. This is why materials science requires a fundamental corpus of knowledge on defects and disorder. In particular, the fundamental study of atomically disordered systems allows to develop theoretical models, and to validate numerical simulations (Monte-Carlo, molecular dynamics, etc…) which are then applied to understand and modelize "real materials". Particularly important is the extrapolation of their properties at long time in operating conditions, and the prediction of their behaviour under thermal, chemical, or irradiation-induced ageing.

1. DISORDERED SYSTEMS

1.1. Introduction

The scientific activity of LLB in the field of disordered systems is mainly concentrated on the study of local atomic arrangements in topologically or chemically disordered solids or liquids, by elastic diffuse neutron scattering. Two instruments are entirely devoted to these studies :

- the 7C2 diffractometer, installed on the "hot" source, with short wavelength (generally ≈ 0.7 Å) neutrons, and equipped with a 640 cell position sensitive linear multidetector, for liquid and amorphous systems,
- the G4.4 diffractometer, installed on a "cold" neutron guide, managed by ONERA and CEA/LSI, with time-of-flight analysis, devoted to the "in situ" high temperature study of local order in single crystals.

In the case of systems presenting a tendency towards phase separation, complementary studies by Small-Angle Neutron Scattering (SANS) are necessary.
Some studies of dynamics, mainly on glass transition, are also performed at LLB by external users, in particular with the time-of-flight inelastic spectrometer MIBEMOL.

1.2. Metallic alloys : from diffuse scattering to kinetics

(X. Flament, PhD, and R. Caudron, LLB and LEM-ONERA).

The face-centered cubic (f.c.c.) lattice contains equilateral triangles of first neighbours. If the interactions between these first neighbours dominate and are repulsive (antiferromagnetic), this results in a localized frustration. This frustration induces a degeneracy which is source of disorder and entropy, even at zero temperature. This phenomenon is at the origin of the complexity and of the richness of phase diagrams of systems built on the f.c.c. cubic lattice.

As shown by the diffuse neutron scattering study on Pd_3V, most of the order-disorder properties of this alloy, the structure DO_{22} of which is built on a f.c.c. cubic lattice, can be deduced from an Ising model limited to two interactions. In this model, the interactions J_2 between second neighbours are of the same sign, but much weaker than those between first neighbours J_1 (J_2/J_1~0.05). The work described here has allowed to show that, in this situation, the quasi-degeneracy presented by the DO_{22} phase can induce special ordering paths.
The Long-Range Order DO_{22} is characterised by 100 and 1 ½ 0 type superstructure reflections. We have followed by X-ray diffraction the time dependence of the intensities of these two lines after in situ quenching. In the usual situations, one expects that, depending if the quench temperature is above or below the spinodal temperature, the two waves present, or not, an incubation time. In our case, two distinct spinodals exist, one for each concentration wave. If the quenching temperature is lower, or larger than the two spinodals, the two waves will increase instantaneously or not. This is what was found experimentally. Nevertheless, if the quenching temperature is intermediate, the wave with the lowest spinodal temperature will form instantaneously, while the other will undergo an incubation time. Figure 1a shows indeed that, for a quench from 660°C, the 1 ½ 0 wave forms with a delay, when the 100 which, in the disordered state, corresponds to the maximum of short-range order intensity, develops immediately. On Fig.1b, a Monte-Carlo simulation reproduces clearly this situation, with J_1 and J_2 potentials compatible with the diffuse scattering determined by neutron scattering on G4.4.

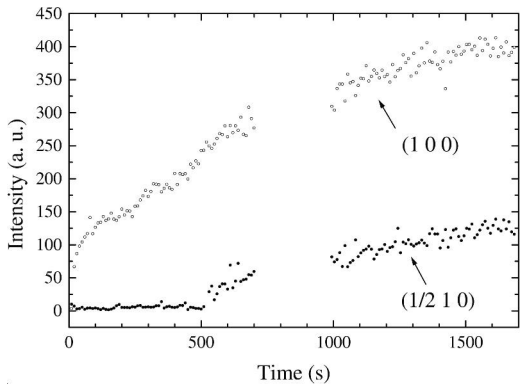

Figure 1a : Time evolution of the 210 (type 100) and 1 5/2 0 (type 1 ½ 0) Bragg peak maximum intensities following quenching from 660°C, determined by X-ray scattering (experiment performed at Brookhaven National Laboratory Synchrotron)

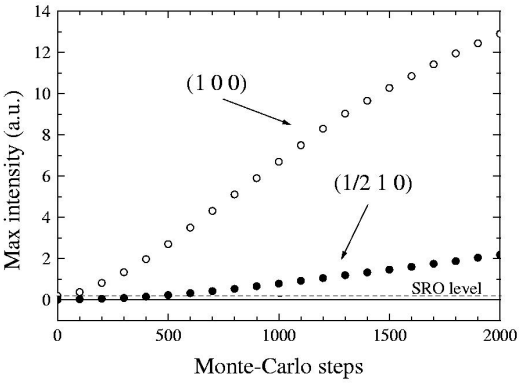

Figure 1b : Monte Carlo simulation of the results shown in Fig.1a . The dotted line shows the short-range order intensity in 100, confirming that the LRO concentration wave shows up instantaneously.

1.3. Short range order and phason fluctuations in icosahedral AlPdMn

(N. Shramchenko, PhD, R. Bellissent, LLB, D. Gratias and R. Caudron, LEM-ONERA)

The powder diffraction diagrams of quasicrystals were rapidly indexed after their discovery in1984. This indexation was confirmed on single grains as soon as they became available. However, the exact location of the sites and their atomic occupancy are not yet known. The best models available nowadays concern only 90% of the sites.

Diffuse scattering can provide us with information about partial occupancy of sites. We have studied at least four single crystals of Al Pd Mn icosahedral phase, elaborated by different teams, by Bridgeman or Czochralsky methods, and submitted to various heat treatments. All these crystals yielded, quantitatively, the same distribution of diffuse scattering. This situation can be attributed to the narrow domain of existence of the icosahedral phase (less than 3 at.%), and also to a low sensitivity of the diffuse scattering to the concentration and thermal treatment.

As an example, fig.2 shows this distribution in a two-fold symmetry plane containing two two-fold, two three-fold and two five-fold axes. The latter axes are indicated on the figure 2.

Spots corresponding to Bragg peaks are strongly broadened. This is not exactly peak broadening, but, in fact, a well identified diffuse scattering, due to phason fluctuations. We checked that this diffuse scattering varies as the inverse square of the distance to the peak. It should also be proportional to the effective quench temperature, but we did not detect any change from sample to sample, notwithstanding the various heat treatments of the samples.

Far away from any obvious Bragg peak (gray-green zone on fig.2) we estimated the order of magnitude of the diffuse background to 0.03 barn/steradian. Unless it results from the superimposition of the diffuse feet coming from the neighbouring Bragg peaks, it can be attributed to chemical disorder. The partial site occupancy found on the approximant phase ξ' corresponds to 0.01 barn/steradian.

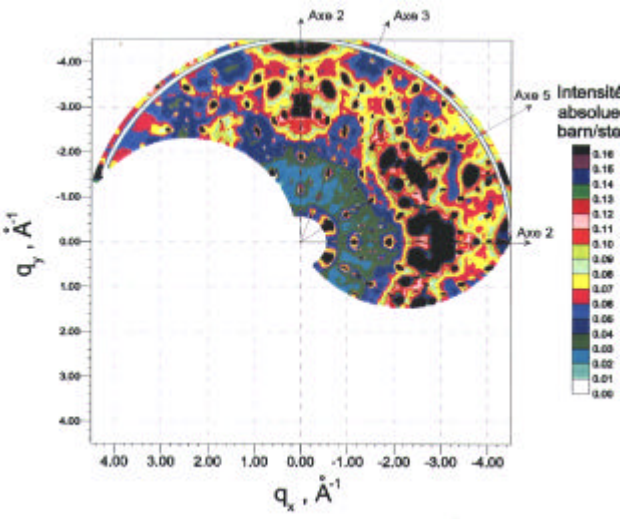

Figure 2. Elastic diffuse scattering map of the "mono-quasi-crystal" ($Al_{0.704}Pd_{0.214}Mn_{0.082}$) measured at LLB on G4.4 at room temperature

1.4. Structure and Dynamics of Supercritical Water

(M.C. Bellissent-Funel, P. Calmettes, LLB, M. Bonetti, CEA/SPEC)

Liquid water has been studied extensively near ambient conditions. Much less is known about water under extreme conditions. Beyond the critical point (H_2O: T_c~374°C, Pc ~221 bar, ρ_c ~0.32 g.cm^{-3} and D_2O: T_c~371°C, Pc ~220 bar, ρ_c~0.36 g.cm^{-3}), water exhibits many peculiar properties such as the variation of dielectric constant, viscosity, ion product as a function of the density. Supercritical water is a very reactive medium that is very well adapted in many industrial applications.
Small-angle neutron scattering (SANS) measurements were performed on supercritical water to understand its peculiar behavior. This technique can probe length scales from the correlation length of the critical density fluctuations to the intermolecular distances. SANS spectra were recorded along the critical isochore at temperatures between (T_c + 0.48 K) and (T_c + 22.02 K). At the lowest values of the wave vector transfer q, the scattered intensity shows a pronounced increase due to the divergence of density fluctuations at the critical point. In the studied q range, from 0.07 Å^{-1} to 0.34 Å^{-1}, all the spectra can be accurately described by the Fisher-Langer correlation function provided that a multiplicative additional term describing both the molecular structure and the local order are taken into account. The value found for the amplitude of the critical correlation length is x_0 = (1.36 ±0.05) Å. This was the first measurement of x_0 for water.

The microscopic structure of supercritical water has been studied by neutron scattering at different thermodynamic states, for densities ranging from 0.2 to 0.7 g.cm^{-3}. The experimental partial pair correlation functions $g_{OH}(r)$, $g_{HH}(r)$ and $g_{OO}(r)$ are compared with the results of molecular dynamics simulations using the (SPCE) model potential for water (see figure 3). The tetrahedral arrangement is lost but hydrogen bonding persists in dense supercritical water via the presence of dimers. This is revealed by the proton density of states that exhibits strong differences with that of ambient water, and is in good agreement with data obtained by NMR and Raman spectroscopies.

Hydrogen-bond dynamics of supercritical water has been investigated for the same thermodynamic states by quasi-elastic neutron scattering. The results have been analysed using a jump diffusion model; τ_0, the residence time and D, the translational diffusion coefficient have been determined as a function of the densityof supercritical water. Values of D are in very good agreement with those measured by NMR and increase strongly as the density of the medium decreases. The residence time τ_0 slightly increases as the density of supercritical water decreases, with a value ten times shorter than that measured in ambient liquid water (1ps). The whole results confirm that some degree of hydrogen bonding is present in dense supercritical water even though the tetrahedral coordination number leading to an extended network at room temperature is lost

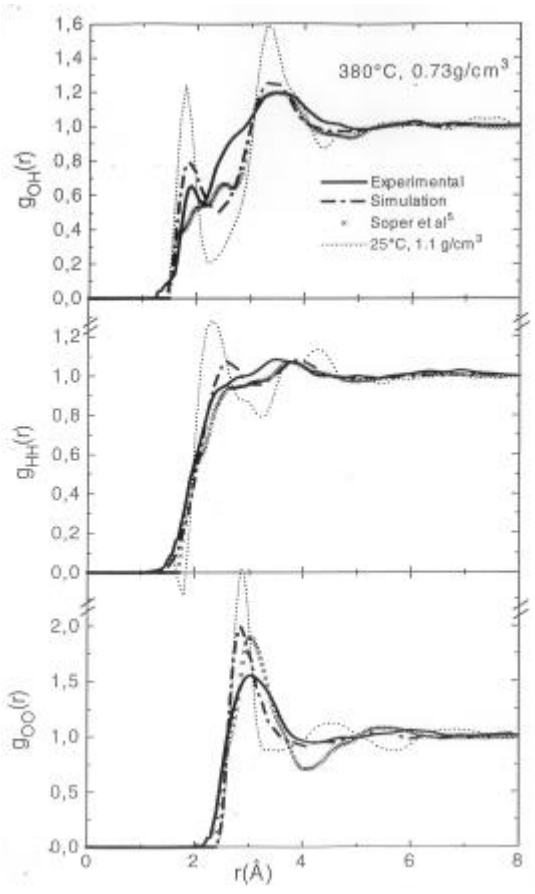

Figure 3. The experimental and simulated partial pair correlation functions g_{OH}, g_{HH} and g_{OO} of supercritical water at T=380°C and ρ=0.73g/cm^3. The data of Soper *et al.* J. Chem. Phys., 106 (1997) 313-322, have been reported for comparison together with that for ambient liquid water.

1.5. Dynamics of ^{4}He confined in porous media at very low temperatures

(F. Albergamo, PhD, LLB)

The measurements of helium adsorption isotherms (at temperatures as low as 1.2 K) have been made possible by building up a suitable equipment at the laboratory; by this technique, a number of porous samples (Vycor glass, Geltech silica and MCM-41 powders) have been characterised. Subsequent inelastic neutron scattering measurements on MIBEMOL spectrometer (at T = 1.2 K) on ^{4}He confined into the 32 Å MCM-41 pores at different pore fillings have revealed that the bulk-like response (elementary excitations) comes from the ^{4}He in the capillary condensate phase.
Further investigation has been conducted on the same system at very low temperatures (down to 0.4 K) with the IN6 spectrometer at the ILL. Special sample cells, filled and sealed at room temperature, have been developed in order to avoid the use of the injection capillary on the ^{3}He cryostat that was found to allow condensation of unknown amounts of liquid helium. In this way, the thermodynamic state of the system was kept known through the whole experiment. For the first time, evidences for phonon confinement phenomena have been collected. In particular, a perturbation of the long wavelength phonon dispersion (up to q = 0.55 Å^{-1}) was observed. Further theoretical developments are in progress to account for this anomalous behaviour.

2. MATERIALS SCIENCE

2.1 Introduction

Materials Science aims to understand the properties of solid systems in their full complexity, and to optimize these properties by acting on the composition, atomic structure, and microstructure. This is a different approach to that of condensed matter physics, which focuses on model systems to study a given property or phenomenon. Obviously, materials science has an immediate bearing on industry and applications.
Neutrons are an ideal probe for studying the structure of materials, particularly because of their low absorption, which makes it possible to work on centimetre-thick parts, and the relative ease with which experiments can be carried out under complex or extreme conditions, such as high temperatures or applied stress.
Research currently under way at LLB includes studies on :

- Residual stress evaluation in complex systems,
- Evolution of textures with thermal or mechanical processing,
- Structure heterogeneity, precipitation, ageing of materials,
- Properties of coated glasses and gratings.

Studies on industrial materials are usefully complemented by studies of model materials that are easier to interprete. Methods for analysing the reciprocal lattice (neutron and X-ray scattering) and the real lattice (electron microscopy, atomic probe, near-field microscopy) are complementary, and always used together, especially for complex industrial materials.

2.2 Engineering - Residual stresses

(M. Ceretti, LLB; A. Lodini, University of Reims Champagne-Ardenne)

Residual stresses in materials have a considerable effect on material properties, including fatigue resistance, fracture toughness and strength. Neutron Strain Scanning provides a powerful non-destructive tool for stress analysis deep within a crystalline material. The principle of the technique is to use crystal lattice as an atomic strain gauge to measure strain distributions with a sub-millimetre spatial resolution. The stresses are thus calculated from the measured strains using elasticity laws. The main research activities developed in the last years at the LLB in this field can be summarised as follows:

- measurement of bulk stress in engineering components,
- understanding deformation processes in technological relevant materials,
- peak broadening analysis,
- development of a strain dedicated diffractometer, "DIANE" (G5.2) (in coll. With INFM, Italy).

Engineering activity at the LLB has strongly developed in the last two years. A large number of real industrial problems have been studied in collaboration with academic (see "Highlight" by M. Grosse et al) and industrial partners, or through European programmes (TRAINSS).

Among the principal industrial contracts we had last year, we mention the works carried out in collaboration with MAN Technologie AG (influence of thermal treatments on the residual stress evolution in ARIANE tank), with Aerospatiale (residual stresses in a welding between aluminium alloy plates for Airbus) and with SNECMA. The latter is described in more detail below.
New aeroengines design requires innovative materials offering high performances in term of lightness, stiffness and strength. At present SNECMA Moteurs studies the possibility to replace the traditional titanium alloy rotor bladed disc with Ti/SiC composite reinforced rotor bling (bladed ring), offering an improved strength-to-weight ratio. A prototype structure is shown in Fig. 4a. However, thermal residual stresses caused by the differences in thermal expansion coefficient between the two phases could have important consequences during the service life of the component. Neutron diffraction technique is the only tool to determine residual stresses non-destructively in depth. Moreover, as the technique is phase selective, it provides information for each phase of the composite separately. A set of experiments has been performed on the G52 strain diffractometer of the LLB, in order to analyse the stress evolution on a single component before (as fabricated) and after fatigue loading. For example, figure 4b reports the evolution of the phase stresses in the hoop direction for the as-fabricated bling. As it might be expected, large compressive hoop stresses are observed in the SiC fibres (-1000 MPa), together with lower tensile hoop stresses in the Ti alloy matrix (+500 MPa).

Figure 4a: The prototype Ti/SiC bling

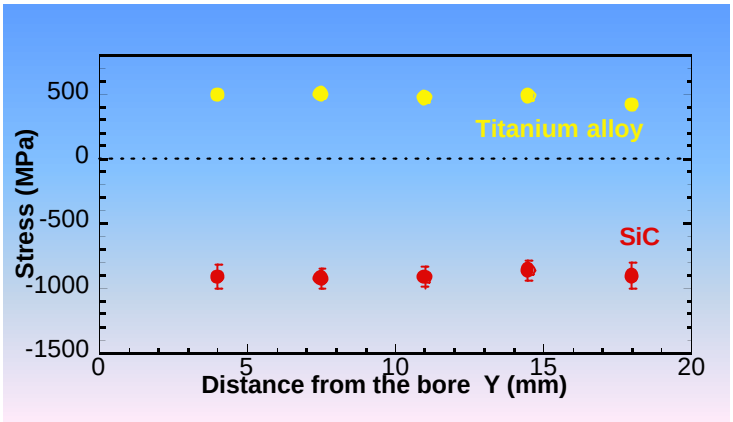

Figure 4b: Evolution of the hoop phase stresses as a function of the distance of the bore of the bling

In collaboration with the Czech team of Prague a spread activity on G52 is dedicated to peak broadening analysis to extract microstructural parameters from the measured profiles. The used approach includes both the influence of microstrain and size of coherently diffracting blocks as well as the instrumental resolution corrections. Modelling is performed in the reciprocal space and the microstrain contribution is treated according to the simple de Keijser's approach.
Recent studies in this field have been carried out to characterise stresses generated by shape memory alloy (P. Sittner, P. Lukas) and Nickel base superalloy (P. Lukas, J. Zrnik). In the latter case, the good instrumental resolution ($\Delta d/d \leq 2\text{x}10^{-3}$) of the G52 diffractometer allows to distinguish the two overlapping peaks from γ' and γ phases, obtaining information on microstrains in matrix and precipitates.

Experiments over the last years have shown a varied research programme with stress analysis in a variety of materials from metals to rocks.
In the field of geology, the residual elastic strains determination by neutron diffraction has been performed on quartzite samples from a former texture study. The measured complete residual strain tensor has been considered as representative of the "natural" finite plastic deformation. Such tensors fitted to plastic tensors have been introduced in texture modeling, based on a self-consistent model. A good agreement between the experimental and the simulated results has been observed. This work was done in collaboration with the University of Cergy Pontoise and the LMS of Orsay University.

TRAINSS is a 4-year (1998-2001) european network, of the Brite-Euram III programme, involving neutron sources, Universities and industrials, aimed to train european industrial laboratories to the use of neutron

diffraction for determination of internal stresses. Two weeks per year of neutron beam time on the DIANE diffractometer are devoted to this programme to study specific problems brought by industrials, in our case SNCF and PSA-Peugeot-Citroen. The PSA problem is the determination of residual stresses in the discs of motor-car brakes, in order to define quality control criteria and to optimize the lifetime of the disks. SNCF is interested in the influence of residual stresses on the propagation of cracks in the wheel axles of railway engines and carriages sollicitated by oligocyclic fatigue in rotative flexion.

VAMAS TWA 20 is an international programme, the aim of which is to establish accurate and reliable procedures for making reproducible and standardized non-destructive neutron diffraction residual stress measurements. It includes representatives from industry, universities and 13 worldwide neutron sources. Different types of samples, in which residual stresses have been introduced by various procedures, are examined, according to a common protocol ("round-robin" testing). LLB has contributed significantly to this programme in the case of surface treatments (nickel alloy peened sample); the application of a software developed in collaboration with ENSAM, allowed to correct the systematic errors induced by close-surface effects, and to evaluate correctly the residual stresses as close as 25 μm from the surface.
The VAMAS programme is now finished; it will be followed by an European network entitled CEN/TC 138/AHG 7 : "NDT (Non Destructive Testing) - Residual stress measurement by neutron diffraction".

2.3 Textures
(M.H. Mathon, V. Branger, LLB; A. Baudin, A.L. Etter, LPCES, Orsay University)

Crystallographic texture (preferred orientation of grains) is one of the parameters describing the microstructure of a polycrystalline material. In metallic alloys, the texture appears during the solidification, then transforms during rolling or wiredrawing, and ultimately during recrystallization. The understanding and the mastering of its texture during thermomechanical and/or annealing treatments are necessary in order to optimise the mechanical behaviour of a material.
Neutron diffraction is the best technique for obtaining precise texture of bulk specimens (≈ 1 cm^3), under the form of a distribution function of crystalline orientations. Its use is in particular necessary in the case of coarse-grained materials (~ a few mm^3), where conventional X-rays are inapplicable.
LLB has a diffractometer specially devoted to the determination of crystallographic textures : 6Tl, equipped with an Euler cradle.
These last years, an important part of the texture activity has been dedicated to the study of recrystallization phenomena and to the evaluation of the stored energy. Indeed, during cold-work of a metal, a small fraction of the energy of deformation is stored in the crystal in the form of the elastic energy associated with the strain field of the generated dislocations. Grains of different crystallographic orientations are expected to store different amounts of energy during deformation. Since the stored energy is the driving force for recrystallization, its orientation dependence can influence the development of recrystallization texture components. The neutron peak broadening method was developed at the LLB to evaluate the stored energy as a function of the crystallographic orientations and it was applied to the FeNi alloys study.

The Fe53%-Ni alloy is widely used as soft magnetic sheet material. After high reduction (80%), this alloy exhibits copper-type cold-rolled texture with three main components : {110}<112> (B), {123}<634> (S) and {112}<111> (C). During recrystallization, a sharp cube texture {100}<001> appears, which is the case for fcc metals and alloys with medium or high stacking fault energy. On the other hand, for weaker cold-rolling, the recrystallization texture is similar to the rolling texture. The reason of this different behaviour is not clearly understood.
To study the kinetics of the recrystallization, we have performed “in-situ” isothermal texture measurements at the Risoe National Laboratory (Denmark) on the TAS3-TXTU spectrometer, equipped with a dedicated furnace. Figure 5a shows the kinetics evolution of S, B, C and cube components versus annealing time at 580°C. This reveals that the incubation time and the kinetics of the cube component development and of the deformation components disappearance are identical. These two phenomena seem to occur simultaneously, which proves that the recrystallization mechanism is not governed by oriented growth. Furthermore, the activation energy of the process involved during recrystallization, deduced from the evolution of the cube component (figure 5b), is equal to 2.5 eV, which is compatible with self-diffusion of fcc iron.

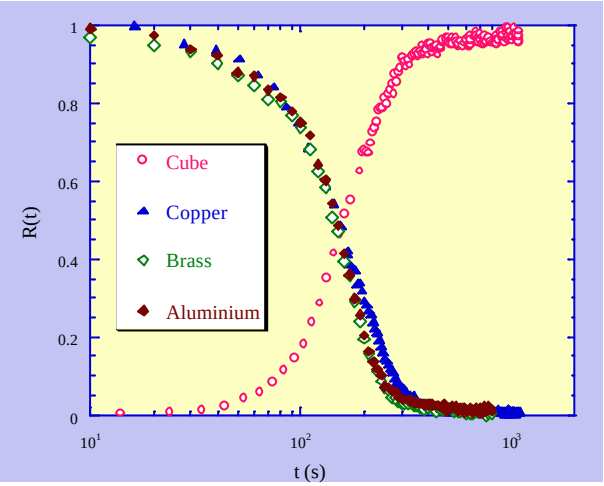

Figure 5a : S, B, C and cube components through the reaction advancement factor R(t) (defined by (I(t)-I(0))/ (I(∝)-I(0)) with I the diffracted intensity), versus time during annealing at 580°C.

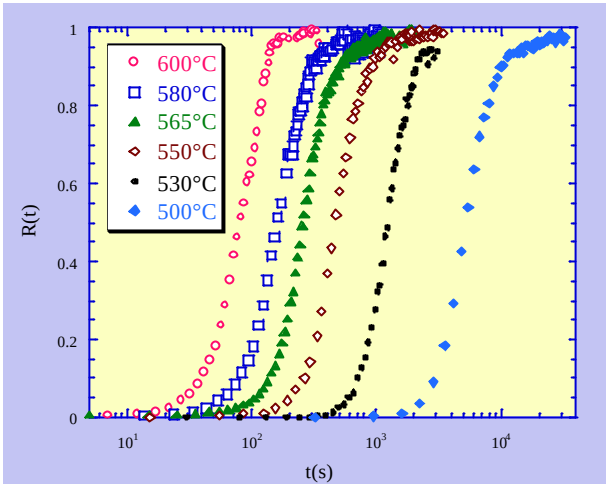

Figure 5b: Cube component formation, through the reaction advancement factor R(t), versus time for annealing temperatures between 500°C and 600°C.

To improve our understanding of the complex recrystallization mechanisms, the influence of the cold-rolled reduction on the stored energy was also studied. Low energy values are found for Cube grains present in a weak volume fraction after deformation whatever the reduction rate, and the energy gap between the Cube and the other texture components increases with reduction, promoting the Cube growth during recrystallization. For low reduction, no energy gap is observed and all orientations can grow simultaneously.

Furthermore, other fundamental and industrial studies have been performed at the LLB.

- A fundamental study of the deformation and recrystallization in a 50-50 austeno-ferritic steel has been undertaken in collaboration with the LPCES and the Institute of Metallurgy and Materials Science of Krakow (J. Jura). A surprising result is that the crystallographic texture of the b.c.c. α phase decreases, whereas that of the f.c.c. γ phase increases, with the deformation.
- A study of the relationships between the texture variation occurring during $\beta \rightarrow \alpha+\beta$ transformation and the microstructure has been performed on the high strength titanium alloy "βCEZ" developed for medium temperature compressor discs applications. This study has shown that whatever the microstructure, the texture components do not vary, but that their sharpness is sensitive to the morphology of the α phase. They were found to be insensitive to the intermediate ω phases, formed eventually during the precipitation sequence.
- Deformed quartz-rich rocks, which are rather ubiquitous in the upper part of the earth crust, show a wide range of microstructures and directional arrangements of the grains, producing a texture. Both the microstructures and crystallographic textures store informations about the deformation history of the host rock, which has recorded a complex strain path during its evolution, and therefore were used to supplement the macroscopic features of the deformation in rocks for the assessment of their kinematics. From samples collected in the Betic Cordillera (southern Spain), two principal components of the texture $\{\bar{1}2\bar{1}0\}<\bar{1}010>$ and $\{\bar{1}10\bar{1}\}<\bar{1}\bar{1}20>$ have been clearly identified and linked with specific proportions of grains considered respectively deformed and recrystallized. This work will now be completed by the study of annealed samples.

2.4. Nanomaterials prepared by mechanical alloying

(PhD thesis of S. Galdeano, coll. between M.H. Mathon, C.H. de Novion, LLB; L. Chaffron, CEA/SRMP; E. Vincent, CEA/SPEC; A. Traverse, LURE)

Mechanical alloying allows the synthesis of nanostructured materials, difficult or impossible to produce by classical routes, such as the $Cu_{80}(Fe_{0.3}Co_{0.7})_{20}$ compound which is constituted of a nanocrystalline Cu matrix in which are dispersed small $Fe_{0.3}Co_{0.7}$ clusters. The aim of this study is to precise the role of the milling

conditions on the nanostructure and on the spatial distribution of the magnetic atoms (Fe and Co), which influence the GMR properties of the material.
Batches of this ternary compound were produced by mechanical alloying elemental powders in a two-stage procedure involving first the preparation of binary $Cu_{88}Fe_{12}$ and $Cu_{72}Co_{28}$ f.c.c. metastable supersaturated solid solutions. At each stage of the preparation, the samples were characterised by X-ray and neutron powder diffraction, by SANS, by magnetic measurements, and by EXAFS.
These complementary techniques proved that in the ternary compound, the majority (60%) of the Fe and Co atoms are in form of superparamagnetic particles, either rich in Fe or mixed (Co+Fe). The rest is in a spin-glass type Cu-rich f.c.c. solid solution. The increase of the milling temperature (from 30 to 200°C) was shown to have important effects on the as-milled state : in particular the size of the magnetic clusters increases, and their internal structure changes from coherent f.c.c. to incoherent b.c.c. Fe-Co precipitates.
Further post-milling annealings, performed at 500°C, allow to enhance the precipitation of the magnetic particles. Even after a short annealing time (15 minutes), most of the superparamagnetic particles became ferromagnetic with a stoichiometry close to $Fe_{0.3}Co_{0.7}$. The increase of the milling temperature was clearly shown to slow down the post-milling precipitation kinetics, which is due to the change of the distribution of the superparamagnetic population (nuclei of the Fe-Co precipitates) with the milling conditions.

2.5. Structural stability of nuclear materials under thermal ageing or neutron irradiation

(M.H. Mathon, C.H. de Novion, LLB; Y. de Carlan, A. Alamo, CEA/SRMA; G. Geoffroy, B. Beuneu, A. Barbu, LSI, CEA/Ecole Polytechnique)

Since 1996, a research program is developed in the CEA on Low Activation Materials for nuclear applications. In order to characterise the microstructural evolution of martensitic steels under neutron irradiation (at 325°C up to a dose of 0.9 dpa), or after long thermal ageing (between 250°C and 550°C up to 22 000 hours), SANS experiments were coupled with Transmission Electron Microscopy (TEM) observations. They showed that above 8.8 at.% Cr in solid solution, the ferritic matrix is unstable at an ageing temperature of 400°C and separates into two b.c.c. phases, a Cr-depleted (α) and a Cr-rich (α'); moreover, a strong radiation-accelerated or induced α' precipitation is observed in alloys irradiated at 325°C. Finally, the precipitation of Laves phase $Fe_2(Mo,W)$ is strongly dependent on the Mo and W contents in the alloys.
Recently, SANS experiments allowed to check that the size and composition of oxide nanoparticles in different ODS (Oxide Dispersion Strengthened) steels, are stable after thermal treatments, which is a prerequisite for their selection as advanced fuel cladding for nuclear reactors.

2.6. Thin films and multilayers

(A. Menelle, F. Ott, P. Humbert (PhD), LLB, in coll. with C. Fermon, CEA/SPEC)

The major use of neutron reflectivity is in the field of magnetism (with polarised neutrons) and in soft matter. For non-magnetic and non-organic materials, X-ray reflectometry is the usual technique. Nevertheless, neutrons are useful in specific cases of poor X-ray contrast : e.g. layers of silicon oxide on silicon, or thin films containing titanium, which has a negative scattering length for neutrons.
This is the case of SiO_y/TiO_x bilayers deposited on glass. Neutron reflectivity performed with Stazione Sperimentale del Vetro (Murano, Italy) provides better information than spectrophotometry and RBS on thickness, roughness and composition. The results have been used directly to calculate and optimise solar light and heat transmission properties of the coated glass.
The long lasting collaboration with Société CILAS on the development of Ti-Ni supermirrors is now going on through a more commercial basis. All technological research necessary before the product release in the market has been done. Now neutron reflectivity is used directly to check that the supermirrors produced by the company meets the specifications of the client.
More specialised are the efforts put in the study of non-specular reflectivity of periodic gratings. By comparison with experiments, we have validated a new program of non-specular intensity calculation. This opens the use of large gratings in instrumentation as a wavelength analysis device.
Another work on instrumentation has been our first surface diffraction experiment performed on the EROS reflectometer in order to demonstrate the efficiency of the new white beam method. It enables a fast and reliable alignment process, while the final diffraction measurements are performed using the usual time-of-flight method. Our main interest being in magnetic surface diffraction, the next experiment will be done using a polarised beam.

DISPERSION FORCES IN SIMPLE FLUIDS PROBED BY NEUTRON DIFFRACTION

U. Bafile[1], F. Barocchi[2], F. Formisano[3], E. Guarini[4], R. Magli[5]

[1] Istituto di Elettronica Quantistica del CNR and INFM Unità di Ricerca di Firenze, Italy
[2] Dipartimento di Fisica di Firenze and INFM Unità di Ricerca di Firenze, Italy
[3] Istituto Nazionale per la Fisica della Materia Operative Group Grenoble, France
[4] Istituto Nazionale per la Fisica della Materia Unità di Ricerca di Firenze, Italy
[5] Dipartimento di Chimica e Biochimica Medica di Milano and INFM Unità di Ricerca di Firenze, Italy

Dispersion forces, acting among the instantaneous electric multipoles arising in each atom of a simple fluid, provide an important contribution to the interaction law $V=V(\boldsymbol{r}_1, \ldots, \boldsymbol{r}_N)$ and represent, in non-polar insulating fluids, the leading term of its long-range tail. Despite the fundamental physical relevance of V, very few (if any) experimental studies of its asymptotic behaviour have been reported in literature until the early nineties. Consequently, this part of V is usually determined using semi-empirical methods which partly rely on experimental data (as polarizabilities, photoabsorption spectra, etc.), while they are heavily based on theoretical calculations [1].

Only quite recently, by taking advantage of the neutron scattering instrumentation and data analysis techniques presently available, it has been experimentally demonstrated that the information contained in the static structure factor $S(k)$ can be profitably used to investigate V and in particular its long-range features. It is worth noting that the search for experimental techniques able to access the asymptotic part of the interaction potential can be of general help, not only to duly verify the computational results and to experimentally constrain the proposed potential models, but also to develop methods of measurement of these fundamental properties in less known or more complicated (e.g., mixtures, conducting fluids, etc.) systems.

In the last decade our group performed a set of experiments on rare gas fluids by means of the Small Angle Neutron Scattering (SANS) diffractometer PAXE (Laboratoire Léon Brillouin, Saclay, France).We shall briefly review some of the results obtained.

For the classical systems considered in the following, we will assume that V can be written as:

$$V(\boldsymbol{r}_1, \ldots, \boldsymbol{r}_N) = \mathrm{S}_{i<j}\, V_2(r_{ij}) + \mathrm{S}_{i<j<k}\, V_3(\boldsymbol{r}_i, \boldsymbol{r}_j, \boldsymbol{r}_k) + \ldots,$$

$$r_{ij} = |\boldsymbol{r}_i - \boldsymbol{r}_j| \qquad (1)$$

where $\boldsymbol{r}_i$ represents the position of the i-th atom. In non-polar insulating fluids, the leading contributions to the long-range part of the pair and triplet interactions are, respectively, the dipole-dipole interaction [2] :

$$V_2(r) \sim - C_6 / r^6 \qquad (2)$$

and the triple-dipole one [3] :

$$V_3(\boldsymbol{r}_1, \boldsymbol{r}_2, \boldsymbol{r}_3) \sim ?_{\mathrm{AT}} [1+3cos?_1\, cos?_2\, cos?_3] / [r_{12}\, r_{23}\, r_{13}]^3 \qquad (3)$$

where r_{12}, r_{23} and r_{13} represent the sides of the triangle formed by three atoms located at $\boldsymbol{r}_1$, $\boldsymbol{r}_2$ and $\boldsymbol{r}_3$, and $?_1$, $?_2$ and $?_3$ are the internal angles of that triangle. For several reasons it is convenient to interpret the results in terms of the direct correlation function $c(r)$ introduced by Ornstein and Zernike in 1914, whose Fourier transform $c(k)$ is connected to the experimentally accessible $S(k)$ via :

$$c(k) = [S(k) - 1] / (n\, S(k)) \qquad (4)$$

where n is the number density of the system. Several methods exist for the interpretation of structural data in terms of microscopic forces and they have been applied in various studies [see, for example, Refs. 4, 5 and references therein quoted]. Two examples are here reported.

For classical insulating fluids, the main result of the theory which relates in an analytical way the long-range behaviour of the pair potential to the features of $c(k)$ at small k-values, can be summarized saying that $c(k)$ is expected to have, at small k, a $|k^3|$ term directly connected to the strength of the long-range Van der Waals interaction. In formulæ, if Eqs.(2) and (3) are assumed to correctly model V_2 and V_3 at long distance, then for k ? 0 :

$$c(k) \sim c(0) + ?_2 k^2 + ?_3 k^3 + O(k^3) \qquad (5)$$

with :

$$?_3 = p^2 ß [C_6 - 8 p n ?_{AT} / 3] / 12 \qquad (6)$$

where $ß = 1 / k_B T$. A density dependence of the k^3 term in the low-k expansion of $c(k)$ provides a direct way of measuring both the dipolar coefficient C_6 and the strength $?_{AT}$ of the triple dipole interaction and represents a clear-cut evidence of three-body effects. Fig. 1 reports the quantity $?_3/ß$ as a function of the density for krypton (for comparison, the density of krypton at critical point is 6.55 nm^{-3}) as measured in a set of experiments performed on PAXE [6]. It turns out that, if low-k structural investigations are performed in a wide density range, from the dilute gas case up to densities close to that of the triple point, a significant density dependence of $?_3$ can be detected, thus obtaining $C_6 = (12.5 \pm 0.6)\ 10^{-78}$ J m^6 and $?_{AT} = (2.3 \pm 1.6)\ 10^{-107}$ J m^9, in agreement with the semi-empirical estimates present in literature. It is worth noting that this determination of $?_{AT}$, though affected by a large uncertainty, is independent of any assumed model for the pair interaction. More accurate results for $?_{AT}$ can be obtained with other methods, as it has been done for example in [5, 7].

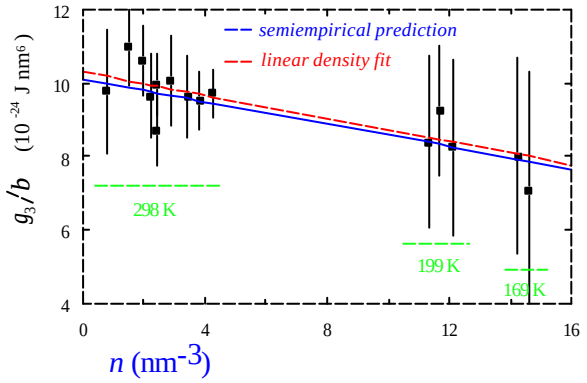

Figure 1. Cubic term $?_3$ in the measured $c(k)$, times $k_B T$, as a function of the density (squares with error bars) for Kr. The solid line represents the theoretical prediction, as calculated from eq. (6) using the averages of the semiempirical estimates for C_6 and $?$ found in the literature. The dashed line is the least-squares fit to all the experimental $?_3 / ß$ values with the model function $A + B n$.

Further knowledge of the microscopic interaction law can be gained comparing the k-dependence of experimental structural quantities with theoretical predictions of reliable liquid state theories, based on different model potentials. In Fig. 2 the experimental density derivatives of $H(k) = [S(k)-1]/n$ are reported for Kr at 169 and 199 K. They are compared with theoretical results obtained using the MHNC and the SC-HRT theories [see Ref. 8 for details] and three interaction models: a pure two-body (AS, [9]), a two-body plus a usual Axilrod-Teller contribution (AS+AT), and a two-body plus the three-body modification of AT ($AS+AT_{eff}$) required for a good theoretical description of critical-point thermodynamic data [8]. It is seen that deviations of the pure two-body model from the neutron data reach even 100%, while the use of AT and AT_{eff} models greatly improves the agreement. In conclusion, this comparison proved the major role of three-body forces in determining the structure of a simple liquid for k values smaller than the position of the first minimum of $S(k)$, and provided also a convincing evidence of the presence of additional many-body contributions beyond the long-range triple-dipole AT interaction.

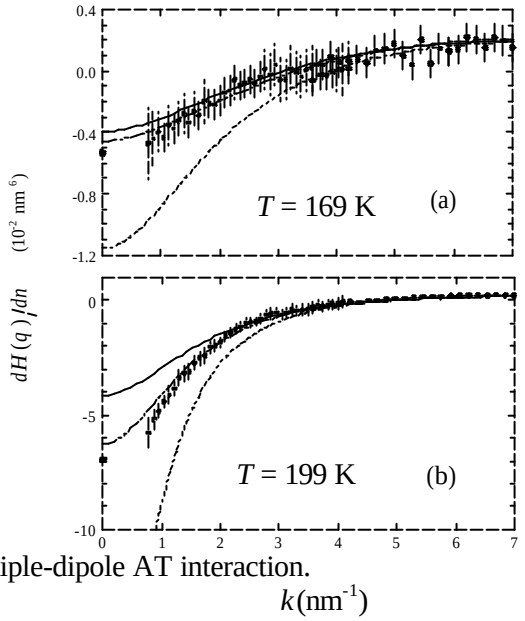

Figure 2. Experimental density derivative of $H(k)$ (dots with error bars) of liquid Kr. Data at higher k-values (open circles) are from Ref. [10]. The SC-HRT prediction based on the Ref. [9] V_2 pair potential plus $(\text{Axilrod-Teller})_{\text{eff}}$ interaction (dash-dotted curve) is shown, together with the MHNC results based on the V_2 (dashed curve) and on the V_2 plus (Axilrod-Teller) interaction (solid curve). Full squares at k=0 are the thermodynamic limits. (a) $dH(k)/dn$ at T=169 K and n=14.40 nm^{-3}. (b) $dH(k)/dn$ at T=199 K and n=11.66 nm^{-3}. The derivative from the data of Ref.[10] is at the slightly different density n=11.57 nm^{-3}.

[1] G. C. Maitland, M. Rigby, E. B. Smith and W. A. Wakeham (1981) *Intermolecular Forces. Their Origin and Determination*, Clarendon Press, Oxford.

[2] F. London, *Z. Phys. Chem. B*, **11**, 222 (1930).

[3] R. M. Axilrod and E. Teller, *J. Chem. Phys*., **11**, 299 (1943).
[4] F. Barocchi, U. Bafile and R. Magli, *J. Phys.: Condens. Matter*, **8**, 9111 (1996).
[5] E. Guarini, G. Casanova, U. Bafile and F. Barocchi, *Phys. Rev. E*, **60**, 6682 (1999).
[6] E. Guarini, G. Casanova, U. Bafile, F. Formisano, R. Magli and F. Barocchi, *Europhys. Lett*., **49**, 62 (2000).
[7] C. J. Benmore, F. Formisano, R. Magli, U. Bafile, P. Verkerk, P. A. Egelstaff and F. Barocchi, *J. Phys.: Condens. Matter*, **11**, 3091 (1999).
[8] E. Guarini, R. Magli, M. Tau, F. Barocchi, G. Casanova and L. Reatto, *Phys. Rev. E*, **63**, 52201-1 (2001).
[9] R. A. Aziz and M. J. Slaman, *Mol. Phys.*, **58**, 679 (1986).
[10] F. Barocchi, P. Chieux, R. Magli, L. Reatto and M. Tau, *Phys. Rev. Lett.* **75**, 1779 (1995)

NEUTRON SCATTERING STUDY OF SULPHUR-TELLURIUM LIQUID ALLOYS : STRUCTURAL EVIDENCE FOR A CLOSED LOOP MISCIBILITY GAP.

M.-V. Coulet [a], R. Céolin [b], R. Bellissent [c] and C. Bichara [d]

[a] Laboratoire TECSEN, Université Aix-Marseille 3, 13397 Marseille cedex 20, France
[b] Faculté de Pharmacie, 4 av de l'Observatoire, 75006 Paris, France
[c] CENG, 22 av. des Martyrs, 38000 Grenoble, France
[d] CRMC2, Université Aix-Marseille 2, Campus de Luminy ,13288 Marseille cedex 9, France

The homogeneity of liquids at various length scales is a challenging question specially as far as liquid metals are concerned. In order to contribute to these kind of studies, we focused on the homogeneity of sulphur-tellurium liquid alloys. Pure tellurium is a twofold coordinated semiconductor in the solid state, and undergoes a transition to a metallic state upon melting. As shown by many neutron and x-rays experiments [1,2] as well as computer simulations [3], this transition is characterised by an increase of the number of first neighbours up to three in the liquid state when increasing the temperature. On the contrary, liquid sulphur remains essentially twofold coordinated and insulating [4]. When alloying these two elements, a closed loop miscibility gap is reported to appear in the liquid state [5]. This phase separation, a unique feature in a binary inorganic system, is assumed to occur in a very narrow temperature and concentration range around 40% at. sulphur and 700°C.

In previous works, we studied the local order of sulphur-tellurium melts by neutron scattering in a broad range of concentration and temperature. The results combined with a modelling of the structure factors allow to determine the evolution of the partial coordination numbers [6,7]. We could explain some of the mechanisms responsible of the phase separation : neglecting chain breaking effects, at 700°C, pure liquid tellurium is a mixture of 2- and 3- fold coordinated atoms. Adding sulphur reveals a phase separation between two phases with different coordination numbers. In order to explicit the link between structure and thermodynamics, we developed a regular solution model with multiple connectivity [8]. Using the measured coordination number, we could deduce the thermodynamic quantities of mixing in the melt. The mixing enthalpy displays a change in concavity when increasing the temperature, characteristic of the presence of two phases in equilibrium. Howsoever consistent with a tendency to phase separation, this previous work does not provide a direct experimental proof of the closed loop miscibility gap.

Two kinds of experiments are reported here that try to give a structural evidence of the phase separation. First, small angle experiments were performed in order to reach gain a knowledge of the structure at large scale. Then, owing to the success of previous experiments, a first attempt in the determination of the local order of the two phases in equilibrium is reported.

Small angle scattering experiments were performed on PACE spectrometer. The wavelength was fixed to 5Å and the momentum transfer range was from 0.02 to 0.2 $Å^{-1}$. The experiments were realised at the concentration of the miscibility gap (40% at. S), the temperature range between 450°C (temperature of the liquidus) and 688°C. The high vapour pressure of sulphur turned out to be the critical parameter of the experiment : the highest temperature that could be reached was measured as 688°C, just below the reported lower critical temperature of the closed loop miscibility gap.

Figure 1 shows the small angle intensities obtained after usual data corrections. Up to 600°C, the signal is flat on the whole q range, which is characteristic of a homogeneous liquid. Above this temperature, the small angle intensities are increasing at low q values, showing

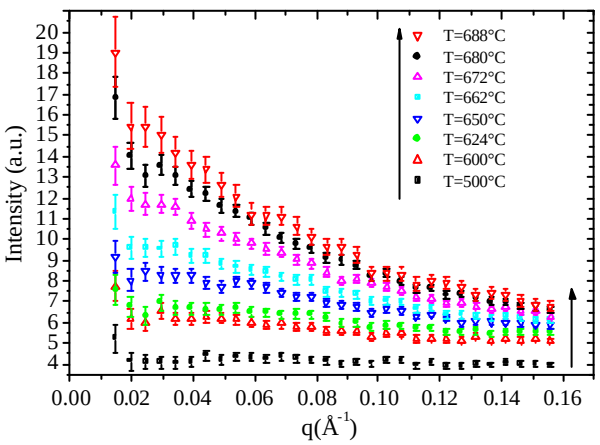

Figure 1 : Small angle scattered intensity versus q at various temperatures.

that the melt becomes inhomogeneous. In order to quantify the concentration fluctuations that develop in the liquid, an Ornstein-Zernike formalism was used. It consists in writing the intensity I(q) as a function depending on q^2 and ξ, where ξ is the correlation length of the concentration fluctuations. We showed that the correlation length reaches a maximum value of 16Å in the temperature range that could be analysed [7].

Then, using a new experimental device (rotating furnace and diaphragm) developed on the 7C2 spectrometer, local order measurements of the two phases in equilibrium were performed. The sample consists in cylindrical quartz tube filled by powder of sulphur and tellurium at the desired concentration (40 % at. S) and is set-up vertically in the furnace. On the one hand, the rotating furnace allows *in situ* "shaking" of the sample and thus ensures the homogeneity of the melt. On the other hand, the automatically driven diaphragm enables one to measure separately the lower and the upper part of the sample which correspond respectively to the denser and the less dense phase in equilibrium.

The sample was slowly molten until 450°C and homogenised by turning the furnace upside down. For each temperature the top and bottom parts of the sample were analysed in turn during the same experiment. The time evolution of the signal was checked by alternating small counting sequences on top and bottom parts.

Figure 2 shows the structure factors measured in the two parts of the tube at various temperatures. At a temperature below the miscibility gap (fig.2a), as shown by the difference plot, the two structure factors are the same within the statistical accuracy.

At 720°C (fig.2b), differences appear between the two spectra. They are predominant at low q values : in the upper part of the tube, the structure factor presents a shoulder around 1.5 $Å^{-1}$, and the first peak around 2$Å^{-1}$ is lower than the second. These features are characteristic of a sulphur rich phase as shown by our previous works [6]. If we look at the difference spectrum we can observe oscillations until 8$Å^{-1}$, the statistics being not sufficient to observe them at higher q values.

At even higher temperature (780°C), the two structure factors became the same again (fig.2c). Owing to entropy effects, the system is homogeneous again.

Although small, a difference is observed at 720°C between the structure factors measured in the top and bottom parts of the tube. Combined to the

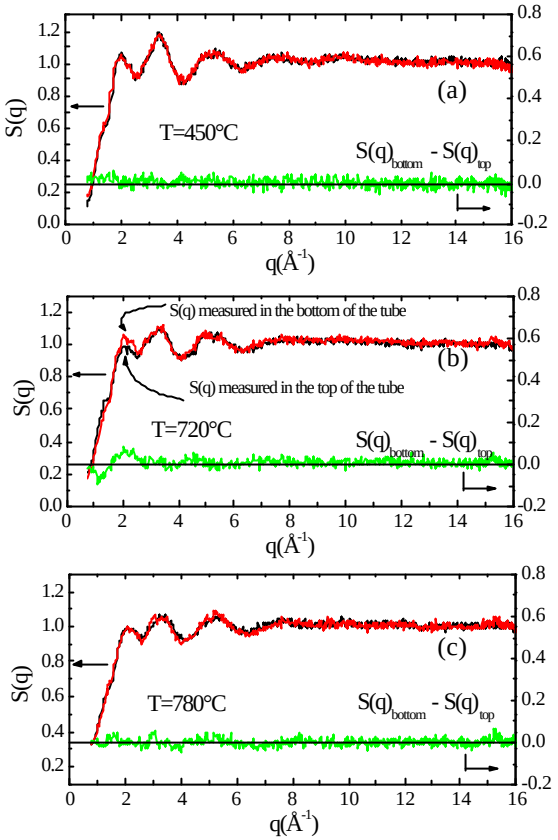

Figure 2 : Structure factors measured in the lower (red) and upper (black) part of the tube for various temperature. In green is represented the difference between the two.spectra.

small angle scattering measurements, this work gives a direct structural proof of the existence of this closed loop miscibility gap. Concerning the mechanisms at the origin of this phenomenon, local order measurements together with a thermodynamic modelling allowed us to conclude [7] that structural changes undergone by the tellurium rich liquid when the temperature is increased are responsible of the miscibility gap.

[1] A. Menelle, R. Bellissent and A. Flank, Physica B 156-157 (1989) 174
[2] S. De Panfilis and A. Filipponi, Europhys. Lett. 37 (1997) 397
[3] R. Bellissent, L. Descotes, F. Boué and P. Pfeuty, Phys. Rev. B 41 (1990) 2135
[4] C. Bichara, J.-Y. Raty and J.-P. Gaspard, Phys. Rev. B 53 (1996) 206
[5] Y. Tsuchiya, J. Phys. Condens. Matter 4 (1992) 4335
[6] M.-V. Coulet, R. Bellissent, M. Bionducci and C. Bichara, Europhys. Lett. 45 (1999) 175
[7] M.-V. Coulet, Thèse de Doctorat, Université de Provence , 1999
[8] H. Amzil, C. Bichara, M. Gilbert and J.-C. Mathieu, J. Phys. Condens. Matter 8 (1996) 5281

STRUCTURE OF GLASSFORMING LIQUIDS CONFINED IN MESOPOROUS MATERIALS

D. Morineau and C. Alba-Simionesco
Laboratoire de Chimie Physique
Bât. 349, Université de Paris-Sud, 91405 Orsay, cedex, France

Viscosity and structural (α)-relaxation times in supercooled liquids can vary over 14 orders of magnitude when changing temperature by a mere factor of 2 at atmospheric pressure leading to the glass formation. The dramatic increase of relaxation times and the manifestation of heterogeneous dynamics close to the calorimetric glass transition temperature T_g are most naturally interpreted as resulting from collective and cooperative behavior. Several experiments showing dynamical heterogeneity have been developed during the last decade (multidimensional NMR, dielectric hole burning, light scattering). They provide a new supermolecular length scale of few molecular diameters whose lifetime is somewhat larger than the α-relaxation time just above T_g. The possible existence of this mesoscopic characteristic length in deeply supercooled liquids has constantly won attention and the notions of cooperativity, correlation length, heterogeneities or domains have been introduced in many theoretical models[1]. However no structural indication of these clusters has been found so far[2].

When confined within a pore of a few molecular diameters the properties of a liquid are strongly modified. The cooperative length postulated above will not be able to extend to distances greater than the pore diameter thus leading to a different dynamical regime and then to indirect information on this length scale. Moreover changing the system size from a few molecular diameters to the macroscopic limit largely affects the phase diagram and the occurrence of long range ordered phases; as a consequence freezing can be avoided which may give rise to a glass transition at lower temperature for very simple model liquids that always crystallize in bulk conditions .

Most experiments have been performed with Controlled Porous Glasses (CPGs) or Vycor[3] as a confinement matrix. These mesoporous materials present a rather irregular porous geometry due to a broad distribution of size and shape of the interconnected cavities leading to a complex interplay of various effects. However recent advances in the synthesis of mesostructured porous silicates[4] of the MCM-41 series and SBA-15 offer a unique possibility to study confined phases in highly regular structure made of a hcp array of non-connected cylindrical pores (with 1.8 to 14 nm pores). Their structural parameters are obtained from nitrogen adsorption and neutron scattering. The structure factor of MCM-41 exhibit Bragg peaks at low Q due to the hcp structure. At higher Q, the structure factor of amorphous silica that formed the walls is restored as presented in Fig.1.

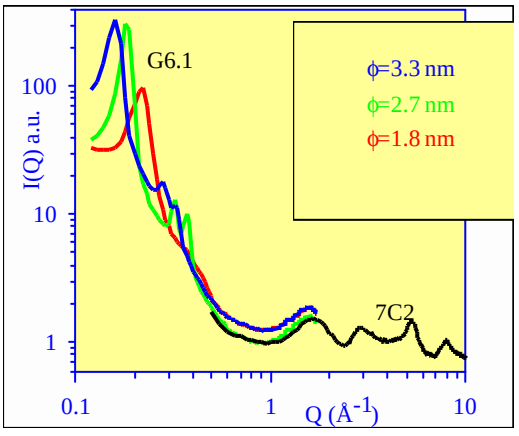

Figure 1 : Structure factor of empty MCM-41, over a wide Q-range, taking advantage of the two spectrometers G6.1 and 7C2 at the L.L.B

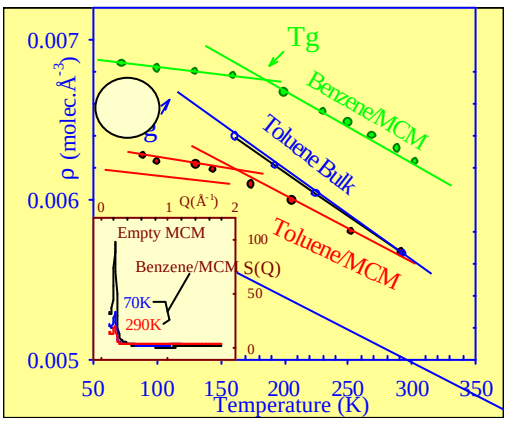

Figure 2 : Density of confined liquids estimated from contrast effects at the MCM-41 (100) Bragg peak (see insert)

Surprisingly the dynamical experiments of confined liquids performed so far do not give a clear answer as to the cooperative dynamics of supercooled liquids. It was not yet possible to distinguish between the influence of the fluid wall interaction and pure confinement effects on one hand, and, on the other hand, no thermodynamic and structural properties were available to describe properly the conditions (isochoric, isobaric,..) under which the glass is obtained and compared to the bulk system. In order to elucidate these points, we focus on weakly interacting model molecules (benzene and toluene) confined in monodisperse cylindrical pores.

The static structure factors of bulk and confined toluene and benzene in MCM-41 have been measured at the L.L.B. on the two double-axis spectrometers G6.1 and 7C2 encompassing an extended Q-range from 0.13 $Å^{-1}$ to 10 $Å^{-1}$ over a wide temperature range from the liquid at 290K down to the glass at 70K. The samples are prepared from a mixture of empty outgased MCM-41 with a proper amount of liquid in order to completely fill the pores. The density changes of the confined liquid can be controlled in an unique and consistent way by taking advantage of the regular hcp structure and from contrast effects considerations at the (100) Bragg peak of the matrix (Fig. 2). For the first time, we observe that the macroscopic density of a liquid in a small pore does not follow the density of the bulk, with a thermal expansivity of the half. This leads to much smaller value of the density of the glass obtained at a higher Tg than the bulk.

A complete discussion on the shape of the structure factor of bulk toluene is provided in [2]. Most of the possible changes of the intermolecular short range order may be illustrated by changes of the shape of the main diffraction peak in the Q range from 1 to 2 $Å^{-1}$. For the small pore size presented on Fig.3, confinement (and surface presumably) induces noticeable changes of the local order in the fluid, which is consistent with the density measurements. This affects the overall properties of the liquid such as dynamics giving rise to a toluene glassy state at lower density and higher temperature than the bulk. Its also affects possible crystallization of benzene. For the first time, it gives access to a description of the structure of benzene in the vitreous state.

The investigation of the heterogeneities of supercooled bulk liquid through confinement would hopefully benefit from the combination of highly regular novel mesopores and microscopic description of confinement effects.

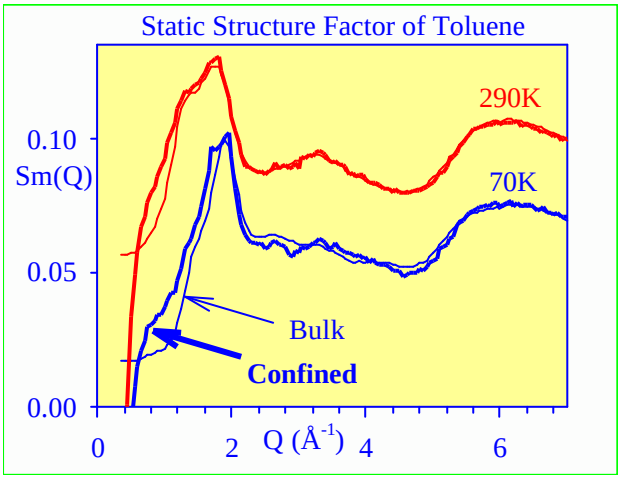

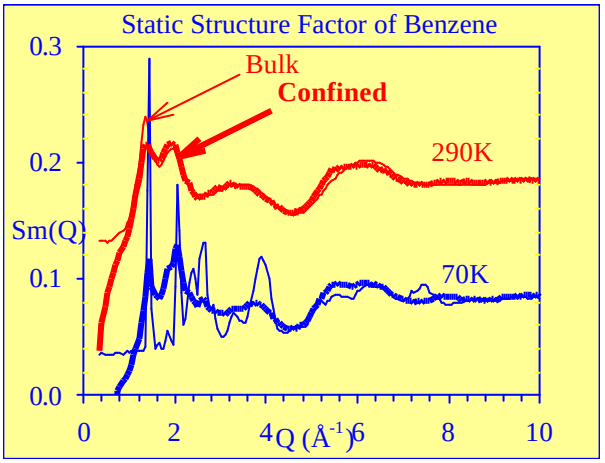

Figure 3 : Static Structure Factor of bulk liquid and confined liquid in MCM-41 with pore diameter ϕ=1.8nm, above their melting point (290K), and below their glass transition (70K) : (a) toluene, (b) benzene.

The authors are indebted to Drs M.-C. Bellissent-Funel and I. Mirebeau for their help and fruitful discussions, and thank J.-P. Ambroise for experimental assistance.

[1] see reviews : Sillescu H., J. of Non-Cryst. Solids, **243** (1999), 81; Alba-Simionesco C., C.R.Acad.Sci.Paris, **t.2**, Série IV, 203, 2001.
[2] Morineau D. and Alba-Simionesco C., *J. Chem. Phys.*, **109** (1998), 8494; Morineau D., Dosseh G., Pellenq R. J.-M., Bellissent-Funel M.-C., Alba-Simionesco C., Molec. Sim. **20**, 95 (1997).
[3] Bellisssent-Funel M.-C., Bosio L., Lal J., J.Chem.Phys. 98, 4246 (1993).
[4] Kresge, C.T.; Leonowicz, M.E.; Roth, W.J.; Vartuli, J.C.; Beck, J.S, *Nature*, **359**, 710-712 (1992), Zhao D., Feng J., Huo Q., Melosh N., Fredrickson G.H., Chmelka B.F. and Stucky G. D., *Science* **279**, 548 (1998).

DISTRIBUTION OF THE RADIAL STRAIN COMPONENT OVER THE CROSS SECTION OF A RAILWAY WHEEL

M. Grosse[1], U. Stuhr[1], M. Ceretti[2], L. Köszegi[3]

[1]Paul Scherrer Institut, CH-5232 Villigen PSI, Switzerland
[2]Laboratoire Leon Brillouin, CEA Saclay, F-91191 Gif sur Yvette, France
[3]SZFKI, KFKI, H-1121 Budapest, Hungary

Introduction

Recent railway disasters in Germany and other countries caused by material failure of wheels are showing that a better understanding of failure mechanism is needed. One limitation of the life-time of railway wheels is the accumulation of plastic strains and formation of micro-cracks due to cyclic loading. Residual stresses are the result of local micro-structural changes especially of local cold-work hardening. The locations of cold work hardening depend on the manufacturing engineering and are re-distributed by interaction between rail and wheels.

Object of the investigation

A 35° section of the hoop of a wheel with rubber suspension (type 064) was used for the investigation. Such wheels are applied in the German ICE high speed trains. The hoop under investigation run about 1.4×10^6 km without any detected damages. The usage level of this hoop is comparable with the usage of the hoop which was broken in the railway disaster of Eschede (Germany) in 1998. It is close to the projected end of live usage.

Strain scanning

Due to the radial load during service the radial strain direction gives sufficient information about local plastic deformations. The measurements were performed using the G5.2 diffractometer at the Orphée reactor (Saclay, France) with a wavelength $\lambda = 0.31$ nm. The measurement on a powder of the wheel hoop material confirms the expectation, that the theoretical lattice constant of pure iron (0.2866 nm) can be used as the strain-free reference state. A gauge volume of about 2mm (axial) × 3 mm (radial) × 10 mm (hoop) was achieved by slits of 2 mm (horizontal) × 10 mm (vertical) in the incident and diffracted beams.

Results and Discussion

Fig. 1 shows the distribution of the radial strain for radial cuts at different distances from the inner surface. Close to the tread, small tensile strains were found. These strains increase with increasing depth. At a depth of about 8mm,

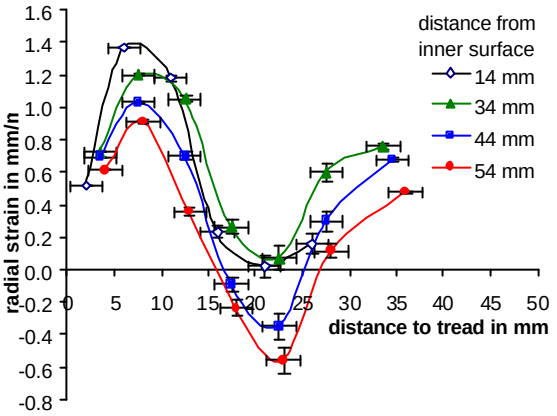

Figure 1. Measured radial strain as a function of depth

maximal tensile strain values exist. At deeper positions the strains decrease and reach minimum tensile strain or maximum compressive strain values in a depth of about 23 mm. At deeper positions, close to the opposite surface the strains increase again and reach values close to those at the tread. This distribution can be understood if local plastic deformation is taken into account. Hertz pressure shall reach maximum values at locations were maximal tensile strains are found [1]. A strain reversal after release of the pressure during contact between railway and wheel occurs. The plastic deformed regions are much more strained than the only elastic deformed ones. After release of the pressure, the elastic strain can not compensate the plastic deformation. In order to fit to the neighbour regions, an elastic strain with opposite sign is formed. The axial distribution of the radial strain is shown in Fig. 2

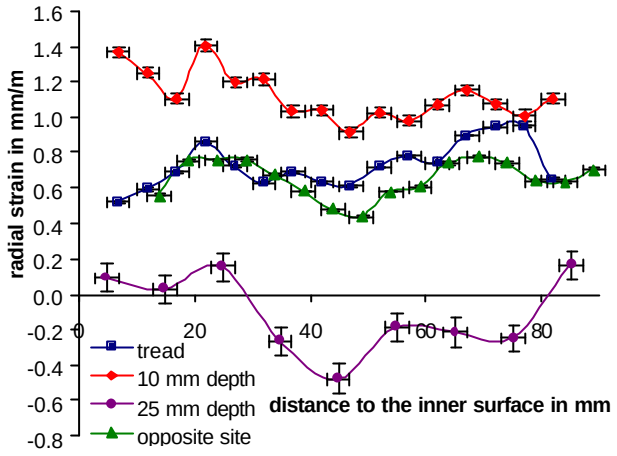

Figure 2. Axial distribution of the radial strain component

for different depths. A gradient in this direction occurs only in a depth where compressive strain was found in Fig. 1. Compressive strain was measured only below the middle of the tread. Fig. 3 shows the distribution of the radial strain over the hoop cross section. Compressive strain was found only in the middle part of the hoop cross section. In a band between a distance of 5 to 12 mm from the tread, relative large tensile strain was quantified. The other regions show only small strains. The fracture surface of a broken wheel hoop with comparable usage is shown in Fig. 4. A comparison with the strain in Fig. 3 shows correlations between strain distribution and fracture appearance. The crack starts at the surface opposite to the tread. At locations with compressive radial strain, the crack growth was stopped. The crack had to bypass this region. At the boundaries of this region, crack branching occurs. Close to the tread, where the highest radial strains were measured, rupture was observed.

Conclusions

Compressive strains were found only in the central part of the hoop cross-section. In a band between a distance of 5 to 12 mm from the tread, relative large tensile strain exist. In other regions, only low strains were obtained.

A comparison of the estimated strain distribution with the fracture surface of a broken hoop shows correlation between the strain distribution and the fracture appearance. The strain and stress distributions strongly influence the fracture process. This shows that the residual stress distribution formed during service has a high relevance for the fracture behaviour.

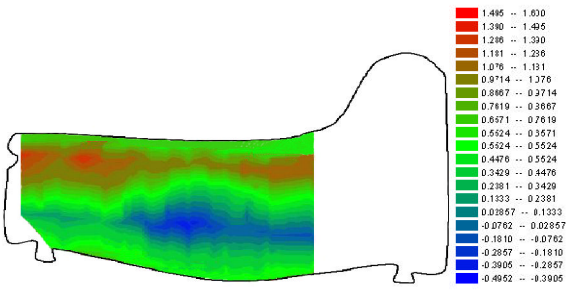

Figure 3. Distribution of radial strain in the hoop cross section.

Figure 4. Fracture surface of a broken railway wheel hoop.

[1] K.L.Johnson: "Contact mechanics", Cambridge University Press, (1985), ISBN 0 521 34796 3

HYDRATION KINETICS OF CEMENT PASTE FOLLOWED BY QUASI-ELASTIC NEUTRON SCATTERING

E. Fratini[1], P. Baglioni[1], S.-H. Chen[2], M.-C. Bellissent-Funel[3]

[1]Florence University, Italy, [2]M.I.T, Boston, USA, [3]LLB, Saclay

A key to improve the properties (strength and durability) of a cement material is to understand and control its hydration.

The major component of ordinary Portland cement is tricalcium silicate (Ca_3SiO_5 or "C_3S"). When water is added to C_3S, the hydration reaction generates calcium-silicate-hydrate ("CSH") and $Ca(OH)_2$ in a semi-crystalline-amorphous gel form surrounding colloidal cement particles. CSH is the main factor in the setting and hardening of the cement paste.

We have shown that the hydration kinetics of C_3S can be followed quantitatively by quasi-elastic neutron scattering (QENS). Indeed, the incoherent QENS cross-section is extremely sensitive to hydrogen, and therefore reveals as a unique technique to study the translational diffusion of water.

The studied samples consisted of a paste obtained by mixing pure crystalline C_3S powder with water (65% in weight). The effect of a retarder additive ("Dequest 1086") was also studied. QENS experiments were performed on the time-of-flight spectrometer MIBEMOL at LLB, at high energy resolution (28 μeV), and the quasi-elastic spectra were recorded each hour of the ageing process at 30 and at 15°C. Figure 1 shows the obtained spectra after ageing times ranging from 1 hour to 42 days at 30°C. The analysis of spectra has been realized using a dynamical model (see caption of Fig. 1), taking into account the existence of two types of water : "immobile water" (non detectable at the time-scale of Mibemol, 2 ps <t< 50 ps) which is bound inside the colloïdal cement particles, and "glassy water" which is incorporated in the gel region between the colloïdal particles (1). At one hour delay time, only a single quasi-elastic component was appreciated, which is attributed to glassy water rather than to free water. An additional elastic peak appears at larger delay times, and its amplitude gradually increases as the cement paste ages. **We interprete the drying process as a transformation from "glassy" to "immobile" water.** The fraction p of immobile water and the relaxation time of "glassy water" can be obtained as a function of ageing time of the cement paste.

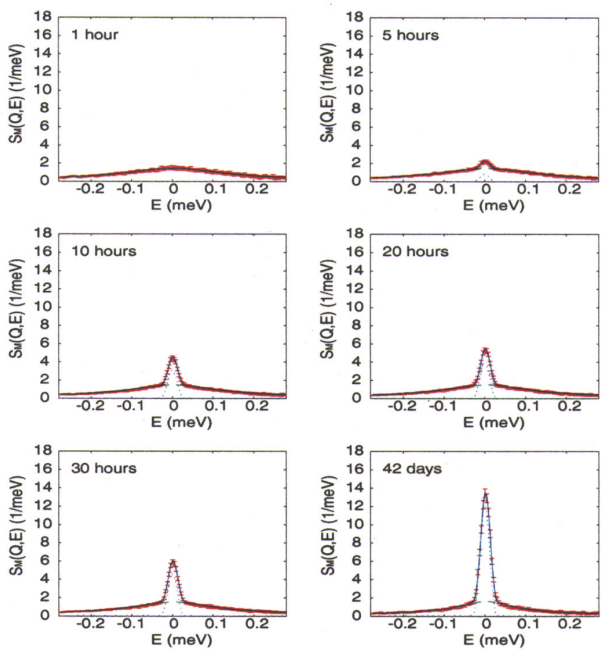

Figure 1. Time evolution of quasi-elastic incoherent neutron scattering spectra of a hydrated cement paste, for Q=1.04 $Å^{-1}$ and T=30°C. The data fitting is made with an elastic peak and the Fourier transform of a stretched exponential characterised by the relaxation time τ and the exponent β.

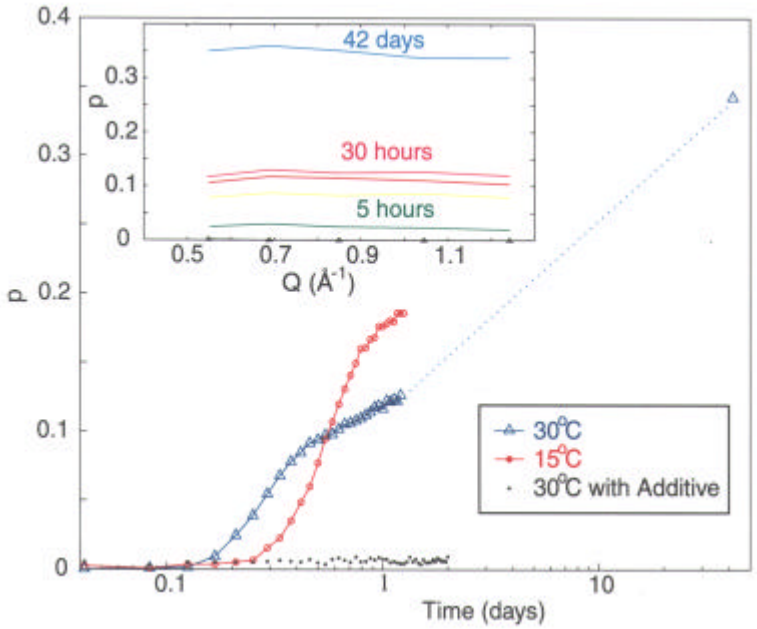

Figure 2. Time evolution of the fraction p of immobile water for different ageing conditions. The inset shows the dependence of p on magnitude of the scattering vector Q for different ageing times at 30°C.

From the evolution of p as a function of time (fig. 2), one could follow the kinetics of the hydration réaction. The dependence of p versus log(t) is in good agreement with a three-stage (induction, acceleration and diffusional periods) kinetic model reported in the literature (2).

The time evolution of the average relaxation time τ of water is depicted on figure 3. It clearly indicates a slowing down of the relaxation time of the "glassy" water as a function of age, which depends on temperature (4).

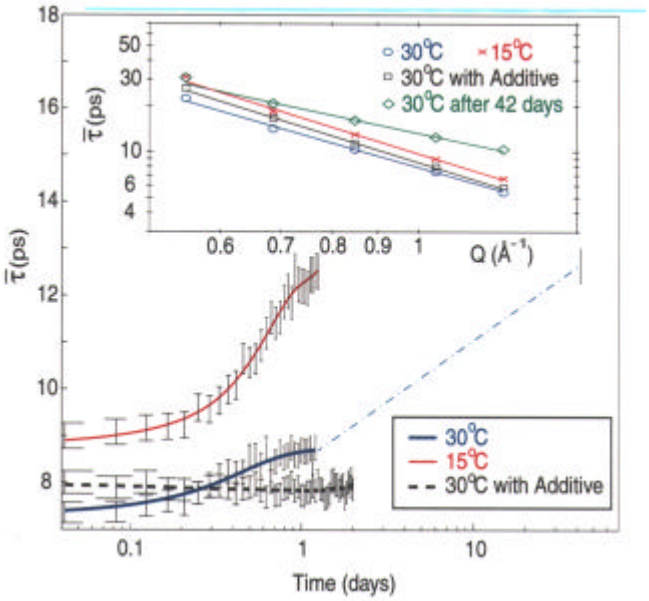

Figure 3. Time evolution of the average relaxation time of vitreous water, τ, obtained for Q=1.04 Å^{-1}. The inset shows that τ follows a power-law Q dependence characteristic of "glassy" or super-cooled water (3).

(1) Jennings, M. H. : *Cem. Conc. Res*. **30**, 101-116 (2000).
(2) Taylor, H.W.F. : *Cement Chemistry* (Academic Press, London, 1990)
(3) Bellissent-Funel, M.C., et al. : *Phys. Rev. Lett.* **85**, 3644-3647 (2000).
(4) Fratini, E., et al. : Phys. Rev. E **64**, (2001).

CHEMICAL PHYSICS

The research in the field of chemical physics at LLB involves mostly soft matter, studied by the Small Angle Neutron Scattering (SANS), Neutron Spin Echo (NSE) and Neutron Reflectivity (NR) techniques (with a strong weight on SANS at present), together with Static and Dynamic Light Scattering. The present chapter intends to summarize the work done by LLB researchers, either entirely inside the laboratory or in close collaboration, and covers the field of colloids from polymers to nanoparticles, including surfactants self-assembly. Besides, a considerable number (more than 100) of experiments in chemical physics are performed each year on the LLB spectrometers by external users (see for example the highlight "Structural properties of helical self-assembled polymers with hydrogen bonding" by *A. Ramzi et al., Eindhoven University*).

OVERVIEW

The basic systems are often **one component** systems, studied in **volume** by SANS :

Polymers (mostly) : Polyelectrolytes, Liquid crystalline polymers, New Polymers,

Vesicles,

Biological materials : Methyl Cellulose, large proteins (including denatured proteins).

But it is now a common trend in Soft Matter to study more complex systems, **with two or more components**, which can be observed separately due to the wide range of neutron scattering length densities (through deuteriation in particular). This is the case for two important axes : polymer systems mechanically reinforced by nanoparticle fillers, and vesicles with membranes stabilised by polymers, but also for rising themes, such as Polyelectrolytes with charged particles, like proteins. The Dynamic Light Scattering study of protein gels including of latex probes also involves such a mixed system.

In many of these bulk systems, LLB is interested in the **mechanical** or **rheological** properties : this has been the origin for several studies under deformation; **Rheo-SANS** has involved stretching for Liquid Crystalline Polymers and silica reinforced polymers, and shear flow for Liquid Crystalline Polymers, semi-dilute polymer solutions, copolymers, micellar phases and vesicles.

Leaving progressively the bulk case, some LLB researchers have been interested in systems of reduced dimensions such as **chains confined in porous media**, on one hand, and **thin films** on another hand.

Going further down to the two-dimensional case, SANS can be used to characterise interfaces in multi-component systems – as done formerly, and planned for nanocomposites, but in the last two years model systems have rather been studied using **neutron reflectivity**. This is the case for liquid – air interface of thermo-sensitive polymers : PNIPAM and Methyl Cellulose, and for solid-solid **interdiffusion profiles** between a polymer and a **polymer network**, in relation with their **adhesion.**

Studies at these large scales can obviously involve also **dynamics**. The use of **Neutron Spin Echo** to measure Inelastic Scattering has been dedicated to **dynamics of polymer stars**, while Inelastic Light Scattering has been used, at the LLB, for the studies of vesicles, and of **latex spheres in biological gels**.

Finally, work on **Instruments or Methods** is not forgotten. On one hand, a new Very Small Angle spectrometer is under development (*J. Oberdisse, D. Lairez*) : it is composed of a new 2D detector made of a neutron sensitive image plate developed in collaboration with MAR-Research, with a very small-angle collimation, the problem being the reduction of γ-rays background (see Chapter on "Technical and instrumental developments"). On the other hand, many developments have been achieved on induced nuclear polarisation (*E. Leymarié, C. Fermon, H. Glattli*).

POLYELECTROLYTES

The advantages of neutrons for direct measurements of the form factor of polyelectrolyte chains via the Zero Average Contrast (ZAC) technique have been thoroughly used in the case of totally charged chains *(J.P. Cotton, G. Jannink, F. Boué).* The model polymer is here the Sodium Polystyrene Sulfonate, (PSS)Na. Semi-dilute solutions have been studied in presence of various co-ions, introduced by addition of salts. One of the questions is the relation between the persistence length L_p which characterises the worm-like conformation of a chain stretched by electrostatic repulsion between monomers, and the electrostatic parameters. The first parameter should give the best estimate of charge screening ; it is expected to be the nominal ionic strength, I, which controls the Debye screening length $\kappa^{-1} \sim I^{-1/2}$. In spite of the most current prediction $L_p \sim \kappa^{-1} \sim I^{-1/2}$,

we observed a lower exponent, $L_p \sim \Gamma^{1/3}$ (*J.P. Cotton, G. Jannink, F. Boué*). In order to distinguish from another possible law, $L_p = L_0 + L_e$, with $L_e \sim \Gamma^{1/2}$, where L_0 is the intrinsic length and L_e the electrostatic contribution, we tried (delicate) measurements at the lowest possible concentration, which confirm the 1/3 exponent (*with E. Dubois and O. Vidal, post-docs*). We also varied the valence of added counter-ions. In the case of anions, the result shows that ionic strength remains the best parameter, combined with a weak dependence on the nature of ions (*with O. Vidal*). In the case of cations, a similar conclusion can be drawn for low ionic strengths. On the reverse, for high ionic strength the chain is no longer worm-like. This is visible at the most for trivalent Lanthanum counter-ions, La^{3+}, for which the chain shape can be determined close to the phase separation observed above a given salt/polymer concentration ratio (C_s /C_p). This enlightens theories of the separation process, addressing electrostatic bridging between monomers *(with E. Dubois)*. For divalent Ca^{2+}, the same trend is observed ; since $(PSS)_2Ca$ is soluble, we also measured (using LURE, ESRF and laboratory X rays) the structure factor in absence of added salt. The "polyelectrolyte peak" in such scattering, shows a behaviour surprisingly different from (PSS)Na (*coll. with J. Combet and M. Rawiso, Strasbourg*).

Polyelectrolytes plus proteins. This system illustrates how SANS is a good tool for mixed systems. We have studied mixtures of negatively charged polystyrene sulfonate with positively charged Hen Egg White Lysozyme (pH 4) ; the phase diagram shows a solubility range, bordered by coacervation lines. In this range we have undergone measurements of the three partials form factors, and extraction of the form factor, over an as wide as possible molecular weight and concentration range (*O. Vidal, J. Bonin, F. Boué*).

LIQUID CRYSTALLINE POLYMERS : STATIC AND RHEO -INDUCED EFFECTS

Liquid crystalline polymers (LCP) have been an extended matter of study at LLB (*J.P. Cotton, P. Keller, L. Noirez, and later F. Boué, A. Brûlet*). Several studies still concern the **static** state, in particular the **nematic phase**, which for some of comb-like liquid crystal polymers studied here shows signs of **pre-smectic** fluctuations which depend on the molecular mass. Studies on five narrowly distributed masses show that, in the direction perpendicular to the mesogenic groups, the backbone adopts a random walk conformation, on which, surprisingly, the nematic order has almost no influence. Moreover, the backbone conformation, in the nematic direction, does not remain Gaussian as predicted, but is contracting when decreasing the temperature (*J.P. Cotton, A. Brûlet*). This is to compare with former results (*L. Noirez, coll. with Germany*). Some studies also explored the effect of **stereo-regularity** on the liquid crystalline state (*L. Noirez, coll. with Austria*).

LCP and rheo-SANS. But most of the recent work on LCP has been dedicated to **deformation** effects. Results of the PhD thesis of *V. Fourmaux-Demange (with J.P. Cotton, A. Brûlet, F. Boué)*, dedicated to detailed studies of chain conformation under **stretching** (coupled with rheology measurements), have been published extensively these last two years. The behaviour in the "isotropic" phase should be close to any amorphous polymer; however, on the one hand, the degree of entanglement is very low, on the second hand, rheometry as well as rheo-SANS suggest additional links leading to clusters of chains. In the nematic phase, there exists a clear difference in the orientation response, probably associated with the nematic domains. In all cases, the relaxation processes are different from amorphous polymers. *L. Noirez* studied **shear-induced** effects, with *V. Casteletto (post-doc)*, showing that pre-smectic fluctuations can counteract the chain flow-alignment, and now with *C. Pujolle (PhD)*, coupling chain conformation observations, optical observations and rheology (*coll. with ESPCI*). Hence, last year, the most striking result came from these three combined techniques : starting from the isotropic phase, **a shear-induced transition** towards a nematic state, has been chosen as our internal "highlight". This last field is rich enough to deserve extensions in the next couple of years. Pressure is also interesting *(G. Pepy)* : it can increase a lot the smectic ordering of a side-chain liquid crystal polymer, and extend its range to higher temperatures (PA-CN reentrant phase, studied using a new sapphire window high pressure cell up to 1200 bar) (see Figure 1). The shape of the smectic domain versus temperature and pressure looks very different from that of reentrant (non polymer) liquid crystals.

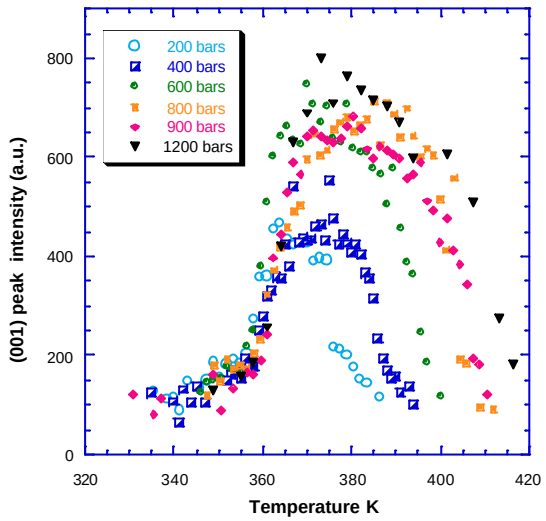

Figure 1. Maximum intensity of the 001 smectic reflection versus temperature, at various pressures. The convergence of the intensity values at low temperature indicates that the Nre-SAd remains unaffected by the external pressure.

RHEOLOGY OF POLYMERS : RHEO-SANS.

Other systems implying mostly polymers have been studied with Rheo-SANS (in situ SANS measurements under applied strain).

Copolymers. Though copolymers are widely studied (including now on LLB instruments the groups of *B. Hamley and K. Mortensen, Risö)*, we believe that a careful description of the crystalline phase has been established for the first time in a close collaboration with the University of Pau (*A. Lapp, coll. with J. Peyrelasse, thesis of C. Perreur*). The method used comes from an analogy with the rotating-crystal method used in WAXS (Wide Angle X-ray Scattering). Comparison with the diffraction spots obtained under shear orientation of a copolymer (Pluronic) micellar crystalline phase makes clear that the scattering is due to an ensemble of different crystalline domains of all orientations, but all with their <111> aligned axis along the flow. This analysis definitely establishes the existence of a unique type of crystal of cubic B.C.C structure (see Figure 2).

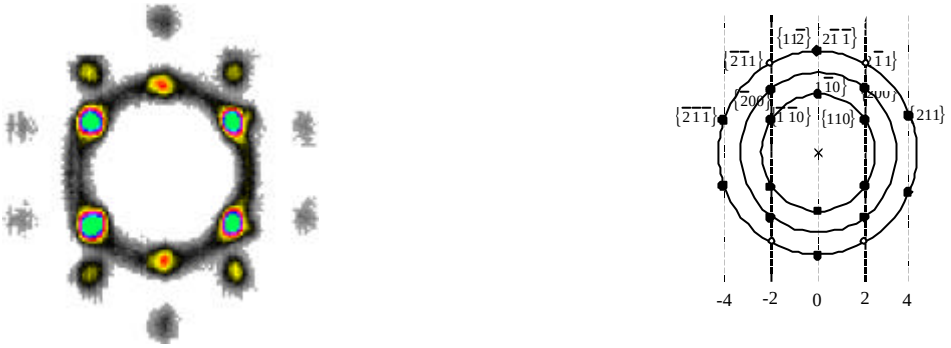

Figure 2. Scattering map for a Tetronic 908 (4 branches star polyPOE co POP) solution at 30% in D_2O (T = 47°C) oriented by a shear rate $\dot{\gamma}$ = 371 s^{-1} (left hand side) compared with theoretical figures for body centered cubic lattice.

Semi-dilute polymer solutions , under shear, have been studied (*F. Boué, thesis of I. Morfin, in coll. with P. Lindner, ILL*), because they show surprising shear-induced concentration fluctuations. These effects had yet been studied only using light radiation : eye (induced turbidity was first detected 20 years ago), static wide angle light scattering (WALS), dichroïsm, polarised light, and during the beginning of our SANS studies, small angle light scattering (SALS) and microscopy. However, all these observations had to be done close to the bad solvent regime, in other words below or close to the theta temperature Θ which separates the good solvent from the bad solvent regime. The reason was that the sizes had to be large enough for light (0.1 to 10 μm). SANS probing smaller sizes, and being quite sensitive too, allowed us to see the onset of enhancement much above Θ. It turned out that far above Θ, fluctuations are simply enhanced along the flow, and do not correspond to a phase separation. Such “first stage” is encountered for polystyrene (PS) in DiOctylPthallate (DOP) above its theta temperature (22°C), as well as for PS in DiEthylPthallate (as seen for the first time),

which is a good solvent at any temperature above crystallisation. When getting closer to Θ (i.e. for DOP), results are sensitive to the vicinity of the phase separation line (cloud point $T_c < \Theta$). One proof is that the scattering does not depend only upon the Weissenberg number $W_i = \dot{\gamma}.\tau$, but also upon $T - T_c$. Using W_i corrects results from the temperature dependence of the terminal time. This would be enough if it was a purely mechanical effect. But the larger and larger fluctuations couple with the stress, and result in a kind of shear-induced phase separation, which we called "second stage". To understand better the evolution of this second stage, we coupled **SANS with SALS** measurements, which has been the opportunity of a collaboration with *T. Hashimoto, Kyoto*. The theoretical predictions do not seem to agree neither with the first stage nor with the second one, which is highly non-linear, and thus requires numerical simulations.

NANOCOMPOSITES

The effect of stretching is also studied for nanocomposite polymer materials : these were first made by mixing aqueous suspensions of polymer beads – called polymer latex, with aqueous colloidal silica, drying and letting filmify. This technique has been re-examined in detail (*J. Oberdisse*); we have also tried other ways like in situ silica precipitation in PolyDiMethylSiloxane (PDMS) networks, developed in coll. with ICSI, Mulhouse (*B. Haidar, P. Ziegler, thesis of O. Spyckerelle*), and finally silica particles grafted with polymer chains. After few trials of grafting PDMS chains to the surface (as previously done by *J.C. Castaing at LLB*), a different route of initiating the polymerisation from the surface ("grafting from") has been started recently (*G. Carrot*). Firstly, Atom Transfer Radicalar Polymerisation (ATRP) has been successfully developed by G. Carrot while in post-doc (*with J.P. Vairon, B. Charleux, Chimie Macromoléculaire, Jussieu*). Secondly, PolyCaproLactone has been “grafted from” silica via Ring Opening Metathesis (ROM) for the first time (*G. Carrot, coll. with Ph. Dubois, Mons*). Thirdly, a collaboration with Rhodia Silica Systems including chemistry, rheology and SANS has been initiated (*A. El Harrak, PhD thesis, planned October 2001*). On the other hand, "grafting from" has been developed this year on functionalised platinum particles (*with Xavier, DEA, in coll. with H. Perez, DRECAM*).

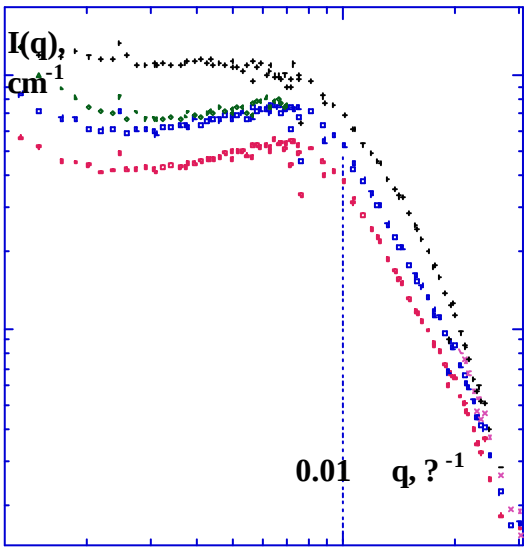

Figure 3. Scattering from a polymer film, reinforced with silica of different volume fractions ϕ : the peak indicates the distance between silica clusters, and therefore their aggregation number, constant with ϕ This indicates that we can control the separation process between the silica spheres and the polymer beads, hence control the dispersion.

STUDIES ON NEW POLYMERS

We are currently focusing more efforts on **new polymers** synthesised via novel routes, in coll. with the LCMO in *Bordeaux (A. Brûlet, J.P. Cotton, with S. Lecommandoux, R. Borsali*) : for preparing stiff polymers (also called bottle-brushes), different controlled polymerizations are combined (*Schappacher, Deffieux*), cationic for the polyvinyl ether backbone and anionic for the PS-Li living branches, which are finally grafted on the backbone (1% of the mass).

This gives well controlled architectures of extremely high branching density with equal branch length. Recent SANS and X-ray experiments show that their shape crosses over from spherical shape to rod-like and eventually worm-like shape when increasing the ratio of the backbone length (i.e. the degree of polymerization DP) to the branch length. Besides, the persistence length appeared much higher for the graft copolymer than for the precursor PCEVE (see Figure 4), due to the high grafting density of PS. We are also interested in measuring how the lateral polystyrene chains are elongated. Further SANS experiments with appropriate labeling and contrast conditions will be performed in order to determine behaviors of the PECE backbone and of polystyrene lateral chains.

Other hyperbranched polymers (as shown in Fig. 4c) are already envisaged.

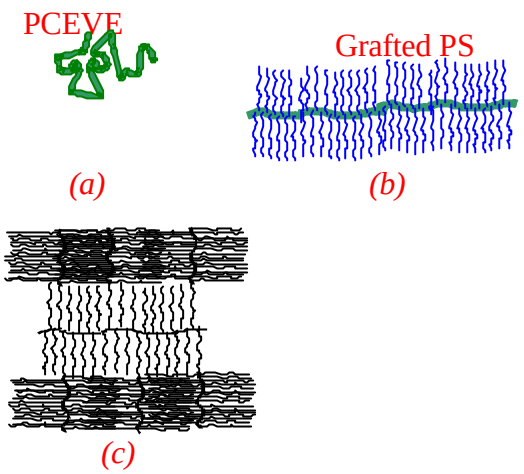

Figure 4. Schematic representation of PCEVE polymer chain (a), and the same chain grafted with polystyrene (b) $PS_{DP=30}$-$PEVE_{DP=1042}$. The persistence length increases from 13 Å up to 106 Å. Hyperbranched objects (c) can be built step by step by using controlled living polymerizations.

Our project is to study now structures made using ROM polymerization of macro-monomers based on Poly-Norbornene. It has a high potential due to the efficiency of the polymerization for a large range of dangling parts, including different species on the same backbone. This will be investigated by SANS, rheology, and possibly inelastic scattering, in order to understand their physical properties in a co-directed thesis work (*Y. Gnanou, V. Herroguez, thesis of S. Desvergnes*, planned October 2001).

CONFINED POLYMERS

SANS is also well suited to studies in confined environment, as illustrated by two different works. A first one (*J.P. Cotton, A. Brûlet, A. Menelle, F. Boué*) uses SANS at its limits, by measuring the chain form factor in a thin film as thin as 10 nm ! One can distinguish three q ranges : in the low q range, the scattering is very sensitive to film preparation (cf. problems reported by Jones, Russel et al.) ; in the medium q range, the chain conformation is the usual one (as found by the same other authors); finally, in the large q range, we have detected some differences in the apparent persistence length, which remain to be understood.

A second work looks at chains trapped in a Vycor porous glass made of kinds of channels of several nm diameter; the signal of the Vycor can be masked by using a deuterated/non deuterated mixture, which is also suitable for ZAC (Zero Average Contrast) investigation of the chain form factor, for amorphous polymers (PDMS) as well as for polyelectrolytes (*L. Auvray, coll. J. Lal, Argonne*). They find that the chains are more stretched in confined geometry than the bulk, as evidenced by the 1/q scattering region. They are also sufficiently extended as to highlight the large-scale disordered structure of Vycor; this effect increases with molecular weight. In addition, we have determined S(q) for both the bulk and confined states. The asymptotic behaviour of the observed interchain structure factor is $1/q^2$ for free and 1/q for confined chains and is a consequence of the local rod-like structure of the chains (see Figure 5). While the observed increase in chain rigidity may be the dominant factor, since the weakly charged Vycor surface is unlikely to significantly reduce the bound counterion fraction around the highly charged (fully-sulfonated) backbone.

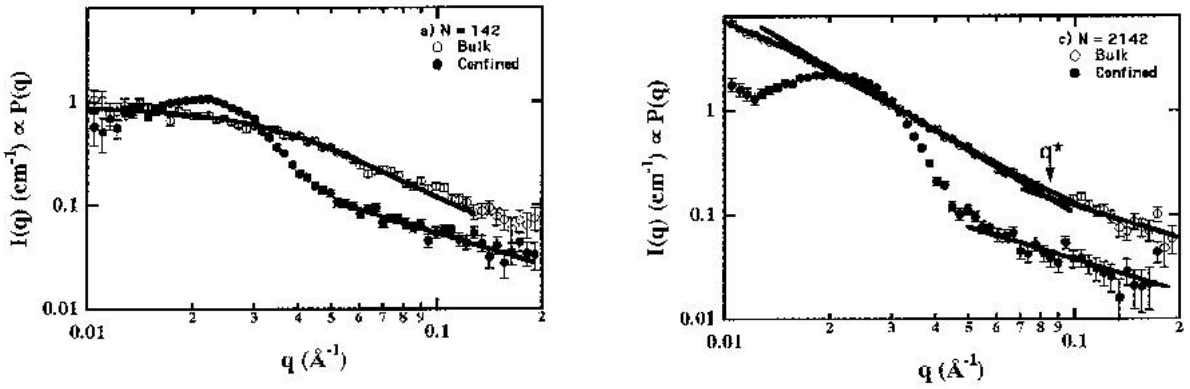

Figure 5. SANS from polyelectrolytes in ZAC condition in **bulk and confined geometry**. Low (a, N_w= 142 units) and large (b, N_w= 2142 units) molecular weight at 0.306 g cm^{-3} . Bulk data have been fitted to the Sharp and Bloomfield model for wormlike chains for $q l_p < 2$. Also shown in (b) are q^{-2} and q^{-1} regions in the SANS which crossover at q*.

SURFACTANT ASSEMBLIES : VESICLES

Recent work on surfactants has been focussed on lipids vesicles. The lipid bilayer forming such bags can be compared with the phospho-lipid membrane enveloping of a cell. One aim of the work has been to make small vesicles (radius : 30 nm < R <150 nm) in aqueous suspension, by extruding larger vesicles through 6 to 10 µm thick polycarbonate films of controlled pore size (10 nm < R_{pore} < 200 nm). When the pore radius is smaller than the one of vesicles, the vesicles break into smaller ones of final radius R_f smaller than their initial radius R_i. SANS and DLS measurements have shown that R_f depends on R_{pore}, but not on the flow rate (which determines the shear rate) (see Figure 6). Breaking is due to bending effects rather than to shear stresses on the membrane. Variation of the elastic modulus and bending modulus has been realized (by adding a polymer for example), in order to understand their relation with breaking.

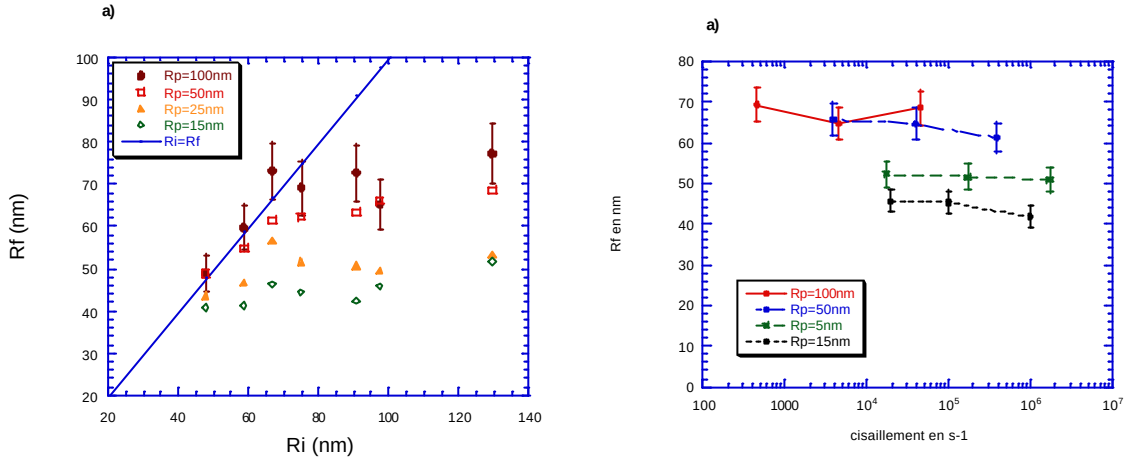

Figure 6. a) Radius of vesicles after extrusion (R_f) versus their initial radius (R_i), for various values of the pore size (R_p) b) R_f versus shear rate.

BIOMATERIALS

A first type of biomaterial is industrially extracted from living systems, e.g. for food or agro-industry, like cellulose from vegetal. One of its water soluble derivatives is Methylated Cellulose. It is a central polymer in the science of modified natural polymers, with many applications. It presents, among other cellulose derivatives, a peculiar phase diagram : not only it forms gels when C is increased, via association of the methyl groups, but also it phase separates when T is increased (Lower Critical Separation Temperature ~ 40 °C) due to temperature sensitive balance between methyl groups hydrophobicity and H bonds. The final texture can therefore be quenched by gelation, with kinetics aspects ; it was important to study it precisely on a very large q range (*S. Guillot, PhD thesis, co-direction D. Lairez – M. Axelos, INRA Nantes*) using SANS, Static Light Scattering (SLS), Dynamic Light Scattering (DLS), and Small Angle Light Scattering (SALS, *coll. with M. Delsanti, CEA/SCM*). The phase separation is not completed, since it does not lead to a Porod law (variation in q^{-4} characteristic of sharp interfaces). The second half of the work deals with interfacial properties, studied using tensiometry in *Nantes* and also neutron reflectivity (see below).

Other types of biomaterials are directly involved in biology. This the case of fibronectin, a protein important in the Extra Cellular Matrix (ECM); its shape in solution, a kind of necklace of successive spheres, has been studied both in the native state and in a reversible denatured state (*D. Lairez, coll. J. Pelta, Univ. Cergy - Pontoise*). It was interesting to study gels formed by this protein, gelled materials being involved in the ECM, and moreover, in order to understand the motion of cells in the ECM, the local mechanical properties, and their response to enzymatic degradation. In a first step, for the sake of simplicity, a smaller scale has been studied : latex beads have been introduced in simple gels like gelatine, and their motion studied by DLS. It is planned to cover these beads by enzymes able to degrade the gel (protein gels, with latex additions (*G. Fadda, thesis, with D. Lairez and J. Pelta)).*

Finally, a new bio-chips project is starting on interfaces (see below)

INTERFACES

Neutron reflectivity (NR) has been developed very early in LLB. It can be used, as in a very recent work, to characterise the different layers of bio-chips (*L. T. Lee, F. Boué, A. Menelle, F. Cousin (military service)*; *coll. with B. Cabane, Paris; C. Pichot and A. Te, UMR Biomérieux-CNRS*).

But one of the LLB expertises is the study of polymers at the **liquid-air interface**. This involved recently thermo-sensitive polymers, e.g. the case of PNIPAM solutions, which phase separates at a LCST of 32°C (*B. Jean, thesis, L.T. Lee, coll. with B. Cabane*); the interaction with surfactants and the eventual association between polymers and micelles has been studied in volume (SANS) and at the interface, which explains the interfacial surface tension and the existence of a complex interface with layers of different species (see "highlight" in the former 1997-98 report). A few measurements have also been done on Methyl Cellulose : they correlate well with the bulk phase separation behaviour, and are currently discussed at the light of tensiometry data (*S. Guillot, thesis, D. Lairez, M. Axelos, L.T. Lee*)

The structure of another type of interface, of the **solid-solid** type, has also been cross-checked with **mechanical properties** : a thin layer of deuterated polystyrene, cross-linked or not, is created on a wafer by spin-coating. A second layer of cross-linked polystyrene, made by spin-coating or solvent casting, is deposited on top of the first one. Such sandwich is annealed for a given time, which permits interdiffusion of the two layers. Former experiments on this system gave access to various tracer diffusion, self-diffusion, mutual diffusion coefficients for different rates of cross-links of the layers. These results were obtained by NR for short sizes, as well as by Ion Beam Analysis (ERDA in particular) for larger sizes, both techniques being sensitive to the presence of deuterium (*with M. Geoghegan*).

We then created an interface as similar as possible to the one studied by NR, confined this time between two thick polystyrene plates ; we finally measured the interface strength as a function of the annealing time, using the "razor blade" test of Brown et al. The aim is to correlate interdiffusion and adhesion. Different regimes were observed depending on the degree of interpenetration. If both layers are networks, equilibrium interpenetration is the number of units between two cross-links, N_c. If one layer is an uncross-linked polymer ("melt", with number of units N), a controlling parameter is the ratio N/N_c. When $N/N_c > 1$, interpenetration is limited to ~ one network mesh, ~ $N_t^{1/2}$. However the mechanical strength of the interface may show surprising behaviours. This has been enlightened by coupling again NR with ERDA and other Ion Beam techniques : this permitted to reconstitute the crack path. Since one of the layers was deuterated, it was possible to know inside which layer, or between which layers, had the crack propagated. Other analysis such as profilometry have been used (*G. Bacri, thesis, with F. Boué, A. Menelle, M. Geoghegan, Leeds, F. Abel, GPS- Jussieu, C. Creton, ESPCI*).

DYNAMIC NUCLEAR POLARIZATION

Time resolved nuclear polarization has been observed by SANS (*H. Glättli, thesis of E. Leymarié, collaboration with PSI, Switzerland*). Dynamic nuclear polarization (by «solid effect » as named by A. Abragam) of some nuclei in the vicinity of paramagnetic centers (of reduced concentration) polarized by NMR, has an obviously strong interest in SANS when applied to H nuclei : it modifies their scattering cross-section and thus permits tuned labeling instead of deuteriation chemistry. For a better understanding of this mechanism, the group of *H. Glättli* (*LLB – SPEC*) has studied spatial inhomogeneity of polarization in the first instants after applying the polarizing field. The data acquisition was time- resolved in 200 frames of 0.1 s, synchronized with a flipping each 10 seconds of the dynamic polarization orientation. The paramagnetic center was a Chrome V complex diluted in a 90% deuterated solvent. The scattering can be fitted by the form factor of two concentric spheres around each Chrome complex (Figure 7). It is clear that proton polarization close to the paramagnetic impurity increases much faster than the one of the bulk proton (Figure 8).

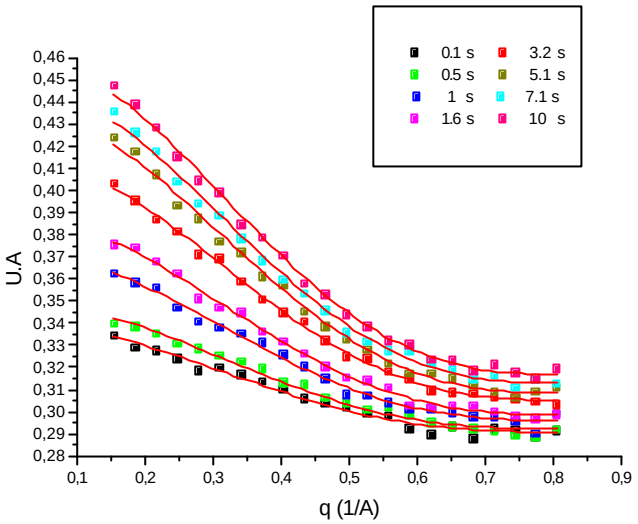

Figure 7 : Time evolution of the SANS signal during the negative polarization of protons, fitted by the form factor of two concentric spheres (measured at D22, ILL).

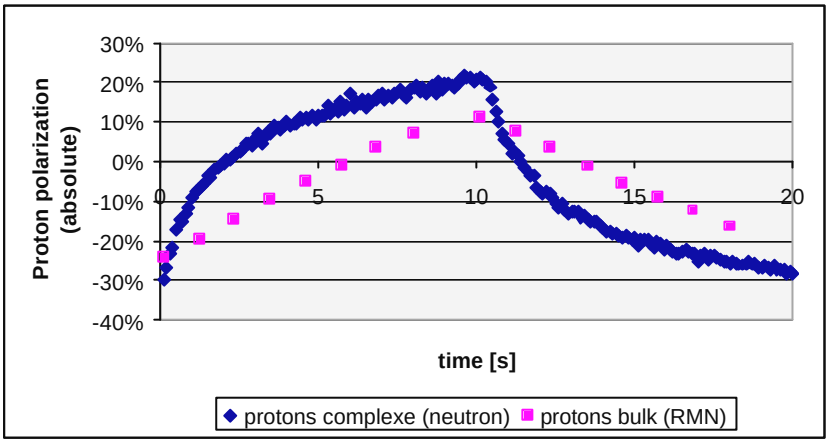

Figure 8 : Dynamic proton polarization as a function of their spatial localization. The polarization in the Cr-complex (blue line) is measured by time resolved SANS, while that of the bulk protons is given by NMR –pink dots).

NUMERICAL SIMULATIONS

It would be particularly useful for SANS to have some ways of modeling the shapes and arrays in many materials : this is a unique way of calculating precisely their scattering and compare to complex models. We hope to be able to develop it in the future. A seed for this activity is the work of J. Oberdisse. A first part concerns nanocomposites (*J. Oberdisse, Y. Rharbi, F. Boué*) : the shapes and arrays of silica clusters of one to several hundreds of particles have been modeled following different mechanisms of aggregation. Then, the motion of these clusters during stretching has been simulated. Their center of mass is moved affinely to the macroscopic elongation, as long as two particles do not hit. This occurs because stretching produces shrinking along the transverse directions. When hitting onsets, different local rearrangement have been tested. The choice of a mutual local shear permitting the two objects to avoid each other gives a simulated scattering with the same features as observed experimentally : namely, butterfly patterns are observed in a 2d contours map, but with four maxima.

The second work has been initiated during the post-doc stay of *J. Oberdisse* in Italy *(coll. with G. Marucci and G. Ianniruberto, Napoli).* The influence of trapped entanglement on the stress has been calculated. The polymer chains are cross-linked, but also entangled with each other : each one can be simulated as a Gaussian chain passing through some "slip link" between two cross-links. Beautifully, the analytical result of *Ball, Doi, Warner and Edwards* is recovered! This work is under development (influence of limited extensibility of one chain between cross-links).

NON-LINEAR RHEOLOGY OF LIQUID CRYSTALLINE POLYMERS

C. Pujolle, L. Noirez
Laboratoire Léon Brillouin (CEA-CNRS), CEA-Saclay, 91191 Gif-sur-Yvette cedex

Under flow, molecules gain new dynamical properties. Close to phase transitions, flow produces a shift of the transition temperatures and changes the critical behaviours. Flow is also expected to induce non-equilibrium phase transitions. Such non-equilibrium transitions were up to now experimentally observed in solutions of worm-like micelles only[1,2] and are still a subject of intensive research. Very recently, we have discovered that high molecular weight **thermotropic** liquid crystals and more particularly side-chain liquid crystalline polymers[3] (Fig.1) display a non-linear behaviour related to the shear induced isotropic-nematic phase transition appearance. Despite more than 20 years of extensive investigation in thermotropic polymers for both academic and technological interests, such a fundamental shear-induced transition has never been identified. We show here that it is a general property of the side-chain liquid crystalline polymers.

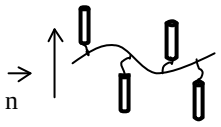

Figure.1. Equilibrium conformation in the nematic phase of a side-chain liquid crystalline polymer with a perpendicular main-chain/side-chain orientation:

Different criteria have driven to the identification of the shear-induced isotropic-nematic phase in side-chain liquid crystalline polymers. These are : - a non-linear behaviour of the birefringence, - a strong birefringence, - a non-linear shear stress behaviour versus shear rate (existence of a stress plateau), and - the singularity of the main-chain conformation (determined by SANS) in the shear induced phase.

- The crossed polariser microscopic observation of the isotropic phase of the side-chain polymers, shows the emergence at a critical shear rate of a strong birefringence ($\Delta n \approx 10^{-3}$) which is consistent with the formation of an uniform nematic phase oriented with the director parallel to the velocity axis.
- The constitutive behaviour of a typical flow induced phase transition exhibits, under stationary conditions, the existence of a stress plateau in a shear stress versus shear rate diagram. However, to identify such a mechanical response, the conditions of the stationary regime have to be necessarily determined. The liquid crystalline bulk displays indeed a transient regime characterised by a shear stress time dependence as illustrated in Fig.2. The instantaneous stress response of the material to the shear flow decreases following a sigmoïdal time decay until reaching a stationary regime after about 1000s. Three distinct regimes can be distinguished : (i) at $\dot{g} < \dot{g}_{c1}$, the bulk behaves as an ordinary homogeneous liquid; (ii) at $\dot{g}_{c1} < \dot{g} < \dot{g}_{c2}$, the shear stress presents a transient regime characterised by a stress overshoot which relaxes and then converges with time to the same stress value indicating the existence of a plateau and finally; (iii) at $\dot{g} > \dot{g}_{c2}$, the final stress value becomes again shear dependent, the sample has been fully converted into the induced nematic phase.

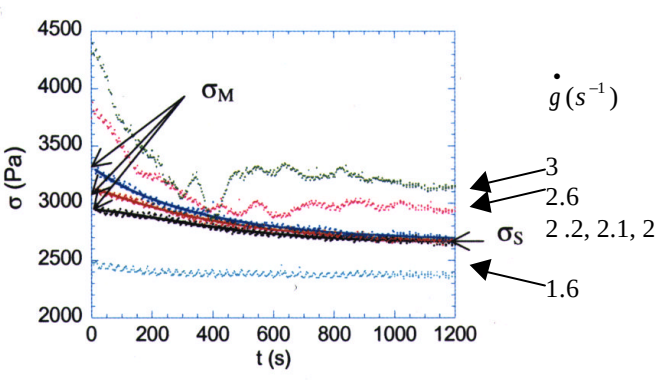

Figure 2. Time dependent shear stress experiments carried out at ΔT=+7°C above the isotropic-nematic transition. These measurements reveal that side-chain polymers show a transient response similar to that seen in wormlike micelles.
Depending of the strain rate $\dot{g}$, three distinct regimes can be distinguished following the steady state value obtained in the stationary regime. These are : the isotropic branch ($\dot{g}$ = 1.6 s^{-1}), the stress plateau ($\dot{g}$ = 2.2, 2.1 and 2 s^{-1}) and the shear-induced nematic branch ($\dot{g}$ = 3 s^{-1}).

The stress plateau is the signature of a flow heterogeneity and corresponds to coexisting isotropic and nematic phases which share the sample volume in proportion relative to the shear rate. Fulfilling the stationary conditions, a steady state flow curve can be determined. Figure 3 shows the variation of the shear stress as a function of the shear rate at $T=T_{NI}$ + 5°C. As can be seen, a stationary state stress plateau separates the low shear regime from the high shear regime.

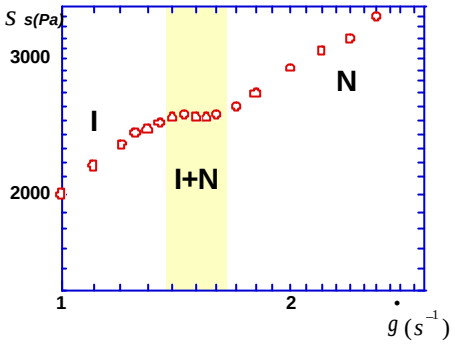

Figure 3. Bulk response of a side-chain polymer under shear stress : Evolution of the shear stress versus shear rate at $\Delta T=+5°C$ above the isotropic-nematic transition $T_{NI}=110°C$. The yellow area corresponds to the stress plateau where isotropic and nematic phases coexist. The lower branch (left side) corresponds to the isotropic phase and the upper branch (right side) to the induced nematic phase.

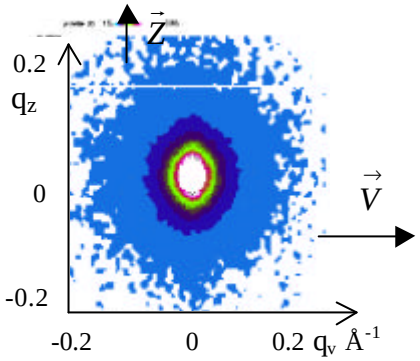

Figure 4.a. Neutron scattering pattern obtained in the (velocity, neutral axis) plane displaying the form factor anisotropy of the main-chain at $T>T_{NI}$ in the shear induced phase. The velocity axis is horizontal – PAXY (λ=8Å, d=2m) - LLB

1. V. Schmitt, F. Lequeux, A. Pousse, D. Roux, Langmuir **10** (1994) 955.
2. J.F. Berret, D.C. Roux, G. Porte, P. Linder, Europhys. Lett. **25** (1994) 521.

From the evolution of the width of the stress plateau versus temperature, a non-equilibrium phase diagram can be built. The disappearance of the stress plateau at large temperature far from the equilibrium transition temperature reveals that the diagram is closed by a critical point.

Finally, by SANS experiments, using a specifically designed shear cell device, homogeneous in temperature and adapted to a simultaneous optical and neutron study of highly viscous fluids at high temperature[4], we have demonstrated that the main-chain of the polymer (backbone) is elongated in the shear induced nematic phase along the flow direction. Main-chain and side-chain mesogens are thus both oriented along the velocity in this configuration (Fig.4).

This orientation is singular since the main-chain conformation is mostly perpendicular to the mesogen director in the usual nematic phase at equilibrium (Fig.1). This feature underlines the specificity of the non-equilibrium phase which thus does not result from a simple temperature shift of the equilibrium nematic phase.

The discovery of this transition in thermotropic systems opens the prospect of non-equilibrium systems. The possibility to control the molecular weight, the force of the interactions and the molecular architecture, opens new routes which were not accessible in the frame of the study of worm-like micellar solutions.

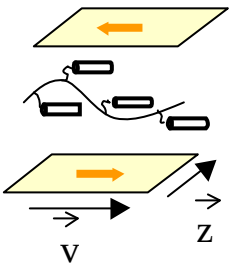

Figure 4.b. Corresponding conformation : in the shear induced phase, the main-chain is oriented parallel to the mesogens. $\vec{v}$ and $\vec{z}$ are the velocity and the neutral axis respectively.

3. C. Pujolle, L. Noirez, Nature **409** (2001) 167.
4. P. Baroni, C. Pujolle, L. Noirez, Rev. of Sci. Instruments **72**, 6 (2001)

STRUCTURAL PROPERTIES OF HELICAL SELF-ASSEMBLED POLYMERS WITH HYDROGEN-BONDING.

Aissa Ramzi[*], Ky Hirschberg, François Boué[†], Annie Brûlet[†]

Department of Chemical Engineering, Eindhoven University of Technology, P.O. Box 513, 5600 MB, Eindhoven The Netherlands.
[*] The Dutch Polymer Institute.
[†] Laboratoire Léon Brillouin, CE-Saclay, F-91191 Gif-sur-Yvette Cedex, France.

SANS allows us to establish and follow self-assembly of molecules into polymers of controlled length, shapes and chirality, with chemistry enabling a rich variety of interactions.

First interactions are **hydrogen bonds** : ureidotriazine is the elementary unit which associates via a quadruple hydrogen bond with another ureidotriazine, see sketch below. Molecule (**1**), **monofunctional** (as far as H-bonds are concerned), selfassociates into **dimers**. Molecule (**2**), ***bifunctional*** *(two* ureidotriazines *linked covalently)* forms **H-bonded chains**.

A second attraction implies **1** as well as **2**, the **stacking of** the extended p-p **-surfaces** of both molecules. Such solvophobic interaction can induce **columnar order**.

Thirdly, **side molecules** (R = **a** or **b** in Figure) gives a third control : they stabilize the self-assembly, and if they possess **chirality** (case **b**) they can induce it along the chain (for reasons clarified below, we focussed on **1b**, **2a** and their mixture).

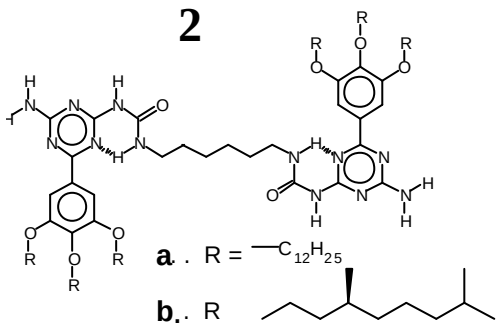

Therefore, all interactions depend on the type of solvent. DiMethylFormamide kills both **hydrogen and** p-p **bonds**. In **chloroform** (deuterated for SANS), **H-bonds take place** : large particle scattering is observed for **2a** (**random chain**), but not for the *monofunctional* molecules (**1b**) which only exist as dimers[3]. In (deuterated) **dodecane** solutions both **1** and **2** display **columnar architecture**. Scattering patterns for **1b** have been fitted by the cylindrical-like form factor : the radius, 15 (± 1) Å, is independent on concentration, matching nicely with a column built up of stacked dimerized molecules of **1b**. The length of the columns is concentration dependent and increases from 100 Å for a 0.2 wt.% solution to 190 Å for a 1.0 wt.% solution (~ 60 molecules). At **elevated temperatures** (~ 100 °C) the scattered intensity decreases strongly : the molecules only exist as dimers as in chloroform at room temperature, because the π–π stacking is overcome (**figure 2**).

The scattering of **2a** in dodecane has also been fitted to a cylinder form factor (interpretation at higher concentrations is hampered by inter-columnar gelation). The radius is constant, 17 (± 1) Å, larger than for **1b** in agreement with the difference in side-chain length of (a) and (b).

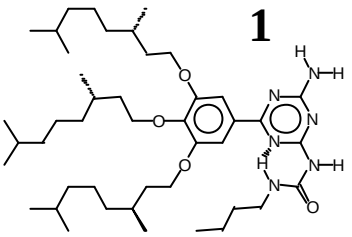

We can also make a **chain-stopper experiment**: monofunctional **1b** is mixed with bifunctional **2a** in deuterated dodecane, at constant 0.5 wt.% concentration (**figure 1**). The radius of the columns slowly changes from 17 to 15 Å as expected, while the length decreases rapidly after addition of small amounts of **1b**, showing the formation of shorter and less stable columns than pure bifunctional **2a**. The length of the columns is

shorter for **1b** due to the absence of the supramolecular polymeric backbone created in **2a** by the covalent links between pairs of H-bonded ureidotriazine units.

This shows how precise can be SANS investigation of these assemblies, in various solvents as soon as they are deuterated ; extensions like contrast variation, partial deuteration, are obvious. From such basis, **most interesting is combination of SANS measure-ments with circular dichroïsm :** it allows us to see how helicity can be controlled by

the chirality of the R radicals together with strength and shape of the assemblies. E.g., **1b**, in spite of its end position in a **1b**/**2a** chain, can induce helicity all along the **2a** sequence.

Finally, let us stress that such selfassembly can occur in water, since aromatic regions creates a hydrophobic environment, preventing water to kill H-bonds. One can then fully control such synthetic helices, which can be compared to DNA assemblies in biology.

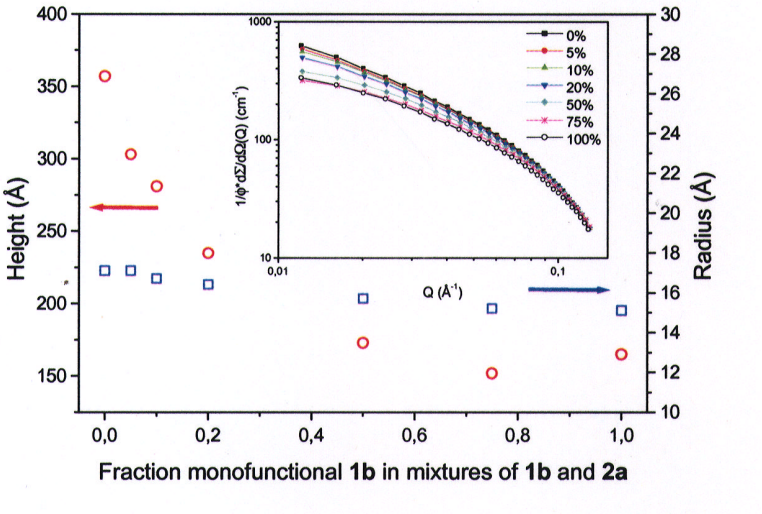

Figure 1. Height (circle) and radius (square) of columns formed by a **2a** + **1b** mixture at a constant total weight percentage (0.5 %). Inset : corresponding observed scattering patterns in log-log plots.

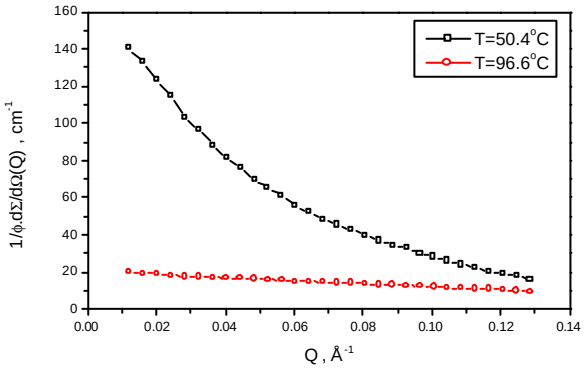

Figure 2. Temperature effect on SANS from monofunctional (1b) solution in dodecane at 0.96% (v/v) concentration

1. Lehn, J.-M., Makromol. Chem. Makromol. Symp. ***1993*** *69*, *1*.
2. Sijbesma, R.P.; Beijer, F.H.;Brunsveld, L; Folmer, B.J.B.; Hirschberg, J.H.K.K.; Lange, R.F.M.; Lowe, J.K.L.; Meijer, E.W. *Science* **1997**, *278*, 1601.
3. Hirschberg, J.H.K.K.; Brunsveld, L; Ramzi, A.; Vekemans, J.A.J.M.; Sijbesma, R.P.; Meijer, E.W. *Nature* **2000**, *407*, 167.

BIOLOGY

1. INTRODUCTION

The research activities in Biology at LLB focus on two main fields of interest that are in full development.

1.1. Conformation of proteins in solution.

The understanding of protein folding remains one of the major goals of Biology. This requires, at least, a detailed structural characterization of both the folded and the unfolded states.
If we raise the temperature sufficiently, or make the pH extremely acid or alkaline, or add guanidinium chloride to the buffer, the protein structure will unfold. Thus, characterisation of the denatured states of protein is important for a complete understanding of the factors stabilising their folded conformation. Whereas X-ray crystallography or nuclear magnetic resonance allows this for native proteins, only few techniques can provide precise information about the mean conformation of flexible denatured states. Among these techniques, small-angle scattering, of either X-rays or neutrons, is a very powerful tool giving structural information at low and medium resolution. Complementary information from circular dichroïsm, fluorescence and differential scanning calorimetry is used.
An emerging and very promising field concerns biofunctional assemblies at lipid interfaces studied by neutron reflectivity (See “highlight” by Tristl et al).

1.2. Protein dynamics and role of water in Biology.

It is now admitted that a protein is a flexible entity and that this flexibility is required for protein to function.
At physiological temperatures internal motions in proteins are partly vibrational and partly diffusive. The description of internal diffusion in proteins is complicated by the variety of existing motions. These involve groups of atoms undergoing a plethora of continuous or jump-like diffusion. Because of the high incoherent scattering cross section of hydrogen (80 barn) with respect to that of other atoms in proteins (C, O, N) inelastic neutron scattering is the most direct probe of diffusive dynamics on the 10^{-12} - 10^{-9} s scale (time of flight, spin echo techniques). Our strategy is to combine the neutron results with that of light scattering and NMR and to compare them with that of Molecular Dynamics (MD) simulations. This strategy offers a unique opportunity to validate potential of MD simulations and get a detailed knowledge of protein dynamics. Dynamics of water that plays an essential role in Biology becomes also accessible on a detailed way.
Analysis of MD simulations is made using some theoretical results obtained for polymeric systems, from which geometry of motions and distribution of relaxation times of various parts of the protein are obtained. Mode Coupling Theory (MCT) that is well appropriate to describe supercooled liquids allowed us to provide with a model for confined or interfacial water.
The knowledge of structural and dynamic properties of bulk water as well as that of confined water is of primary concern. The hydrophilic and hydrophobic interactions have also been studied.

2. DYNAMICS OF WATER

2.1. Hydrogen-bond dynamics model

The problem of hydrogen bond lifetime in liquid water has been analysed in a new way. Even if several incoherent scattering experiments have shown in the past that it is possible to identify a breaking mechanism for hydrogen bond through librational motions, other analysis of the scattered intensity remains possible. The new experiment is based on the decomposition of the structure factor, S(Q), of liquid heavy water in its components. Actually, S(Q) is a weighted sum of three partials corresponding to the pairs OO, OD and DD. Selecting the values of the exchanged momentum Q, it is possible to analyse in a selective way the contribution of each pair. The experiment consists to measure the quasielastic scattered intensity at two different values of Q. For a value at which most of the intensity is due to the OO pairs, it is the dynamics of the whole molecule that is dominant and one finds the classical broadening due to diffusive motions. Instead, at a value of Q at which the intensity is dominated by the pairs DD, one finds the characteristic short time that corresponds to hydrogen bond breaking. This time is very short (1 ps) and depends weakly on temperature, in contrast with the strong and anomalous temperature dependence of transport properties. Such

a separation of the two times with an experimental technique emphasises the importance of hydrogen bond dynamics in liquid water [1].

2.2. Structural relaxation of water supercooled in a porous glass

We have carried out neutron-spin echo measurements of the intermediate scattering function S(Q,t) of supercooled D_2O contained in a porous Vycor glass on the new spin echo spectrometer (MUSES). The results establish clearly the existence of an α-relaxation with the relaxational parameters, consistent with that of Computer Molecular Dynamics data of SPC/E model water. These observations suggest that the dynamics of supercooled water can be described in the general frame of the MCT scheme of glass forming liquids [2].
Figure 1 displays the structure factor S(Q) of D_2O and gives the values of the three fitted parameters: the Debye-Waller factor A(Q), the stretch exponent β and the relaxation time τ, at 258 K.

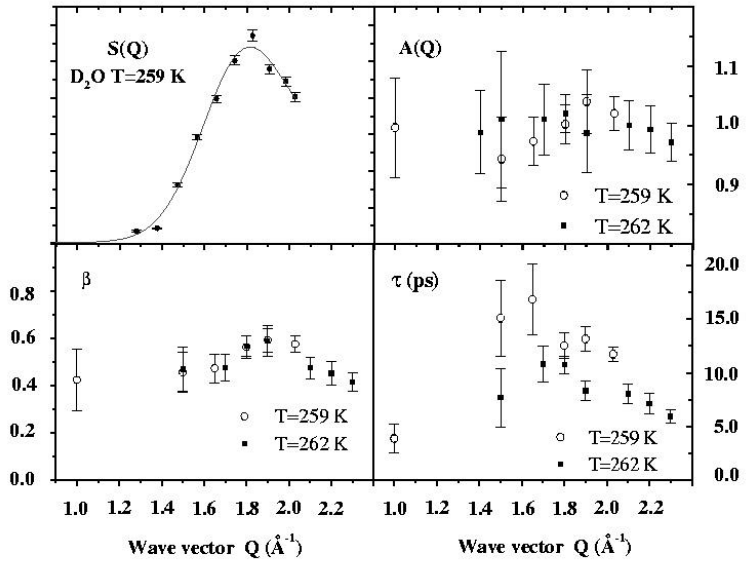

Figure 1. The values of the three fitted parameters, A(Q), β (Q), and τ (Q) according to the α-relaxation model. Also shown (upper left pannel) is the experimental structure factor obtained from the elastic scan of the sample (with the signal due to the Vycor subtracted) at 259 K using the neutron spin-echo spectrometer MUSES. The peak position is in agreement with an independent neutron diffraction measurement performed on the 7C2 spectrometer of LLB.

2.3 Aqueous solutions

The effect of hydrophilic and hydrophobic solutes on dynamics of water has been studied in case of water/DMSO[3] (Stage of J. Tavarès-Cabral, 1999), water/trehalose (Thesis of I. Koper), water/pyridine (Thesis of L. Almasy) solutions.
There is evidence of some slowing down of the translational diffusive motion of water. At the opposite, the effect on hydrogen bonding is not significant.

3. CONFORMATIONS OF PROTEINS IN SOLUTION

The effect of secondary structure on protein folding has been studied. Different proteins, such as yeast phosphoglycerate kinase (PGK), β-casein (Thesis of A. Aschi) and apo-neocarzinostatin (NCS) (Thesis of D. Russo, 2000) were completely unfolded by guanidinium chloride (GdmCl). Small angle neutron scattering (SANS) spectra from these denatured proteins were recorded at wave number transfers, Q, ranging from 0.006 to 0.4 $Å^{-1}$. Among the previous proteins, NCS is the only one that can be denatured by heat without aggregating. Scattering from thermally unfolded NCS was also measured (Figure 2).

[1] J. Teixeira, to be submitted
[2] M.C. Bellissent-Funel, S. Longeville, J. M. Zanotti and S. H. Chen, Phys. Rev. Lett., 85 , (2000) 3644
[3] J.T. Cabral, A. Luzar, J. Teixeira and M.-C. Bellissent-Funel, J. Chem. Phys., 113, (2000) 8736-8745

The randomness of the final protein states depends on the denaturing conditions. In very concentrated GdmCl solutions, excluded volume interactions are generally present. This means that all the amino acids are fully solvated and repel each other at short distances. As a result, the configurational space available to the polypeptide chain is restricted. On the contrary, at 78°C NCS behaves as an ideal chain (Figure 2). Such a behavior, which can also be observed at moderate GdmCl concentrations, is prerequisite to folding. These properties of unfolded proteins can be directly inferred from the variation of the forward scattered intensity as function of protein concentration[4].

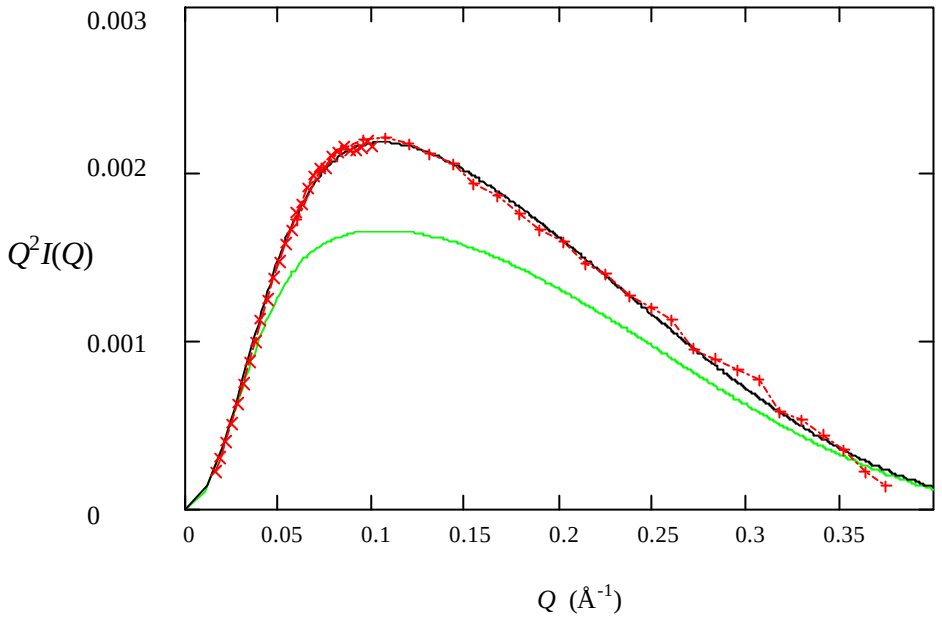

Figure 2. Kratky plot of the neutron intensity, $I(Q)$, scattered from apo-neocarzinostatin unfolded at 78°C. Q is the wave number transfer. Crosses: Experimental data. Lines: Theoretical model of Pedersen and Schurtenberger for an ideal chain (black) and an excluded volume one (green). This clearly shows that neocarzinostatin behaves as an ideal chain at 78°C.

Using Pedersen's description of semi-flexible polymers chains[5], important structural parameters can be inferred from the scattering profiles. Values of the radius of gyration, of the fractal dimension, of the statistical length, and of the apparent radius of the chain cross-section were obtained is this way for the three proteins in various denaturing conditions. As far as the statistical length is concerned, its value depends on the protein and varies between 12 Å for NCS at 78°C and 32 Å for β-casein at room temperature. These values are the first correct experimental determinations of the statistical length of proteins. All the results previously published by other authors were actually based on incorrect theoretical predictions.

4. STRUCTURE-DYNAMICS-FUNCTION RELATIONSHIP

Our investigations have been performed on hydrated powders in order to limit the contribution of bulk water as well as on protein solutions. The protein is isolated from bacteria (cyanobacteria, purple bacteria), blood cells, pike muscles. When the protein is a commercial product, a special care is devoted to its purification (myoglobin). The studied proteins are representative of the following biological functions:

- Photosynthesis: soluble proteins (C-phycocyanin) and membrane proteins (reaction centre RC, light harvesting protein LH2 and complex RC-LH1).
- Calcium/magnesium regulation: parvalbumin
- Oxygen-carrying : hemoproteins (myoglobin, hemoglobin)
- Enzymatic catalysis : aspartate transcarbamylase (ATCase),
- Antibiotic function : neocarzinostatin (NCS)

[4] V. Receveur, D. Durand, M. Desmadril and P. Calmettes, F.E.B.S. Lett. 426 (1998) 57.
[5] J. S. Pedersen and P. Schurtenberger, Macromolecules 29 (1996) 7602.

Biology

4.1. Influence of hydration on the internal dynamics of globular proteins

Powders at different hydration levels, as well as solutions, were investigated by incoherent quasielastic neutron scattering. In particular, the quasielastic component of the spectrum reveals dynamical aspects related to diffusive motions that might be functionally important by participating to the general flexibility of the protein. From these components, one has inferred that diffusive motions of protein protons occur within a confined volume and that about 25% of the protons in the protein are involved in short-time (MIBEMOL, 10 ps time range) diffusive motions. These protons belong to the surface residues of the protein. For a hydrated C-phycocyanin protein (h = 0.5, h in gram of water per gram of protein), the volume of diffusion is close to that of a sphere of radius 2 Å (Thesis of S. Dellerue, 2000). The same findings are obtained for hydrated powders of parvalbumin[6], and solutions of ATCase (see "highlight", Hervé et al) and hemoglobin, (postdoctoral work of C. Loupiac), at the same 10 ps time scale. At higher resolution (IN13, 100 ps time range), backbone motions are observed. Analysis of MD simulation leads to similar results.

Nanosecond MD simulation and analytical theory have been used to model diffusive motions in hydrated C-phycocyanin (h = 0.5). The simulation-derived scattering function is in good agreement with experiment and is decomposed to find the essential contributions. It is found that the geometry of the atomic motions can be modelled as diffusion in spheres with a distribution of radii that is different for backbone (average radius = 1.1 Å) and side chains (average radius = 2.0 Å). The time dependence follows a stretched exponential behaviour, reflecting a distribution of relaxation times. With this description, the average side-chain and backbone dynamics are quantified and compared. The dynamical parameters are also shown to present a smooth variation with distance from the core of the protein. This is reflected in a progressive increase of the mean sphere size of diffusion and in the narrowing and shift to shorter times of the relaxation times distribution. This smooth, 'depth-dependent' dynamics may have important consequences for protein function. It may allow local reorganisation of the structure for efficient ligand binding without affecting the internal stability.

(Thesis of S. Dellerue, 2000).

4.2. Influence of ligand binding on the internal dynamics of globular proteins

(Postdoctoral work of C. Loupiac)

Previous studies of Benson et al [7] using H-D or H-T exchange led to observe some modification of the kinetics exchange after ligandation of oxygen to hemoglobin. On the basis of these previous observations, dynamics of human hemoglobin without O_2 (Hbdeox) and with O_2 ligand (HbO2) in solution has been studied by quasi-elastic and inelastic neutron scattering. The results of experiments carried out, on spectrometer MIBEMOL (energy resolution of .96 μeV) show very small changes between the EISF's of Hbdeox and HbO_2. There is no variation of the proportion of mobile protons (close to 20 %) meaning that, at the picosecond time scale, the dynamics of Hb is not affected by O_2 ligand binding. The evolution of vibrational density of states as a function of temperature has been studied. In collaboration with D. Perahia (Orsay), some MD simulations are in development.

4.3. Influence of trehalose on the internal dynamics of globular proteins

(Thesis of I. Koper)

Among protecting agents, trehalose has the highest effectiveness to stabilise and protect biomaterials against denaturation caused by external stresses. Neither the protecting mechanisms of trehalose nor its highest effectiveness are clear. A strategy to elucidate this mechanism has been to study the interactions between trehalose and a protein, the C-phycocyanin (CPC), by quasi-elastic neutron scattering. Figure 3 compares the intermediate scattering function of hydrated CPC powder[8] with that of a hydrated powder when deuterated trehalose is added to water. In the latter case, one observes a slowing down in the dynamics of the protein by one to two orders of magnitude. Addition of trehalose to the protein affects only slightly the geometry of movements, thus leaving no evidence for direct interactions between sugar and protein.

[6] J.-M. Zanotti, M.-C. Bellissent-Funel and J. Parello, Biophys. J., 76 (1999) 2390

[7] Benson et al, Biochem., 12 (1973) 2699

[8] S. Dellerue, A. Petrescu, J.C. Smith, S. Longeville and M.-C. Bellissent-Funel, Physica B, 276-278 (2000 514-515

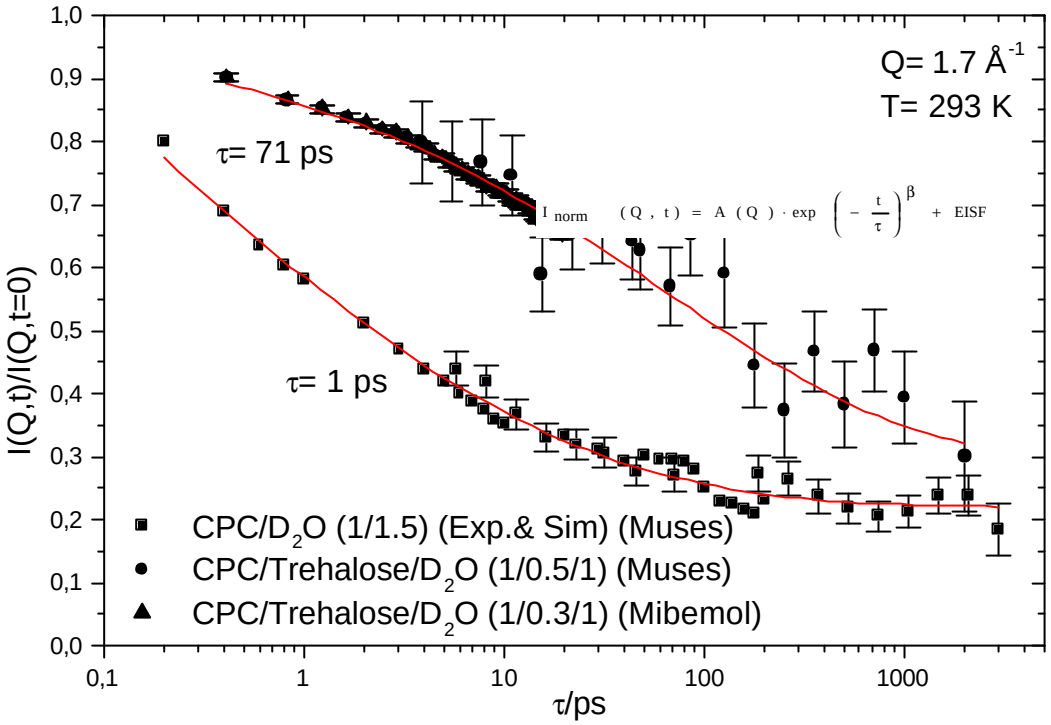

Figure 3. Intermediate scattering function combining different instruments and techniques. Results obtained at a scattering vector of 1.7 $Å^{-1}$ and at 293K for a sample containing hydrated powers of CPC. 1.) A sample of CPC protein, hydrated to 1.5 g D_2O per g protein, combined with results obtained by molecular dynamics simulation; 2.) A sample containing hydrated CPC/trehalose mixtures. Combination of results obtained on the time-of-flight spectrometer MIBEMOL and the neutron spin-echo spectrometer MUSES. Red lines are results of a fit of the combined curves using a stretched exponential function, taking into account an elastic incoherent structure factor (EISF) to describe the plateau value at longer times.

4.4. Influence of concentration. Oxygen transport in crowded protein solutions

(Postdoctoral work of S. Longeville, LLB, W. Doster, T.U. Munich)

When increasing the concentration of macromolecules in solutions, self-diffusion becomes hindered by interactions with neighbours. Above a certain concentration, molecules are trapped in transient cages formed by neighbours. In biological systems such as cells, biological reactions become limited by protein diffusion. Does myoglobin facilitate oxygen transport in muscle cells by macromolecular diffusion at high concentration ? How does the kinetics of oxygen exchange in blood cells depend on hemoglobin mobility ? To understand oxygen assisted protein diffusion, a detailed study of myoglobin and hemoglobin diffusion in very concentrated or *crowded* solutions has been undertaken. In this case, neutron spin-echo spectroscopy provided a very fruitful and unique tool to study diffusion of protein solution on length scales corresponding to the centre-of-mass distances. In fact, dynamic light scattering experiments are impeded by strong absorption by the heme and multiple scattering. For the first time, *in vivo* hemoglobin diffusion from blood cells has been studied using the new spin echo spectrometer MUSES. For myoglobin, the diffusion coefficient is reduced by a factor of 15 when going from dilute solutions to 32 mM solutions.

4.5. Internal dynamics of the membrane mediated photosynthetic apparatus from purple photosynthetic bacteria. (Postdoctoral work of A. Gall)

During 1999-2000, the experimental work was divided into four parts: (i) large scale preparation of H/D-exchanged RC-LH1 and LH2 pigment-protein complexes. The exogenous detergent was then replaced by a deuterated lipid (DMPC) environment. Protein integrity was verified by electronic absorption and infrared spectroscopies. (ii) Incoherent quasi-elastic neutron scattering (IQENS) experiments using the above proteins were undertaken. (iii) Structural studies of these same proteins (in detergent or native membrane) by

electronic absorption and Raman spectroscopies under applied hydrostatic pressure were made as a prelude to neutron scattering experiments under similar conditions. (iv) Small-angle neutron scattering measurements on the LH1 subunit called B820 established that the structure is a dimer of two single membrane-spanning polypeptides with non-covalently attached bacteriochlorin molecules[9].

Compared to previous IQENS studies using MIBEMOL (λ = 6Å, Resolution 96 µeV, Q_{max} = 2 $Å^{-1}$) of detergent-isolated RC-LH1 in full solution (Thesis of S. Dellerue, 2000), in a lipid environment the internal dynamics is more restrained. Since the RC is encircled by the LH1 protein, it is unclear to which extent each component is influenced by the hydrophobic region of the lipids. This work is continuing using a range of different resolutions such as those obtained at ILL with IN13 (Resolution 8 µeV, Q_{max} = 5 $Å^{-1}$) and IN16 (Resolution 1.2 µeV, Q_{max}= 2 $Å^{-1}$). This allows us to cover the largest temporal and Q-space windows with the aim of better characterising the dynamics of the system.

In collaboration with the University of Tartu, Estonia, electronic absorption and pre-resonance FT-Raman spectra for the RC, LH1 and LH2 proteins using their bacteriochlorins as internal molecular probes show that the proteins are still intact at pressures where globular proteins, such as lysozyme, are generally denatured. It should be noted that Raman spectroscopy is a vibrational technique complementary to inelastic neutron scattering.

It was established that the stability of LH2 is both strain and medium specific, and that under optimised conditions protein denaturation was not observed. In the case of the RC from *Rhodobacter sphaeroides*, two proteins were studied, one where large internal cavity is produced (mutant) and the second (wild type) where no such internal void is present. It was established that there are at least 3 pressure domains where different structure changes occur without denaturing the proteins between atmospheric and 0.8 GPa[10]. Thus, we have established the pressure parameters that will enable us to develop inelastic neutron scattering of membrane proteins, something that has never before been achieved. To this end, this protein system provides an important contribution to the overall understanding of the inherent differences between integral membrane proteins, and globular proteins, which are located in the cytosol. Finally, in collaboration with R.J. Cogdell FRSe (University of Glasgow, Scotland) who elucidated the structure of the LH2 protein and a number of RC mutants, the biochemical aspects of the project have been optimised. More specifically, we have characterised numerous altered LH2 proteins by resonance Raman spectroscopy. These studies were preceded by more general Raman studies, into the structure and conformation of the molecular interactions assumed by the pigment cofactors with the polypeptide scaffold [11 12].

5. CONCLUSION

5.1. Perspectives

During the coming years, the fruitful strategy applied to C-phycocyanin protein will be extended to other systems. In order to get a full landscape of the dynamics of biological systems in relation with their function, it is necessary to do experiments at different energy or time resolutions. For this purpose, efforts will be devoted to get samples fully and specifically deuterated. Membrane proteins are good candidates for that, but some soluble proteins are envisaged. Combined with the proposed strategy, the MD simulations will be performed to access a detailed knowledge of the protein dynamics in terms of relaxation times and geometry of motions of various parts of proteins (domains, backbone, side chains,…). Up to now, the effect of temperature on conformational changes and dynamics of protein has been considered. Aother interesting parameter is the pressure and its influence on protein folding. It is now well accepted that a protein strongly interacts with its environment. Hydrostatic pressure allows the properties of a solvent to be modified in a simple way and may lead to a better understanding of some of the solvent effects on the protein structure and function. Preliminary SANS measurements on horse myoglobin (Postdoctoral work of C. Loupiac) have shown that no significant structural changes occurs up to 3 kbar. Higher pressures may lead to protein denaturation. The conformation of the pressure denatured states is unknown and is one of the future research

[9] A. Gall, S. Dellerue, K. Lapouge, B. Robert and M.-C.Bellissent-Funel, Biopolymers, 58 (2001) 231-234
[10] A. Gall, A. Ellervee, M.-C. Bellissent-Funel, B. Robert and A.Freiberg, Biophys. J., 80, (2001) 1487-1497
[11] A. Gall A, N.J. Fraser, M.-C.Bellisent-Funel, H.Scheer, B.Robert, R.J.Cogdell, FEBS Letters, 449 (1999) 269-272
[12] A. Gall and B. Robert, 1999, Biochemistry, 38, (1999), 5185-5190

ways. For such a study, it is interesting to use horse myoglobin as a model protein to take advantage of the experimental results previously obtained under pressure. In particular, results from infrared spectroscopy show an increase of the strength of hydrogen bond network with a reorganisation of the α-helices for pressures up to 12 kbar[13]. Finally, the studies of dynamics of protein solutions under pressure will be extended to membrane proteins. New pressure cells are being designed to sustain 12 kbar.

5.2. Responsabilities at the interface Physics-Biology and Chemistry-Biology

The expertise of LLB in the field of water is internationally recognised. Two LLB researchers (M.-C. Bellissent-Funel and J. Teixeira) have organised, in August 2000, the Research Gordon Conference on Water, held in Plymouth (USA).

LLB has an active participation at the Physics-Biology and Chemistry-Biology interfaces as demonstrated by its involvement to organising schools, congress, Hercules Practicals, LLB Fan etc.. Examples are the organisation of a -NATO School, entitled 'Hydration Processes in Biology', with the publication of the book in 1999, and of a minicolloquium at the interface Physics-Biology held during the Congress of Physics of Condensed Matter in 2000 in Poitiers. LLB has also participated at the session on Biology during the Table Ronde ESS Evaluation Stratégique (TRESSES) on january 2001 and contributed to the resulting report.

The Department of Life Sciences of CNRS created in 2000 the GDR- 1862 entitled 'Fonction et Dynamique des Macromolécules Biologiques' (Responsibles : M.-C. Bellissent-Funel and J. Parello), for which a congress took place at Saclay on January 2001.

In collaboration with the IBS (Grenoble) and INFM (Italy), LLB has participated to the creation of IN13 CRG, at ILL. Because of its unique characteristics (resolution 8 μeV associated to a wide Q range, Q_{max} = 5 $Å^{-1}$), this backscattering instrument allowed us to fill a gap between the time of flight (MIBEMOL) and spin echo (MUSES) instruments.

[13] Le Tilly, Eur. J. Biochem. 205 (1992) 1061

DYNAMICS OF TWO-DIMENSIONALLY CONDENSED WATER ON HYDROXYLATED CHROMIUM (III) OXIDE SURFACE

Yasushige Kuroda[a], Shigeharu Kittaka[b*], Shuichi Takahara[b], Toshio Yamaguchi[c], and M.-C. Bellissent Funel[d]

[a]Okayama University, Japan; [b]Okayama University of Science, 1-1 Ridaicho, Okayama 700-0005, Japan
[c]Fukuoka University, Japan; [d]LLB.CEA Saclay, France

The dynamic properties of water molecules adsorbed on the hydroxylated chromium (III) oxide surface were investigated around the two-dimensional critical temperature (303 K) by FT-IR, quasielastic neutron scattering and dielectric relaxation techniques. The Cr_2O_3 sample covered with a water monolayer gives a broad band at 3400 cm^{-1} due to the mutual hydrogen bonding between the adsorbed water molecules. The quasielastic neutron scattering data have revealed that when crossing the two-dimensional critical temperature, the motion of the adsorbed water molecules changes from that of a supercritical fluid to that of a solidified phase. The dielectric spectra observed at 298 K have been interpreted in terms of two relaxations due respectively to interfacial and orientational polarizations. The interfacial polarization was explained in terms of a hopping model of protons of adsorbed molecules. As a result, from the behaviour of conductivity, one concludes that below the monolayer coverage, small clusters are formed on the Cr_2O_3 surface.

The knowledge of interactions of water molecules with metal oxide surface is of essential interest. In effect, metal oxide surface is covered with hydroxyls carrying various physico-chemical properties such as heterogeneity, acidity, hydrophilicity. Among metal oxide surfaces, hydroxylated chromium oxide (Cr_2O_3) surface is specifically characteristic because of its exceptionally high homogeneity. As a result, adsorbed water molecules are considered to perform some uniform two-dimensional (2D) phase. Figure 1 shows the phase diagram of a water monolayer on the hydroxylated Cr_2O_3. A 2D critical temperature has been determined to be 303 K, but the triple point has not been observed. Thus, the question is raised if the condensed phase is either liquid or solid on the basis of physico-chemical point of view. Dynamic properties of water molecules in this system was investigated by using FT-IR, quasi-elastic neutron scattering, and dielectric techniques.

Results and Discussion

In a previous work (1), a broadening of OH stretching band of monolayer water at ~3400 cm^{-1} was observed above 2D critical temperature, suggesting the easing of the lateral bonding of monolayer water. FT-IR measurements of the surface hydroxyls and monolayer water at low temperatures suggested that there were no definite phase changes below the 2D critical temperature.

Quasielastic neutron scattering experiments were realized on a water monolayer as a function of temperature using the cold neutron beam of MIBEMOL. The obtained spectra were fitted with one delta function and one Lorentzian function. Fig. 2 represents the half-width at half maximum (Γ) of the quasielastic part of the spectra as a function of the momentum transfer Q. Below the 2D critical temperature, Γ values are independent on Q, while above this temperature, Γ exhibits some increase at large Q values. The latter tendency becomes marked as temperature increases. This change in Γ-Q relation above 297 K suggests some change in rotational motion from three sites to higher sites model: this suggests that the environment of the water molecule evolves from some ice-like water to some hypercritical liquid (2).

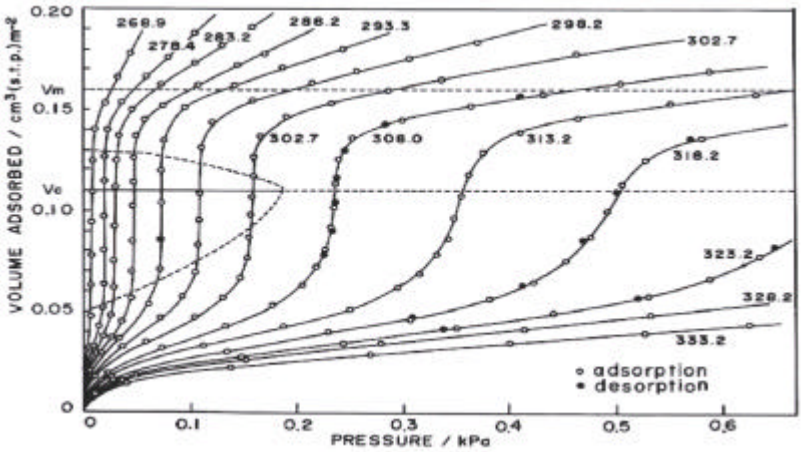

Figure 1. Adsorption isotherms of water on hydroxylated Cr_2O_3 surface at various temperatures.

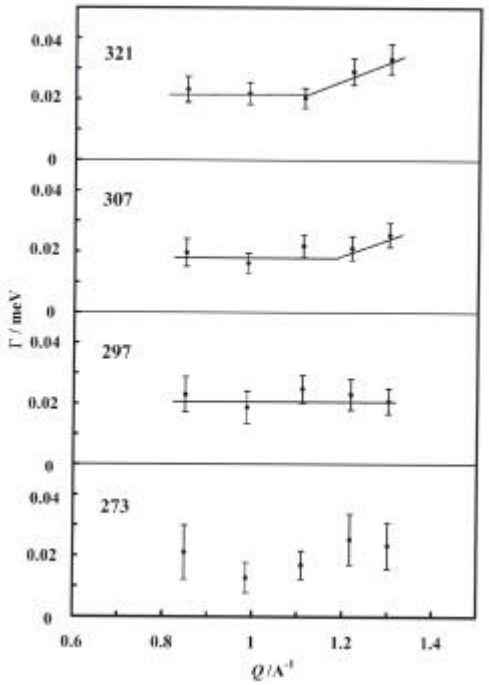

Figure 2. HWHM-Q relation for the adsorbed water on the hydroxylated Cr_2O_3 surface.

The structure and dynamic properties of adsorbed water below the critical temperature were inferred, into details, from dielectric measurements. Figure 3 shows the effect of coverage on the dielectric permittivity (ε') of the system determined at various frequencies (numbers in Hz in figure 3). Constancy of values of dielectric permittivity at the 2D condensation region shows that the increase in adsorbed water molecules does not directly lead to an electric conductivity increase and thus the relaxation is not of Onsager type (3). In other words, we may say that the 2D condensed phase is composed of monolayer patches on the hydroxylated Cr_2O_3 surface.

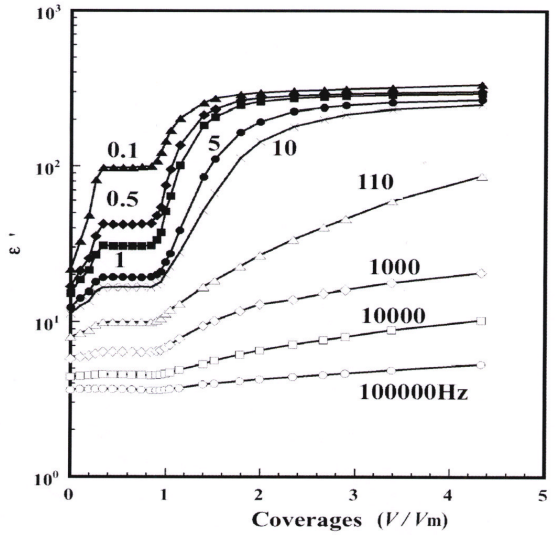

Figure 3. Dependence of dielectric permittivity, ε', versus coverage of H_2O adsorbed on Cr_2O_3 at 288 K for various frequencies.

Figure 4 shows one example of Cole-Cole plots of relaxation for the system including water monolayer (coverage 1.1) at 298 K. The inset is an expanded figure of the smaller part of the full plot, corresponding to the contribution of dipolar polarization relaxation. The characteristic frequency (peak point of dielectric loss curve) for this relaxation is about 300 Hz, which is much smaller than 2.5 kHz for ice at 273 K and 18 GHz for liquid water at 293 K (4,5). Furthermore, this is smaller than 33 kHz for a water monolayer on SrF_2 at 159 kHz (6), as shown by a neutron study which will soon be reported. It is clear that water on the hydroxylated Cr_2O_3 has strongly hindered rotational motion below the 2D critical temperature due to ice-like structure originating from commensurating structure with (001) Cr_2O_3 surface.

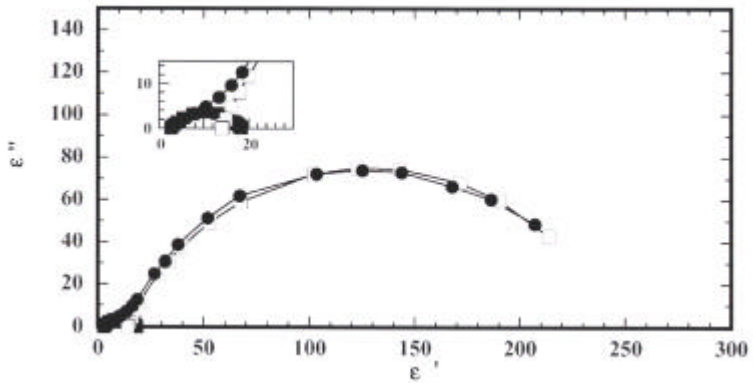

Figure 4. Cole-Cole plot (●) for the relaxations observed at 298 K and the coverage of 1.1. Interfacial (□) and dipolar (■) polarizations.

1. Kittaka, S.; Sasaki, T.; Fukuhara, N., Kato, H., *Surf. Sci*., **282**, 255 (1993).
2. Bee, M., *Quasielastic Neutron Scattering*, Adam Hilger,197 (1988).
3. Onsager, L., J. Am. Chem. Soc., **58**, 1486 (1936).
4. Auty, R. P.; Cole R. H., *J. Chem. Phys.*, **20**, 1309 (1952).
5. Collie, C. H.; Hasted, J. B.; Riston, D. M., *Proc. Phys. Soc.* **60**, 145 (1948). Lane, J.A.; Saxton, J. A., *Proc. R. Soc. London, A,* **213**, 473 (1952).
6. Nagao, M.; Kumashiro R.; Matsuda, T.; Kuroda Y., *Thermochim. Acta* **253**, 221, (1995).

TOWARDS AN UNDERSTANDING OF THE INTRAMOLECULAR SIGNAL TRANSDUCTION THROUGH ENZYMES 3D STRUCTURE

G. Hervé[1], J.-M. Zanotti[2] and M.-C. Bellissent-Funel[2]

[1]Biochimie des Signaux Régulateurs Cellulaires et Moléculaires, Université Pierre et Marie Curie, Paris
[2]Laboratoire Léon Brillouin (CEA-CNRS), CEA-Saclay, 91191 Gif-sur-Yvette cedex

E. coli aspartate transcarbamylase (ATCase) is an allosteric enzyme which catalyses the first committed step in pyrimidine biosynthesis. As shown by X-ray crystallography, the binding of the substrates into the protein induces significant conformational changes. The protein switches from a T form towards a R form which results in an increase of 5% of the radius of gyration of the protein. We study the effect of substrate binding on the local picosecond dynamics of ATCase by incoherent quasi-elastic neutron scattering. The implication of these results in the field of signal transduction within enzymes 3D structure is tentatively discussed.

Introduction

In the field of biomolecular regulation, ATCase is an interesting molecular machinery. This 310 kDa enzyme, whose structure is reversibly and co-operatively modified by the presence of its substrates, presents all the known regulation modes of catalytic activity. The latter is in particular strongly activated by ATP, a puric base, but inhibited by CTP and UTP, the two pyrimidic bases that are the final products of the reaction catalysed by ATCase. This interplay of activation and retro-inhibition that ensures the intracellular balance of puric and pyrimidic bases for DNA and RNA synthesis in healthy organisms is seen as a promising powerful tool to be used in cancer therapy.

At the molecular level, how does the fixation of a first substrate on one of the six catalytic sites influence the affinity for the substrate of the other five sites, distant of as far as 70 Å? This is the central problem of "signal transduction". The enzymatic activity of ATCase is modulated by large structural changes (Fig. 1). As a consequence of this structural modification, the radius of gyration of protein, as measured by small angle X-ray scattering increases by 5% [1].

Is enzymatic activity modulated by internal dynamics? The inspection of high resolution structures only enables to estimate enthalpic contributions. Entropic contributions, originating partly from dynamic contributions, are difficult to deduce from structures. Inelastic neutron scattering can help to solve the problem.

Material and method

ATCase was purified from overproducing strains [2]. The protein concentration of the solution was determined by absorbance measurement and found to be 18 mg/ml (0.06 mM). The switch from the T form towards the R form has been obtained by dissolution of exchanged N-(phosphonacetyl)-L-aspartate (PALA) in the solution. The corresponding buffer solution was prepared by addition of same amount of exchanged PALA to buffer solution. Each sample was sealed in a 3.0*4.0*0.8 mm^3 aluminium cell.

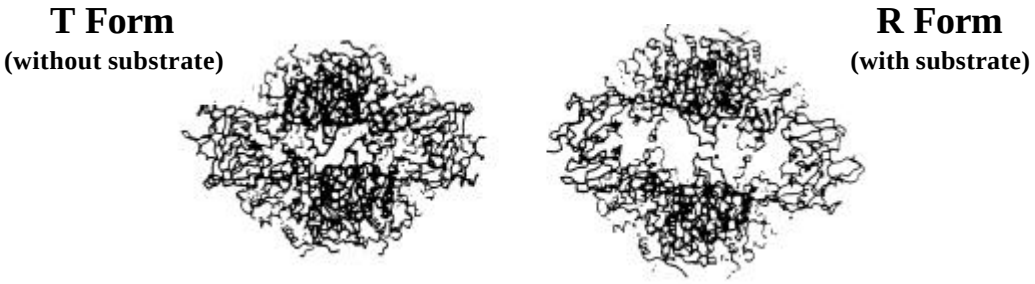

Figure 1: ATCase conformation without substrate (T form) and in liganded state (R form). View along the C_2 axis from [1].

Inelastic neutron scattering

Incoherent quasi-elastic neutron scattering is a unique tool to get experimental information on protein dynamics in the 0.1 to several hundreds ps range. It takes advantage of the large incoherent scattering cross-section of hydrogen atoms (σ_{inc} = 80 barn) with respect to that of other atoms (C, O, N) in proteins. In the present case, we have recorded the difference induced by a slight modification of the system by stabilising the protein in the R state with a non-metabolisable substrate analogue: PALA.

Experiments

The experiments have been performed on MIBEMOL time-of-flight spectrometer of LLB using two different energy resolutions (96 μeV, λ = 6 Å and 410 μeV, λ = 4 Å). Figure 2 presents a quasi-elastic spectrum obtained at a resolution of 96 μeV.

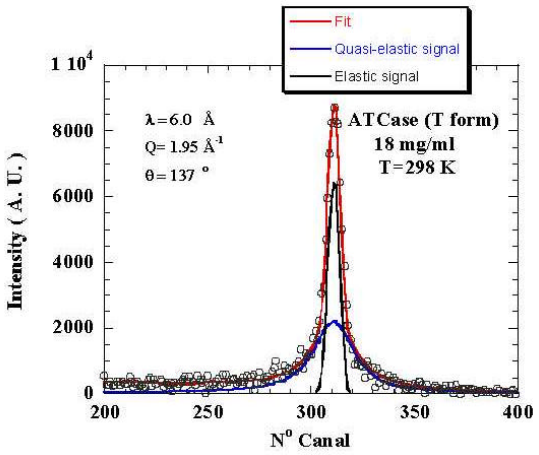

Figure 2. Incoherent quasi-elastic spectrum of T form of ATCase 18 mg/ml at T=298 K. The buffer signal has been subtracted. The resolution is 96 μeV. Circles are the experimental points, the red solid line is the model fit using an elastic peak and a single Lorentzian line. The elastic and quasi-elastic contributions are shown as black and blue lines respectively.

Results

From the Q dependence of the integrated intensity of the quasi-elastic region, the averaged mean-square vibrations of protons $\langle u^2 \rangle$in the protein are obtained. There is no significant effect of PALA on their values given below:

$\langle u^2 \rangle_{ATCase}$ /3=0.09 ±0.05 Å^2 and $\langle u^2 \rangle_{ATCase+PALA}$/3=0.07 ±0.05 Å^2.

The spectra are well described by an elastic peak (correlation times longer than the time resolution) and a quasi-elastic component with a Lorentzian line shape (Fig. 2) [3]. The self-diffusion coefficient of the protein in solution has been taken into account in the analysis of the spectra. From the Elastic Incoherent Structure Factor (EISF) we access the geometry of motions. Due to the narrow time window of the instrument, the dynamics of the system is well described by a single Lorentzian line providing with a single correlation time, even if a broad distribution of correlation times exists in the system. Due to the complexity of the system, we have chosen to describe the EISF in terms of a simple model: a model of a particle diffusing inside a sphere of radius a allows to fit properly the data and to show that the diffusive motions are experienced by surface residues (Fig. 3).

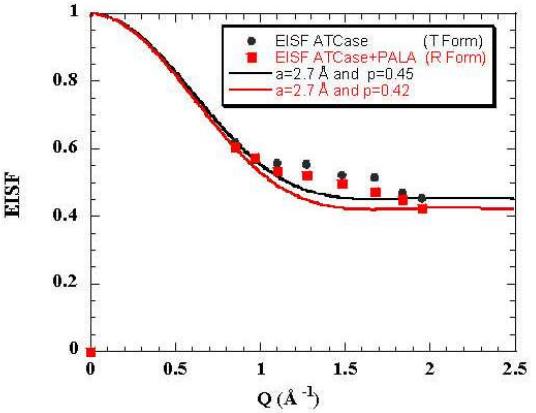

Figure 3. Experimental Elastic Incoherent Structure Factor of T and R forms of ATCase. Error bars are of the size of the points. Fit using the model from ref. 3 (red and black full lines). The extra broad contribution around 1.4 Å is due to a coherent contribution, not taken into account by the model.

Conclusion

Short-time dynamics of ATCase has been studied by quasi-elastic neutron scattering. At room temperature, about 55% of protons experience diffusive motions inside a sphere of radius 2.7 Å, on a time-scale of 15 picoseconds. The fraction of mobile protons essentially accounts for protons of the polar and charged side-chains at the surface of the protein. A slight, but significant difference in the dynamics of T and R forms of ATCase, is revealed by an increase of 3% of the fraction of protons experiencing diffusive motions upon ligand binding (see EISF). The obtained difference is not due to a modification of the whole protein dynamics**.** It is a consequence of the modification of the structure protein upon ligand binding. The protein accessible surface

area is increased by 16000 Å^2. This large increase of surface accessibility is consistent with the take up of 200 water molecules as measured by Li Cata et al. [4] by osmotic stress technique. This important finding shows how much careful comparison between neutron scattering data from different proteins has to be made. This is particularly the case for homologous proteins (extremophiles as an example) that have the same function but different sequences and so slight difference between accessible surface areas or conformations.

[1] L. Fetler, P. Tauc, G. Hervé, M. Moody and P. Vachette, J. Mol. Biol., 251 (1995) 243.
[2] S. F. Nowlan and E. R. Kantrowitz, J. Biol. Chem., 260 (1985) 14712-14716.
[3] J.-M. Zanotti, M.-C. Bellissent-Funel and J. Parello, Biophys. J., 76 (1999) 2390;
J. Perez, J.-M. Zanotti and D. Durand. Biophys. J., 77 (1999) 454.
[4] V. J. Li Cata and N. M. Allewell, Biochemistry, 36 (1997) 10161-10167

BIOFUNCTIONAL ASSEMBLIES AT LIPID INTERFACES THROUGH RECOMBINANT SPHERICAL BACTERIAL PROTEIN

M. Tristl[1], I. Haase[2], S. Marx1[1], L.T. Lee[3], M. Fischer[2] and E. Sackmann[1]

[1] Physik Department, Technische Universität München, James Franck Str. D-85748 Garching (Germany)
[2.] Lehrstuhl für Organische Chemie und Biochemie, Technische Universität München, Lichtenbergstr. 4 D-85748 Garching (Germany)
[3.]Laboratoire Léon Brillouin (CEA-CNRS)

A novel strategy to construct biomimetic assemblies of bio macromolecules on supported membranes is presented. It is based on the anchoring of a 15 nm ball-like recombinant protein, lumazine synthase, on a phospholipid membrane. These proteins have functional groups pointing in solution. They are coupled to phospholipids in solution exhibiting different functional headgroups like biotin and Ni chelator complexes. In this feasibility study we probe the adsorption dynamics of LuSy molecules on phospholipid membranes functionalised with different key-lock like binding mechanisms. The density of adsorbed protein is followed by neutron reflectivity experiments. The influence on the adsorption process of the concentration of a competing inhibiting lipopolymer (phospholipid with polyethylene-glycol headgroup called PEG) at the interface was also measured.

Introduction

The interest in microstructured biofunctional surfaces has increased dramatically during the last years owing to numerous potential practical applications as for example the design of smart biosensors on electrooptical devices (Fromherz [1] , Sackmann [2]) and the surface anchoring of proteins under non-denaturing conditions e.g. for applications in the rapidly developing field of proteomics or to stimulate tissue growth on transplants (Kanthlehner [3]).

These biofunctional surfaces have also a fundamental interest. They allow the study of the physical basis of self-assembly of biomembranes and lipid/protein interaction mechanisms by various surface sensitive techniques. They also allow the design of mimetics of cell and tissue surfaces which permit to study the regulation of cell adhesion by the interplay of receptor mediated lock-and-key forces which are universal interfacial forces. Finally, it plays a key role in the understanding of the cell membrane elasticity (Sackmann [4]).

Lumazine Sythase

In the present work, we introduce a versatile new tool for the design of smart biomimetic solid surfaces based on a large recombinant protein: the lumazine synthase (LuSy) from Bacillus subtilis. Lusy is composed of 60 β subunits and has a ball-like structure with a diameter of 15 nm and a hole of 5 nm in it.

The Lusy proteins are prepared by genetic engineering. They can thus be easily modified and selectively conditioned by coupling of functionalized groups. Lumazine Synthase can exist in a number of different oligomerization states[5-9] and has been studied in considerable detail [8,10-11]. An outstanding feature of Lusy is that the amino as well as the carboxyl end of each subunit are located on the outer surface of the protein, enabling the recombinant coupling of anchoring groups (such as biotin, histidin tags or even other proteins like hisactophilin).

A major advantage of this coupling techniques is that direct contact of the bound protein with the surface is largely avoided and thus non-specific binding is minimised. By using proteins with histidin tags the reversible binding and unbinding of, for example, actin can be induced by small changes in pH (as shown in Behrisch 1995) or by chelator antagonists such as EDTA or Imidazole.

Neutron reflectivity experiments

Over the last years, it has been shown that neutron reflectivity is a very powerful technique to characterise bio-active surfaces with grafted films (Deme [12]). It opens new possibilities to study the interaction of water-soluble amphiphilic proteins with lipid membranes and to observe protein-protein recognition processes.

The experiments were performed at the liquid-air interface using the EROS reflectometer. A teflon tray of a size of 4 cm by 10 cm and 1 mm deep containing 13 ml of D_2O buffer was used. A waterbath was used to control the temperature. To prevent exchange of D_2O with H_2O, a lid with quartz glass windows for the neutron beam was

used to cover the whole cell. To measure and control the surface pressure, a Wilhelmy plate attached to a spring balance was used.
The neutron reflectivity technique allows us to measure, in real time, the amount of the protein adsorbed to a lipid surface.
We present here the evolution with time of the structure of the protein layer for two different functional binding groups: histidin and biotin. In the case of histidin, the effect of the concentration of inhibiting polymers (*i.e* PEG) at the lipid interface has also been tested.
This study shows that different binding behaviour must be considered depending on the functional groups of the protein and the phase of the lipid interface (crystalline or liquid).

NTA protein and PEG

Reflectivity curves have been obtained after adsorption of LuSy functionalized with histidin tags, to the lipid interfaces. These interfaces consist of 90 mol% of DMPC lipids and 10 mol% of DOGS-NTA-Ni lipids which can bind histidin. Curves are represented on figure1. The lipid layer was spread to a surface pressure of about 30 mN/m, where DMPC is known to be still in a liquid phase. The fit enables us to obtain the evolution of the absorbed quantity of protein to the interface as a function of time and to determine the saturation value (Figures 3 and 2).

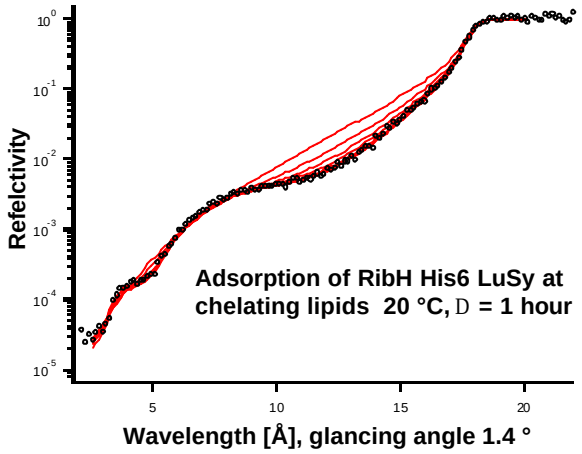

Figure 1. Reflectivity data obtained during the adsorption of LuSy to a Ni Chelator covered surface. The lines correspond to the best fits of the neutron reflectivity data sets, plotted over wavelength. The time distance between two sets of data is one hour.

In order to quantify the influence of the inhibiting polymers at the lipid interface, the same measurements were performed while introducing increasing concentration of PEG lipid in the DMPC matrix (still containing 10 mol% of DOGS-NTA). The results are reported on Figure 2, and show clearly that the amount of LuSy bond to the surface is reduced. The steep decrease of LuSy adsorption between 0.8 and 1.7 mol% PEG can be explained with a phase transition of PEG from a pancake to mushroom like phase.

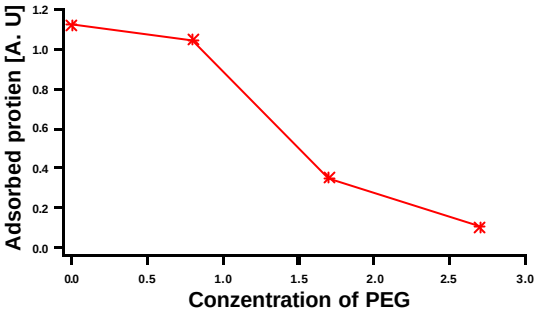

Figure 2. Saturation values of adsorbed LuSy depending on PEG concentration at the lipid layer.

NTA protein and Biotin

The binding dynamics also depends on the phase of the lipid layer or binding interface. To check that fact we choose to measure also the adsorption kinetics of LuSy using another locking process to the interface. This new locking process consist of LuSy functionalized with biotin and streptavidin in solution, a protein which can strongly bind biotin. The binding constant of the streptavidin-biotin binding is much stronger than the one of the histag-Ni chelator binding used previously. Therefore a faster binding process (and eventually a denser protein layer) was expected. In fact, the opposite was observed (see figure 3). One possible reason for this is, that streptavidin forms at the interface a crystallised layer with much less in plane diffusion than the previous liquid DMPC resulting in a slower process. Another possible reason is that the free streptavidin available in the solution, results in aggregation of LuSy. These big aggregates have a much lower diffusion constant in the subphase and this results also in a slower adsorption process leading to a lower effective LuSy concentration.

The presence of a streptavidin mediated interaction between LuSy molecules also gives rise to a new situation at the surface. The LuSy adsorbs to the interface not in the form of a monolayer but in a more complicated fashion (figure 4). This is shown by the fact that it is no longer possible to adequately fit the data with a monolayer model. The correct model consists of a dense monolayer followed by progressively more dilute protein layer.

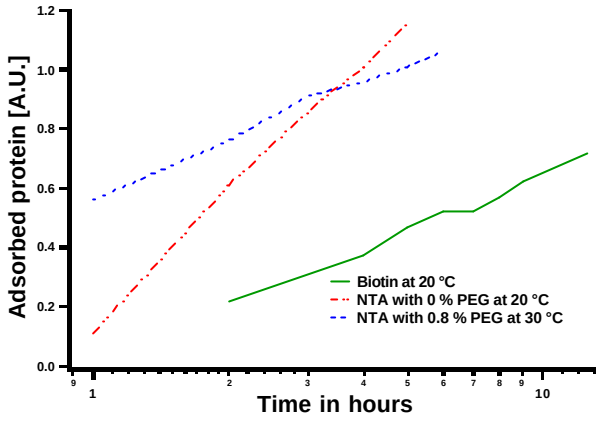

Figure 3. Dynamic adsorption of protein to the interface. The graph shows different dynamical adsorption processes: the adsorption of histidin tagged LuSy without and with 0.8 mol% PEG lipid and compares the two processes with the adsorption of a biotin coated LuSy to a streptavidin interface. Considering the fact that the streptavidin biotin binding is much stronger than the NTA Ni-Chelator binding, this dynamic behaviour needs further explanation (see text).

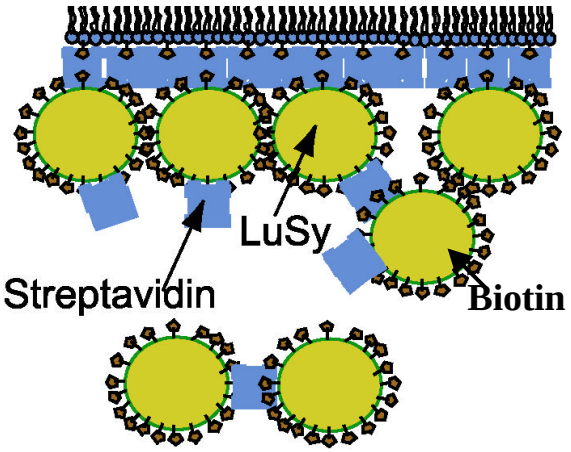

Figure 4. Model of multilayers to fit the data of biotin Lusy adsorbed to a streptavidin interface

[1] P. Fromherz, A. Offenhauser, T. Vetter, I. Weiss, *Science* **1991,** *252*, 1290-1293.
[2] E. Sackmann, M. Tanaka, *Trends Biotechnol* **2000**, *18* pp 57-64.
[3] M. Kantlehner, D. Finsinger, J. Meyer, P. Schaffner, A. Jonczyk, B. Diefenbach, B. Nies, H. Kessler, *Angew. Chem.* **1999,** 111, Nr.4, 587-590.
[4] E. Sackmann, *Science* **1996,** *271*, 43-48.
[5] B. C. Braden, C. A. Velikovsky, A. A. Cauerhff, I. Polikarpov F. A. Goldbaum, *J. Mol. Biol.* **2000**, *297*, 1031-1036.
[6] W. Meining, S. Mörtl, M. Fischer, M. Cushman, A. Bacher, R. Ladenstein, *J. Mol. Biol.* **2000**, *299*, 181-197.
[7] K. Persson, G. Schneider, D. B. Jordan, P. V. Viitanen, T.Sandalova, *Protein Sci.* **1999,** *8*, 2355-2365.
[8] R. Ladenstein, K. Ritsert, R. Huber, G. Richter, A. Bacher, *Eur. J. Biochem.* **1994**, *223(3)*, 1007-1017.
[9] W. Zhang, X. W. Meining, M. Fischer, A. Bacher, R. Ladenstein, *J. Mol. Biol.* **2001,** (in press).
[10] R. Ladenstein, M. Schneider, R. Huber, H. D. Bartunik, K. Wilson, K. Schott, A. Bacher, *J. Mol. Biol.* **1988**, *203(4)*, 1045-1070.
[11] K. Ritsert, R. Huber, D. Turk, R. Ladenstein, K. Schmidt-Bäse, A. Bacher, *J. Mol. Biol.* **1995,** *253(1)*, 151-167.
[12] B.Demé, D.Hess, M.Tristl, L.T. Lee, E. Sackmann, *Eur.Phys.J. E 2* **2000,** *1999*, 125–136.

TECHNICAL AND INSTRUMENTAL DEVELOPMENTS

The development of the neutron technique and the research of new methods are two permanent goals of the LLB activity. Due to the wide field of condensed matter research in which the neutron spectrometry is involved and often even unique, this domain of activity is very large. It ranges from the designs of new spectrometers, but also implies improvements of the existing instruments (neutron flux, versatility). Optimised neutron focussing and better polarising systems are now installed on the spectrometers. Technical developments also concern the sample environment facilities: high magnetic fields (12T), cryostats (down to 50mK), furnaces (1800°C), pressure systems (40GPa)… The wide use of these devices also requires the development of raw data acquisition and data treatment systems, as simple as possible to use. All this specific neutron instrumentation generally results of collaborations between the researchers and the technical staffs (designs and drawings, "small" mechanics, electronics, computing) of the LLB, and more recently European networks between centers.

During the period 1999-2000, among the activities of the LLB, we find some important technical realisations. The major one is the rebuild of the 2T channel with a larger geometry of the output neutron beam. This important change close to the reactor core was accompanied with a new more brilliant thermal triple axis spectrometer with the polarised neutron option, owing to the higher flux of 2T. The experimental installations of LLB are continuously modernised or implemented with new options, such as the grazing angle diffractometer. Several specific neutron instrumentation projects are also developed at LLB, generally for peculiar needs of the laboratory. As example, microstrip detectors and polarising multilayers have been and will be produced and installed on several spectrometers of the laboratory. We wish to mention the powerful data acquisition and control system realised by the electronics staff of LLB, which is spread not only in neutron spectrometry, but also for X-rays or light diffraction in other laboratories.

Besides these important developments, numerous other realisations in various domains have been carried out (new sample environments, new acquisition or data treatment programs…), which render the domain of application of neutron scattering always larger.

DEVELOPMENT OF SPECTROMETERS.

A recurrent demand in neutron spectroscopy concerns the **increase of the neutron flux**. Huge progresses have been obtained in this way, due to important improvements either in multilayers guides or in the single crystal manufacture. For instance, with supermirrors guides (even polarizing), the maximum critical angle for neutron reflection (keeping a good reflectivity) is now around $3\theta_c$ (θ_c is the critical angle of naturel Nickel). These improvements, eventually combined with focussing methods, are more and more applied to the instrumentation of LLB.

Such upgrades can be heavy works, as the 2T operation almost finished this year. The latter consisted in an increase of the size of the neutron beam cross-section, 50*120mm^2 instead of 40*75mm^2. The aim of this operation was of course to get higher flux at the sample position, but also owing to the higher flux to provide a world leading ***thermal triple axis spectrometer with polarized neutrons***. Several solutions have been adopted to increase the flux. Better single crystals of Heusler alloy ($AlCu_2Mn$) have been realized in collaboration with ILL. The size of both the monochromator and the analyzer were increased; composed respectively of around 40 and 27 elements, they are bent vertically as well as horizontally. In order to fully benefit from these improvements of the spectrometer, an increase of the beam size of the 2T output was required and thus a ***major modification of the thermal beam tube 2T*** and of its dense concrete shielding. The dismounting of the old 2T neutron beam output and the installation of the new one have been performed during the reactor shut-down, in April 1999. The operation was a full success, realized in due time by the team of the Orphée reactor.

Now the thermal flux on the 2T spectrometer is much higher: the counting rate has been increased by a factor 3. Optimising this spectrometer thus offers new opportunities. Recently, non-polarised experiments on molecular beam epitaxy grown samples have been performed. They successfully led to the determination of

the spin-wave spectrum of MnTe samples, of thickness of about 4-6µm and even of 1µm. Such a sample volume (~0.25mm^3) is well below that usually needed in neutron studies (typically a few cm^3). These experiments on small samples are very encouraging and promise a new way for the development of the neutron scattering spectrometry. The polarized option is being installed in 2001.

A new surface diffraction spectrometer has been mounted on the reflectometer EROS at LLB. Its originality lies in its working mode, a Laue type configuration. It is diffraction measurements at grazing incidence by a white neutron beam. In the grazing incidence geometry, a part of the beam is reflected while another part is transmitted. The latter, the evanescent wave, may be diffracted by Bragg planes perpendicular to the surface. It is then possible to get information concerning the in-plane ordering of a sample from the diffraction signal recorded by a position sensitive detector. Preliminary experiments have already been performed on non-magnetic crystals and on a magnetic Co epitaxial thin film. With the latter, four evanescent Bragg peaks have been measured, corresponding to the four possible spin combinations (++,--,+-,-+). After these promising first measurements, the ***grazing incidence diffraction*** set-up will be installed as a new option of the reflectometer EROS.

The renewal of the detection system of the spectrometer 7C2, the spectrometer devoted to studies of liquids and disordered systems, has started this last year. The wavelength used on this spectrometer is 0.07nm. The old detector was a "banana" (640 cells covering 128°) filled with BF_3 gas. It had a bad detection efficiency (17%), especially for this low wavelength. On the opposite, the microstrip detector technique developed at LLB (see the description in the next paragraph) is filled with 15 bars of ^{3}He gas, which gives a detection efficiency of 80-85%! Thanks to the latter improvement of the detection, the replacement of the banana detector was decided. The spatial resolution of the first microstrip detector of the future spectrometer, has been especially adapted for 7C2. The resolution is 2mm in the horizontal direction and 5mm in the vertical direction. Thirteen detectors of this type will be placed closer to the sample (radius of 1m instead of 1.5m), in quincunx (see Fig. 1) in order to avoid blind detection angles. The total angular detection range will be 130°, with a better resolution in the horizontal plane (0.12° instead of 0.2° previously).

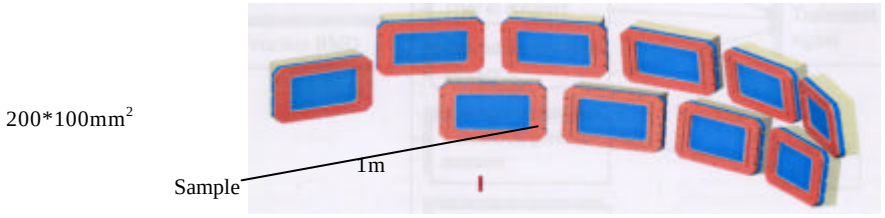

Figure 1. Layout of the future detection system of the spectrometer 7C2: 13 microstrip ^{3}He detectors (200*100mm^2) are placed in quincunx around the sample. One central detector will cover the small q domain.

Finally, we would like to stress the progress in the development of a new spectrometer, the project named **TPA** (Très Petits Angles), for small angle neutron scattering at very low q. The scattering vector range aimed with this new instrument is 10^{-4} - 10^{-2}Å^{-1}. It would allow the studies of large scale objects (1000Å) such as giant micelles, cell membranes, cavities, precipitation in alloys, biophysical gels… The principles are those of classical small angle spectrometers, pin hole collimation and 2D detection, but with a good resolution. For the collimation, methods to increase the neutron flux, such as focusing mirrors or neutron lens, will be studied later on. Concerning the detection, as the manufacture of big detectors for neutrons with a resolution of about 1mm is a present problem, the choice of the image plate technique has been made. An image plate for neutrons designed by MAR Research is now optimised on the guide G5ter. However, this kind of detector being very sensitive to γ radiation, studies of collimator and detector shielding are presently performed. The replacement of the mechanical selector by a supermirror monochromator is envisaged to get rid of the γ coming from the selector.

TECHNICAL DEVELOPMENTS, SAMPLE ENVIRONMENT AND DATA TREATMENT.

A major element in neutron spectrometry concerns the neutron detection. Unfortunately, the manufacture of large multidetectors is now a big problem for all neutron laboratories. The LLB has participated during the period 1996-1999 in the area multidetector of the XENNI program (the 10-Member European Network for

Neutron Instrumentation). In this frame, the LLB has developed ***microstrip gas detectors***. The latter are filled with high pressure He^3 gas to capture the neutrons. The conversion into electric signal is performed through a glass plate, on which a network of anodes and cathodes has been etched. Such device allows a two dimensional detection with a very good resolution (1.5 - 2mm). Several prototypes of such microstrip detectors have been tested on PRISM and EROS (the two reflectometers of LLB). They display a large dynamics and a low noise. At this moment, a large size detector 200*100mm^2 is installed for a test period on the spectrometer 7C2, the spectrometer devoted to studies of liquids and disordered systems. It is a prototype for the renewal of the whole detection system of this instrument (described in the previous paragraph).

Besides, optical gratings used for the manufacture of microstrip detectors could also be used in the field of neutron optics. As a matter of fact, UV lithography makes possible to achieve large surface arrays (several cm^2) with periods down to 200nm. The neutron beam can be diffracted by such gratings. We envisage to use these gratings for the ***energy analysis of the white neutron beam***. As a matter of fact, the diffraction direction is a function of the wavelength. Thus, after diffraction by the grating, one can measure on a multidetector the whole reflectivity curve of a sample, without any 2θ rotation or use of a chopper.

Another improvement of the spectrometers at LLB concerns the replacement of the **mechanical selectors** of the SANS spectrometers. As a matter of fact, due to the supermirror guides installed in the past years, neutrons of short wavelength are now available at the end of the guides where the SANS machines are located. The wavelength corresponding to the maximum flux of the wavelength distribution, is now around 2 and 3Å. In order to meet the repeated demand of users to increase the q range, the PACE spectrometer is now equipped with a Dornier selector. An intensity gain of about 20% (due to a better transmission than the previous Hungarian selector) and a possible choice of small wavelengths (down to 2Å at 24000 rpm when tilting the selector) are expected. On this spectrometer, it is now also possible to remove automatically this mechanical selector and replace it by a guide element in order to perform with an additional chopper, **SANS measurements by time of flight** (TOF) on the white neutron beam. This technique has been used few times in the past at LLB. It allows us to perform SANS measurements in the whole q range in the same time with a good wavelength resolution (1-2%). We thus plan to get larger experience in the TOF procedure, in view of the future European Spallation Source (ESS). We also wish to develop TOF on the XY-multidetectors (PAXE, PAXY). As a matter of fact, thanks to the recent EuroPSD modules developed by the electronic group of LLB, such technical developments could be achieved rapidly and more easily now than previously at LLB.

Developments of the sample environment facilities are also under progress. In particular, neutron scattering experiments under **pressure** are carried out at LLB since several years. On the one hand, in soft matter, even low pressure (<1GPa) may strongly change the inter-atomic distances and the physical properties. In solids, much higher pressures are required to induce a phase transition as example. In the domain of neutron diffraction, the single-crystal diffractometer 6T2 can be used in a so-called "lifting detector" mode, which allows a variety of complex sample environments to be implemented. The equipment suite has been recently extended to encompass a powerful combination of high field (***6 Tesla*** with a ***cryomagnet*** from Oxford Instruments), very low temperature (***50 mK*** with the ***^{3}He-^{4}He dilution insert*** from Air Liquide) and high pressure (***7 GPa*** with the Kurchatov-LLB ***sapphire-anvil pressure cell***) devices (see Fig. 2). The potential of this experiment was demonstrated by recent studies of field-temperature-pressure phase diagrams in TmSe and TmTe compounds.

Figure 2. 6T2 spectrometer equipped with the cryomagnet (6Tesla), ^{3}He-^{4}He dilution insert (50mK). The high pressure cell (mounted inside the cryomagnet) allows to perform experiments up to 7GPa.

Since several years, numerous physical-chemistry systems (lamellar phases, giant micelles, liquid-crystalline polymers) are studied under shear. The experiments consist in applying a shear deformation with a

characteristic time $1/\dot{\gamma}$, where $\dot{\gamma}$ is the velocity gradient. When this time is about some characteristic relaxation times of the complex fluid, important structure changes can be observed. The Small Angle Neutron Scattering technique is especially well adapted to such studies. Several in-situ **shear devices** have been realised: Couette or cone-plate shear cells. Recently, one Couette cell, with quartz windows, was improved since its velocity gradient range extended from 10^{-2} to 800 s^{-1}: this shear cell is specially adapted to the study of soft systems such as colloids. Another Couette cell, allowing studies at higher and better controlled temperature (up to 140°C), has been specially designed for small sample volumes (<500mm^3) (see Fig. 3).

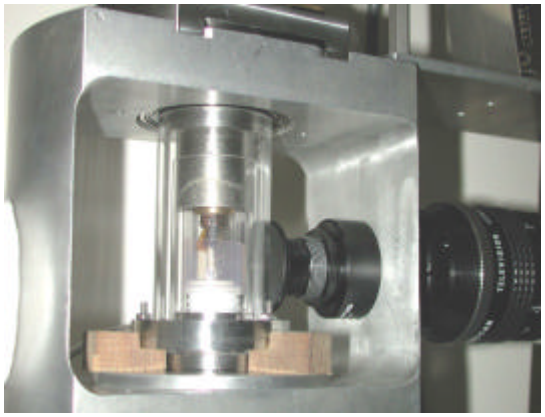

Figure 3. Couette cell, transparent for neutrons, designed to perform in situ small angle neutron scattering experiments under shear. The temperature is controlled up to 140°C. The gradient velocity range is 0.1 to 100 s^{-1}. A video camera records images of the sheared sample.

←→
20mm

The neutron scattering techniques are also very interesting to study materials or devices of technological interest. At LLB several spectrometers are specially devoted to applied research in materials science and technology, for texture and strain-stress measurements. The neutron radiography instrument, installed at the end of the guide G4 of the Orphée reactor, is widely used as a non-destructive testing technique. Such a technique is also interesting to measure some physical properties of materials. Recently, in collaboration with the University of Kiel, ***dynamic neutron imaging*** has been used for the first time to determine in situ ***viscosities and densities of silica melts***. The method consists in monitoring small neutron absorbing spheres falling in silicate melts. The furnace designed for these experiments allows measurements at temperatures up to 2000°C.

Other aspects of the neutron technique are data acquisition and control. All the spectrometers at LLB and several spectrometers in other laboratories in the world are equipped with the intelligent control systems for data acquisition developed by the ***electronic group*** of LLB. In the past, most contracts of this group were scientific collaboration projects, but ever since they integrated the Orphée Technologie's structure, their approach is more commercial and they are very reactive to the client's needs. In this way, the hardware designs have integrated downloading procedures so that the customer can upgrade the system as well as receive maintenance testing programs. Recently, they sold a data acquisition system for 2D detector to ILL, and have completed a contract with the Optic Institute of Orsay to renovate their X-ray spectrometer. In South Africa, they brought up-to-date the control and driving system of a 4-circles neutron diffractometer. A contract for the equipment of a light scattering spectrometer has been signed with the Tunisian Ministry of Education. Thus, the electronic group of the LLB has, since a long time, acquired enough experience to export and promote its know-how in spectrometer process control and data acquisition. Now, the trend is to equip, at LLB and abroad, not only neutrons but also X-rays and laser spectrometers.

On its side, the ***computing group*** of LLB has been working for the last years on a new instrument control software for data acquisition, named "***Programme Orienté Objet de Pilotage de Spectromètres***". The software architecture mimics the architecture of spectrometers, which are all doing different physical studies, but have all many common points (electronic counting devices, sample environments, motors, choppers). The instrument configuration (experiment and environment description) is defined in specific files. From these descriptions, the software adapts itself and constructs the corresponding Graphical User Interface and list of functions available on the spectrometer. It has been carefully defined to help its maintenance and its evolution. The software is now controlling 6 spectrometers of LLB.

To the development of instrumentation, are added those of **programs for data analysis** suited to each method. As example, in some treatment programs of diffraction measurements, new fits to various functions (the Rietveld analysis, pseudo-Voigt decomposition method…) are always implemented. ***FullProf***, a LLB-made program for the determination of complex crystalline structures from powder and single-crystal diffraction patterns, is widely used in physics, chemistry of condensed matter. It has recently been extended to data treatments of X-rays, including from synchrotron radiation sources. Now, crystal superstructures, like incommensurate structures, can be treated. A simulated annealing optimisation has also been included in the program to solve crystal and/or magnetic structures. Fullprof program, including a lot of examples and help, is at the disposal of the scientific community on Internet (http://www-llb.cea.fr/fullweb/powder.htm). Started in 1990, important developments of CRystallographic Imaging using Maximum Entropy (CRIME) have resulted in the maturation of two programs: GIFTED (Generalized Inverse Fourier Transforms for Electron Densities) aimed at x-ray / unpolarized-neutrons, powder / single-crystal, Patterson / Fourier densities and ACE (ACEntric) aimed at Polarized Neutron data and used to reconstruct 3D magnetization densities no matter how large the flipping ratios. Recent applications involve imaging disordered protons in molecular crystals (aspirin, $Ni(NH_3)_6Cl_2$), field-induced magnetic symmetry breaking in ($Nb_{3-x}S_4$) and detection of fractional oxygen in Hg-based high-Tc superconductors.

PERSPECTIVES.

Among the improvements planned for the forthcoming years, one can mention:
- the renewal of the detection system of 7C2 (described in a previous paragraph): thirteen microstrip detectors filled with ^{3}He gaz with an efficiency of 80-85% will increase the counting rate by a factor 4.
- the upgrade of MUSES, the Neutron Resonance Spin-Echo (NRSE) spectrometer, recently installed at G1bis. The NRSE spectrometry, an alternative version of high magnetic field Neutron Spin Echo, is especially well suited for large angle measurements. It allows to measure intermediate scattering functions, from 0.05 to 3 $Å^{-1}$. In order to improve the counting rate of the spectrometer, we plan to implement a multi-angle analysis device. This requires the construction of a second "precession" arm covering a scattering angle of 15°. It includes 25 ^{3}He detectors, the development of appropriate symmetry NSE coils for the measurements of the small time part of the spectrum and two curved or "banana like" resonance coils. The data acquisition unit developed by the electronic group of the LLB will be installed. A possible future development of TOF spin echo spectrometry could be made on this spectrometer. The development and construction of the proposed options will be performed in the frame of the collaboration with the Technische Universität München.

The LLB is also involved into European networks for the forthcoming years (2000-2003). One program concerns the neutron polarisation (in particular the supermirror polarisers and analysers), the European Neutron Polarisation Initiative (ENPI). Besides, the LLB is a member of the European contract, TECHNI (Technology for Neutron Instrumentation program), for the studies of microstrip detectors and gratings.

For the neutron physicist community, the European Spallation Source is a big challenge for the future. The LLB, with respect to its position and responsibility, should play an important role in this project. Namely, concerning the instrumentation, several techniques can be modified and/or developed in order to operate in TOF mode. We have already mentioned the possibility to perform SANS experiments by TOF on PACE (the spectrometer devoted to isotropic scattering). The SANS technique is, at the present, not considered to have a big advantage of the TOF mode. For this reason, a lot of experience could be gained on the SANS spectrometers at LLB, including measurements on multidetectors. Several other possibilities could be also settled, like in the powder diffraction spectrometry. Concerning the TOF, a lot of improvements, as focusing guides, could be made on MIBEMOL, the high resolution TOF machine of LLB, in order to increase the flux.

As a conclusion, all these developments are very encouraging as well as motivating. They render the neutron spectrometry more and more useful and determinant to any research at the microscopic level (structure and dynamics) in physics, chemistry, biology and materials science.

MODIFICATION OF THE THERMAL BEAM TUBE 2T

(Orphée reactor team)

Triple-axis spectrometry is the ideal technique to determine the complete set of vibrational and magnetic excitation dispersion curves in crystalline solids. Important results were obtained recently at the LLB by this technique, in particular on high Tc superconductors and GMR manganites, due to the high flux on thermal and cold instruments, 1T/2T and 4F1/4F2 respectively, built very close to the Orphée reactor core. Nevertheless, the method is limited by the (relatively) low counting rates, and therefore by the necessity to work on large single crystals (typically 0.1 cm^3).

In 1996, it was decided to increase the size of the 2T neutron beam cross-section and to rebuild the corresponding thermal triple-axis instrument with optimized neutron optics, in order to obtain largely increased counting rates, and to install a (new) polarized neutron option. This would make of 2T a world leading instrument.

The aim of this operation was of course to allow to work on smaller samples or to detect weaker effects, owing to the higher flux, but in priority to allow an experimental separation of the magnetic and lattice excitations in solids, in the energy range 10 to 100 meV, using polarized neutrons and polarization analysis.

The first stage of this project consisted to modify the 2T beam output, with an increased beam cross-section of 50×120 mm^2 (instead of 40×75 mm^2 in the "old" version).

This required a safety study in order to optimize the thickness of the zircaloy window, the dimensions of the screws and of the safety gate (made in neutron absorbing Al-Gd alloy), taking into account the case of a BORAX accident (water splash inducing a shock wave of 40 bars during 5 ms) in the new geometry. The safety tests were realized on a mock up (scale 1/2) by the Company SODERA in 1997-98, with direct pressure measurements in front and behind the zircaloy window during the tests, and measurement of the residual strains induced by the tests. Their results were submitted for agreement to the safety authorities (DSIN). The optimization of the new zircaloy window thickness (3.5 mm instead of 1 mm in the "old" version) required an elasto-plastic finite element calculation.

The technical study and detailed plans were performed by GEC-Alsthom. The new beam output was realized in 1998-99 by the Company OMG. The quality (homogeneity and density) of the filling with heavy neutron absorbing concrete (biological shielding) was checked on a transparent mock-up.

The dismounting and the removal of the old 2T neutron beam output, and the installation of the new one, were performed during the reactor shut-down of april 1999 by the team of reactor Orphée. The operation was a full success.

The three following figures show :

Figure 1 : the change of incident neutron beam geometry allowed by the increase of 2T neutron beam cross-section;

Figure 2 :the disposition of beam 2T relative to the reactor core, and a plan of the 2T output (barrel, plug, collimator, shielding device);

Figure 3 : a series of photos, taken during the replacement of the beam tube part, in april 1999, and showing the different stages of the operation.

The description of the new 2T triple-axis instrument and first results are given as a highlight.

The success of this "2T operation" shows that increase of the size of neutron beams issued from presently existing reactors can be performed satisfactorily, if safety tests and calculations are carefully made, and this results in strong improvements of the flux on the instruments. In the case of Orphée, this gives confidence that the ORPHEE-PLUS (second cold neutron guide hall with increased 4F beam size) and ALTOR (enlargement of the 8F neutron output allowing to duplicate the guides G1 to G4) projects are quite feasable technically and would considerably improve the quality of the ORPHEE-LLB neutron source.

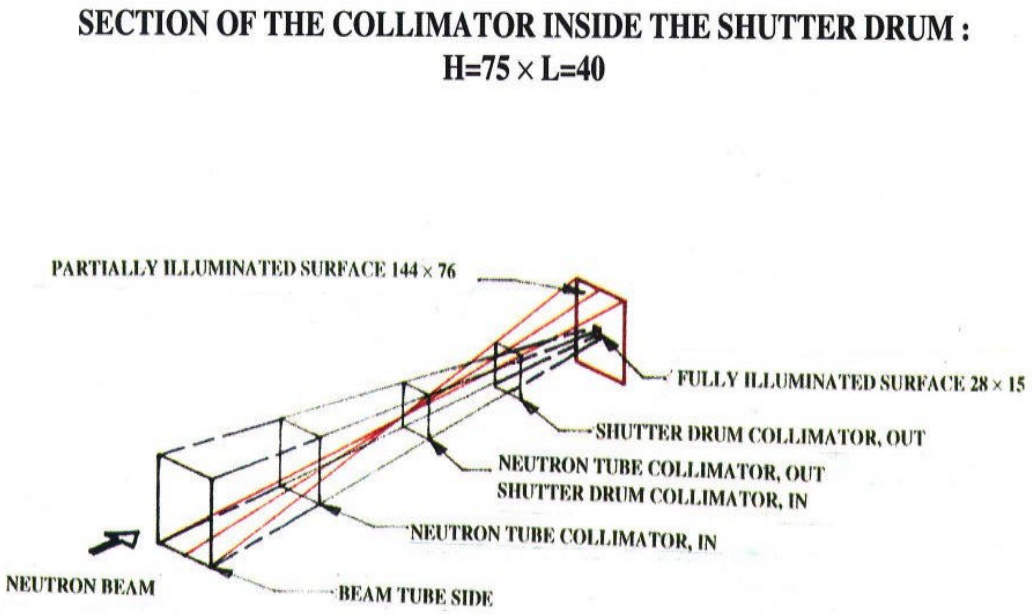

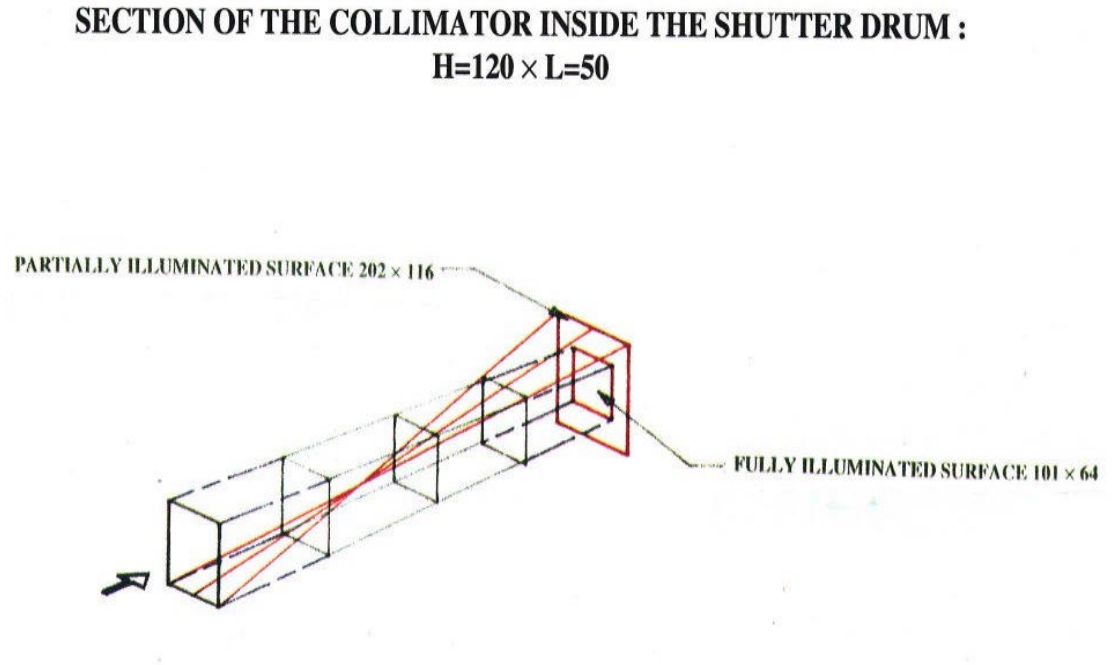

Figure 1. View graphs of the geometry of 2T chanel.

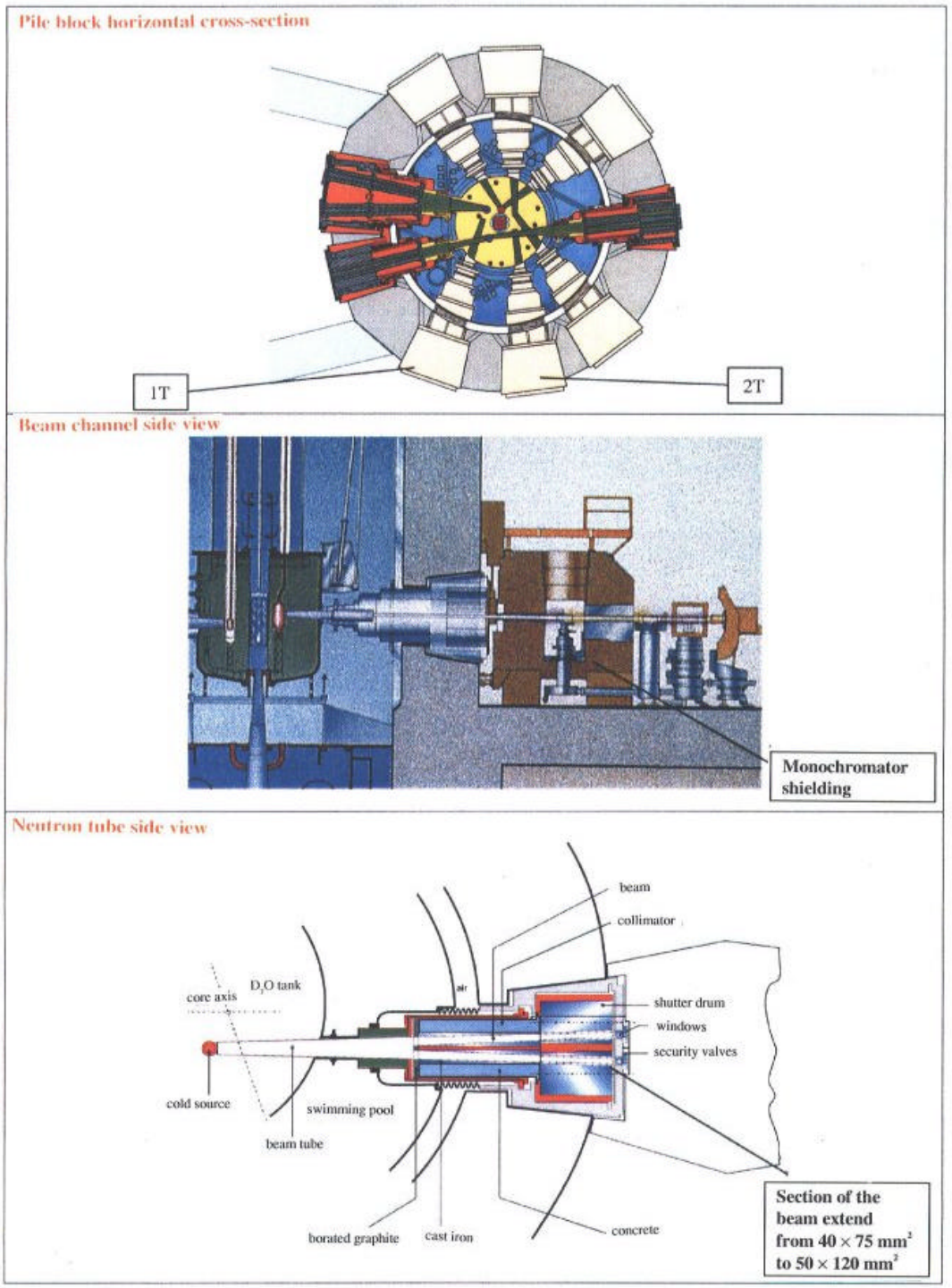

Figure 2. Schemes of the new beam output 2T

1. Before disassembling

2. The instruments are removed

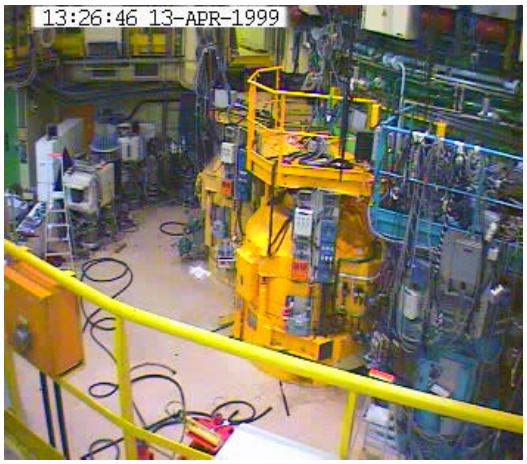

2. The monochromator shielding is displaced

4. The plug is pulled out

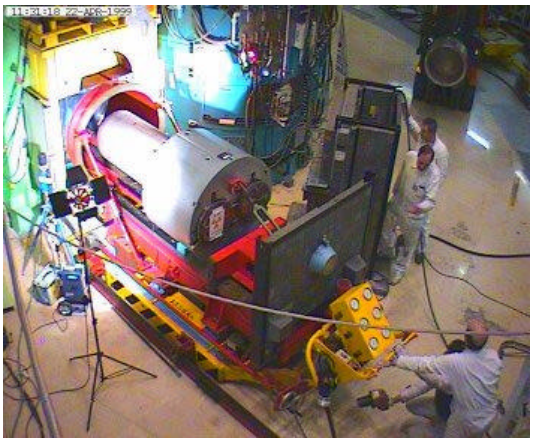

5. Installation of the new

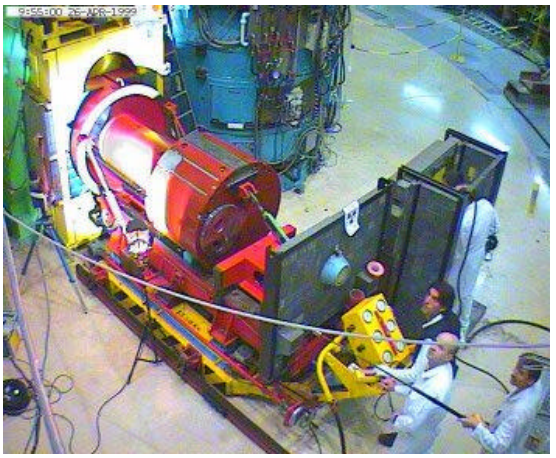

6. Reassembling of the shielding

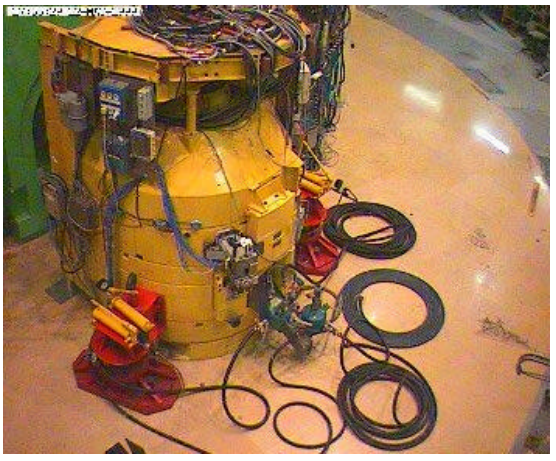

Figure 3. Replacement of the beam tube 2T in april 1999

IMPROVEMENT OF THE 2T TRIPLE AXIS SPECTROMETER

P. Bourges, B.Hennion, P. Boutrouille, J.P. Beauchef, P. Baroni, F. Maignen
LLB (CEA-CNRS)

In order to improve the thermal neutron flux available on the french triple axis spectrometer and to get the opportunity to have a polarized neutron option on this spectrometer, the size of the neutron beam has been changed to get a 5x12 cm^2 surface at the monochromator site. This necessitated a change of the beam port inserted in the beam tube. The wish to keep the possibility to transform the channel 1 from a thermal beam to a cold one, as well as the need for a vertical accessibility of the sample table for the polarized neutron option, led to the decision to swap the french and german spectrometers. The german spectrometer, managed by the group of Karlsruhe, was thus transferred from 2T on 1T. A new design of the beam port of 2T was realized, tested and installed by the Orphee group, while the PG002 and Cu111 monochromators of previous 1T french triple axis spectrometer were enhanced and set up on a new changer, designed by AZ-Systems. A copy of the monochromator unit, mechanics and shielding, was done and adapted to receive the new Heusler monochromator, so to have the possibility to go easily from the non-polarized option to the polarized one. 18 pieces of Heusler single crystals of 1.5x7 cm^2 grown and tested at the ILL, were used to achieve a 13.5x14 cm^2 vertically focusing monochromator, maintained in a horizontal magnetic field of 1.5 kGauss to get a polarized thermal neutron beam in an energy range from 5 to 75 meV, which hopefully will be extended to 100 meV. The non-polarized neutron option was first undertaken. Modifications of the drum were needed to take a full advantage of the new beam size. The beam entrance had to be enlarged as well as the exit of the monochromatic beam. This implied a dismantling of the whole drum.
During this operation, the 35 years old needle bearings used for the 20 tons drum rotation went stuck! A lot of patience and skill from the technical staff was needed to get it fixed up…

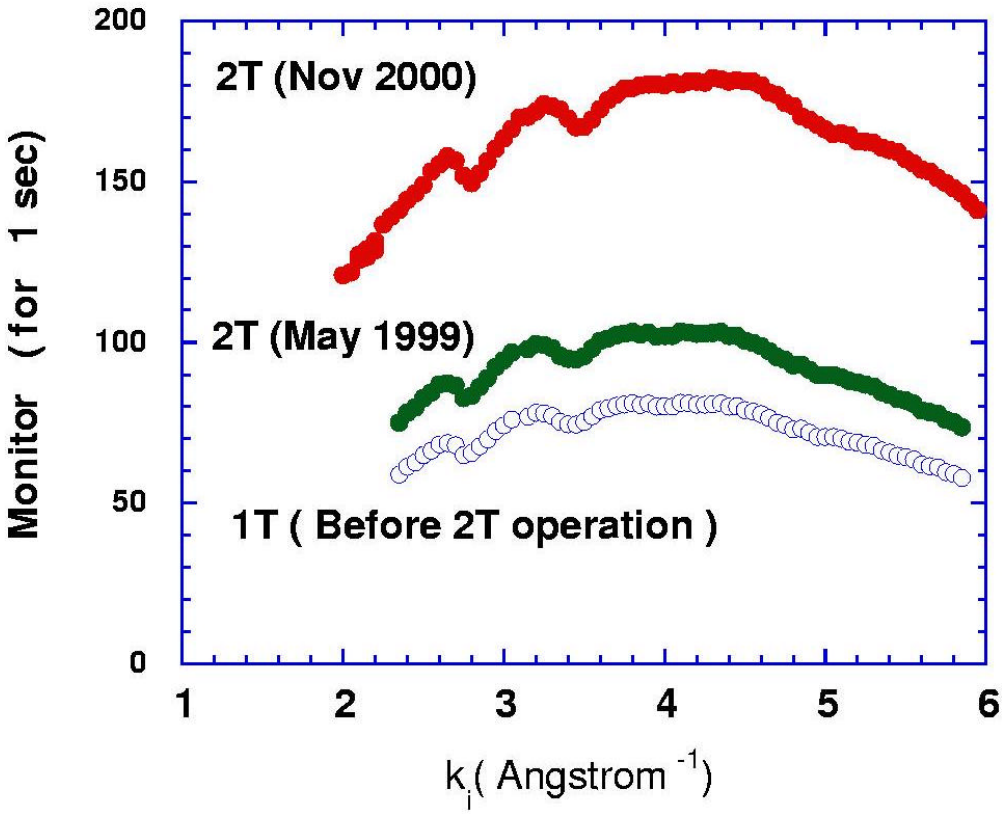

Figure 1 Monitor count evolution. May 1999: new beam port, old monochromator. Nov 2000: final state

Finally the spectrometer, in its new version, could be settled in. The improvement obtained on the thermal flux is illustrated on Figure 1 where the successive steps of the operation are reported. The gain is indeed about a factor 2.25 for the monitor count and nearly a factor 3 at constant time for a Vanadium measurement, which is even better than had been estimated initially. This is due to intrinsic differences between channels 1T and 2T: the distance between source and monochromator is slightly shorter on 2T, but it also appeared that the luminance of the beam is less on 1T, for yet unclear reason.

The completion of the polarized option is now nearly achieved. First tests have been undertaken, pointing out the need of a few modifications: a change in the curvature control of the vertical focusing of the monochromator and a modification of the guide field in the vicinity of the monochromator. On the other hand, a new shielding has been built up to allow the use of a new horizontally focusing polarizing Heusler analyzer. It will be installed during summer 2001 together with the above mentioned modifications. The polarized option on the 2T thermal beam will thus be fully operational at the end of 2001. The success obtained with the non polarized beam allows us to expect very good numbers for this new option.

To illustrate the current possibility of the non polarized thermal beam, we have reported on Figure 2 measurements performed on Molecular-Beam-Epitaxy-grown samples. Spin waves have been measured in pure MnTe, obtained in the cubic Blende structure because of the epitaxial growth, while otherwise it would have been of hexagonal structure. After a series of measurements on a 6 µm thick sample in the type III antiferromagnetic phase below ~ 65 K, where a complete spin wave spectrum has been obtained, we tried to look at the spin waves in a superlattice made of a stacking of blocks of MnTe (20 monolayers, with about 3.15 ? spacing) interspaced by block of non magnetic ZnTe layers (6 monolayers). Indeed this superlattice exhibits a surprisingly long range coherency of the same magnetic order as the pure material. On Figure 2 are superimposed results obtained on a 1 µm thick superlattice and those on the 6 µm thick MnTe. In both case the sample surface was ~ 2.5 cm^2. This illustrates the feasibility of this kind of measurements for a total sample volume of ~ 0.25 mm^3.

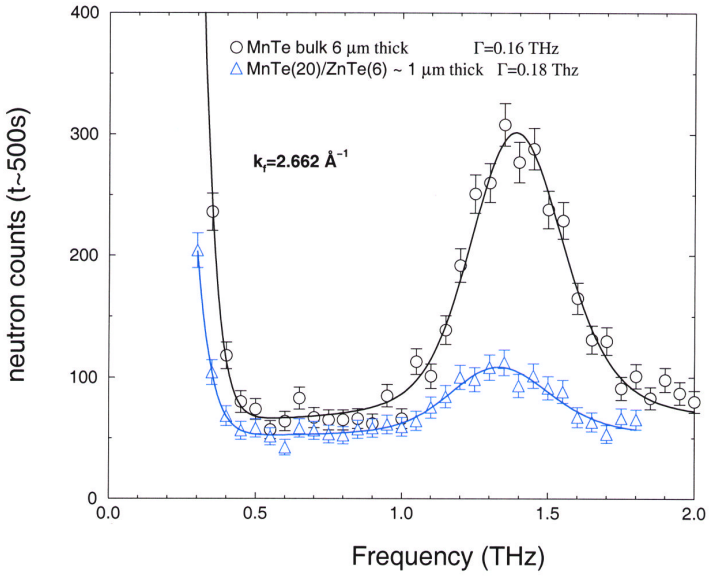

Figure 2: Zone boundary spin wave for MnTe (6 µm) and MnTe(20)/ZnTe(6) (1µm) at 13 K.
(ref : B.Hennion, W.Szuszkiewicz et al. to be published)

MEASUREMENTS OF THE VISCOSITIES AND DENSITIES OF SILICATE MELTS BY DYNAMIC NEUTRON IMAGING

A. Kahle [1], B. Winkler[1], B. Hennion[2], G. Bayon[3], P. Boutrouille [2]

[1]Inst. f. Geowissenschaften, Universität Kiel, Kiel, Germany
[2] DSM/DRECAM/LLB, CE A-Saclay, Gif sur Yvette, France
[3] DRN/DRE/SIREN, CEA-Saclay, Gif sur Yvette, France

Introduction

Volcanic processes such as magma ascent and emplacement are governed to a large extent by the viscosities and densities of the magmas involved. The physical properties of magmas strongly depend on temperature and composition. For example, the viscosity decreases by 10 orders of magnitude when going from a pure silica (SiO_2) melt to a melt with diopside ($CaMgSi_2O_6$) composition at a constant temperature of 1500 K [1]. Other factors determining the viscosities of geologically relevant magmas are the amount of crystals in the melt, the concentration and size of bubbles formed during degassing and the amount of dissolved volatiles. While an understanding of the rheological behaviour of magmas is of fundamental importance in the Earth Sciences, the amount of reliable experimental data on physical properties of melts is limited and mostly restricted to homogenous melts. This severely constraints our ability to model volcanic processes. In order to provide more data on the physical properties of melts, we have developed a novel method for the simultaneous *in situ* determination of viscosities and densities of silicate melts which is accurate and can be used to investigate chemically inhomogeneous melts. In addition, rheological processes in magmas can be directly observed.

Method

We modify the well known falling sphere technique by using dynamic neutron imaging for a real-time, *in situ* observation of spheres falling in silicate melts. We use spheres of Gd, Er, Hf and Ta, which strongly absorb neutrons and are practically inert with respect to the melt, where the latter is essentially transparent for neutrons. The spheres have diameters between 2-5 mm, the sample height is typically 80 mm. The sample is illuminated by a parallel white neutron beam, and after transversing the sample and conversion to visible light, the transmitted intensity is recorded with a video camera.
A set of typical video frames is shown in figure 1.

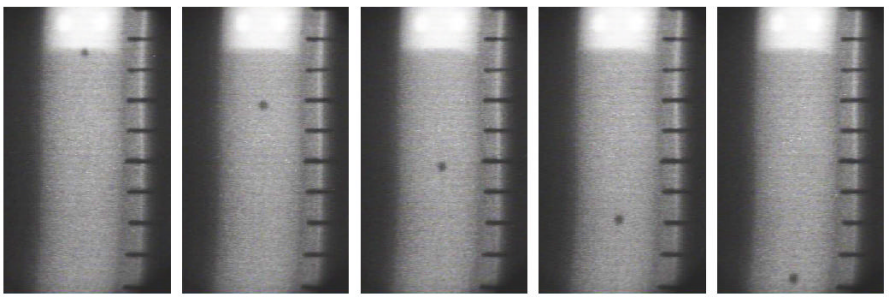

Figure 1: Frames from a video recording of a falling sphere experiment. The sphere has a diameter of 3 mm, the time between the first and last image is 30 min.

With software based on pattern recognition, the time-dependence of the position of the sphere is analysed. Typical data are shown in figure 2.

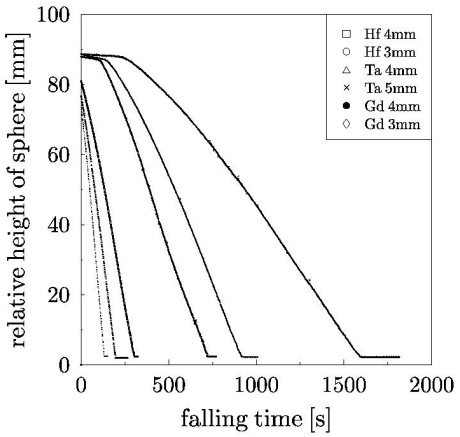

Figure 2: Plot of the relative height of spheres with different composition and diameter falling down in a melt as a function of time. The respective velocities are obtained from the slope of the lines.

The data analysis is based on Stokes' law. As we independently vary both sphere diameters and sphere densities, we can solve a set of equations at constant temperature and obtain the viscosity and density to within a few percent. This has been confirmed by comparison to standard samples. The high accuracy of this method is partially due to the absence of convection. This can be demonstrated by partially doping the melt, which is also the technique used to visualize rheological processes (see figure 3).

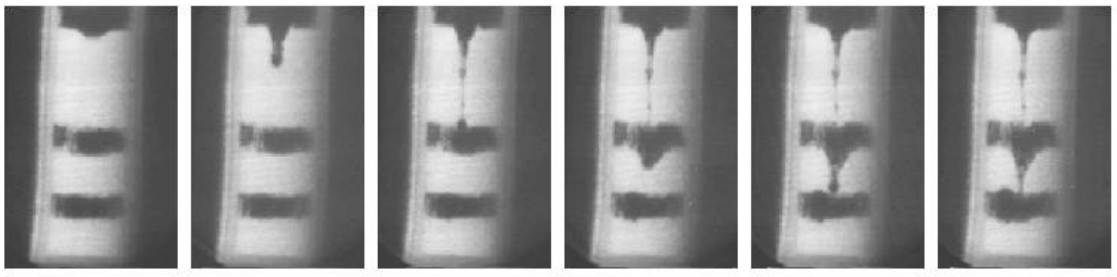

Figure 3: Real-time observation of a sphere falling through a silicate melt at 1050°C. The black and white layers are of equal density but the black ones are doped with gadolinium oxide. The boundaries between the layers stay sharp, indicating the absence of convection.

Summary and Outlook

Dynamic neutron imaging has been used to monitor spheres falling in silicate melts, thereby allowing an accurate *in situ* determination of melt viscosities and densities. In contrast to other methods, our approach does not require any calibration and can be used for partially crystalline melts. A new furnace designed for these experiments allows measurements at temperatures up to 2000°C. An autoclave for high-pressure experiments of volatile-containing melts is currently being constructed. Furthermore, the direct observation of rheological processes is possible. This is currently used to investigate magma mingling.

[1] Stebbins J.F., McMillan P.F., Dingwell D.B. (eds): Structure, Dynamics and Properties of Silicate Melts, Reviews in Mineralogy, MSA, Vol.32.

Acknowledgement

This project is funded by the German Science Foundation (project Wi 1232/9)

MICROSTRIP GAS DETECTORS

C. Fermon, V. Wintenberger and F. Ott
Laboratoire Léon Brillouin

The LLB is currently developing micro-strip gas counters (MSGC) based on the charge division principle. These detectors are suitable for small area 200x100mm², good spatial resolution (< 2mm) neutron detection. They allow to avoid the possible mechanical problems related to wire grid detectors by replacing the wires with anode and cathode metal stripes deposited on a glass substrate.

A MSGC consist of a gap filled with high pressure ^{3}He gas (up to 10 bars) to capture the neutrons and create an electrical charge. A high electrical field (~1000 V/m) The charge amplification is performed by a high electrical field between anodes and cathodes amplifies the charge (gain of 10^4). This electrical charge is split in two by a resistive line. The position of the neutron is determined by measuring the charge ratio between the two ends of the resistive line (see figure 1). The charge division design has been chosen because of the very low cost of the associated electronics (the number of charge amplifiers is limited to 3.)

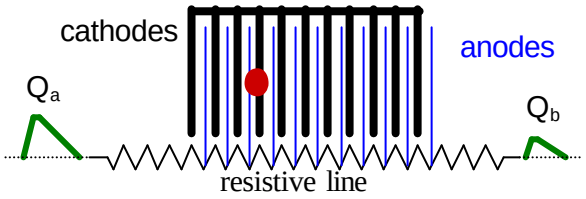

Figure 1 : charge division principle. The electrical charge created by the neutron are amplified and collected on both sides of a resistive line Q_a and Q_b. The neutron position is calculated by $Q_a/(Q_a+Q_b)$.

The gamma discrimination is performed by measuring the total electrical charge collected on the cathodes.

At the moment, the larger size available is 200x100mm². It is limited by the fabrication and the capacitance of the micro-strip glass plate itself. A 2D position detection can be achieved by using two perpendicular sets of stripes (on the front and on the back of the glass substrates).

Ultra High Vacuum techniques have been used for the design of the detectors casings (see fig. 2) in order to maintain the purity of the detection gas. This is essential to prevent any deterioration of the metallic anodes stripes and to avoid parasitic signals.

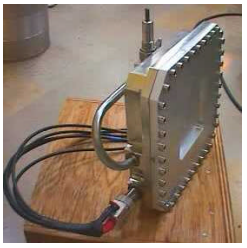

Figure 2 : 100x100 mm² MSGC detector

The electronics is composed of a compact electronic chain including the charge amplification and the charge division calculation, a conversion board with two 12 bits ADC converters, an interface board to communicate with the standard LLB EuroPSD and EuroScaler counting boards.

The speed of the electronics counting rate is limited at 5MHz, but the actual limitation is given by the detector itself (due to the resistance of the charge division line.)

These MSGC can achieve a 1.5-2 mm spatial resolution (see Figure 3). The background noise is 30 counts/min on a 100x200mm² detector.

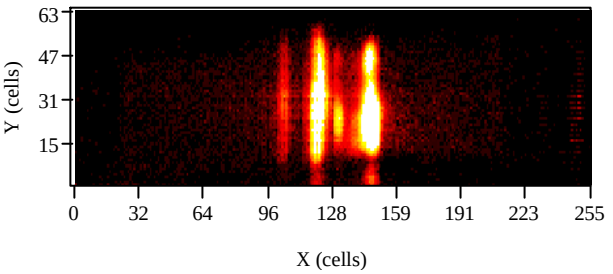

Figure 3 : picture of the reflectivity measured on a grating (right, direct beam ; left reflected beams).

This year, the spectrometer 7C2 (designed for the study of liquids and disordered systems) will be equipped with a set of 10 new MSGC (200x100mm²). The resolution of each individual detector is 2 mm in the horizontal direction and 5 mm in the vertical direction. The wavelength of this spectrometer is 0.05 nm. The ^{3}He pressure in each detector is 15 bars and allows a detection efficiency of 85%.

Acknowledgement
These detectors have been developed in the frame of the European XENNI and TECHNI (n° HPRI-CT-1999-50005) contracts.

NEUTRON ENERGY ANALYSIS USING GRATINGS.

F. Ott, A. Menelle, P. Humbert, C. Fermon
Laboratoire Léon Brillouin CEA/CNRS, CE Saclay.

Gratings have become standard optical elements in the field of X-ray synchrotron radiation. The field of neutron instrumentation has not yet seen much use of these artificial structures. A noticeable realisation is however the use of gratings for neutron interferometry. At the LLB, we are evaluating the use of optical gratings in the field of neutron optics to perform an energy analysis of a neutron white beam in a reflectivity geometry. In a reflectivity geometry (grazing incidence) it is possible to perform highly efficient diffraction on gratings which have periods in the micron size range (see fig. 1). These gratings are easy to produce by standard UV lithography on large surfaces (several cm²).

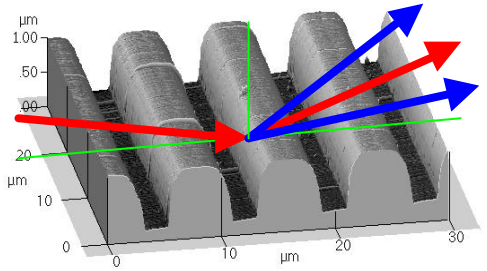

Figure 1 : diffraction on a grating: neutron incident beam and specular reflection (red) ; the beam is diffracted (blue) in the plane of incidence (green).

The use of gratings in neutron optics requires an increase in the diffraction efficiency. Several approaches have been tested in order to maximise this efficiency : use of high index materials, titanium coating, super-mirror coatings. We have shown that an appropriate coating can allow to reach a diffraction efficiency as high as 25%. We have also shown that these efficiencies can be obtained over a wide scattering wave-vector range (0.02 nm^{-1}) (with respect to a neutron reflectivity geometry) [1-2]. Figure 2 shows the example of the diffraction on a nickel grating.
These gratings could have a direct application in time-of-flight (TOF) neutron reflectometers built around steady state reactors and could lead to very large gains in measuring time. The sample is illuminated by a white beam (covering the whole guide wavelength spectrum available). After reflection on the sample, the neutron beam is diffracted by the grating (see figure 3).

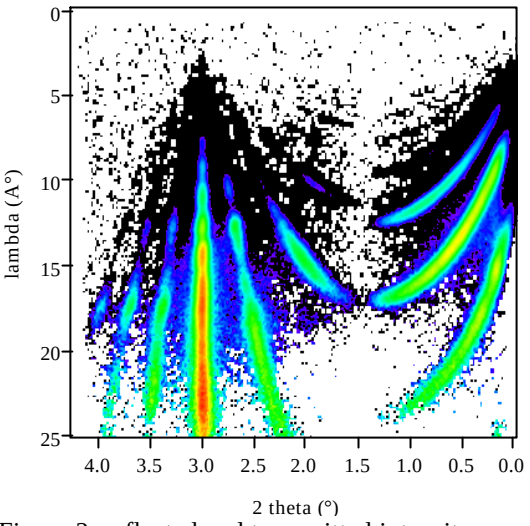

Figure 2: reflected and transmitted intensity on a nickel grating (the neutron beam incidence angle on the grating is 1.5°). The horizontal axis represents the position on the detector. The vertical axis represents the wavelength. The colour scale represents the neutron intensity. The measurement has been made on the D17 reflectometer at the ILL with the help of R. Cubbit. The diffracted intensities can amount up to 10% of the incident beam.

The diffraction direction is a function of the wavelength. By using a position sensitive detector, one can then instantly measure the whole reflectivity curve. Assuming a grating diffraction efficiency as low as 5%, this device could allow a gain of a factor 10 in measuring time (by avoiding the chopping stage).

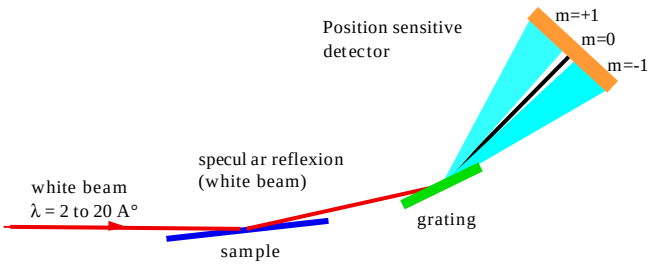

Figure 3 : principle of the energy analysis using gratings.

This work is supported by the European contract TECHNI nr. HPRI-CT-1999-50005.

[1] F. Ott, A. Menelle, C. Fermon, P. Humbert, Physica B **283** (2000) 418-421.
[2] F. Ott, P. Humbert, C. Fermon, A. Menelle, Physica B **297** (2001) 189-193.

A NEW GENERATION OF SOFTWARE TO CONTROL SPECTROMETERS

Alain Buteau, Nathalie Ravenel, Katy Ho

The computing group of the LLB has been working for the last years on a new instrument control software called « Programme Orienté Objet de Pilotage de Spectromètres »

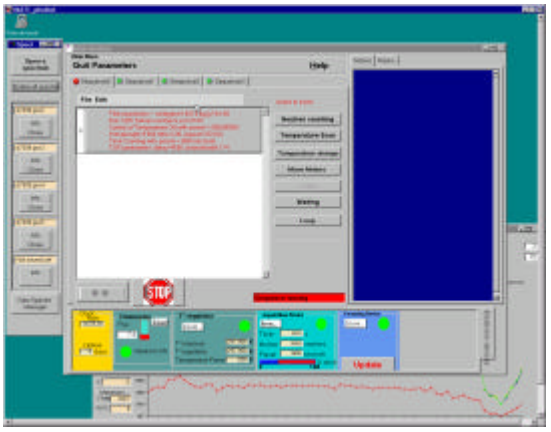

Figure 1. Graphical User Interface on spectrometer 7C2

The design guidelines

This new software generation has been designed with the following architectural guidelines :

- The software architecture should mimic the spectrometers architecture which are all different (and are all doing different physics studies) but have all many common points (electronic counting devices, sample environments, motors)
- Easy maintenance : The ability to provide a short response time to problems or required evolutions with a low manpower was a key point in the technical choices done for this software. The architecture must help the maintenance and evolution of the software. We reached this goal in describing the common points between spectrometers in high levels « modules » and let the differences be expressed in well isolated « modules »
- Extensibility: It should also be easy to integrate the control of new devices in the system to integrate as quickly as possible the experimental changes.
- Instrument driven : the complete instrument, experiment and environment description is done in configuration files. From these descriptions, the software adapts itself and constructs the corresponding Graphical User Interface and list of operations available on the spectrometer
- Friendly user interface : The experiment control software is the interface between the spectrometer and the physicist. Because the LLB has a lot of external beam users, a particular care should be brought to the design of the Graphical User Interface (see figure 1).
- Portability : the software must run on a Windows NT platform in a first time, but may also be used on Unix operating systems in the future.

The technical choices

To fullfill these requirements, the choice of Object Oriented (O-O) technologies seemed very natural. The O-O concepts of « modules » (called Class) and the inheritance and polymorphism mechanisms were potentially able to give us solutions to our problems. We decided to use the following techniques and tools to help us through the project.

1. An Object-Oriented notation : OMT and its successor UML has been used to help us during the analysis phase to :

- capture user requirements through Use Case and Sequence diagrams
- construct state models for objects with related life-cycles (example: Devices States)
- express the static structure of the system with Class Diagrams

1. An UML modelisation tool has been used to generate code skeletons from Class diagrams.
2. The « Design Pattern » techniques are used to bridge the gap between analysis and design. Patterns are an attempt to describe successful solutions to common software problems. They helped us construct a really modular software with documented solutions. In particular, it has allowed a clear separation between the Kernel part of the system in charge of the experiment control and the Graphical User Interface (GUI)
3. Portable and high level librairies : ILOG Views for the GUI construction, and STL for objects collection management.
4. Integration of the emerging Common Data Format of the Neutrons/Xrays community : NeXus.
5. And at least portable hand written C++ …..

And the (final) results

The software is now controlling 6 spectrometers of 3 different types :

- 1 Time of flight reflectometer : **EROS**
- 4 Two axis spectrometers : **G41, G61, 7C2, G52**
- 1 quasi-elastic time of flight spectrometer : **MIBEMOL**

The initial choices have proved to be adequate to our needs and are in the spirit of modern software engineering practices. The software is still evolving and the maintenance tasks have been contained at acceptable levels. We must nevertheless underline that the learning curve of Object Oriented technology has proved to be quite long and painful ! !

The future

The use of this software on the first 6 instruments since more than a year has proven the validity of the concept. Our goal now is to install the software on other spectrometers in order to check that it is able to be adapted easily on all type of spectrometers.

However, nothing is perfect and we are now working on the second generation software that will improve some weak points of the current version reported by the users. The data visualisation tools provided with the software are far from the standards met in common commercial program and should be updated. Another requirement is to provide a better remote access which will enable a easy and flexible remote control of the instrument. The use, in the next version, of a distributed architecture using CORBA as a software bus between the subsystems will enables us to provide this access through a Web Browser Graphical User Interface.

EXPERIMENTAL PROGRAMME AND USER ACTIVITIES

1. SUMMARY OF THE USER ACTIVITIES IN 1999 AND 2000

1.1 Operation of Orphée reactor and LLB facility

The reactor Orphée operated 215 days in 1999 and 208 days in 2000.
4196 and 3953 experiment days were realized respectively in 1999 and in 2000 on the 25 scheduled instruments. These values do not take into account the beam time given to the CRG teams on the following instruments : 2T (Kf Karlsruhe), G4.2 (PNPI, Gatchina), G4.3 (University of Wien) and G5.2 (INFM, Italy). The CRG time is usually 1/3 of the Orphée operating time (25% for G5.2). They include the full beam time for G4.4 (managed by ONERA) and 5C2 (managed by University of Aachen).
In spring 1999, in order to increase the beam size and the intensity on the thermal triple-axis spectrometer 2T1, and to install a polarized neutron option, the 2T beam tube before the monochromator and the collimators was completely replaced (see "highlight") during a 2 months shut-down of the reactor.
Within a period of 6 months in winter 1999-2000 and spring 2000, several (5) cold neutron guide tube elements (1.25 m long each), close to the reactor, broke, probably because of various ageing effects. This led us to put in place in 2000 and 2001 a systematic replacement programme of the oldest elements (installed between 1981 and 1985).

1.2. Instruments

The list and main characteristics of LLB instruments and a layout of their implantation are given in the introducing chapter "Presentation of LLB".
In Table 1 are summarized the numbers of realized experiments and scheduled beam days, on the different instruments.
The reflectometer DESIR was closed in 2000, the corresponding beam port (G5bis) being used to build a very-small angle diffractometer (see section "Technical and Instrumental Developments"). The reflectivity experiments on soft matter and liquids are now all performed on the more recent and higher flux time-of-flight reflectometer EROS, installed on the cold neutron guide G3bis.
The new instruments MUSES (Neutron Resonant Spin-Echo, built and managed in collaboration with the Technical University of Munich) and PAPOL (Small-Angle Neutron Scattering with polarized neutrons and nuclear dynamic polarization) have been partially (50%) opened to external users in 2000 (autumn 1999 selection panel).

1.3. User statistics

Table 2 indicates the distribution of beam time per country (based on the location of the laboratory of the main applicant), for experiments realized in 1999 and 2000.
Around 70% of the total beam time was used by French users in 1999 and 2000, which is similar to the previous years. 30% of the total beam time was used by foreign users; this number includes 18% for European Union, 4% for CEI (Russia and Ukrainia) and 5% for PECO (Eastern and Central Europe) countries.

The distribution of total beam time per scientific domain (Round Table Sessions) was the following :

- 24% for Physical Chemistry and Biology (session A),
- 19% for Structural Studies and Phase Transitions (session B),
- 31% for Magnetism and Superconductivity (session C),
- 26% for Disordered Systems and Materials (session D).

1.4. European Access Programme

Since 1993, the LLB is a large scale facility for the transnational access of european users, in the frame of the Human Capital and Mobility (HCM, 1993-97) and Training and Mobility of Researchers (TMR, 1996-2000) Research and Development programmes of the European Commission. Among the E.U. users of LLB, those involved in the TMR access programme received 342 beam days in 1999 and 298 in 2000 (8.2% and 7.5% of the total beam time respectively).

The LLB TMR access programme finished in november 2000. During the 51 months of the programme, it allowed to perform 182 experiments (1409 experiment days) and to receive 183 individual users (issued from 12 different countries), among which 115 were new users of LLB. Their distribution per nationality is given in the following figure.

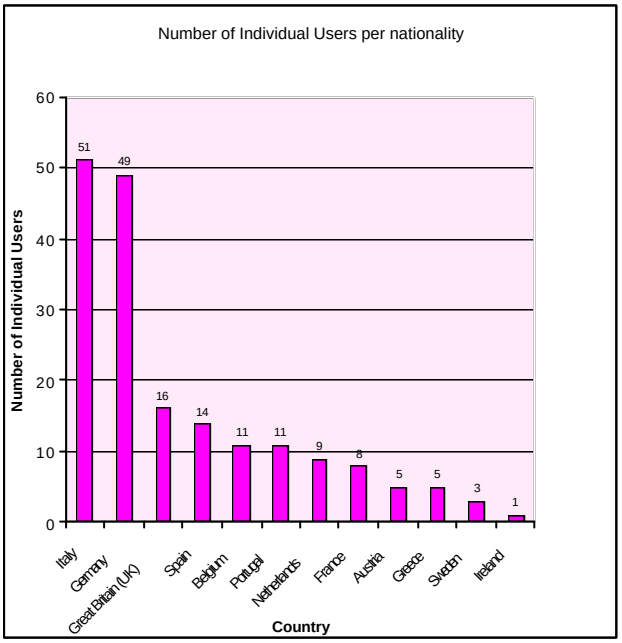

TMR
« Access to LLB » programme

In 1999, the LLB applied successfully for the new E.U. Access to Research Infrastructures action of the Improving Human Potential programme (HPRI). Contrary to TMR, this programme is also opened to researchers of countries associated to E.U. (in particular from Central Europe : Poland, Czech Republic, Hungary, etc…). The contract extends for 3 years, starting from february 1rst 2000; during the first year of the HPRI contract, we received between june 2000 and january 2001 : 20 teams (30 individual users, among which 10 came from Central and Eastern Europe associated countries), corresponding to 129 days of access.

2. BEAM TIME REQUEST AND ALLOCATION

2.1. The present organization

We have kept the system of Round Tables and User Selection Panels put in place in 1996, which aimed to favour long-term projects, but have introduced a new Spring Session. In spring 1999, this was limited to E.U. users of the TMR programme, but in 2000 it was extended to all users.
To perform an experiment at LLB, the researcher must first submit a proposal written on a special form, where he explains his scientific interest and describes the proposed experiment. All the proposals submitted at LLB are examined by a peer review Selection Panel, which encounters twice a year (at the end of november and in may), and which is subdivided in 4 sessions :

- Physical Chemistry and Biology,
- Structural Studies and Phase Transitions,
- Magnetism and Superconductivity,
- Disordered Systems and Materials Science.

Each session of the Selection Panel comprises typically 9 members (3 of LLB, 3 French non-LLB, 3 non-french). The list of members for the Selection Panel of autumn 1999 (which selected the experiments to be performed in the first semester of 2000) is given in Table 3.
The Selection Panels classify the proposals in A, B and C, on the basis of scientific merit :

- A : accepted and to be performed,
- B : eventually performed if beam time available,
- C : rejected.

The applicant is informed by an official mail, of the classification of his proposal and, in case of success, of the allocated beam time. In case of classification C, the reasons are explained to the applicant.

In the autumn session, the Selection Panels are preceeded by user meetings, called "Tables Rondes du LLB". These meetings consist of :

- invited talks (in each "Table Ronde", half a day is devoted to a specific theme, for example "structure and properties of foams" in session A, and "structure and dynamics of molecular crystals" in session B);
- presentation of new long-term projects or programmes;
- presentation of recent scientific results obtained by external or internal users at the LLB ("poster session");
- technical presentations;
- discussions with users.

Typically 30 persons participate in the average to each of these four "Tables Rondes".

2.2. Analysis of the beam time request and allocation

The beam time requests received and the beam time allocated by the spring and autumn User Selection Panels during the year 2000 are summarized per country in Table 4, and per instrument and scientific session in Table 5.

The overload factor of an instrument, defined as the ratio between the required beam time and the foreseen operating time (80% of the operating time of Orphée, the 20% remaining being used for maintenance, repairs, tests, urgent experiments, etc…), depends of the considered instrument and ranges between above 2 (4-circle 5C2, strain scanner G5.2,…) and 1; in average, it is 1.5. These numbers are practically constant since the refurbishment of the ILL reactor (1995).

2.3. Fast access procedure

In order to facilitate the access to neutron scattering instruments, in particular for new users, to perform test experiments, to prepare long term projects or to satisfy in a short delay the sample characterization requirements of chemists, a new fast access procedure, for short experiments (typically 1 day), has been set-up since 2000. This concerns in particular powder and small-angle neutron diffraction experiments.

The demands can be made at any moment of the year, by web, adressed to the Scientific Secretariat of LLB. The answer is given with a delay of two weeks, and the experiment performed, either by the proposer or by the local scientific contact, in principle within 2 months.

Experimental Programme and User Activities

REALIZATION BY INSTRUMENT FOR 1999 AND 2000 **TABLE 1**

INSTRUMENTS	1999		2000	
	Number of experiments performed	Beam time (days)	Number of experiments performed	Beam time (days)
TRIPLE-AXIS SPECTROMETERS				
1T (german CRG)*	15	165	11	135
2T	9	119	19	160
4F1	15	192	15	174
4F2	18	173	21	178
G4.3 (austrian CRG)*	9	106	10	103
POWDER DIFFRACTOMETERS				
3T2	42	188	49	188
G4.1	41	197	47	183
G4.2 (russian CRG)*	16	137	27	136
G6.1	17	178	21	179
MATERIALS DEDICATED DIFFRACTOMETERS				
6T1 (textures)	14	179	10	174
G52 (residual stresses) (1/2 Italian CRG)	19	176	18	137
SINGLE CRYSTAL DIFFRACTOMETERS				
5C1	10	185	12	163
5C2 (german CRG)	16	185	29	208
6T2	16	187	19	167
REFLECTOMETERS				
Eros (G3 bis) / Desir (G5 bis)	23	314	24	189
Prism (G2.4)	20	128	14	95
DIFFRACTOMETERS FOR DISORDERED SYSTEMS				
7C2	21	167	24	149,5
G4.4 (ONERA CRG)	5	190	3	200
SMALL ANGLE NEUTRON SCATTERING				
PACE	32	210	37	151
PAXE	42	200	49	198
PAXY	44	207	36	168,5
PAPOL	5	104	4	82
QUASI-ELASTIC SCATTERING				
Spin Echo	10	149	7	142
TV (Mibemol)	20	160	23	185
G1 bis	-	-	10	108
TOTAL	**479**	**4196**	**539**	**3953**

*** Not included CRG beam time given on 1T to germans, on G4.3 to austrians, on G4.2 to russians**

REALIZATION BY COUNTRY FOR 1999 AND 2000 **TABLE 2**

COUNTRIES	1999			2000		
	Number of experiments performed	Beam time (days)	Total experiment beam time (%)	Number of experiments performed	Beam time (days)	Total experiment beam time (%)
TOTAL FOR FRANCE	***328***	***2990,5***	***71,27%***	***354***	***2685,5***	***67,94%***
AUSTRIA	7	34	0,81%	10	49	1,24%
BELGIUM	2	11	0,26%	2	6	0,15%
GERMANY	28	193,5	4,61%	44	396,5	10,03%
GREECE	1	16	0,38%	2	14	0,35%
ITALY	20	183	4,36%	25	166	4,20%
NETHERLANDS	4	24	0,57%	6	31	0,78%
PORTUGAL	4	33	0,79%	1	6	0,15%
SPAIN	9	86	2,05%	14	77,5	1,96%
SWEDEN				1	12	0,30%
UNITED KINGDOM	5	31	0,74%	10	46	1,16%
TOTAL FOR E.U.	***80***	***611,5***	***14,57%***	***115***	***804***	***20,34%***
TOTAL FOR RUSSIA-CEI	***17***	***154***	***3,67%***	***19***	***127***	***3,21%***
CZECH REPUBLIC	1	7	0,17%	5	44,5	1,13%
HUNGARY	11	64,5	1,54%	11	68	1,72%
POLAND	15	118,5	2,82%	16	100	2,53%
TOTAL FOR PECO	***27***	***190***	***4,53%***	***32***	***212,5***	***5,38%***
ALGERIA	1	7	0,17%			
AUSTRALIA	1	14	0,33%			
CUBA	1	5	0,12%			
INDIA	1	9	0,21%			
JAPAN	3	37	0,88%	2	26	0,66%
MEXICO	1	7	0,17%			
MOROCCO	5	32	0,76%	5	9	0,23%
SOUTH AFRICA	1	3	0,07%			
SWITZERLAND	7	68	1,62%	9	58	1,47%
UNITED STATES	6	68	1,62%	3	31	0,78%
OTHERS	***27***	***250***	***5,96%***	***19***	***124***	***3,14%***
TOTAL	**479**	**4196**	**100,00%**	**539**	**3953**	**100,00%**

TABLEAU 3

User Selection Panel - "Tables Rondes" - Autumn 1999

SESSION A : Physical Chemistry, Biology				
LLB MEMBERS	**FRENCH MEMBERS**		**NON-FRENCH MEMBERS**	
F. Boué	F. Nallet (Président)	C.R.P.P. Pessac	W. Doster	T.U. München
L.-T. Lee	S. Pouget	I.L.L. Grenoble	G. Hadziioannou	Université Groningen
J. Teixeira	M. Rawiso	I.C.S. Strasbourg	R.E. Lechner	HMI Berlin

SESSION B : Structural Studies, Phase Transitions				
LLB MEMBERS	**FRENCH MEMBERS**		**NON-FRENCH MEMBERS**	
J. Etrillard	H. Cailleau	G.M.C.M. Rennes	W.-F. Kuhs	Université Goettingen
M. Braden	E. Elkaïm	LURE Orsay	J. Kulda	I.L.L. Grenoble
R. Kahn	A. Hewat (Président)	I.L.L. Grenoble	W. Prandl	Université Tübingen
J. Rodriguez-Carvajal	E. Lorenzo-Diaz	Lab. Cristallo. Grenoble		

SESSION C : Magnetism, Superconductivity				
LLB MEMBERS	**FRENCH MEMBERS**		**NON-FRENCH MEMBERS**	
G. André	A. Ivanov	I.L.L. Grenoble	J.C. Gomez-Sal	Université Cantabria
P. Bourges	H. Noël	Université de Rennes I	G. Mc Intyre	I.L.L. Grenoble
C. Fermon	P. Mangin (Président)	LMPSM, Nancy	L. Paolasini	E.S.R.F. Grenoble
A. Goukassov				
P. Pfeuty				

SESSION D : Disordered Systems, Materials				
LLB MEMBERS	**FRENCH MEMBERS**		**NON-FRENCH MEMBERS**	
F. Bourée	J.-L. Bechade	SRMA, CEA/Saclay	J.-P. Gaspard (Président)	Université de Liège
C.-H. de Novion	A.J. Dianoux	I.L.L. Grenoble	G. Krexner	Université de Vienne
	F. Hippert	Université Paris-Sud	R. Magli	Université de Florence
	J.-M. Sprauel	ENSAM, Aix en Provence		

Request and allocations (priority A) per country received in the year 2000 **TABLE 4**

Country	Number of proposals submitted	Beam time requested (days)	Allocated beam time (days) (as priority A)				Total	% of total allocated beam time
			Session A	Session B	Session C	Session D		
FRANCE	284	2904	350	417	553	459,5	1779,5	66,23%
TOTAL FOR FRANCE	284	2904	350	417	553	459,5	1779,5	66,23%
AUSTRIA	10	92,5	0	25	10	25,5	60,5	2,25%
BELGIUM	3	14	7	0	0	0	7	0,26%
GERMANY	37	318,5	50,5	37	79	57,5	224	8,34%
GREECE	1	10	0	0	10	0	10	0,37%
ITALY	34	253,5	11	0	60	18	89	3,31%
NETHERLANDS	4	30	3,5	0	17	0	20,5	0,76%
PORTUGAL	4	24	7	10	0	0	17	0,63%
SPAIN	5	23	0	9	8	5	22	0,82%
SWEDEN	4	33	5	0	0	7	12	0,45%
UNITED KINGDOM	14	97	7	21	18	29	75	2,79%
TOTAL FOR E.U.	116	895,5	91	102	202	142	537	19,99%
MOLDAVIA	1	6	0	0		0		
RUSSIA	23	161	0	7	64	44	115	4,28%
TOTAL FOR RUSSIA-CEI	24	167	0	7	64	44	115	4,28%
CZECH REPUBLIC	3	17,5	3,5	0	0	10	13,5	0,50%
HUNGARY	11	79	7	7	0	13,5	27,5	1,02%
POLAND	22	224	2	10	82	24	118	4,39%
TOTAL FOR PECO	36	320,5	12,5	17	82	47,5	159	5,92%
AUSTRALIA	1	3,5	3,5	0	0	0	3,5	0,13%
INDIA	1	2	0	0	2	0	2	0,07%
ISRAEL	1	3	3,5	0	0	0	3,5	0,13%
JAPAN	8	63	13	0	14	0	27	1,00%
MAROCCO	1	2	0	2	0	0	2	0,07%
SWITZERLAND	4	19	0	0	6	7	13	0,48%
TUNISIA	1	18	0	6	0	0	6	0,22%
UNITED STATES	7	59,5	17,5	17	0	5	39,5	1,47%
TOTAL FOR OTHER COUNTRIES	24	170	37,5	25	22	12	96,5	3,59%
TOTAL	**484**	**4457**	**491**	**568**	**923**	**705**	**2687**	**100,00%**

Request and allocations per instrument received in the year 2000 **TABLE 5**

INSTRUMENT	Request		Allocated beam time (as priority A)				
	Number of proposals	Beam time (days)	Session A	Session B	Session C	Session D	Total
1T1	15	123	0	47	56	0	103
2T1	15	202	0	28	98	21	147
4F1	19	218	0	68	91	3	162
4F2	10	121	0	21	49	0	70
G4.3	9	108	0	35	0	54	89
TRIPLE-AXIS SPECTOMETERS	68	772	0	199	294	78	571
3T2	33	170	0	75	51	0	126
G4.1	39	181	0	16	104	6	126
G4.2	16	64	0	31	32	0	63
G6.1	28	222	0	19	100	20	139
POWDER DIFFRACTOMETERS	116	637	0	141	287	26	454
6T1	10	206	0	0	0	132	132
G5.2	23	248	0	0	0	95	95
MATERIALS DEDICATED DIFFRACTOMETERS	33	454	0	0	0	227	227
5C1	13	208	0	0	97	0	97
5C2	28	437	0	120	28	0	148
6T2	18	202	0	65	94	0	159
SINGLE CRYSTAL DIFFRACTOMETERS	59	847	0	185	219	0	404
G2.4	13	167	0	0	77	14	91
G3.Bis	21	227	80	0	20	55	155
REFLECTOMETERS	34	394	80	0	97	69	246
7C2	23	185	22	11	4	62	99
G4.4	2	60	0	0	0	60	60
DIFFRACTOMETERS FOR DISORDERED SYSTEMS	25	245	22	11	4	122	159
G5.5			0	0	7	0	7
PACE	32	217	98,5	0	0	28,5	127
PAXE	24	135,5	54,5	0	0	19,5	74
PAXY	41	241,5	91	0	8	21	120
SMALL ANGLE NEUTRON SCATTERING	97	594	244	0	8	69	321
G1.Bis	9	109	19	7	0	29	55
Spin Echo	6	86	56	0	0	28	84
TV	35	307	70	25	7	41	143
QUASI-ELASTIC SCATTERING	50	502	145	32	7	98	282
G4.5	2	12	0	0	0	16	16
NEUTRON RADIOGRAPHY	2	12	0	0	0	16	16
Total	**484**	**4457**	**491**	**568**	**916**	**705**	**2680**

PUBLICATIONS

LLB - Publications 1999-2000

This list includes publications involving LLB researchers and publications relative to experiments performed on LLB instruments by external users.

ADELMANN P., RENKER B., SCHOBER H., BRADEN M., FERNANDEZ-DIAZ F. – Lattice dynamics of Li-ZrNCl : an electron doped layered superconductor
Journal of Low Temperature Physics **117** (1999) 449-453

AGUIE-BEGHIN V., LECLERC E., DAOUD M., DOUILLARD R. – Asymmetric multiblock copolymers at the gas-liquid interface. Phase diagram and surface pressure
J. Colloid Interface Sci. **214** (1999) 143-155

AIN M., PETITGRAND D, DHALENNE G., REVCOLEVSCHI A - Dispersion curve of magnetic excitations in dimerized $CuGeO_3$.under applied field.
In Physical Phenomena at High Magnetic fields-III, Edited by Z. Fisk, L. Gorkov, R. Schrieffer, World Scientific, Singapore (1999).

AIN M., BLUNDELL S.J., LORD J., JEGOUDEZ J. REVCOLEVSCHI A. - Muon spin relaxation in NaV_2O_5
Physica B **284-288** (2000) 1633-1634

AIN M., BLUNDELL S.J., LORD J., JEGOUDEZ J. REVCOLEVSCHI A. - Muon spin relaxation in NaV_2O_5 in its spin-Peierls phase
Physica B **281-282** (2000) 648-649

ALBERTINI G., BRUNO G., CARRADO A., FIORI F., RUSTICHELLI F.- Residual stress determination by neutron diffraction
Measurement Science and Technology , **10** (1999) R56-R73

ALBERTINI G., CAGLIOTI G., CERETTI M., FIORI F., MONZANI R., VIVIANI L. - Residual stresses in an AA6082 shrink-fit thermoplastic junction
Ater. Sci. Forum **347-349** (2000) 674-677

ALEKSEEV P.A., MIGNOT J.-M., LINK P., HAHN W., OCHIAI A., FILOPPOV V., NEFEODOVA E.V., CLEMENTYEV E.S. – Spin-orbit transitions in mixed-valence samarium compounds
Physica B **259-261** (1999) 351-352

ALEKSEEV P. A., MIGNOT J.-M., KAHN R., OCHIAI A., CLEMENTYEV E.S., LAZUKOV V.N., NEFEODOVA E.V., SADIKOV I.P., FABI P. – Neutron scattering study of the magnetic excitation spectra in mixed-valence $^{154}Sm_3Te_4$
J. Phys. : Condens. Matter **12** (2000) 2725-2736

ALEKSEEV P..A., LAZUKOV V.N., MIGNOT J.-M., SADIKOV I.P. – Neutron scattering studies of intermediate-valence compounds
Physica B **281-282** (2000) 34-41

ANDRE G ., BOUREE F., KOLENDA M., LESNIEWSKA B., OLES A., SZYTULA A. - Magnetic structure of $RAgSb_2$ compounds
Physica B **292** (2000) 176-189

ANDRE G ., BOUREE F., KOLENDA M., LESNIEWSKA B., OLES A., SZYTULA A. - Magnetic ordering of $RAgSb_2$ compounds
Acta Phys. Pol. A **97** (2000) 771-774

ARZEL L., HEHLEN B., CURRAT R., HENNION B., SAINT-PAUL M., COURTENS E. - The effect of domains on spectral anomalies of $SrTiO_3$ below the structural transition
Ferroelectrics **236** (2000) 81-92

ARZEL L., HEHLEN B., CURRAT R., HENNION B., COURTENS E. - Dynamics of coupled modes in $SrTiO_3$
Physica B **276-278** (2000) 230-231

ASMUSSEN B., BALSZUMAT D., GUTT C., PRESS W., LANGEL W., CODDENS G. - Orientational ordering in methane condensates in mesoporous SiO_2 modifications at low temperatures
J. Phys. IV France **10** (2000) 137-141

ASSERIN O., BRAHAM C., COPPOLA R., LODINI A. - Unstressed lattice parameter and microstructural evolution in electron beam welded martensitic steel
Proceedings " Residual Stresses – ICRS 6 " (2000) 459-466

AUVRAY L., KALLUS S., GOLEMME G., NABIAS G., RAMSAY J.D.F. - SANS analysis of anisotropic pore structures in alumina membranes
Stud. Surf. Sci. Catal. **128** (2000) 459-466

AUVRAY L. - Polymer at interfaces
C.R. Acad. Sci., Ser.IV 1 (2000) 1123-1124

BACZMANSKI A., BRAHAM C., LODINI A. - Internal stresses in two phases polycrystalline materials
Archives of Metallurgy **44** (1999) 1182-1187

BACZMANSKI A., BRAHAM C., LODINI A., WIERZBANOWSKI K. – Evolution of microstresses in plastically deformed duplex steel
Materials Science Forum **347-349** (2000) 253-258

BACZMANSKI A., BRAHAM C., GIGOUT D., LODINI A., WIERZBANOWSKI K. - Self consistent model and FEM methods used by stress prediction
Proceedings " Residual Stresses – ICRS 6 " (2000) 1182-1187

BALATSKY A., BOURGES P. – Linear dependence of peak width in $\chi(q,\omega)$ vs. T_c for $YBa_2Cu_3O_{6+x}$
Physical Review Letters **82** (1999) 5337-5340

BALAGUROV A.M., RASPOPINA E.V., SIKOLENKO V.V., LYUBUTIN I.S., STEPIN A.S., GRIBANOV A.V., ANDRE G., BOUREE F., DUH H.M. - Neutron diffraction study of the $U(Pd_{1-x}Fe_x)_2Ge_2$ magnetic structure
J. Magn. Magn. Mater. **210** (2000) 225-232

Publications

BARILO S.N., SHIRYAEV S., SOLDATOV A.G., SMIRNOVA T.V., GATALSKAYA V.I., REICHARDT W., BRADEN M., SZYMCZAK H., SZMCZAK R., BARAN M. – Potassium doped barium bismuthates coexisting near the tetra(ortho) and cubic phases boundary : crystal growth and properties
Supercond. Sci. Technol. **13** (2000) 1145-1150

BAROCCHI F., GUARINI E., CASANOVA G., BAFILE U.- Low-q structure of Kr gas at undercritical densities : an accurate SANS determination of triplet forces
Physica B **276-278** (2000) 448-449

BASTER M., BOUREE F., KOWALSKA A., LATACZ Z. – The change of crystal and exchange parameters in the vicinity of T_N in Cr_2O_3
J. Alloys Compounds **296** (2000) 1-5

BATTAGLIN C., CACCAVALE F., MENELLE A., MONTECCHI M., NICHELATTI E., NICOLETTI F., POLATO P. - Characterisation of antireflective TiO_2/SiO_2 coatings by complementary techniques
Thin Film Solids **351** (1999) 176-179

BATTAGLIN C., MENELLE A., MONTECCHI M., NICHELATTI E., POLATO P. - Characterisation of silver-based coatings by neutron reflectometry and complementary techniques
Proceedings of «The Surface : a bug in new and old glasses », S. Servolo Island, Venice (Italy), Rivista della Stazione sperimentale del vetro **6** (2000) 111-116

BAYON G., WINKLER B., KAHLE A., HENNION B., BOUTROUILLE P. - Application of dynamic neutron imaging in the earth science to determine viscosities and densities of silicate melts
6th World Conference on Neutron Radiography, Osaka, Japan, 1999

BEAUDOIN E., GOURIER C., LAPP A., FRANCOIS J. - Influence of salt on hydrophobically end-capped polyethylene oxides in aqueous solution
Macromol. Symp. **146** (1999) 171-177

BECHADE J.L., BOUCHE G., MATHON M.H., BAUDIN T. - Texture of welded joints of 316L stainless steel
12th International Conference on Texture of Materials (ICOTOM 12), Edited by J.A. Szpunar, NRC Research Press, Ottawa 1999, pp. 922-927

BELLISSENT-FUNEL M.-C., TEIXEIRA J. - Structural and dynamic properties of bulk and confined water
In « Freeze-Drying/Lyophilization of Pharmaceutical and Biological Products » edited by L. Rey and J.C. May, Publishers Marcel Dekker, New York (1999) p.53-77

BELLISSENT-FUNEL M.-C.(Editor) – Hydration Processes in Biology : Theoretical and Experimental Approaches
[In :NATO Sci.Ser., Ser.A (1999) 305], 430 pages
Edited by IOS Press, Amsterdam, Netherlands.

BELLISSENT-FUNEL M.-C. – Water in protein dynamics and function
Books of abstracts, 218th ACS National Meeting, New-Orleans (1999)

BELLISSENT-FUNEL M.-C., LONGEVILLE S., ZANOTTI J.-M., CHEN S.H. - Experimental observation of the α-relaxation in supercooled water
Physical Review Letters **85** (2000) 3644 -3647

BELLISSENT-FUNEL M.-C. - Hydration in protein dynamics and function
Journal of Molecular Liquids **84** (2000) 39-52

BENGUIGUI L., BOUE F. – Homogeneous and inhomogeneous polyacrylamide gels as observed by small angle neutron scattering : a connection with elastic properties
European Physical Journal B **11** (1999) 439-444

BENOIT H., JANNINK G. - A new approach to the problem of radiation scattering by multicomponent systems
European Physical Journal E **3** (2000) 283-290

BERGMAN C., COULET M.V., BELLISSENT R., SEIFERT-LORENZ K., HAFNER J. - Structure of liquid potassium-antimony alloys : neutron scattering experiments and ab initio molecular dynamics calculations
J. Non Cryst. Solids **250-252** (1999) 253-257

BERRY H., LAIREZ D., PAUTHE E., PELTA J. – Statistical conformation of human plasma fibronectin
J. Biosciences **24** (1999) 50

BERRY H., PELTA J., LAIREZ D., LARRETA-GARDE V. - Gel-sol transition can describe the photeolysis of extracellular matrix gels
Biochim. Biophys. Acta **1524** (2000) 110-117

BERTI D., PINI F., BAGLIONI P., TEIXEIRA J.- Micellar aggregates from short-chain phospholiponucleosides : a SANS study
J. Physical Chemistry B **103** (1999) 1738-1745

BERTI D., LUISI P.L.L., BAGLIONI P. - Molecular recognition in supramolecular structures formed by phosphatidylnucleoside based amphiphiles
Colloids and Surfaces A **167** (2000) 95-103

BIENFAIT M., ZEPPENFELD P., RAMOS Jr. R.C., GAY J.M., VILCHES O.E., CODDENS G. – Isotopic ordering in adsorbed hydrogen monolayers
Physical Review B **60** (1999) 11773-11782

BIKAKI A., VOULGARAKIS N.K. AUBRY S., TSIRONIS G.P. – Energy relaxation in discrete nonlinear lattices
Physical Review E **59** (1999) 1234-1237

BIONDUCCI M., NAVARRA G., BELLISSENT R., CONCAS G., CONGIU F. – Local order in amorphous Fe_2Zr prepared by mechanical alloying and mechanical grinding
J. Non-Cryst. Solids **250-252** (1999) 605-610

BIOTTEAU G., HENNION M., MOUSSA F., RODRIGUEZ-CARVAJAL J., PINSARD L., REVCOLEVSCHI A.- Static Ferromagnetic Modulation Revealed by Neutron Scattering in $La_{1-x}Ca_xMnO_3$
Journal of Superconductivity **12** (1999) 261-262

BIOTTEAU G., HENNION M., MOUSSA F., RODRIGUEZ-CARVAJAL J., PINSARD L., REVCOLEVSCHI A. - Anomalous spin dynamics in $La_{1-x}Ca_xMnO_3$
Physica B **259-261** (1999) 826-827

BIOTTEAU G., MOUSSA F., HENNION M., RODRIGUEZ-CARVAJAL J., WILDES A., PINSARD L., REVCOLEVSCHI A. – Strong change in spin dynamics close to percolation in $La_{1-x}Ca_xMnO_3$
Physica B **276-278** (2000) 562-563

BIOTTEAU G. - Etude par diffusion élastique et inélastique de neutrons de systèmes perovskites dopés au calcium $La_{1-x}Ca_xMnO_3$ présentant des propriétés de magnétorésistance géante.
Thesis, University of Paris VII, October 16, 2000

BOBROFF J., M acFARLANE W.A., ALLOUL H, MENDELS P., BLANCHARD N., COLLIN G., MARUCCO J.F. – Spinless impurities in high-T_c cuprates : Kondo-like behavior
Physical Review Letters **83** (1999) 4381-4384

BONNARME V., BACHMANN C., COUSSON A., MONDON M., GESSON J.P. – Diels-Alder reaction of 4-bromo-6-spiroepoxycyclohexa-2,4-dienone with electron-rich and neutral dienophiles
Tetrahedron **54** (1999) 433-448

BONNARME V., BACHMANN C., MONDON M., GESSON J.P., COUSSON A. – Cyclodimerization and Diels-Alder reaction of a spiroepoxycyclohexadienone with an o-quinodimethane structure
Chem. Commun n°12 (1999) 1143-1144

BONETTI M., AMBROISE J.P., CALMETTES P. – A small-angle neutron scattering cell for the study of supercritical fluids at elevated pressure and high temperature : a study of heavy water
Rev. Sci. Instrum. **70** (1999) 4015-4019

BONETTI M., ROMET-LEMONNE G., CALMETTES P., BELLISSENT-FUNEL M.-C. – Small-angle neutron scattering from heavy water in the vicinity of the critical point.
J. Chem. Phys. **112** (2000) 268-274

BONETTI M., CALMETTES P. – Small angle neutron scattering from heavy water in the vicinity of the critical point.
« Steam, Water and Hydrothermal Systems : Physical and Chemistry Meeting the Needs of Industry », Proc. of the 13th ICPWS, P.R. Tremaire, P.G. Hill, D.E. Irish and P.V. Balakrishnan, (Editors) NRC Research Press, Ottawa, Canada, 2000, pp. 347-354

BORGES R.P., OTT F., THOMAS R.M., SKUMRYEV V., COEY J.M.D., ARNAUDAS J.I., RANNO L. - Field-induced transition in the paramagnetic state of $(Sm_{0.65}Sr_{0.35})MnO_3$ associated with magnetic clusters
Physical Review B **60** (1999) 12847-12851

BOTTI S., CICOGNANI G., COPPOLA R., GIORGI L., LAPP A., MAGNANI M. - Particle size and optical performances of photoluminescent laser synthesized Si nanopowders
Physica B **276-278** (2000) 860-861

BOUCHE G., BECHADE J.L., MATHON M.H., ALLAIS L., GOURGUE A.F., NAZE L - Texture of welded joints of 316L stainless steel multi-scale orientation analysis of a weld metal deposit
Journal of Nuclear Materials, **277** (2000) 91-98

BOUCHERLE J.X., GIVORD F., SCHWEIZER J., GUKASOV A., MIGNOT J.-M., LELIEVRE-BERNA E., AOKI H., OCHIAI A. – Polarized neutron investigation in the mixed-valence compound Sm_3Te_4
Physica B **267-268** (1999) 37-40

BOUCHERLE J.X., GIVORD F., SCHWEIZER J., MIGNOT J.-M., LELIEVRE-BERNA E., AOKI H., OCHIAI A. – Polarized neutron investigation of charge ordering in mixed-valence Sm_4Bi_3
Physica B **267-268** (1999) 47

BOUCHERLE J.X., GIVORD F., SCHWEIZER J., MIGNOT J.-M., LELIEVRE-BERNA E., AOKI H., OCHIAI A. – Polarized neutron investigation in the mixed-valence compound Sm_3Te_4 at different temperatures
Physica B **281-282** (2000) 139-140

BOUDJADA F., MEINNEL J., COUSSON A., PAULUS W., MANI M., SANQUER M. - Tribromomesitylene structure at 14 K. Methyl conformation and tunneling
AIP Conf. Proc. **479** (1999) 217-222

BOUIS F. - Deux systèmes d'électrons fortement corrélés : le modèle de réseau Kondo dans la limite du couplage couplage fort et un modèle bidimensionnel d'électrons au voisinage d'une transition topologique électronique
Thesis, Ecole Polytechnique, October 14, 1999

BOUIS F., KISELEV M.N. - Effective action for the Kondo lattice model. New approach for S=1/2
Physica B **259-261** (1999) 195-197

BOUIS F., PFEUTY P. – From the Kondo-Hubbard model to the spin brush model
Physica B **259-261** (1999) 206-207

BOUIS F., KISELEV M.N., ONUFRIEVA F., PFEUTY P. - Various ordered states in a 2D interacting electron system close to an electronic topological transition
Physica B **284-288** (2000) 677-678

BOULET P., GROSS G.M., ANDRE G., BOUREE F., NOEL H. - Crystal and magnetic structure of new ternary uranium intermetallics : U_3TiX_5, X=(Ge, Sn)
Journal of Solid State Chemistry **144** (1999) 311-317

Publications

BOULET P., POTEL M., ANDRE G., ROGL P., NOEL H. - Crystal and magnetic structure of the binary uranium germanide U_3Ge_5
Journal of Alloys and Compounds **283** (1999) 41-44

BOURGES P., SIDIS Y., FONG H.F., KEIMER B., REGNAULT L.P., BOSSY J., IVANOV A., MILLIUS D.L., AKSAY I.A.. – Spin dynamics in high-T_c superconductors
AIP Conference Proceedings "High Temperature Superconductivity" **483** (1999) 207-212

BOURGES P., SIDIS Y., FONG H.F., REGNAULT L.P., BOSSY J., IVANOV A., KEIMER B. - The spin excitation spectrum in superconducting $YBa_2Cu_3O_{6.85}$
Science **288** (2000) 1234-1237

BOURGES P., KEIMER B., REGNAULT L.P., SIDIS Y. - A critical examination of the spin dynamics of high-T_c cuprates
Journal of Superconductivity : Incorporating Novel Magnetism **13** (2000) 735-740

BOURGES P. - Spin dynamics in cuprates and its relation to superconductivity
Neutron Scattering Novel Mater., Proc. Summer Sch. Neutron Scattering 8th (2000) 252-265

BRADEN M., HENNION B., PFEUTY P., DHALENNE G., REVCOLEVSCHI A. - High-energy magnetic excitation in $CuGeO_3$
Physical Review Letters **83** (1999) 1858-1861

BRADEN M., BÜCHNER B., KLOTZ S., MARSHALL M., BEHRUZI M., HEGER G. - Pressure dependence of the crystal structure of $CuGeO_3$-à 6.2 GPa by neutron diffraction
Physical Review B **60 (**1999) 9616-9622

BRADEN M., REICHARDT W., ELKAIM E., LAURIAT J.P., SHIRYAEV S., BARILO S.N. - Structural distortion in superconducting $Ba_{1-x}K_xBiO_3$
Physical Review B **62** (2000) 6708-6715

BRADEN M. - Inelastic neutron scattering : phonons and magnons
Mater. Mater. **5** (2000) 13/1-13/25

BRAND R.A., CODDENS G., CHUMAKOV A.I., CALVAYRAC Y. – Partial phonon density of states of Fe in an icosahedral quasicrystal $Al_{62}Cu_{25.55}Fe_{12.5}$ by inelastic nuclear-resonant absorption of 14.41 keV synchrotron radiation
Physical Review B **59** (1999) R14145-R14148

BRANGER V., MATHON M.H., BAUDIN T., PENELLE R. - "In situ" neutron diffraction study of the cube crystallographic texture development in Fe53%-Ni alloy during recrystallization
Scripta Mater **43** (2000) 325-330

BRANGER V., MATHON M.H., BAUDIN T., PENELLE R. - Neutron diffraction study of the cube texture development in Fe53%-Ni alloy
Physica B **276-278** (2000) 914-915

BRECHT E., SCHWEISS P., WOLF TH., BOOTHROYD A.T., REYNOLD J.M, ANDERSEN N.H., LÜTGEMEIER H., SCHMAHL W.W. - Antiferromagnetic ordering states of oxygen-deficient $NdBa_2Cu_3O_{6+x}$ and $Nd_{1+y}Ba_{2-y}Cu_3O_{6+x}$ single crystals
Phys. Rev. B **59** (1999) 3870-3878

BRIGANTI G., GIORDANO R., LONDEI P., VALLE F. - Functional role of chaperonin protein complexes
Physica B **276-278** (2000) 516-517

BRULET A., BOUE F., MENELLE A., COTTON J.P. - Conformation of polystyrene chain in ultrathin films obtained by spin coating
Macromolecules **33** (2000) 997-1001

CABAÇO M.I., TASSAING T., DANTEN Y., BESNARD M. - Structural study of 1-3-5 trifluorobenzene dimer stability : from liquid to gas densities using supercritical conditions
Chemical Physics Letters **325** (2000) 163-170

CABAÇO M.I., TASSAING T., DANTEN Y., BESNARD M. - Evolution of the local order in 1,3,5-trifluorobenzene from the liquid state up to supercritical conditions.
Journal of Chemical Chemistry A **104** (2000) 10986-10993

CABRAL J.T., LUZAR A., TEIXEIRA J., BELLISSENT-FUNEL M.-C. - Water dynamics in DMSO-Water mixture
Physica B **276-278** (2000) 508-509

CABRAL J.T., LUZAR A., TEIXEIRA J., BELLISSENT-FUNEL M.-C. - Single particle dynamics in DMSO-water eutectic mixture by neutron scattering
Journal of Chemical Physics **113** (2000) 8736-8745

CALMETTES P. – Diffusion des neutrons aux petits angles : choix de l'échantillon et traitement des données
In "Diffusion de neutrons aux petits angles" Editeurs : J.P. Cotton, F. Nallet, Journal de Physique IV 9 (Pr1) (1999) 83-93

CAPUZZI G., FRATINI E., PINI F., BAGLIONI P., CASNATI A., TEIXEIRA J. – Counterion complexation by calixarene ligands in cesium and potassium dodecyl sulfate micelles. A small angle neutron scattering study
Langmuir **16** (2000) 188-194

CASALTA H., SCHLEGER P., BELLOUARD C., HENNION M., I. MIREBEAU I, EHLERS G., FARAGO B., DORMAN J.-L ., KELSCH M., LINDE M., PHILLIPP F. - Direct measurement of superparamagnetic fluctuations in monodomain Fe particles via neutron spin-echo spectroscopy
Physical Review Letters **82** (1999) 1301-1304

CASALTA H., SCHLEGER P., BELLOUARD C., HENNION M., I. MIREBEAU I, EHLERS G., FARAGO B. – Low Q measurement of super-paramagnetic fluctuations in monodomain Fe particles
Physica B **276-278** (2000) 664-665

CASTAING J.C., ALLAIN C., AUROY P., AUVRAY L. - Rheology of nanosized hairy grain suspensions
European Physical Journal. B **10** (1999) 61-70

CASTELLETTO V., NOIREZ L., VIGOUREUX P. – Equilibrium and shear-induced conformations of a side chain liquid crystal polymer
Europhysics Letters **52** (2000) 392-398

CATHALA B., LEE L.T., AGUIE-BEGHIN V., DOUILLARD R., MONTIES B. -
Organization behavior of guaiacyl/syringyl dehydrogenation polymers (lignin model compounds) at the air/water interface
Langmuir **16** (2000) 10444-10448

CELARD N.J., PATHIRAJ B., NIKBIN K., WEBSTER G.A. - A comparison of residual stress measurements in steels using the X-ray and the neutron diffraction techniques.
Materials Science Forum, Vols **347-349**, Trans Tech Publications, Switzerland, 2000.

CERETTI M., MAGLI R., VANGI D. - Neutron diffraction study of stress field distribution in automotive gears
Materials Science Forum **321-324** (2000) 732-736

CERETTI M. - Recent developments for strain measurements at the LLB
Physica B **276-278** (2000) 932-933

CERETTI M., JANSSEN S., McMORROW D., RADAELLI P., STEIGENBERGER U., - ECNS'99 – Young scientist forum
Physica B **276-278** (2000) 45-51

CHAPON L., RAVOT D., TEDENAC J.C., BOUREE-VIGNERON F. - Skutterudites based new thermoelectric compounds. Cerium filled Ni substituted skutterudites $Ce_yFe_{4-x}Ni_xSb_{12}$ type. XANES and neutron diffraction studies.
Proc. Int. Conf. Thermoelec. 18th (1999) 13-15

CHERNYSHEV V.V., FITCH A.N., SONNEVELD E.J., KURBAKOV A.I., MAKAROV V.A., TAFEENKO V.A. - Crystal and Molecular Structures of [1-(2-aminoethyl)-1,2-dihydroimidazolidene-2] nitroaceto-nitrile ($C_7H_{11}N_5O_2$) and 3,7-diamino-4-nitro-6-hydroxy-8-oxopyrazolo[1,5-a] pyrimidine monohydrate ($C_6H_6N_6O_4$+H_2O) from X-Ray, Synchrotron and Neutron Powder Diffraction Data.
Acta Crystallographica B55 (1999) 554-562.

CHERNYSHOV D.YU., KURBAKOV A.I., TROUNOV V.A. - Crystal structure evaluation of $Sm_{0.6}Sr_{0.4}MnO_3$ in the temperature range 1.5 – 300 K
Physica B **276-278** (2000) 318-319

CHERNYSHOV D.Yu., TROUNOV V.A., KURBAKOV A., DUNAEVSKY S.M., RODRIGUEZ-CARVAJAL J. – Neutron diffraction study of crystal and magnetic structure of samarium-strontium manganite
Materials Science Forum **321-324** (2000) 812-817

CHERRABI R., SAOUT-ELHAK A., BENHAMOU M., DAOUD M. - Phase separation in confined polymer blends
J. Chemical Physics **111** (1999) 8174-8181

CLEMENTYEV E.S., BRADEN M., LAZUROV V.N., ALEKSEEV P.A., MIGNOT J.-M., SADIKOV I.P. HIESS A., LAPERTOT G. - Anomalous phonon softening in intermediate-valence CeNi
Physica B **259-261** (1999) 42-43

CLEMENTYEV E.S., MIGNOT J.-M., ALEKSEEV P.A., LAZUKOV V.N., SADIKOV I.P., BRADEN M. – Magnetic excitations in single crystal CeNi
Physica B **276-278** (1999) 760-761

CLEMENTYEV E.S., MIGNOT J.-M., ALEKSEEV P.A., LAZUKOV V.N., NEFEODOVA E.V., SADIKOV I.P., BRADEN M., KAHN R., LAPERTOT G. – Dynamic magnetic response in intermediate-valence CeNi
Physical Review B **61** (2000) 6189-6195

CODDENS G., STEURER W. - A time-of-flight neutron-scattering study of phason hopping in decagonal Al-Co-Ni quasicrystals
Physical Review B **60** (1999) 270-276

CODDENS G. - Comment on « Direct imaging of lowal chemical disorder and columnar vacancies in ideal decagonal Al-Ni-Co quasicrystals»
Physical Review Letters **82** (1999) 4366

CODDENS G., LYONNARD S., HENNION B., CALVAYRAC Y. - Correlated simultaneous phason jumps in an icosahedral Al-Mn-Pd quasicrystal
Physical Review Letters **83** (1999) 3226-3229

CODDENS G. - Comment on « Hierarchical porosity in real quasicrystals »
Philosophical Magazine Letters **79** (1999) 925-927

CODDENS G. - Comment on « Self diffusion in icosahedral $Al_{72.4}Pd_{20.5}Mn_{7.1}$ and phason percolation at low temperature studied by ^{27}Al NMR »
Physical Review Letters **83** (1999) 884

CODDENS G. - La diffusion quasielastique cohérente des neutrons
J. Phys. IV France **10** (2000) 151-164

CODDENS G., LYONNARD S., HENNION B., CALVAYRAC Y. - Triple axis neutron scattering study of phason dynamics in Al-Mn-Pd quasicrystals
Physical Review B **62** (2000) 6268-6295

COPPOLA R., GIORGI L., LAPP A., MAGNANI M. - SANS investigation of Pt-loaded electrodes for polymer electrolyte fuel cells
Physica B **276-278** (2000) 839-840

COPPOLA R., BOUREE F., GIORGI L. - Neutron diffraction study of lithium cobaltites for molten carbonate fuel cells
Physica B **276-27**8 (2000) 862-863

Publications

COTTON J.P., NALLET F. (Editors) – Livre : Diffusion de Neutrons aux Petits Angles
Ecole M^4 de la Société Française de Neutronique, JDN7, Albé (France), Journal de Physique IV 9(Pr1) (1999)

COTTON J.P. – Diffusion de neutrons aux petits angles : introduction et variation sur le contraste
Journal de Physique IV 9(Pr1) (1999) 21-49

COULET M.V., BERGMAN C., BELLISSENT R., BICHARA C. – Local order and phase separation in sulphur-tellurium melts : a neutron scattering study
J. Non Cryst. Solids **250-252** (1999) 463-467

COULET M.V., BELLISSENT R., BIONDUCCI M., BICHARA C. – Can local order changes induce a phase transition in a liquid ?
Europhysics Letters **45** (1999) 175-185

COULET M.V., BELLISSENT R., BICHARA C. – Small angle neutron scattering study of sulphur liquid alloys : structural evidence for a phase separation
Physica B **276-278** (2000) 415-416

COULOMB J.P., GRILLET Y., LLEWELLYN P.L., MARTIN C., ANDRE G. - Structural properties of krypton confined on MCM-41 (ϕ=40 Å)
Fundam. Adsorpt. (1999) 147-152.

COULOMB J.P., MARTIN C., GRILLET Y., KAHN R. - Different translational mobility types of confined molecules in the one-dimensional micropores of model zeolites : $AlPO_{4\text{-}5}$ and $AlPO_{4\text{-}11}$
Proceedings of the International Zeolite Conference, M.M.J. Tracy, Editor (1999) pp. 51-58

COULOMB J.P., FLOQUET N., GRILLET Y., LLEWELLYN P.L., KAHN R., ANDRE G. – Dynamic and structural properties of confined phase (hydrogen, methane and water) in MCM-41 samples (19 Å, 25 Å. and 40 Å)
Studies in Surface Science and Catalysis **128** (2000) 235-242

COUSSON A., COUSTARD J.-M. - Crystal structure of ethyl (Z)-2-hydroxyimino-2—(methylsulfanyl)acetate, $C_5H_9SNO_3$
Z. Kristallogr. New Cryst. Struct. **214** (1999) 469-470

COUSSON A., COUSTARD J.-M. - Crystal structure of (E)-1-(methylthio)-1-(4'-methoxyphenylamino)-2-nitroethene, $C_{10}H_{12}N_2O_3S$
Z. Kristallogr. New Cryst. Struct. **214** (1999) 467-468

CRUPI V., MAGAZU S., MAJOLINO D., MIGLIARDO P., VENUTI V., BELLISSENT-FUNEL M.-C.- Confinement influence in liquid water studied by Raman and neutron scattering
J. Phys. :Condens. Matter **12** (2000) 3625-3630

CRUPI V., MAGAZU S., MAJOLINO D., MIGLIARDO P., BELLISSENT-FUNEL M.-C. - Dynamical study of confinement ethylene glycol by IQENS
Physica B **276-278** (2000) 417-418

DAHLBORG U., HOWELLS W.S., CALVO-DAHLBORG M., DUBOIS J.M. – Atomic motions in the crystalline $Al_{50}Cu_{35}Ni_{15}$ alloy
J. Physics : Condens. Matter **12** (2000) 4021-4041

DAMAY F., MARTIN C., MAIGNAN A., HERVIEU M., RAVEAU B., JIRAK Z., ANDRE G., BOUREE F. - Magnetic and structural transitions in the half-doped manganites $Pr_{0.5}Sr_{0.5\text{-}x}Ca_xMnO_3$
Chem. Mater. **11** (1999) 536-541

D'ARRIGO G., GIORDANO R., TEIXEIRA J. – Small-angle neutron scattering studies of aqueous solutions of linear alkenediols and triols
Langmuir **16** (2000) 1553-1556

D'ASTUTO M., BOURGES P., CASALTA H., IVANOV A., PETITGRAND D. – Low energy magnetic dynamics of Nd-moments in Nd_2CuO_4
Physica B **259-261** (1999) 875-876

DE CARLAN Y., FOUCHE C., MATHON M.H., GEOFFROY G. - Study of secondary hardening phenomena in F82H steel by Small Angle Neutron Scattering
Progress Report - Contract UT-SM&C - LAM3 NT SRMA 2318 (1999)

DE CARLAN Y., ALAMO A., MATHON M.H., GEOFFROY G., CASTAING A. - Effect of thermal aging on microstructure and mechanical properties of 7-11Cr W steels
J. Nuclear Materials **283-287** (2000) 672-676

DELLERUE S., BELLISSENT-FUNEL M.-C. – Collective and individual dynamics in a photosynthetic protein
Biochimie 81 (2000) 2835

DELLERUE S., BELLISSENT-FUNEL M.-C. - Relaxational dynamics of water molecules at protein surface
Chemical Physics **258** (2000) 315-325

DELLERUE S., PETRESCU A., SMITH J.C., LONGEVILLE S., BELLISSENT-FUNEL M.-C. - Collective dynamics of a photosynthetic protein probed by neutron spin-echo spectroscopy and molecular dynamics simulation
Physica B **276-278** (2000) 514-515

DELLERUE S. - Structure et dynamique de protéines photosynthétiques étudiées par diffusion de neutrons et simulation par dynamique moléculaire
Thesis, University of Paris XI Orsay, January 21, 2000

DEME B., HESS D., TRISTL M., LEE L.T., SACKMANN E. – Binding of actin filaments to charged lipid monolayers : film balance experiments combined with neutron reflectivity
European Physical Journal E **2** (2000) 125-136

DEMIRDJIAN B.
Structure et dynamique des films de glace supportés. Influence de l'adsorption de HCL, implications pour l'environnement.
Thesis, December 2000.

DEROLLEZ P., LAAMYEM A., FOURET R., HENNION B., GONZALEZ J. - Phonons in chalcopyrite compounds
AIP Conference Proceedings « Neutrons and Numerical Methods - N2M » **479** (1999) 127-130

DEROLLEZ P., FOURET R., LAAMYEM A., HENNION B., GONZALEZ J. – Lattice dynamics in copper indium diselenide by inelastic neutron scattering
Journal of Physics : Condensed Matter **11** (1999) 3987-3995

DILIGENT-BERVEILLER S., GAUTIER E., WEISBECKER P., MATHON M.H., IUNG T., REGLE H., ZIMMER P. - Influence of cooling temperature on recrystallization of Cu-bearing Ti-IF steels
Proceedings of the 21st Riso International Symposium on Materials Science : Recrystallization – Fundamental Aspects and Relations to Deformation Microstructure, Editors : N. Hansen, X. Huang, D. Juul Jensen, E.M. Lauridsen, T. Leffers W. Pantleon, T.J. Sabin, J.A. Wert (2000) 321-325

DOOGLAV A.V., EGOROV A.V., MUKHAMEDSHIN I.R., SAVINKOV A.V., ALLOUL H, BOBROFF J., MacFARLANE W.A., MENDELS P., COLLIN G., BLANCHARD N, PICARD P.G. – Antiferromagnetism in hydrated 123 compounds
JETP Letters **69** (1999) 792-797

DORE J., SUFI M.A.M., BELLISSENT-FUNEL M.-C. - Structural change in D_2O water as a function of temperature : the isochoric temperature derivative function for neutron diffraction
Phys. Chem. Chem. Phys. **2** (2000) 1599-1602

DORNER B., PETITGRAND P., GUDEL H.U. – Minute splitting of magnetic excitations due to dipolar interactions in $CsFeCl_3$ and $RbFeCl_3$ observed with polarised neutrons
Physica B **267-268** (1999) 263-265

DUBOIS E., CABUIL F., BOUE F.., PERZYNSKI R. – Structural analogy between aqueous and oily magnetic fluids
Journal of Chemical Physics **111** (1999) 7147-7160

DUBOIS E., PERZYNSKI R., BOUE F., CABUIL F. – Liquid-Gas transition in charged colloidal dispersions : small angle neutron scattering coupled with phase diagrams of magnetic fluids
Langmuir **16** (2000) 5617-5625

DUFAU N., FLOQUET N., COULOMB J.P., ANDRE G., KAHN R., LLEWELLYN P.L., GRILLET Y. – On the ordering of simple gas phases adsorbed within model microporous adsorbents.
Stud. Surf. Sci. Catal. **128** (2000) 289-293

DUFOUR C., DUMESNIL K., MOUGIN A., MANGIN Ph., HENNION M.,- Large wavelength magnetic modulation in (0001) Tb films
J. Phys. Conden. Matter **11** (1999) L497-L503

DUMESNIL K., DUFOUR C., MANGIN Ph., HENNION M., BROWN P.J. – Crystal and magnetic structures of Sm epitaxial thin films and Sm/Y superlattices
Physical Review B **60** (1999) 10743-10746

DUMONT Y., AYACHE C., COLLIN G. – Dragging excitation characteristics from thermoelectric powder in $Bi_2(Sr_{2-y}La_y)CuO_{6+\delta}$ single crystals
Physical Review B **62** (2000) 622-625

EHRENBERG H., WEITZEL H. FUESS H., HENNION B. - Magnon dispersion in $MnWO_4$
J. Phys. Condens. Matter **11** (1999) 2649-2659

EL BADRAOUI E., BAUDOUR J.L., LEROUX C. FRITSCH S., BOUREE F., GILLOT B., ROUSSET A. - Cation distribution, short-range order and small polaron hopping conduction in nickel manganites, from a neutron diffraction study
Phys. Stat. Sol. **212** (1999) 129-139

EL KHAYATI N., CHERKAOUI EL MOURSLI R., RODRIGUEZ-CARVAJAL J., ANDRÉ G., BLANCHARD N., BOURÉE F., COLLIN G., ROISNEL T. - Magnetic structure of compounds $MFePO_5$ (M = Cu, Ni)
Phosphorus Research Bulletin **11** (2000) 107-113.

ETRILLARD J., BOURGES P., LIN C.T. - Incommensurate composite structure of the superconductor Bi-2212
Physical Review B **62** (2000) 150-153

ETXEBARRIA I., HLINKA J., QUILICHINI M., - The role of nearest neighbour anharmonic couplings in the phase diagram of betaine calcium chloride dihydrate (BDDC)
Journal of Physics : Condensed Matter **11** (1999) 5497-5504

FADDA G.C., LAIREZ D. - Rigid structure of fractal aggregates of lysozyme
Europhysics Letters **52** (2000) 712-718

FAURE M.C., BASSEREAU P., LEE L.T., MENELLE A., LHEVEDER C. - Phase transitions in monolayers of PS-PEO copolymer at the air-water interface
Macromolecules **32** (1999) 8538-8550

FERMON C., OTT F., GILLES B., MARTY A., MENELLE A., SAMSON Y., LEGOFF G., FRANCINET G.. – Towards a 3D magnetometry by neutron reflectometry
Physica B **267-268** (1999) 162-167

FERMON C., OTT F., LEGOFF G., GLATTLI H., WINTENBERGER V. - New polarised neutron reflectometer with polarisation analysis PRISM
Physica B **283** (2000) 372-375

Publications

FERMON C., OTT F., MENELLE A. - Neutron reflectometry
in « X-ray and neutron reflectivity : principle and applications » Edited by J. Daillant and A. Gibaud, Springer-Verlag 1999, pp. 163-195

FERMON C., OTT F., LEGOFF G., GLÄTTLI H., WINTENBERGER V. - PRISM, the new polarised neutron reflectometer with polarisation analysis at the LLB
Rev. Sci. Instr . **71** (2000) 3797-3800

FIETZ W.H., GRUBE K., SCHLACHTER S.I., LUDWIG H.A., TUTSCH U., WUHL H., WEISS K.P., LEIBROCK H., HAUFF R., WOLF Th., OBST B., SCHWEISS P., KLASER M. – Joint features of pressure effect and specific heat of $RBa_2Cu_3O_x$ at distinct n_H values
Physica C **341-348** (2000) 347-350

FILLAUX F., LEYGUE N., TOMKINSON J., COUSSON A., PAULUS W. - Structure and dynamics of the symmetric hydrogen bond in potassium hydrogen maleate : a neutron scattering study
Chem. Phys. **244** (1999) 387-403

FITZPATRICK M. E., HUTCHINGS M.T., WITHERS P.J. - Separation of Measured Fatigue Crack Stress Fields in a Metal Matrix Composite Material,
Acta Mater., **47**(1999) 585-593

FITZPATRICK M. E., KENNARD M.J., SMALL C.J. - Problems in Residual Stress Determination for Thick Components.
in 6th Intl Conf. on Residual Stresses, Vol. 2, pp 939-946. Institute of Materials, UK, 2000.

FLOQUET N., COULOMB J.P., MARTIN C., GRILLET Y., LLEWELLYN P.L., ANDRE G. - Neutron diffraction study of phase transitions observed during the sorption of D_2O on MCM-41 (40 Å and 25 Å)
Materials Research Society (1999) 659-666.

FONG H.F., BOURGES P., SIDIS Y., REGNAULT L .P., GUK G.S., NOSHIZUKA N., KEIMER B. - Neutron scattering from magnetic excitations in $Bi_2Sr_2CaCu_2O_{8+\delta}$
Nature **298** (1999) 588-591

FONG H.F., BOURGES P., SIDIS Y., REGNAULT L .P., BOSSY J., IVANOV A. MILLIUS D.L., AKSAY I.A., KEIMER B. – Effect of nonmagnetic impurities on the magnetic resonance peak in $YBa_2Cu_3O_7$
Physical Review Letters **82** (1999) 1939-1942

FONG H.F., BOURGES P., SIDIS Y., REGNAULT L .P., BOSSY J., IVANOV A., MILIUS D.L., AKSAY I.A., KEIMER B. - Spin susceptibility in underdoped $YBa_2Cu_3O_{6+x}$
Physical Review B **61** (2000) 14773-14786

FORMISANO F., TEIXEIRA J. - Critical fluctuations of a binary mixture confined in a porous medium
European Physical Journal E **1** (2000) 1-4

FORMISANO F., TEIXEIRA J. – Appearance of critical fluctuations in a binary fluid mixture confined in vycor glass
J. Physics : Condens. Matter **12** (2000) A351-A356

FORMISANO F., TEIXEIRA J. - Critical fluctuations of a fluid mixture confined in a porous glass investigated through SANS
Notiziario Neutroni e Luce Sincrotone **5** (2000) 16-22

FOURMAUX-DEMANGE V., BRULET A., BOUE F., DAVIDSON P., KELLER P., COTTON J.P. - Influence on the nematic order on rheology and conformation of stretched comb-like liquid crystalline polymers
European Physical Journal E **1** (2000) 301-317

FRONTERA C., GARCIA-MUNOZ J.L., LLOBERT A., RITTER C., ALONSO J.A., RODRIGUEZ-CARVAJAL J. - Dependence of the physical properties of $Nd_{0.5}Ca_{0.5}MnO_{3+\delta}$ on the oxidation state of Mn
Physical Review B **62** (2000) 3002-3005

FUJISHIRO K., IWASE T., UESU Y., YAMADA Y., DKHIL B., KIAT J.M., MORI S., YAMAMOTO N. - Optical and structural studies of long-range order development in relaxor ferroelectric
J. Phys. Soc. Japan, **69** (2000) 2331-2338

GALDEANO S., CHAFFRON L., MATHON M.H., ANDRE G., VINCENT E., de NOVION C.H. - Microstructural characterisation of the mechanically alloyed $Cu_{88}Fe_{12}$ and $Cu_{72}Co_{28}$ compounds and of the ball milled $Cu_{80}(Fe_{0.3}Co_{0.7})_{20}$ pseudo alloy.
Materials Science Forum **343-346** (2000) 715-720

GALL A., FRASER N.J., BELLISSENT-FUNEL M.-C., SCHEER H., ROBERT B., COGDELL R.J.- Bacteriochlorin-protein interactions in native B800-B850, B800 deficient and B800-Bchlap-reconstituted complexes from Rhodopseudomonas acidophila, strain 10050
FEBS Letters **449** (1999) 269-272

GAMEZ-CORRALES R., BERRET J.-F., WALKER L.M., OBERDISSE J. - Shear-thickening dilute surfactant solutions. Equilibrium structurae as studied by small angle neutron scattering
Langmuir 15 (1999) 6755-6763

GEOFFROY G., BARBU A., MAURY F., MATHON M.H. - Etude par diffusion de neutrons aux petits angles d'aciers austéno-ferritiques modèles et de deux aciers prélevés sur les vannes de Chooz
Note Technique CEA/LSI N°129 (1999).

GEOGHEGAN M., CLARKE C.J., BOUE F., MENELLE A., RUSS T., BUCKNALL D.G. – The kinetics of penetration of grafted polymers into a network
Macromolecules **32** (1999) 5106-5114

GEOGHEGAN M., BOUE F., MENELLE A., ABEL F., RUSS T., ERMER H., BUCKNALL D.G. - Surface segregation from a polymer network
J. Physics : Condensed Matter **12** (2000) 5129-5142

GILLON B., AEBERSOLD M., KAHN O., PARDI L., DELLEY B. - Spin density in a triazole-nitronyl-nitroxide radical presenting linear ferromagnetic interactions : role of hydrogen bonding
Chemical Physics **250** (1999) 23-34

GILLON B. – Spin densities in bimetallic compounds : polarized neutron diffraction
Mol. Cryst. Liq. Cryst. Sci. Technol. Sect A **335** (1999) 765-784

GILLON B. - Spin distribution in molecular systems with interacting transition metal ions
In «Magnetism: Molecules to Materials: Models and Experiments », Miller and Drillon eds. (1999) 357-378

GIRARDIN E., MILLET P., LODINI A. - X-ray and neutron diffraction studies of crystallinity in hydroxyapatite coating
J. Biomedical Material Research **49** (2000) 211-215

GLYDE H.R., PLANTEVIN O., FAK B., CODDENS G., DANIELSON P.S., SCHOBER H. - Dynamics of liquid ^{4}He in Vycor
Physical Review Letters **84** (2000) 2646-2649

GOLOSOVSKY I.V., TOREK Gy., MALTZEV E.I., MIREBEAU I. - Neutron diffraction study of nanocrystalline alloys $Fe_{73.5}CuNb_3(Si,B)_{22.5}$
Physica B **276-278** (2000) 918-920

GOLOSOVSKY I.V., GUKASOV A.G., POLYAKOV V.A., ZHIGUNOV D.I., ZOBKALO I.A. – Magnetic structure of lanthanum copper oxide $La_2Cu_2O_5$
Journal of Physics : Condensed Matter **11** (1999) 6959-6967

GONCHARENKO I.N., MIREBEAU I., IRODOVA A.V., SUARD E. - Magnetic and hydrogen ordering in the frustrated Laves hydrides $RMn_2H_{4.5}$ (R=Y, Gd, Tb, Dy, Ho) : a neutron diffraction study
Physical Review B **59** (1999) 9324-9331

GONCHARENKO I.N., MIREBEAU I., OCHIAI A. - Magnetic neutron diffraction under pressures up to 43 GPa. Study of the EuX and GdX compounds
Hyperfine Interactions 128 (2000) 225-444

GONCHARENKO I.N., LINK P., MIGNOT J.M., KOHGI M., IWASA K., HAGA Y., SUZUKI T. - Appearance of ferromagnetism in CeP at high pressure
Physica B **259-261** (1999) 306-308

GREVIN B., BERTHIER Y., MENDELS P., COLLIN G. - Superconducting clusters and phase separation in $Pr_{1-x}Ba_{2-x}Cu_3O_{7+\delta}$: a 63,65Cu nuclear quadrupole resonance and zero-field NMR study
Physical Review B **61** (2000) 4334-4345

GREVIN B., BERTHIER Y., COLLIN G. – Comment on « Low-temperature charge ordering in the superconducting state of $YBa_2Cu_3O_{7+\delta}$ »
Physical Review Letters **84** (2000) 1636

GREVIN B., BERTHIER Y., COLLIN G. – In-plane charge modulation below T_c and charge-density-wave correlations in the chain layer in $YBa_2Cu_3O_7$
Physical Review Letters **85** (2000) 1310-1313

GROENEWEGEN W., EGELHAAF S.U., LAPP A., VAN DER MAAREL J.R.C. - Neutron scattering estimates of the effect of charge on the micelle structure in aqueous polyelectrolyte diblock copolymer solutions
Macromolecules **33** (2000) 3283-3293

GROENEWEGEN W., LAPP A., EGELHAAF S.U., VAN DER MAAREL J.R.C. - Counterion distribution in the coronal layer of polyelectrolyte diblock copolymer micelles
Macromolecules **33** (2000) 4080-4086

GROSSE M. - Additional information about the chemistry of precipitates by variation of the scattering contrast in SANS and SAXS experiments
Proceedings of the International School and Symposium on Small-Angle Scattering, Matrabaza, Hungary, Report KFKI-1999-02/E (1999) p. 38

GROSSE M., BÖHMERT J. - Irradiation damage structure in VVER-440 steels after irradiation at different temperatures and post-irradiation annealing
In Effects of Radiation on Materials, 19th International Symposium, ASTM STP 1366, M.L. Hamilton and A.S. Kumar Eds, West Conshohocken (PA, USA) (1999)

GROSSE M., DENNER V., BOHMERT J., MATHON M.H. - Irradiation induced structural changes in surveillance material of VVER 440-type weld metal
Journal of Nuclear Materials **277** (2000) 280-287

GUARINI E., BAFILE U., BAROCCHI F., CASANOVA G., FORMISANO F., MAGLI R - The three-body interaction in fluids studied by SANS
Physica B **276-278** (2000) 410-412

GUEZOU J.C., BAUDIN T., CERETTI M., MATHON M.-H., SPRAUEL J.-M., PENELLE R. - Study of elastic residual strains in quartzites
C.R. Acad. Sci. Paris Sciences de la terre et des Planètes **328** (1999) 733-738

GUENOUN P., MULLER F., FONTAINE P., DELSANTI M., AUVRAY L., YANG J., MAYS J.W., TIRREL M., DEME B., LESIEUR P. - Charged stars formed by association of charged-neutral diblock copolymers
Polym. Prepr. **40** (1999) 1018-1019

GUENOUN P., MULLER F., FONTAINE P., DELSANTI M., AUVRAY L., YANG J., MAYS J.W., TIRREL M., DEME B., LESIEUR P. - Charged stars formed by association of charged-neutral diblock copolymers
218th ACS National Meeting, New Orleans, 1999, p. 638

GUILLEMET-FRISTCH S., BAUDOUR J.L., CHANEL C., BOUREE F., ROUSSET A. - X-ray and neutron diffraction studies on nickel zinc manganite $Mn_{2.35-x}Ni_{0.65}Zn_xO_4$ powders
Solid State Ionic **132** (2000) 63-69

Publications

GUILLOT S., LAIREZ D., AXELOS M.A.V. - Non-self-similar aggregation of methylcellulose
J. Appl. Crystallogr. **33** (2000) 669-672

GUKASOV A., PLAKHTY V.P., DORNER B., KOKOVIN S. YU., SYROMYATNIKOV V.N., SMIRNOV O.P., CHERNENKOV YU.P. - Inelastic neutron scattering study of spin waves in the garnet $Mn_3Al_2Ge_3O_{12}$ with a triangular magnetic structure
J. Phys. : Condens. Matter **11** (1999) 2869-2878

GUKASOV A. – Left-right asymmetry in polarized neutron scattering
Physica B **267-268** (1999) 97-105

HELLWEG T., BRULET A., SOTTMANN T. - Dynamics in an oil-continuous droplet microemulsion as seen by quasielastic scattering techniques
Physical Chemistry Chemical Physics **2** (2000) 5168-5174

HENNION B. – Structural and magnetic dynamical properties of solids. Experimental approach with inelastic scattering
Acta Phys. Pol. A **96** (1999) 629-640

HENNION M., MIREBEAU I. - Diffusion de neutrons aux petits angles (DNPA) et magnétisme : concepts et applications
J. Phys. IV France **9** (1999) 51-66

HENNION M., BIOTTEAU G., MOUSSA F., RODRIGUEZ-CARVAJAL J., PINSARD L., REVCOLEVSCHI A. - Static Ferromagnetic Modulation in $La_{1-x}Ca_xMnO_3$: Assembly of Interacting Magnetic Polarons
Physica B **259-261** (1999) 814-815

HENNION M., MOUSSA F., BIOTTEAU G., RODRIGUEZ-CARVAJAL J., PINSARD L., REVCOLEVSCHI A.
Magnetic coupling induced by hole doping in perovskites $La_{0.94}Sr_{0.06}MnO_3$ by neutron scattering and comparison with Ca-doped manganites
Physical Review B **61** (2000) 9513-9522

HERNANDEZ O., QUILICHINI M., PEREZ-MATO J.M., ZUNIGA F.J., DUISEK M., KIAT J.M., EZPELETA J.M. - Neutron structural study of a displacively modulated crystal. : a soliton regime in betaine calcium chloride dihydrate
Physical Review B **60** (1999) 7025-7036

HERNANDEZ O., KIAT J.M., COUSSON A., PAULUS W., EZPELETA J.M., ZUNIGA F.J. – Commensurately modulated 1/4 and 1/5 phases of deuterated betaine calcium chloride dihydrate : a neutron structural study
Acta Crystallographica C**55** (1999) 1463-1466

HERNANDEZ –VELASCO J., SAEZ-PUCHE, HOSER A., RODRIGUEZ-CARVAJAL J. - Magnetic structures of R_2BaCoO_5 (R=Rare earth)
Physica B **276-278** (2000) 726-727

HINSEN K., PETRESCU A.J., DELLERUE S., BELLISSENT-FUNEL M.-C. - Harmonicity in slow protein dynamics
Chem. Phys. **261** (2000) 25-37

HIRSCHBERG J.H.K. KY, BRUNSVELD L., RAMZI A., VEKEMANS J.A.J.M., MEIJER E.W. - Helical self-assembled polymers from cooperative stacking of hydrogen-bonded pairs
Letters to Nature **407** (2000) 167-170

HIRSCHI K. - Analyse des contraintes résiduelles et des paramètres microstructuraux par diffraction de neutrons dans un acier inoxydable austénitique.
Thesis, University of Reims Champagne-Ardenne, October 11, 1999

HIRSCHI K., CERETTI M., LUKAS P., JI N., BRAHAM C., LODINI A. - Microstrain measurement in plastically deformed austenitic steel
Texture and Microstructures **33** (1999) 219-230

HOLMBERG K., NYDEN M., LEE L.T., MALMSTEN M., JHA B.K. – Interactions between a lipase and charged surfactants – a comparison between bulk and interfaces
Adv. Colloid Interface Sci. **88** (2000) 223-241

IRODOVA A.V., ANDRE G., BOUREE F. - Phase transition between hydrogen superstructures with k=(001) and k=0 via incommensurate phase in $ZrV_2D_x(2.8\leq x\leq 3.9)$
Journal of Alloys and Compounds **302** (2000) 159-168

ISAKINA A.P., PROKHVATILOV A.I., RODRIGUEZ-CARVAJAL J. - Structure and thermal expansion of the low-temperature phase of SF_6
Low Temperature Physics **26** (2000) 296-304

IVANOV A., BOURGES P , PETITGRAND D. - In-plane copper spin wave gap in Pr_2CuO_4
Physica B **259-261** (1999) 879-880

IWASA K., KOHGI M., HAGA Y., SUZUKI T., KAKURAI K., NICHI M., NAKAJIMA M., LINK P., GUKASSOV A., MIGNOT J.-M. - Polarized neutron study of the magnetic polaron state in CeP
Physica B **259-261** (1999) 285-287

IWASA K., KOHGI M., HAGA Y., SUZUKI T., KAKURAI K., NICHI M., NAKAJIMA M., LINK P., GUKASOV A., MIGNOT J.M. - Polarized neutron study of the magnetic polaron state in CeP
J. Phys. Chem. Solids **60** (1999) 1185-1188

IWASA K., KOHGI M., HAGA Y., SUZUKI T., KAKURAI K., NICHI M., NAKAJIMA M., LINK P., GUKASOV A., MIGNOT J.-M. – Magnetic form factor of magnetic polaron state in CeP
JAERI-Rev. (1999) 122-123

IWASA K., KOHGI M., HAGA Y., OSAKABE T., BRADEN M., MIGNOT J.-M., SUZUKI T.
Phonon dispersions in the low-carrier density system CeSb
JAERI-Rev. (2000) 67

IWASA K., KOHGI M., GUKASOV A., MIGNOT J.M., OCHIAI A., AOKI H. SUZUKI T. – Magnetic states of Yb ions in the charge ordered phase of Yb_4As_3 determined by polarized-neutron scattering
Physica B **281-282** (2000) 460-461

JANKOWSKA-KISIELINSKA J., MIKKE K ., HENNION B. – Inelastic neutron scattering in γ-Mn(12%Ge) alloy and below the Neel temperature
Acta Phys. Pol. A **97** (2000) 559-562

JANKOWSKA-KISIELINSKA J., MIKKE K ., HENNION B., MILCZAREK J.J. – Inelastic neutron scattering at the magnetic Brillouin zone boundary in antiferromagnetic Mn(13.7%Ni) alloy
J. Phys. :Condens. Matter **12** (2000) 161-176

JARY D., SIKORAV J.L., LAIREZ D. – Nonlinear viscoelasticity of entangled DNA molecules
Europhysics Letters **46** (1999) 251-255

JAVIERRE I., NALLET F., BELLOCQ A.-M., MAUGEY M. - Structure and dynamic properties of a polymer-induced sponge phase
Journal of Physics : Condensed Matter **12** (2000) A295-A299

JEAN F., COLLIN G., ANDRIEUX M., BLANCHARD N., MARUCCO J.F. – Oxygen non-stoichiometry, point defects and critical temperature in superconducting oxides $Bi_2Sr_2CaCu_2O_{8+d}$
Physica C **339** (2000) 269-280

JEAN F., MARUCCO J.F., COLLIN G., ANDRIEUX M., BLANCHARD N. – Dependence of oxygen stoichiometry and critical temperature of susceptibility in Kagome-based $Bi_2Sr_2CaCu_2O_{8+\Delta}$ on oxygen partial pressure between 300 and 700°C
Supercond. Sci. Technol. **13** (2000) 1167-1169

JEAN, B., LEE L.T., CABANE B. - Interaction of sodium dodecyl sulfate with acrylamide-N-isopropylacrylamide statistical copolymer
Colloid Polymer Science **278** (2000) 764-770

JEAN, B., LEE L.T., CABANE B. - Polymer-surfactant interactions at the air-water interface
Book of Abstract " 219th ACS National Meeting , San Franscisco ", COLL-156.

JIRAK Z., DAMAY F., HERVIEU M., MARTIN C., RAVEAU B., ANDRE G., BOUREE F. – Magnetism and charge ordering in $Pr_{0.5}Ca_xSr_{0.5-x}MnO_3$ (x=0.09 and 0.5)
Physical Review B **61** (2000) 1181-1188

JOHANSSON M., AUBRY S. - Growth and decay of discrete nonlinear Schrödinger breathers interacting with internal modes or standing-wave phonons
Physical Review E **61** (2000) 5864-5879

JORIO A., CURRAT R., MYLES D., McINTYRE G.J., ALEKSANDROVA I.P., KIAT J.M., SAINT GREGOIRE P. - Ferroelastic phase transition in $Cs_3Bi_2I_9$: a neutron diffration study
Physical Review B **61** (2000) 3857-3862

JOVARI P. - Neutron diffraction and computer simulation study of liquid CS_2 and CSe_2
Molecular Physics **97** (1999) 1149-1156

JULIEN M.H., FEHER T ., HORVATIC M., BERTHIER C., BAKHAREV O.N., SEGRANSAN P., COLLIN G., MARUCCO J.F. – ^{63}Cu NMR evidence for enhanced antiferromagnetic correlations around Zn impurities in $YBa_2Cu_3O_{6.7}$
Physical Review Letters **84** (2000) 3422-3425

KADLEC F., MOUSSA F., SIMON P., SOBOLEV B.P. - Inelastic neutron scattering study of the superionic solid solutions $Ba_{1-x}La_xF_{2+2x}$
Solid State Ionics **119** (1999) 131-137

KADLEC F., MOUSSA F., SIMON P., GRUENER B.P., SOBOLEV B.P. - Defects and lattice distortion in the superionic conductor $Ba_{0.84}La_{0.16}F_{2.16}$
Mater. Sci. Eng. B **57** (1999) 234-240

KADLEC F., SIMON P., MOUSSA F. - Vibrational spectroscopy of $Ba_{1-x}R_xF_{2+x}$ (R=La, Nd) superionic conductors
Ferroelectrics **239** (2000) 47-54

KASTNER J., NEUHAUS J., WASSERMANN E.F., PETRY W., HENNION B., BACH H. – TA1[110] phonon dispersion and martensitic phase transition in ordered allys Fe_3Pt
European Physical Journal B **11** (1999) 75-81

KEARLEY G .J., NICOLAI B. – Méthodes numériques et simulations
J. Phys. IV France **10** (2000)

KEIMER B., BOURGES P., FONG H.F., SIDIS Y., REGNAULT L.P., IVANOV A., MILIUS D.L., AKSAY L.A., GU G.D., KOSHIZUKA N. – Resonant spin excitations in $YBa_2Cu_3O_{6+\delta}$ and $Bi_2Sr_2CaCu_2O_{8+\delta}$
J. Phys. Chem. Solids **60** (1999) 1007-1011

KEIMER B., BOURGES P., FONG H.F., GU G.D., HE H., IVANOV A., MILIUS D.L., KOSHIZUKA N. – LIANG B., LIN C.T., REGNAULT L.P., SIDIS Y., SCHOENHERR E. – Spin excitations in cuprates : from underdoped to overdoped
Physica C **341-348** (2000) 2113-2116

KEIZER R.J., de VISSER A., MENOVSKY A.A., FRANSE J.J.M., FAK B., MIGNOT J.M. - Neutron diffraction study of the evolution of antiferromagnetic order in UPt_3 doped with Pd
Physical Review B **60** (1999) 6668-6677

KENT M.S., MAJEWSKI J., SMITH G.S., LEE L.T., SATIJA S. – Tethered chains in poor solvent conditions : an experimental study involving Langmuir diblock copolymer monolayers
J. Chem. Phys. **110** (1999) 3553-3565

KENTZINGER E., PARASOTE V., PIERRON-BOHNES V., LAMI J.F., CADEVILLE M.C., SANCHEZ J.M., CAUDRON R., BEUNEU B. – Experimental determination of pair interaction energies in a $CoPt_3$ single crystal and phase diagram calculations
Physical Review B **61** (2000) 14975-14983

Publications

KIAT J.M., BALDINOZZI G., DUNLOP M., MALIBERT C., DKHIL B., MENORET C., MASSON O., FERNANDEZ-DIAZ M.-T. – Anharmonicity and disorder in simple and complex perovskites : a high energy synchrotron and hot neutron diffraction study
J. Physics : Condensed. Matter **12** (2000) 8411-8425

KIKOIN K., KISELEV M.N., MISHCHENKO A.S., DE VISSER A. - Themodynamics of CeNiSn at low temperatures and in weak magnetic fields
Physical Review B **59** (1999) 15070-15084

KISELEV M.N., KIKOIN K.A. - Critical dynamics of Heisenberg antiferromagnets : correlation functions above Néel point
Physica B **259-261** (1999) 913-915

KISELEV M.N., BOUIS F. - Comment on «Theory of unconventional spin density wave : a possible mechanism of the micromagnetism in U-based heavy fermion compounds»
Physical Review Letters **82** (1999) 5172

KISELEV M.N., BOUIS F., ONUFRIEVA F., PFEUTY P. - Some consequences of electronic topological transition in 2D system on a square lattice : excitonic ordered states
European Physical Journal B **16** (2000) 601-611

KLOTZ S., BRADEN M. - Phonon dispersion of bcc iron to 10 GPa
Physical Review Letters **85** (2000) 3209-3212

KLOTZ S., BRADEN M., BESSON J.M. – Inelastic neutron scattering to very high pressures
Hyperfine Interact **128** (2000) 245-254

KOEPPE M., BREUEL M., GAHLER R., GOLUB R., HANK P., KELLER T., LONGEVILLE S., RAUCH U., WUTTKE J. – Prospects on resonance spin-echo
Physica B **266** (1999) 75-86

KOHGI M., IWASA K., MIGNOT J.M., PYKA N., OCHIAI A., AOKI H., SUZUKI T. - Magnetic excitations in the charge ordered state of Yb_4As_3 and $Yb_4(As_{0.6}P_{0.4})_3$
Physica B **259-261** (1999) 269-270

KOHGI M., IWASA K., MIGNOT J.M., PYKA N., KADOWAKI H., OAKI H., SUZUKI T . - Low energy excitations in the low-carrier heavy-electron system Yb_4As_3
JJAP Ser**. 11** (1999) 111-113

KOPIDAKIS G., AUBRY S. - Breathers discrets intrabandes dans les systèmes désordonnés
Editions Paris Onze - Rencontres NonLinéaires IHP-Paris, 1999

KOPIDAKIS G., AUBRY S. - Intraband discrete breathers in disordered nonlinear systems :
I : delocalization
Physica D **130** (1999) 155-186

KOPIDAKIS G., AUBRY S. - Discrete breathers and delocalization in nonlinear disordered systems
Physical Review Letters **84** (2000) 3226-3229

KOPIDAKIS G., AUBRY S. - Intraband discrete breathers in disordered nonlinear systems :
II : localization
Physica D **139** (2000) 247-275

KORNEEV D.A., BODNARCHUK V.I., YARADAIKIN S.P., PERESEDOV V.F., IGNATOCICH V.K., MENELLE A., GAEHLER R. - Reflectometry studies of the coherent properties of neutrons
Physica B **276-278** (2000) 973-974

KURBAKOV A., RODRIGUEZ-CARVAJAL J., TROUNOV V.A., STAROSTINA N.V. – Discovery and investigation of the magnetic structure of terbium formate $Tb(DCOO)_3$
Mater. Sci. Forum **321-324** (2000) 971-975

KURBAKOV A., TROUNOV V.A., BARANOVA T.K., BULKIN A.P., DMITRIEV R.P., KASMAN Ya.A., RODRIGUEZ-CARVAJAL J., ROISNEL T. – Russian-French high resolution multi-section neutron powder diffractometer
Mater. Sci. Forum **321-324** (2000) 308-313

KURODA Y., KITTAKA S., TAKAHARA S., YAMAGUCHI T., BELLISSENT-FUNEL M.C. – Characterization of the state of two-dimensionally condensed water on hydroxylated chromium(III) oxide surface through FT-IR, quasielastic neutron scattering, and dielectric relaxation measurements
Journal of Physical Chemistry **103** (1999) 11064-11073

KVARDAKOV V.V., PEPY G., SOMENKOV V.A. – Observation of the periodic and chaotic automodulations of the nonlinear magnetoacoustic vibrations in perfect $FeBO_3$ crystal by neutron diffraction method
Physica B **262 (**1999) 262-266

LAFFARGUE D., BOUREE F., CHEVALIER B., ETOURNEAU J., ROISNEL T. - Magnetic structure of the antiferromagnetic Kondo stannide Ce_2Ni_2Sn
Physica B **259-261** (1999) 46-47

LAFFARGUE D., BORDERE S., BOUREE F., CHEVALIER B., ETOURNEAU J., ROISNEL T. - Crossover from ferromagnetic to antiferromagnetic ground state in the $(Ce_{1-x}U_x)_2Pd_{2.05}Sn_{0.95}$ system
J. Phys. : Conden. Matter **11** (1999) 5195-5208

LAIREZ D. – Résolution d'un spectromètre de diffusion de neutrons aux petits angles
Journal de Physique IV 9 (Pr1) (1999) 67-81

LAL J., AUVRAY L. - Interaction of polymer with clays
J. Appl. Crystallogr**. 33** (2000) 673-676

LANG O., FELSER C., SESHADRI R., RENZ F., KIAT J.M., ENSLING J., GUTLICH P., TREMEL W. - Magnetic and electronic structure of the CMR chalcospinel $Fe_{0.5}Cu_{0.5}Cr_2S_4$
Adv. Mater**. 12** (2000) 65-69

LATROCHE M., PAUL-BONCOUR V., PERCHERON-GUEGAN A., BOUREE-VIGNERON F., ANDRE G. Structural and magnetic properties of low D content YMn_2 deuteride
Journal of Solid State Chemistry **154** (2000) 398-404.

LATROCHE M., PAUL-BONCOUR V., PERCHERON-GUEGAN A., BOUREE –VIGNERON F., ANDRE G. - Neutron diffraction study of $YMn_2D_{1.15}$
Physica B **276-278** (2000) 666-667

LAZEWSKI J., PARLINSKI K., HENNION B., FOURET R. - First principles calculations of the lattice dynamics of $CuInSe_2$
J. Phys. :Condens. Matter **11** (1999) 9665-9671

LEBEDEV V.T., TOROK GY., KALI GY., CSER L., ORLOVA D.N., SIBILEV A.I. – Dynamics of concentrated ferrofluid with labeled particles
J. Magn. Magn. Mater. **201** (1999) 133-135

LE BOLLOC'H D., FINEL A., CAUDRON R. – Concentration dependence of the short range order in the Ni-V and Pt-V systems
Physical Review B **62** (2000) 12082-12088

LECOMMANDOUX S., NOIREZ L., ACHARD M.F., HARDOUIN F. - Smectic C structure and backbone confinement in side-on fixed liquid crystalline polymers
Macromolecules **33** (2000) 67-72

LEE L.T. Polymer-surfactant interactions : neutron scattering reflectivity
Current Opinion in Colloid & Interface Science **4** (1999) 205-213

LEE L.T., JEAN, B., MENELLE A. - Effect of temperature on the adsorption of poly(n-isopropylacrylamide) at the air-solution interface.
Langmuir **15** (1999) 3267-3272

LEE L.T., JHA B.K., MALMSTEN M., HOLMBERG K. – Lipase-surfactant interactions studied by neutron reflectometry and ellipsometry
J. Phys. Chem. B**. 103** (1999) 7489-7494

LEIBROCK H., GRUBE K., FIETZ W.H., SCHLACHTER S.I., WEISS K.P., RYKOV A.I., TAJIMA S., OBST B., SCHWEISS P., WUHL H. – Pressure dependence of the oxygen-ordering process in $RBa_2Cu_3O_x$
Physica C **341-348** (2000) 339-340

LETOUBLON A., ISHIMASA T., DE BOISSIEU M., BOUDARD M., HENNION B., MORI M. - Stability of the F2-(Al-Pd-Mn) phase
Philos. Mag. Lett. **80** (2000) 205-213

LEVY-TUBIANA R. - Etude des composites à matrice métallique par la technique de la diffraction de neutrons : analyse du comportement élastoplastique et évaluation des contraintes résiduelles
Thesis, University of Paris XI, Orsay, November 14, 1999

LEVY-TUBIANA R., BACZMANSKI A., CERETTI M., FITZPATRICK M., LODINI A., WIERZBANOWSKI K. - Study of phase stresses in an Al/SiC metal matrix composite
Mater. Sci. Forum **347-349** (2000) 510-515

LINK P., GUKASOV A., MIGNOT J.-M., MATSUMURA T., SUZUKI T.- Neutron-diffraction study of quadrupole order in TmTe: observation of a field-induced magnetic superstructure
Physica B **259-261** (1999) 319-321

LINK P., MATSUMURA T., GUKASOV A., MIGNOT J.-M., SUZUKI T.- Antiferromagnetism and quadrupolar order in TmTe : a low temperature neutron-diffraction study
Physica B **281-282** (2000) 569-570

LONGEVILLE S., LECHNER R.E. – Light and heavy water dynamics
Physica B **276-278** (2000) 534-535.

LONGEVILLE S. – Null-field or resonance spin echo spectroscopy
J. Phys. IV **10** (2000) 59-75

LOONG C.K., LOEWENHAUPT M., NIPKO J.C., BRADEN M., BOATNER L. – Dynamics coupling of crystal-field and phonon f states in $YbPO_4$
Physical Review B **60** (1999) R12549-R12552

LORENZO J.E., REGNAULT L.P., BOUCHER J.P., HENNION B., DHALENNE G., REVCOLEVSCHI A. - Anisotropy of the spin interactions in the spin-Peierls compound $CuGeO_3$:a new magnetic excitation branch
Europhysics Letters **45** (1999) 619-625

LUKAS P., ZRNIK J., CERETTI M., NEOV D. , STRUNZ P., VRANA M., MIKULA P., KEUERLEBER J.A. –Neutron diffraction as a tool for microstrain characterization of polycrystalline Ni-base superalloy after thermal fatigue
Mater. Sci. Forum **321-324** (2000) 1046-1050

LUTZ P.J., PLENZ-MENEGUETTI S., KRESS J., LAPP A., DUVAL M. – Investigation on the structural parameters of polyethylenes obtained using a Pd catalysis
Polymer Preprints **41** (2000) 1883

MAAZA M., SPEGEL M., SELLA C ., PARDO B., RAYNAL A., MENELLE A., BRIDOU F., CORNO J. - V-Ni multilayered monochromators and supermirrors for cold neutrons
Solid State Communications **111** (1999) 23-28

MAAZA M., CHAUVINEAU J., PARDO B., MENELLE A., SPEGEL M., SELLA C ., PARDO B., CORNO J., GAZIEL R. - Thermal stability of Co-Ti multilayer neutron polarizers
Solid State Communications **112** (1999) 177-181

MAAZA M., GIBAUD A. , SELLA C ., PARDO B., DUNSTETTER F., CORNO J., BRIDOU F., VIGNAUD G., DESERT A., MENELLE A. – X-ray scattering by nano-particles within granular thin films, investigation by grazing angle X-ray reflectometry
European Physical Journal B **7** (1999) 339-345

Publications

MacFARLANE W.A., MENDELS P., BOBROFF J., DOOGLAV A.V., EGOROV A.V., ALLOUL H, BLANCHARD N., COLLIN G., PICARD P.G., KEREN A. – Antiferromagnetism in water doped $YBa_2Cu_3O_{6+x}$ for $x \approx 0.5$
Physica B **289-290** (2000) 291-294

MacFARLANE W.A., BOBROFF J., ALLOUL H., MENDELS P., BLANCHARD N., COLLIN G., MARUCCO J.F. – Dynamics of the local moment induced by nonmagnetic defects in cuprates
Physical Review Letters **85** (2000) 1108-1111

MADIGOU V., BAUDOUR J.L. , BOUREE F., FAVOTTO C., ROUBIN M, NIHOUL G. - Crystallographic structure of lead hafnate, $PbHfO_3$, from neutron powder diffraction and electron microscopy
Philosophical Magazine A **79** (1999) 847-858

MADIH-AYAD K., RAKOTOZAFY S., CEVA T., CROSET B., DUPONT-PAVLOVSKY N., CONVERT P., MIREBEAU I., RESSOUCHE E. -Growth mode of dichloromethane physisorbed on graphite, thermodynamic and structural characterizations
Surface Science **436** (1999) 99-106

MAGLI R., BAROCCHI F., CASANOVA G., GUARINI E., TAU M. - Three-body effects in simple insulating liquids : a small-angle neutron scattering in Kr
Physica B **276-278** (2000) 450-451

MAHAJAN A.V., ALLOUL H., COLLIN G., MARUCCO J.F. – ^{89}Y NMR probe of Zn induced local magnetism in $YBa_2(Cu_{1-x}Zn_y)_3O_{6+x}$
European Physical Journal B **13** (2000) 457-475

MAKAROVA O.L., GONCHARENKO I.N., MIREBEAU I. – Magnetic order and reorientation transitions in the diluted Laves hydride $(Dy_xY_{1-x})Mn_2D_{4.4}$
Physical Review B **59** (1999) 11826-11831

MALEYEV S.V., PETITGRAND D., BOURGES P., IVANOV A.S. - Pseudodipolar interaction in noncollinear antiferomagnets and spin waves in Pr_2CuO_4 compounds (R=Pr, Nd, Sm and Eu)
Physica B **259-261** (1999) 870-874

MALIBERT C., DKHIL B., DUNLOP M., KIAT J.M., BALDINOZZI G., VAKHRUSHEV S.B. - Disorder and harmonicity in simple and complex perovskites
Ferroelectrics **235** (1999) 87-96

MALIBERT C., BALDINOZZI G., BULOU A., KIAT J.M. - Investigation of the relaxor system PBSN by Raman scattering
Ferroelectrics **235** (1999) 241-249

MANIFACIER L., COLLIN G., BLANCHARD N. - Correlation between crystallographic and physical properties in $(Bi,Pb)_2Sr_2(Ca,Y)Cu_2O_{8+\Delta}$ superconductors
Physica B **259-261** (1999) 562-563

MARGACA F.M.A., MIRANDA-SALVADO I.M., TEIXEIRA J. - Small angle neutron scattering study of silica gels : influence of pH
J. Non Crystalline Solids **258** (1999) 70-77

MARTIN C., MAIGNAN A., DAMAY F., HERVIEU M., RAVEAU B., JIRAK Z., ANDRE G., BOUREE F. - Influence of Mn-site doping upon orbital and charge ordering in the $Pr_{0.5}A_{0.5}Mn_{1-x}M_xO_3$ manganites (A = Sr, Ca and M = Cr, Al)
Journal of Magnetism and Magnetic Materials **202** (1999) 11-21

MARTIN C., MAIGNAN A., HERVIEU M., RAVEAU B., JIRAK Z., KURBAKOV A., TROUNOV V., ANDRE G., BOUREE F. - Two C-type antiferromagnets with different magnetoresistive properties : $Sm_{0.15}Ca_{0.85}MnO_3$ and $Pr_{0.15}Sr_{0.85}MnO_3$
Journal of Magnetism and Magnetic Materials **205** (1999) 184-198

MARTIN C., MAIGNAN A., HERVIEU M., RAVEAU B., JIRAK Z., SAVOSTA M.M., KURBAKOV A., TROUNOV V., ANDRE G., BOUREE F. – Structural study of the electron-doped manganites : $Sm_{0.1}Ca_{0.9}MnO_3$ and $Pr_{0.1}Sr_{0.9}MnO_3$: evidence of phase separation
Physical Review B **62** (2000) 6442-6449

MASQUELIER C., WURM C., RODRIGUEZ-CARVAJAL J., GAUBICHE J., NAZAR L. - A powder neutron diffraction investigation of the two rhombohedral NASICON analogs : γ-$Na_3Fe_2(PO_4)_3$ and $Li_3Fe_2(PO_4)_3$
Chemistry of Materials **12** (2000)525-532.

MATHON M.H., DE NOVION C.H. – De l'intensité à la structure des matériaux
Dans « Diffusion de Neutrons aux Petits Angles » Ecole Thématique de la Société Française de Neutronique
Journal de Physique IV, **9** (1999) 127-146

MATHON M.H., GEOFFROY G., de CARLAN Y., ALAMO A., de NOVION C.H. - SANS study of the microstructural evolution of martensitic steels under thermal ageing and neutron irradiation
Physica B **276-278** (2000) 939-940

MATHON M.H., GEOFFROY G., de CARLAN Y., ALAMO A., de NOVION C.H.,. - Microstructural characterization of LA12Ta, LA13Ta and F82H steels by small angle neutron scattering
Contrat LAM3, Note Technique SRMA 00-2359 (Mars 2000)

MATHON M.H., de CARLAN Y., GEOFFROY G., AVERTY X., de NOVION C.H., ALAMO A. - Microstructural evolution of reduced activation and conventional martensitic steels after thermal aging and neutron irradiation
Note Technique SRMA 00-2396 (Déc. 2000)

MATTAUCH S., PAULUS W. , GLINNEMANN J., ROTH G., HEGER G. - Crystal structure of $RbD_2PO_{4x}d_2O$: a new hydrate phase of KDP-type compounds
Cryst. Res. Technol. **35** (2000) 501-509

MAURY F., NICOLAS-FRANCILLON M., BOUREE F., OLLITRAULT-FICHET R., NANOT M. - Local structural changes in lithium-doped $YBa_2Cu_3O_y$
Physica C **333** (2000) 121-132

MAURY F., NICOLAS-FRANCILLON M., BOUREE F., MIREBEAU I.- Structural and magnetic changes in Li substituted $YBa_2Cu_3O_y$ determined by neutron powder diffraction measurements
Physica C **341-348** (2000) 609-610

MEINNEL J., MANI M., COUSSON A., BOUDJADFA F., PAULUS W., JOHNSON M. - Structure of trihalogenomesitylenes and tunneling of the methyl groups porous. II Protoned tribomomesitylene
Chemical Physics **261** (2000) 165-187

MENDELS P., BOBROFF J., COLLIN G., ALLOUL H., GABAY M., Y., MARUCCO J.F. , BLANCHARD N., GRENIER B. – Normal –state magnetic properties of Ni and Zn substituted in $YBa_2Cu_3O_{6+x}$: hole doping dependence
Europhysics Letters **46** (1999) 678-684

MENDELS P., KEREN A., LIMOT L., MEKATA M., COLLIN G., HORVATIC M. – Ga NMR study of the local susceptibility in Kagome-based $SrCr_8Ga_4O_{19}$: pseudogap and paramagnetic defects
Physical Review Letters **85** (2000) 3496-3499

MENELLE A., MONTECCHI M., NICHELATTI E., POLATO P. - Characterisation of double laser coatings on flat glass by neutron reflectivity and spectrophotometry
Glass Technology **40** (1999) 160-166

MENELLE A., MONTECCHI M., POLATO P. - Neutron reflectivity as a tool for the characterization of homogeneous and inhomogeneous single layer coating on glass
Indian Ceram. **41** (1999) 41410-41416

MENELLE A. - Neutron reflectivity, a tool for thin film characterization
Mater. Sci. Forum **321-324** (2000) 246-256

MERZ M., GERHOL S., NÜCKER N.,. KUNTSCHER C.A, BURBULLA B., SCHWEISS P., SCHUPPLER S., CHAKARIAN V., FREELAND J.,. IDZERDA Y.U, KLÄSER M., MÜLLER-VOGT G., WOLF TH. - Site-specific structure of the $RBa_2Cu_3O_{7-y}$ family
Phys. Rev. **B 60** (1999) 9317-9320

MIGNOT J.-M., LINK P., GUKASOV A., MATSUMURA T., SUZUKI T. - Neutron diffraction study of quadrupolar and magnetic order in TmTe
Physica B **281-282** (2000) 470-476

MIGNOT J.-M., GONCHARENKO I., LINK P., MATSUMURA T., GUKASOV A., SUZUKI T. - Neutron diffraction study of magnetic and quadrupolar order in Tm monochalcogenides
Physica B **276-278** (2000) 756-759

MIGNOT J.-M., GONCHARENKO I.N., LINK P., MATSUMURA T., SUZUKI T. - Single-crystal neutron-diffraction under high pressures : valence instabilities in Tm monochalcogenides
Hyperfine Interactions **128** (2000) 207

MIREBEAU I., HENNION M., CASALTA H., ANDRES H., GÜDEL H.U., IRODOVA A.V., GANESCHI A. Low energy magnetic excitations of the Mn_{12}-acetate spin cluster observed by neutron scattering
Physical Review Letters **83** (1999) 628-631

MIREBEAU I., GONCHARENKO I.N., ANDREANI D., SUARD E. - Influence of Aluminium doping and hydrogen disorder on the magnetism in the frustrated Laves hydrides $Y(Mn_{1-x}Al_x)_2H_y$
Physical Review B **62** (2000) 9493-9497

MORAL A., ARBE A., COLMENERO J. - Fast dynamics in Poly(vinyl chloride) below the glass transition : self and pair correlation functions
Physica B **276-278** (2000) 440-441

MOREIRA J.A., CHAVES M.R., ALMEIDA A., KIAT J.M., KLOPPERPIPER A. - X-ray study of the betaine arsenate and deuterated betaine arsenate
Phys. Status Solidi A **178** (2000) 633-643

MORFIN I., LINDNER P., BOUE F. - Temperature and shear rate dependence of small angle neutron scattering from semidilute polymer solutions
Macromolecules **32** (1999) 7208-7223

MORFIN I. - Structures induites par l'écoulement dans une solution viscoélastique de polymère
Thesis, Joseph Fourier University, Grenoble, September 17, 1999

MORGANTE A.M., JOHANSSON M., KOPIDAKIS G., AUBRY S. – Instabilités oscillatoires des ondes stationnaires non-linéaires dans les réseaux unidimensionnels
Editions Paris Onze - Rencontres NonLinéaires IHP-Paris, 1999

MORGANTE A.M., JOHANSSON M., KOPIDAKIS G., AUBRY S. - Oscillatory instabilities of standing waves in one-dimensional nonlinear lattices
Physical Review Letters **85** (2000) 550-553

MORINEAU D., CASAS F., ALBA-SIMIONESCO C., GROSMAN A., BELLISSENT-FUNEL M.-C., RATOVELOMANANA N. - A neutron scattering investigation of the structural properties of glassforming m-toluidine confined in MCM-41
J. Phys. IV France 10 (Pr7) (2000) 95-98

MOUSSA F., BIOTTEAU G., HENNION M., RODRIGUEZ-CARVAJAL J., PINSARD L., REVCOLEVSCHI A. - Precursor Effects of the Giant Magnetoresistance Regime in Calcium Doped Manganites
Journal of Superconductivity **12** (1999) 257-259

MOUSSA F., HENNION M., BIOTTEAU G., RODRIGUEZ-CARVAJAL J. - Magnetic coupling induced by hole doping in perovskites $La_{1-x}Ca_xMnO_3$: a neutron scattering study
Physical Review B **60** (1999) 12299-12308

MOUSSA F., COURTENS E. - Pressure effect on the proton glass $Rb_{1-x}(NH4)_xH_2PO_4$: a neutron study
Feroelectrics **236** (2000) 181-192

Publications

MOZE O., MANFRINETTI P., CANEPA F., PALENZONA A., FORNASINI M.L., RODRIGUEZ-CARVAJAL J.
Magnetic and Crystal Structure of Th-Fe-Sn intermetallics: $ThFe_{0.22}Sn$ and $Th_5Fe_{13}Sn_5$"
Intermetallics **8** (2000) 273-277

MÜLLER C., BAUDOUR J.L., MADIGOU V., BOUREE F., KIAT J.-M., FAVOTTO C., ROUBIN M. - Temperature dependent neutron powder diffraction evidence for splitting of the cationic sites in ferroelectric $PbHf_{0.4}Ti_{0.6}O_3$
Acta Crystallographica B **55** (1999) 8-16

MÜLLER C., BAUDOUR J.L., BEDOYA C., BOUREE F., SOUBEYROUX J.L., ROUBIN M. - Octahedral deformations and cationic displacements in the ferroelectric $PbHf_{0.8}Ti_{0.2}O_3$: a neutron powder diffraction study from 10 to 770 K
Acta Crystallographica B **51** (2000) 27-38

MULLNER R., NOIREZ L., ZOJER E., STELZER F., LEISING G. - Side chain influence on main chain orientation of PPV-type oligomers
Mater. Res. Soc. Symp. Proc. **598** (2000) 16/1-16/4

NASR S., BELLISSENT-FUNEL M.-C., CORTES R. – X-ray and neutron scattering studied of liquid formic acid DCOOD at various temperatures and under pressure
Journal of Chemical Physics **110** (1999) 10945-10952

NATREPOV A., CISOWSKI J., HEIMANN J., MIREBEAU I. - A new ternary compound $YbZn_2As_2$ with mixed valency of Yb
Journal of Alloys and Compounds **290** (1999) 6-9

NAVAZA A., CHEVRIER G., KIAT J.M., BARAN E.J. Neutron diffraction structure of $Y_2V_{10}O_{28}.24H_2O$ at 297 K and 60 K
Journal of Chemical Crystallography **30** (2000) 545-555

NEFEODOVA E.V., ALEKSEEV P.A., MIGNOT J.M., LAZUKOV V.N., SADIKOV I.P., PADERNO YU.B., SHITSEVALOVA N. YU., ECCLESTON R.S. – Magnetic excitation spectrum of Kondo insulator YbB_{12}
Physical Review B **60** (1999) 13507-13514

NEFEODOVA E.V., ALEKSEEV P.A., MIGNOT J.M., LAZUKOV V.N., SADIKOV I.P., PADERNO YU.B., SHITSEVALOVA N. Yu., ECCLESTON R.S. - Inelastic neutron scattering study of the Kondo semiconductor YbB_{12}
Physica B **276-278** (2000) 770-771

NOIREZ L. – Side chain liquid-crystalline polyacrylates : experimental evidence of a coexistence of a double main-chain confinement inside the smectic layer
Europhysics Letter **46** (1999) 728-734

NOIREZ L. - Shear-induced smectic A-smectic-C transition in side-chain- liquid crystalline polymers
Physical Review Letters **84** (2000) 2164-2167

OBERDISSE J., RHARBI Y., BOUE F. - Simulation of aggregate structure and SANS-spectra in filled elastomers
Comput. Theor. Polym. Sci. **10** (2000) 207-217

ONUFRIEVA F., PFEUTY P., KISELEV M. - New scenario for high-T_c cuprates : electronic topological transition as a motor for anomalies in the underdoped regime
Physical Review Letters **82** (1999) 2370-2373

ONUFRIEVA F., PFEUTY P. – Quantum SDW liquid state originating from 2D electronic topological transition as a source for anomalies in the high-T_c cuprates
J. Physique IV 9 (Pr10) (1999) 339-343

ONUFRIEVA F., PFEUTY P. – SC state anomalies in the underdoped regime of high-T_c cuprates as a result of proximity to electronic topological transition
Journal of Low Temperature Physics **117** (1999) 229-233

ONUFRIEVA F., PFEUTY P. – Normal state pseudogap and $(\pi,0)$ feature in the underdoped high-T_c cuprates : a microscopic theory
Physical Review Letters **82** (1999) 3136-3139

ONUFRIEVA F., PFEUTY P. – Normal state pseudogap and $(\pi,0)$ feature in the underdoped high-T_c cuprates : a microscopic theory (Erratum)
Physical Review Letters **83** (1999) 1271

ONUFRIEVA F., PFEUTY P. – Quantum critical point associated with the electronic topological transition in a two-dimensional electron system as a driving force for anomalies in underdoped high-T_c cuprates
Physical Review B **61** (2000) 799-820

OSAKABE T., KOHGI M., IWASA K., KAKURAI K., MIGNOT J.M., GONCHARENKO I., OKAYAMA Y., TAKAHASHI H., MORI N., KUBOTA M., YOSHIZAWA H., HAGA Y., SUZUKI T. - Novel magnetic structure of the low carrier system CeP and CeAs under external fields
JAERI-Rev. (1999) 123-125

OTT F., MENELLE A., FERMON C., HUMBERT P. - Off-specular diffraction on periodic gratings studied by neutron reflectometry
Physica B **283** (2000) 418-421

OTT F., VIRET M., BORGES R., LYONNET R., JACQUET E., FERMON C., CONTOUR J.-P. - Interface magnetism of $La_{0.7}Sr_{0.3}MnO_3$ thin films studied by neutron reflectometry
Journal of Magnetism Magnetic Materials **211** (2000) 200-205

OTT F., MENELLE A., FERMON C., HUMBERT P. - Off-specular diffraction on periodic gratings studied by neutron reflectometry
Physica B **283** (2000) 418-421

OUALI N., MERY S., SKOULIOS A., NOIREZ L. - Backbone stretching of wormlike carbosilane dendrimers
Macromolecules **33** (2000) 6185-6193

PAIXAO J.A., PEREIRA L.C.J., ESTRELA P., GODINHO M., ALMEIDA M., PAOLASINI L., BONNET M., SPIRLET J.C. - Magnetization density distribution in U_2Co_2Sn
J. Phys. : Condensed Matter **11** (1999) 2115-2125

PAOLONE A., ROY P., ROUSSE G., MASQUELIER C., RODRIGUEZ-CARVAJAL J. - Infrared spectroscopy investigation of the charge ordering transition in $LiMn_2O_4$
Solid State Comunications **111** (1999) 453-458

PAPPAS C., - Critical scattering in the disordered ferromagnet $Au_{0.82}Fe_{0.18}$
Report Ber. Hahn-Meitner-Inst. (HMI-B 559) (1999) 106-107

PAUL-BONCOUR V., GUENEE I., LATROCHE M., PERCHERON-GUEGAN A., OULADDIAF B. , BOUREE –VIGNERON F. Elaboration, structures and phase transitions for YFe_2D_x compounds (x=1.3, 1.75, 1.9, 2.6) studied by neutron diffraction
J. Solid State Chemistry **142** (1999) 120-129

PECHEV S. , CHEVALIER B., LAFFARGUE D. , DARRIET B. , ROISNEL T. , ETOURNEAU J. – Magnetic behaviour of the ternary silicide $U_3Cu_4Si_4$.
Journal of Magnetism and Magnetic Materials **191** (1999) 282-290

PELTA J., BERRY H., FADDA G., PAUTHE E., LAIREZ D. - Statistical conformation of human plasma fibronectin in physiological conditions
Biochemistry **39** (2000) 5146-5154

PEPIN-DONAT B., LAIREZ D., DE GEYER A., VIALLAT A. – Light and small-angle neutron scattering studies of well-defined conducting gels
Synth. Mat. **101** (1999) 471-472

PEREZ-CONDE J., BOUIS F., PFEUTY P. - The Kondo Hubbard model at half-filling
Physica B **259-261** (1999) 183-185

PEREZ J., ZANOTTI J.M., DURAND D. – Evolution of the internal dynamics of two globular proteins from dry powder to solution
Biophysical Journal **77** (1999) 454-459

PEREZ-MATO J.M., ARAMBURU I ., QUILICHINI M., IVANTCHEV S., HERNANDEZ O. – Polarisation-flip phase transitions under an electric field in displacive systems with competing periodicities
Physical Review B **62** (2000) 11418-11422

PETITGRAND D., MALEYEV S.V., BOURGES P., IVANOV A.S. - Pseudodipolar interaction and antiferromagnetism in R_2CuO_4 compounds (R=Pr, Nd, Sm and Eu)
Physical Review B **59** (1999) 1079-1104

PETRESCU A.J., CALMETTES P., DURAND D., RECEVEUR V., SMITH J.C. - Change in backbone torsion angle distribution on protein folding
Protein Sci. **9** (2000) 1129-1136

PIERRARD A., GREDIN P., DUPONT N., DE KOZAK A., BOUREE-VIGNERON F., ANDRE G., ROSENMAN I. Magnetic structure and properties of $Pb_8Fe^{II}Fe_2^{III}F_{24}$: a 1-D ferrimagnetic chain compound exhibiting a spin-flop transition
J. Alloys and Compounds **291** (1999) 44-51

PINSARD-GAUDARD L., SURYNARAYANAN R., REVCOLEVSCHI A., RODRIGUEZ-CARVAJAL J., GRENECHE J.M., SMITH P.A.I., THOMAS R.M., BORGES R.P., COEY J.M.D. - Ferrimagnetic order in Ca_2FeMoO_6
J. Applied Phys**. 87** (2000) 7118-7120

PINTSCHOVIUS L., BRADEN M. – Anomalous dispersion of LO phonons in $La_{1.85}Sr_{0.15}CuO_4$
Journal of Low Temperature Physics **117** (1999) 437-441

PINTSCHOVIUS L., SCHREIECK B., EIGENMANN B. - Neutron, X-ray and finite-element stress analysis on brazed components of steel and cemented carbide
Textures and Microstructures, **33** (1999) 263 – 278

PINTSCHOVIUS L., BRADEN M. – Anomalous dispersion of LO phonons in $La_{1.85}Sr_{0.15}CuO_4$
Physical Review B **60** (1999) R15039-15042

PINTSCHOVIUS L., PREM M., FRISCHBUTTER A. - High-precision neutron-diffraction measurements for the determination of low-level residual stresses in a sandstone
Journal of Structural Geology **22** (2000) 1581-1585

PLAKHTY V.P., GUKASOV A.G., PAPOULAR R.J., SMIRNOV O.P. - Spin density on ligands O^{2-} and covalency of Fe^{3+} ions in octahedral sites of $Ca_3Fe_2Ge_3O_{12}$ garnet : a polarised neutron diffraction study
Europhysics Letters **48** (1999) 233-239

PLAKHTY V.P., MALEYEV S.V., WOSNITZA J., KREMER B.K. VISSER D., KULDA J., GOUKASSOV A.G., ZOBKALO I.A., MOSKVIN E. – Polarized neutron scattering study of the spin chirality
Physica B **267-268** (1999) 259-262

POGOSSIAN S.P., LE GALL H., BEN YOUSSEF J., MENELLE A. – Neutron waveguiding properties of Co/Cu exchange coupled magnetic superlattice.
Journal of Magnetism and Magnetic Materials **214** (2000) 276-280

POJTINGER A., LAMPARTER P., STEEB S. - Medium range structure of hydrogenated amorphous $Ti_{54}Si_{16}$
Z. Natursforsch. **A 54** (1999) 704-710

PRIGENT G., BELLISSENT R., CEOLIN R., FISCHER H.E., GASPARD J .P. - Local order and metal-non-metal transition in Cd_xTe_{1-x} : a neutron diffraction study
Journal of Non-Crystalline Solids **250-252** (1999) 297-300

PRIGENT G., GASPARD J .P., BELLISSENT R., BICHARA C. – Effect of charge transfer on the local order in liquid group IV isoelectronic compounds : neutron diffraction data versus numerical tight-binding simulations
AIP Conference Proceedings « Neutron and Numerical Methods-N2M » 479 (1999) 83-89

PROKES K., BOURDAROT F., BURLET P., OLSOVEC M., SECHOVSKY V., JARORSKY P., BRUCK E., GOUKASSOV A., DE BOER F.R., MENOVSKY A.A. – Magnetic structures of UNiAl in magnetic fields
Physica B **259-261** (1999) 246-247

Publications

PROKES K., SECHOVSKY V., GUKASOV A., ANDREEV A.V., NAKOTTE H. – Direct measurement of the magnetic anisotropy in UCoGa using polarized neutrons
Physica B **276-278** (2000) 564-565

PROVILLE L., AUBRY S. - Small bipolarons in the 2-dimensional Holstein-Hubbard model. I. The adiabatic limit
European Physical Journal B **11** (1999) 41-58

PROVILLE L., AUBRY S. – Mobilité bipolaronique dans le modèle de Holstein Hubbard à deux dimensions
Editions Paris Onze - Rencontres NonLinéaires IHP-Paris, 1999

PROVILLE L., AUBRY S. - Small bipolarons in the 2-dimensional Holstein-Hubbard model. II. Quantum bipolarons
European Physical Journal **15** (2000) 405-421

PYKA N., d'ASTUTO M., METZ A., IVANOV A.S., LOEWENHAUPT M., CASALTA H., PETITGRAND D., BOURGES P.- High resolution study of the supposed fourfold Nd spin-wave degeneracy of Nd_2CuO_4
Physical Review B **61** (2000) 14311-14314

QUESNE C., MATHON M.H., BAUDIN T., BERNARDONI P., PENELLE R. – Influence of phase transformation and heat treatments in β and α+β fields on texture evolution in βCEZ alloy
The 9th World Conference on Titanium, Saint-Petersbourg, Russia, editors : I.V. Gorynin and S.S. Ushkov, CRISM, Prometey, Vol**. 3** (2000) pp. 1711-1717

RAGHUNATHAN V.A., RICHETTI P., ROUX D., NALLET F., SOOD A.K. - Phase transitions in colloidal dispersions in a liquid crystalline medium
Langmuir **16** (2000) 4720-4725

RASMUSSEN K.O., AUBRY S., BISHOP A.R., TSIRONIS G.P. - Discrete nonlinear Schrödinger breathers in a phonon bath
European Physical Journal B **15** (2000) 169-175

RATHGEBER S., WILLNER L., RICHTER D., BRULET A., FARAGO B, APPEL M., FLEISCHER G. – Polymer dynamics in bimodal polyethylene melts : A study by neutron spin echo spectroscopy
Journal Chemical Physics **110** (1999) 10171-10187

RATY J.Y., GASPARD J.P., BIONDUCCI M., CEOLIN R., BELLISSENT R. – On the structure of liquid IV-VI semiconductors
Journal of Non Crystalline Solids **250-252** (1999) 277-280

RATY J.Y., GASPARD J.P., BICHARA C., BERGMAN C., BELLISSENT R., CEOLIN R., – Re-entrant Peierls distortion in IVA-VIA compounds
Physica B **276-278** (2000) 473-474

REGNAULT L.P., BOUCHER J.P., MOUDDEN A.H., LORENZO E., HIESS A., A. VIETKIN A., REVCOLEVSCHI A. - Spin Dynamics in the Magnetic Chain Arrays of $Sr_{14}Cu_{24}O_{41}$
Physical Review B **59** (1999) 1055

REICHARDT W., BRADEN M. – Anomalous features in the bond stretching vibrations of $La_{1-x}Sr_xMnO_3$
Physica B **263-264** (1999) 416-420

RENKER B., SCHOBER H., BRADEN M. – Alignment of polymer chain in RbC_{60} by uniaxial pressure
Solid State Commun. **109** (1999) 423-426

RENZI R.D., ALLODI G., GUIDI M.C. , GUIDI G., HENNION M., PINSARD L., AMATO A. - Magnetic order in pure $LaMnO_3$ and in Ca-doped single crystals
Physica B **289-290** (2000) 52-55

RHARBI Y., CABANE B., VACHER A., JOANICOT M., BOUE F. – Mode of deformation in a soft/hard nanocomposite : a SANS study
Europhysics Letters **46** (1999) 472-478

RIETVELD I.B., BEDEAUX D., SMIT J.A.M. - Equation of state of poly(propylene imide) dendrimers in deuterated methanol as obtained from the osmotic compressibility
J. Colloid Interface Science **232** (2000) 317-325

RIOS S., QUILICHINI M., KNORR K., ANDRE G. - Study of the (P,T) phase diagram in TlD_2PO_4
Physica B **266** (1999) 290-299

ROEPKE M., HOLLAND-MORITZ E., BUCHNER B., BERG H., LECHNER R.E., LONGEVILLE S., FITTER J., KAHN R., CODDENS G.., FERRAND M. – 4f-spin dynamics $La_{2-x-y}Sr_xNd_yCuO_4$
Physical Review B **60** (1999) 9793-9800.

ROGL P., ANDRE G., BOUREE F., NOEL H. - Magnetic structures of $U_3M_2M'_3$, M = Al, Ga ; M' = Si, Ge : a neutron powder diffraction study
Journal of Magnetism and Magnetic Materials **191** (1999) 291- 300

ROGL P., BOUREE F.- A novel boroncarbide $Y_2B_3C_2$, X-ray single crystal and neutron powder diffraction analysis
J. Alloys Compounds **298** (2000) 160-163

ROISNEL T., NUÑEZ P., TRESSAUD A., MOLINS E., RODRIGUEZ-CARVAJAL J. - Investigation of $K_2MnF_5.H_2O$ by Neutron Diffraction
Journal of Solid State Chemistry **150** (2000) 104-111

ROLS S.
Structure et dynamique des nanotubes de carbone. Une étude par diffraction et diffusion inélastique de neutrons.
Thesis, December 21, 2000

ROLS S., ANGLARET E., SAUVAJOL J.L., CODDENS G., DIANOUX A.J. – Neutron scattering studies of the structure and dynamics of nanobundles of single-wall carbon nanotubes
Applied Physics A **69** (1999) 591-596

ROLS S., ANGLARET E., SAUVAJOL J.L., CODDENS G., SCHOBER H., DIANOUX A.J. – Structure and dynamics of single-wall carbon nanotubes probed by neutron scattering
Physica B **276-278** (2000) 276-277

ROLS S., BENES Z., ANGLARET E., SAUVAJOL J.L., PAPANEK P., FISCHER J.E., CODDENS G., SCHOBER H., DIANOUX A. J. - Phonon Density of States of Single-Wall Carbon Nanotubes
Physical Review Letters **85** (2000) 5222-5225

ROUEDE D., LE GRAND Y., RABILLER P., SCHERF CH. – Study of antiparallel pyroelectric twins in $KLiSO_4$
Optics Communications **178** (2000) 225-232

ROUSSE G., MASQUELIER C., RODRIGUEZ-CARVAJAL J., HERVIEU M. - Cubic ↔ Orthorhombic Transition in the Stoichiometric Spinel $LiMn_2O_4$.
Electrochemical and Solid Letters **2** (1999) 6-8

ROUSSE G., MASQUELIER C., RODRIGUEZ-CARVAJAL J., ELKAIM E., LAURIAT J.P., MARTINEZ J.L. - X-ray study of the spinel $LiMn_2O_4$ at low temperatures
Chemistry of Materials **11** (1999) 3629-3635

RUNOV V.V., KOPITSA G.P., OKOROKOV A.I., RUNOVA M.K.
Spin correlations and magnetonuclear cross-correlation in Sm(Sr)-Mn-O perovskite in the low-temperature
JETP Letters **69** (1999) 353-360.

RUNOV V.V., GLATTLI H., KOPITSA G.P., OKOROKOV A.I., RUNOVA M.K. -
Small angle polarized neutron scattering in $Sm_{1-x}Sr_xMnO_3$ ($x < 0.5$) perovskite
Physica B **276-278** (2000) 795-796

RUNOV V.V., CHERNYSHOV D.YU., KURBAKOV A.I., RUNOVA M.K., TRUNOV V.A., OKOROKOV A.I.
Mesoscopic Magnetic Inhomogeneities in the Low-Temperature Phase and Structure of $Sm_{1-x}Sr_xMnO_3$ ($x < 0.5$) Perovskite
JETP **91** (2000) 1017-1028.

RUSSO D., PEREZ J., DESMADRIL M., CALMETTES P., DURAND D. – IQNS-monitored dynamical transition of a small β-protein following heat denaturation.
Physica B **276-278** (2000) 499-500

RUSSO D., DURAND D., DESMADRIL M., CALMETTES P. - Study of thermally and chemically unfolded conformations of a small β-protein by means by small-angle neutron scattering
Physica B **276-278** (2000) 520-521

RUSSO D. - Etude structurale et dynamique de l'état natif et des états dénaturés de la néocarzinostatine, par microcalorimétrie différentielle, spectroscopies optiques et diffusion de neutrons et rayons X
Thesis, University of Paris XI, Orsay, April 4, 2000

RUSTICHELLI F., CERETTI M., FIORI F., LODINI A., MENELLE A. - Residual Stress Measurements at the DIANE Diffractometer
Proc. of the 1st International Congress on Radiation Physics, High Current Electronics, and Modification of Materials, Ed. D. Vaisburd, p.243 (2000).

SAUVAJOL J.-L., ANGLARET E., ROLS S., JOURNET C., GOZE C., BERNIER P., MASER W.K., MUNOZ E., BENITO A.M., MARTINEZ M.T., CODDENS G., DIANOUX A.J. – Structure and vibrational properties of single wall carbon nanotubes
Synth. Met. **103** (1999) 2537-2539

SCHERF CH., PAULUS W., HEGER G., HAHN TH.
Crystal structure analysis of the orthorhombic phase II of $KLiSO_4$
Physica B **276-278** (2000) 247-249

SCHIEBEL P., PAPOULAR R.J., PAULUS W., ZIMMERMANN H., DETKEN A., HAERBERLEN U., PRANDL W. - Isotope induced proton ordering in partially deuterated aspirin
Physical Review Letters **83** (1999) 975-978

SCHIEBEL P., PRANDL W., PAPOULAR R.J., PAULUS W., DETKEN A., HAERBERLEN U., ZIMMERMANN H., - Isotope orientational order in acetyl salisylic acid
Physica B **276-278** (2000) 816-817

SCHOBINGER-PAPAMANTELLOS P., RODRIGUEZ-CARVAJAL J., ANDRE G., DE GROOT C.H., DE BOER F.R., BUSCHOW K.H.J. - Magnetic Ordering of $ErFe_4Ge_2$ Studied by Neutron Diffraction and Magnetic Measurements
Journal of Magnetism and Magnetic Materials **191** (1999) 261-276

SCHOBINGER-PAPAMANTELLOS P., RODRIGUEZ-CARVAJAL J., HAGMUSA I.H., DUONG N.P., BUSCHOW K.H.J. - Uniaxial Antiferromagnetic Ordering in $HoFe_2Ge_2$: a Neutron and Magnetic Study
Journal of Alloys and Compounds **284** (1999) 42-46

SCHOBINGER-PAPAMANTELLOS P., RODRIGUEZ-CARVAJAL J., BUSCHOW K.H.J., DOORYHEE E., FICH A.N. - The Double Phase Transition on $ErFe_4Ge_2$. An XRPD Study
Journal of Magnetism and Magnetic Materials **210** (2000) 121-137

SCHOBINGER-PAPAMANTELLOS P., ANDRE G., RODRIGUEZ-CARVAJAL J., DUIJN H.G., BUSCHOW K.H.J. - Magnetic ordering in $DyMn_{6-x}Cr_xSn_6$ (x=1,2) compounds studied by neutron diffraction and magnetic measurements.
Journal of Magnetism and Magnetic Materials **219** (2000) 22-32

SCHOBINGER-PAPAMANTELLOS P., ANDRE G., RODRIGUEZ-CARVAJAL J., DUIJN H.G., BUSCHOW K.H.J. - Magnetic ordering in $Tb_xCr_xSn_6$ (x=1,2) compounds studied by neutron diffraction and magnetic measurements.
Journal of Alloys and Compounds **306** (2000) 47-55

SCHRAMCHENKO N., KLEIN H., CAUDRON R., BELLISSENT R. - Comparison of local order in icosahedral Al-Pd-Mn quasicrystal and in approximant phase by thermal neutron scattering
Mat. Sci. Eng. A **294-296** (2000) 335-339

Publications

SCHWEIZER J., GILLON B. - Neutron diffraction studies of spin densities in magnetic molecular materials
Chapitre de « Magnetic Properties of Organic Materials »
Marcel Dekker inc Editor, pp. 449-473

SCHWEIZER J., PAPOULAR R.J. RESSOUCHE E., TASSET F., ZHELUDEV A.I. - Maximum entropy reconstruction of spin densities involving non-uniform prior
Understanding Chem. React. **21** (2000) 37-44

SENAS A., ESPESO J.I., RODRIGUEZ FERNANDEZ J., GOMEZ SAL J.C., GARCIA SOLDEVILLA J., RODRIGUEZ-CARVAJAL J. - Complex magnetic structures in $TbPt_{1-x}Cu_x$ compounds
Physica B **276-278** (2000) 612-613

SENAS A., ESPESO J.I., RODRIGUEZ FERNANDEZ J., GARCIA SOLDEVILLA J., GOMEZ SAL J.C., RODRIGUEZ-CARVAJAL J., IBARRA R. - Multiphase magnetic analysis through the martensitic transition of TbCu
Physica B **276-278** (2000) 614-615

SIDIS Y.,BRADEN M., BOURGES P., HENNION B., NISHIZAKI S., MAENO Y., MORI Y. - Inelastic neutron scattering studies on Sr_2RuO_4
Physica B **281-282** (2000) 967-968

SIDIS Y.,BRADEN M., BOURGES P., HENNION B., NISHIZAKI S., MAENO Y., MORI Y. - Evidence for incommensurate spin fluctuations in Sr_2RuO_4
Physical Review Letters **83** (1999) 3320-3323

SIDIS Y., BOURGES P., FONG H.F., KEIMER B., REGNAULT L .P., BOSSY J., IVANOV A., HENNION B., GAUTIER-PICARD P., COLLIN G., MILIUS D.L., AKSAY I.A. - Quantum impurities and the neutron resonance peak $YBa_2Cu_3O_7$: Ni versus Zn
Physical Review Letters **84** (2000) 5900-5903

SIMONET V., HIPPERT F., AUDIER M., BELLISSENT R., - Local icosahedral order and magnetism in AlMn and AlCr liquids in equilibrium with μ-phase solids
Journal Non Cryst. Solids **250-252** (1999) 824-828

SIMONET V., HIPPERT F., AUDIER M., BELLISSENT R., - Structure .of liquid Al-Mn-Cr alloys in equilibrium with the $\mu Al_4(Mn_yCr_{1-x})$ approximant phase
Mater Sci. Eng. A **294-296** (2000) 116-119

SKUMRYEV V., OTT F., COEY J.M.D., ANANA A., RENARD J.P., PINSARD-GAUDART L., REVCOLEVSCHI A.– Weak ferro-magnetism in $LaMnO_3$
European Physical Journal B **11** (1999) 401-406

SOLDATOV A.G., BARILO S.N., SHIRYAEV S., FINSKAYA V.M., USTINOVICH S.N., REICHARDT W., BRADEN M., SZYMCZAK H. – Crystal structure and possible superconductivity in $BaBi_3$-$KBiO_3$ system outside the cubic phase
Physica B **284-288** (2000) 1059-1060

SOMENKOV.A.,. GLAZKOV V.P, SHIL'SHTEIN S.SH., ZHUKOV V.P., BEZMEL'NITSYN V.N., KURBAKOV A.I. - Neutron Diffraction Study of the Structure of Deuterated and Fluorinated Fullerene C_{60}.
Metal Science and Heat Treatment **42** (2000) 319-325.

SPRAUEL J.M., BARRALLIER L., LODINI A., PYZALLA A., REIMERS W. - Determination of residual stresses in nitrided layers generated by gas nitriding
Proceedings " Residual Stresses – ICRS 6 " (2000) 1343-1348

STARR F.W., BELLISSENT-FUNEL M.-C., STANLEY H.E. - Structure of supercooled and glassy water under pressure
Physical Review E **60** (1999) 1084-1087

STRIDE J.A., JAYASOORIYA U.A., MBOGO N., WHITE R.P., KEARLEY G.J., LONGEVILLE S. – Restricted proton mobility in the self-organizing system 3,5-dimethylpyrazole
Physica B **276-278** (2000) 308-309

SUARD E., FAUTH F., CAIGNAERT V., MIREBEAU I., BALDINOZZI G. - Charge ordering in the layered Co based perovskite $HoBaCo_2O_5$
Physical Review B Rapid Communications **61** (2000) 11871-11874

SYROMYATNIKOV V.G., MENELLE A., TOPERVERG B.P., SOROKO Z.N., SIEBRECHT R., PLESHANOV N.K., PUSENKOV V.M., UL'YANOV V.A. - Observation of peculiarities in magnetic off-specular polarized neutron scattering from rough interfaces in Co/Ti periodic multilayer
Physica B **276-278** (2000) 700-701

SYROMYATNIKOV V.G., MENELLE A., TOPERVERG B.P., SOROKO Z.N., SCHEBETOV A.F. - Off-specular polarized neutron scattering from rough interfaces in Co/Ti and Fe/Al multilayer structures
Physica B **267-268** (1999) 190-193

SZUSZKIEWICZ W., DYNOWSKA E., GORECKA J., WITKOWSKA B., JOUANNE M., MORHANGE J.F., JULIEN C., HENNION B. - Peculiarities of the lattice dynamics of cubic mercury chalcogenides
Phys. Status Solidi B **215** (1999) 93-98

SZUSZKIEWICZ W., HENNION B., JOUANNE M., MORHANGE J.F., DYNOWSKA E., JANIK E., WOJTOWICZ T. - Selected properties of AFM-III structures – cubic MnTe and diluted magnetic semiconductors CdMnTe and MgMnTe
J. Magn. Magn. Mater. **196-197** (1999) 425-427

SZYTULA A., KOLENDA M., ANDRE G., BOUREE F., OLES A. - Magnetic ordering of $TbTSb_2$ (T=Cu, Pd, Ag) compounds
Physica B **276-278** (2000) 618-619

TABTI T., CHIKINA J., JACQUINOT J.F., DAOUD M. – Nuclear magnetic relaxation without spin diffusion in polymers at interfaces
Physical Review E **60** (1999) 645-653

TAKAHARA S., KITTAKA S., KURODA Y., YAMAGUCHI T., FUJII H., BELLISSENT-FUNEL M.C. – Interlayer water molecules in vanadium pentoxide hydrate, $V_2O_5nH_2O_{,7}$. Quasi-elastic neutron scattering study
Langmuir **16** (2000) 10559-10563

TAKZEI G.A., MIREBEAU I., GUN'KO L.P., SYCH I.I., SURZHENKO O.B., CHEREPOV S.V., TROSCHENKOV YU.N. - Study of the onset of a long range ferromagnetic order in an ensemble of small particles with giant magnetic moments
Journal of Magnetism and Magnetic Materials **202** (1999) 376-384

TASSAING T., BELLISSENT-FUNEL M.-C. - The dynamics of supercritical water : a quasi elastic incoherent neutron scattering study
Journal of Chemical Physics **113** (2000) 3332-3337

TASSAING T., CABAÇO M.I., DANTEN Y, BESNARD M. - The structure of liquid and supercritical benzene as studied by neutron diffraction and molecular dynamics
J. Chem. Physics **113** (2000) 3757-3765

TEIXEIRA J., LUZAR A. – Physics of liquid water. Structure and dynamics
In « Hydration Processes in Biology» NATO Science Series, vol 305, edited by M.-C. Bellissent-Funel, (1999) pp. 35-65

TEIXEIRA J. - L'eau, liquide ou cristal déliquescent ?
La Recherche n°234 (1999) 36-39

TEIXEIRA J. – El agua. liquido o cristal delicuescente ?
Mondo Cientifico **207** (1999) 24-27

TEIXEIRA J. - Dynamics of liquids in porous materials
Ecole Thématique du CNRS « Les Matériaux Poreux Désordonnés » , Les Houches, France, 4-8 octobre 1999

TEIXEIRA J. – Scattering by fractals
Ferroelectrics **235** (1999) 231-234

TEIXEIRA J. – SANS : an introduction
in Lecture Notes of the Introductory Course to the ECNS'99, CKFKI, Budapest, Editors : G. Kadar and L. Rosta, (1999) pp. 129-136

TEIXEIRA J. – Agua, el enlace de hidrogenio
Investigacion y ciencia **291** (2000) 33-34

TRAN Y., AUROY P., LEE L.T., STAMM M. – Polyelectrolyte brushes : counterion distribution and complexation properties
Physical Review E **60** (1999) 6984-6990

TRAN Y., AUROY P., LEE L.T., STAMM M. – Determination of the structure of polyelectrolyte brushes
Macromolecules **32** (1999) 8952-8964

TRAN V.H., TROC R., ANDRE G., BOUREE F., KOLENDA M. – Structural properties and magnetic structure of the heavy-fermion compound UCu_5Sn
J. Physics :Condens. Matter **12** (2000) 5879-5888

TROUNOV V.A., KURBAKOV A.I., TSERKOVNAYA E.A., NECHITAYLOV A.I., NECHITAYLOV A.A. - The Possibility of Catalyst Preparation for Oxidation of Monoxide Carbon (CO) by help of System Types $CuCr_{2-x}Co_xO_4$ +nCuO and TiO_2+nCuO
(Neutron Diffraction Study, Oxidation Efficiency)
Physica B **276-278** (2000) 934-935

TURQUIER F, CERETTI M., HAIRY P., TITEUX I., LODINI A. - Residual stress measurements in a tool steel coated with plasma-sprayed zirconia and submitted to thermal fatigue in liquid aluminium
Physica B **276-278** (2000) 872-873

VAN DER MAAREL J.R.C., GROENEWEGEN W., EGELHAAF S.U., LAPP A. - Salt induced concentration of polyelectrolyte diblock copolymer micelles
Langmuir **16** (2000) 7510-7519

VAN DIJK N.H., FAK B., CHARVOLIN T., LEJAY P., MIGNOT J.M. - Magnetic excitations in heavy-fermion $CePd_2Si_2$
Physical Review B **61** (2000) 8922-8931

VELASQUEZ M., HAUT C., HENNION B., REVCOLEVSCHI A.- Crystal growth and characterization of the CMR compound $La_{1.2}(Sr,Ca)_{1.8}Mn_2O_3$
Journal of Crystal Growth **220** (2000) 480-487

VENUTI V., CRUPI V., MAGAZU S., MAJOLINO D., MIGLIARDO P., BELLISSENT-FUNEL M.-C.- Diffusional and vibrational properties of water confined in very thin nanoporous glasses probed by light and neutron scattering
J. Phys. IV 10(Pr7) (2000) 211-214

VERNIERE A., BOUCHERLE J.X., LEJAY P., GILLON B. – Field-induced magnetic form factor in UIr_2Si_2
Physica B **267-268** (1999) 41-46

VERSLUIJS J.J., BARI M., OTT F., COEY J.M.D., REVCOLEVSCHI A. - Non-linear I-V curves in nanocontacts between crystals of $(La_{0.7}Sr_{0.3})MnO_3$
E-MRS Spring Meeting 1999, Strasbourg, June 1-4, 1999 (invited paper)
Journal of Magnetism Magnetic Materials **211** (2000) 212-216

VERSLUIJS J.J., OTT F., COEY J.M.D. – Potentiometric imaging of $(La_{0.7}Sr_{0.3})MnO_3$ thin films
Applied Physics Letters **75** (1999) 1152-1154

VIEIRA L.G., HERNANDEZ O., ALMEIDA A., QUILICHINI M., RIBEIRO H.L., CHAVES M.R., KLOPPERPIEPER A. – Elastic neutron scattering and dielectric behavior of 4% brominated betaine calcium chloride dihydrate (BCCD)
European Physical Journal B **10** (1999) 447-456

VIEIRA L.G., RIBEIRO H.L., HERNANDEZ O., QUILICHINI M., ALMEIDA A., CHAVES M.R., KLOPPERPIEPER A. – On the transition to the X-phase in highly brominated betaine calcium chloride dihydrate (BCCD)
Ferroelectrics **240** (2000) 1435-1442

Publications

VIRET M., DELFOSSE L., WARIN P., OTT F., FERMON C. - Domain wall scattering in submicron cobalt bridges
C.R. Acad. Sci. Paris **327** (1999) 907-913

VIRET M., SAMSON Y., WARIN P., MARTY A., OTT F., SONDERGARD E., KLEIN O., FERMON C. - Anisotropy of domain wall resistance
Physical Review Letters **85** (2000) 3962-3965

WERNER R., GROS C ., BRADEN M. – Microscopic spin-phonon coupling constants in $CuGeO_3$
Physical Review B **59** (1999) 14356-14366

WISNIEWSKI P., GUKASOV A., HENKIE Z., WOJAKOWSKI A. - Polarized neutron diffraction study of spin and orbital moments in UAsSe
J. Phys. : Condensed Matter **11** (1999) 6311-6317

WISNIEWSKI P., GUKASOV A., HENKIE Z. - Spin and orbital moments in U_3X_4-type pnictides (X=P, As, Sb, Bi) :Polarized neutron diffraction study
Physical Review B **60** (1999) 6242-6245

WISNIEWSKI P., GUKASOV A., HENKIE Z. – Spinowe i orbitalne skladowe momentow magnetycznych w pniktydkach uranu typ U_3X_4 (X=P, As, Sb i Bi)
Dzialalnosc Naukowa **8** (1999) 110-112

WOLCYRZ M., HORYN R., BOUREE F. - Structural peculiarities of $BiLa_2O_{4.5+\delta}$ examined by X-ray and neutron powder diffraction
J. Phys. : Condens. Matter **11** (1999) 5757-5765

WUTTKE J., OHL M., GOLDAMMER M., ROTH S., SCHNEIDER U., LUNKENHEIMER P., KAHN R., RUFFLE B., LECHNER R., BERG M.A. - Propylene carbonate reexamined : Mode-coupling β scaling without factorization ?
Physical Review E **61** (2000) 2730-2740

YATSENKO A.V., CHERNYSHEV V.V., KURBAKOV A.I., SCHENK H. - Structure of p-Phenylazoaniline hydrochloride from powder data: protonation site and UV-visible spectra
Acta Crystallographica C**56**, (2000) 892-894

YONG G., TOULOUSE J., ERWIN R., SHAPIRO S., HENNION B. - Pretransitional diffuse neutron scattering in the mixed perovskite relaxor $K_{1-x}Li_xTaO_3$
Physical Review B **62** (2000) 14736-14743

ZAHARKO O., SCHOBINGER-PAPAMANTELLOS P., RODRIGUEZ-CARVAJAL J., BUSCHOW K.H.J. - Magnetic Ordering in $HoFe_6Ge_6$ Studied by Neutron Diffraction
Journal of Alloys and Compounds **288** (1999) 50-56

ZANNA J.J., MAUZAC M. BOUE F. – SANS experiments on swollen mesomorphous Networks
Macromolecules **32** (1999) 2962-2966

ZANOTTI J.M., BELLISSENT-FUNEL M.-C, PARELLO J. - Hydration coupled dynamics in Proteins studied by neutron scattering and NMR : the case of the typical EF-hand calcium binding parvalbumin
Biophysical Journal **76** (1999) 2390-2411

ZANOTTI J.M., BELLISSENT-FUNEL M.-C, CHEN S.H. - Relaxation dynamics of supercooled water in porous glass
Physical Review E **59** (1999) 3084-3093

ZATTARIN P., BACZMANSKI A., LIPINSKI P., WIERZBANOWSKI K. – Modified self-consistent model for time independent plasticity of polycrystalline material
Archives of Metallurgy **45** (2000) 163-184

ZEGHAL M., AUVRAY L. - Structure of polymer complexes in water
Europhysics Letters **45** (1999) 482-487

ZRNÍK J.
Neutrónová difrakcná analýza vnútorných pnutí nukleovaných pri tepelnej únave niklovej superzliatiny, 5. Medzinárodné metalurgické sympózium, 9.-10. September, 1999, Rajecké Teplice, SR, p. 198

LLB – Complementary Publications 1997-1998 related to experiments performed on LLB instruments

(which were not included in the previous Scientific Report)

ALBA-SIMIONESCO C., MORINEAU D., FRICK B., HIGONENQ N., FUJIMORI H. - An analysis of the short and intermediate range order in several glass-forming liquids from the static structure factor under pressure
J. of non-Crystalline Solids **235-237** (1998) 367-374

BACZMANSKI A., WIERZBANOWSKI K., TARASIUK J. - Internal Stresses in Metal Matrix Composite - Diffraction Experiment and Elasto-Plastic Model, Proc. Int. Conf.: Analyse des Contraintes Residuelles, MATTEC 97, p.269, Reims, France, 1997

BIENFAIT M., ZEPPENFELD P., VILCHES O.E., PALMARI J.P., LAUTER H.J. - Structure and phase transitions of D_2+Ar mixtures adsorbed on graphite
Surf. Sci. **377-379** (1997) 504

BIENFAIT M., ZEPPENFELD P., BOVIE L.J., VILCHES O.E., LAUTER H.J. - Structure of monolayer films of hydrogen isotope mixtures
Physica B **234-236** (1997) 159-163

BILL J., SEITZ J., THURN G., DÜRR J., CANEL J., JANOS B., JOLOWIECKI A., SAUTER D., SCHEMPP S., LAMPARTER P., MAYER J., ALDINGER F. - Structure analysis and properties of Si-C-N ceramics derived from polysilazanes
Physica Status Solidi A –**16** (1998) 269-296

BING K., PINTSCHOVIUS L., EIGENMANN B., MACHERAUCH E. - Combination of X-Ray and Neutron Diffraction, Hole Drilling and FE-Calulations for the Determination of the Residual Stress State in Brazed Joints of Steel and Cemented Carbide
in Proceed. of the Fourth Europ. Conf. on Res. Stresses ECRS4, June 4-6, 1996, S. Denis et al (eds), (Soc. Franc. de Métall. et de Mat. , ENSAM, 1998), p. 627

BRIGANTI G., GIORDANO R., LONDEI P., PEDONE F. - SANS measurements on S. solfataricus ribosomes as a function of temperature and magnesium concentration
Physica B **225**(1997) 234-236

BRIGANTI G., GIORDANO R., LONDEI P., PEDONE F. - SANS analysis of thermal stability of 23S rRNA and the bulk 50S subunit of sulfolobus solfataricus ribosomes
Biophys. Acta **1379** (1998) 297-301

CABAÇO M.I., DANTEN Y., BESNARD M., GUISSANI Y. , GUILLOT B. - Structural investigations of liquid binary mixtures : neutron diffraction and molecular dynamics studies of benzene, hexafluorobenzene and 1,3,5-trifluorobenzene
J. Phys. Chem. B **102**(1998) 10712-10723

CHERNYSHEV V.V., YATSENKO A.V., TAFEENKO V.A., ZHUKOV S.G., ASLANOV L.A., SONNEVELD E.J., SCHENK H., MAKAROV V.A., GRANIK V.G., TROUNOV V.A., KURBAKOV A.I. – Crystal structures of Pyrazolo[1,5-a]pyrimidine derivatives solved from powder diffraction data.
Zeitschrift für Kristallographie **213** (1998) 477-482

DANTEN Y., BESNARD M., GUISSANI Y., GUILLOT B. - Neutron diffraction and molecular dynamics study of liquid benzene and its fluorinated derivative as a function of temperature
J. Phys. Chem. **101** (1997) 6977- 6987

FITZPATRICK M. E., EDWARDS L., D. WANG Q., BURDETT C. – Neutron diffraction Study of the Effects of Vibrational Stress Relief.
Fifth Intl. Conf. on Residual Stresses, T. Ericsson, M. Oden and A. Andersson, eds. Vol. 2, pp. 1090-1095. Univ. of Linkoping, 1997.

FITZPATRICK M. E. - The Effect of Plasticity Caused by Cold Working on the Misfit Stresses in a Metal Matrix Composite.
Fifth Intl. Conf. on Residual Stresses, T. Ericsson, M. Oden and A. Andersson, eds. Vol. 2, pp. 886-891. Univ. of Linkoping, 1997.

FITZPATRICK M. E., EDWARDS L. - Fatigue Crack / Residual Stress Interactions and their Implications for Damage Tolerant Design,
J. Mater. Engng Performance **7** (1998) 190-198

GRADZIELSKI M., LANGEVIN D., SOTTMANN T., STREY R. - Droplet microemulsions at the emulsification boundary : The influence of the surfactant structure on the elastic constants of the amphiphilic film
J. Chem. Phys. **106** (1997) 8232-8238

GRADZIELSKI M. - Effect of the cosurfactant structure on the bending elasticity in nonionic oil-in-water microemulsions
Langmuir **14** (1998) 6037-6044

GROSSE M., BÖHMERT J., GILLES R. - Small-angle neutron scattering investigations of the microstructure of VVER-440-type reactor pressure vessel steel after irradiation at 60°C
J. Nucl. Mater. **254** (1998) 143

HANK P., BESENBOCK W., GAHLER R., KOPPE M. – Zero-field neutron spin echo techniques for incoherent scattering
Physica B **234-236** (1997) 1130-1132

Publications

KYRIOPOULOU I., BUIRON N., MICHAUD V., PRIOUL C., PANTÉLIS D. - Étude microstructurale et mécanique d'assemblages brasés de nitrure de silicium/fonte à graphite
La Revue de Métallurgie, p.227-239, (1997).

KRATZ K., HELLWEG T., EIMER W. - Internal dynamics of colloidal poly (N-isopropylacrylamide) microgel particles (in german)
Ber. Bursenges Phys. Chem. **102** (1998) 1603-1608

LUKAS P., ZRNIK J., KOURIL Z., STRUNZ P., MIKULA P., VRANA M. - Využitie neutrónovej difrakcie pri stúdiu vnitrných pnutí termálnej podstaty v tvárnené niklové supeslitine
Zborník z mezinárodnej konferencie TECHNOLÓGIA´97, Bratislava, September 1997, Vol. 1, P. 134

LUKAS P., ZRNIK J., VRANA M., KOURIL Z., STRUNZ P., MIKULA P. - High Resolution neutron diffraction study of thermal fatigue of polycrystalline nickel base superalloy EI698 VD
EUROMAT 97, april 1997, Maastricht (NL), p. 4/227

LUKAS P., ZRNIK J.
Analyza mikropnut v kovech pomoci neutronove difrakce s vysokym rozlisenim, 240th ROZHOVORY o aktualnych otazkach rontgenove a neutronove strukturni analyzy, Krystalograficka spolecnost, UJF Rez uPrahy, October 1997

MIKULA P., LUKAS P., VRANA M., KLIMANEK P., ULRICH H.J., ZRNIK J. - Nondestructive strain/stress Measurements by neutron diffraction,
Proc. of the 7th International Metallurgical Symposium METAL 98, May 1998, Ostrava, Czech Republic, p. 110

MORINEAU D., ALBA-SIMIONESCO C. Hydrogen-bond-induced clustering in the fragile glass-forming liquid m-toluidine: Experiments and simulation
J. Chem. Phys. **109** (1998) 8494-8503

MORINEAU D. :
Structure de liquides moléculaires 'fragile' à l'approche de la transition vitreuse par diffusion de neutrons et simulation Monte Carlo
Thesis, University of Paris-XI , Orsay, March 28, 1997.

PEDONE F., BONINCONTRO A., BRIGANTI G., GIANSANTI A., LONDE P., RISULEO G., MENGONI M. - Effects of magnesium and temperature on the properties of E. Coli and sulfolobus solfataricus ribosomes
Biochim. Biophys. Acta **1335** (1997) 283-289

PINTSCHOVIUS L., SCHREIECK B., EIGENMANN B. - Neutron, X-ray and finite-element stress analysis on brazed components of steel and cemented carbide
In MAT-TEC 97, A. Lodini (ed.), IITT-International (1997) 307-312

REYNAUD A., PRIOUL C., DUJIN S., LE STRAT J. M. , LASCAR G. - Etude des possibilités de brasage céramique/fonte GS en vue de renfort local des pièces en fonte
Fonderie Fondeur d'aujourd'hui **161** (1997) 44-54

SCHEMPP S., DÜRR J., LAMPARTER P., BILL J., ALDINGER F. - Study of the atomic structure and phase separation in amorphous Si-C-N ceramics by X-ray and neutron diffraction
Z. Naturforschung **53a**. (1998) 127-133

ZRNIK J., LUKAS P., VRANA M., KOURIL Z., STRUNZ P., MIKULA P. - The thermal fatigue residual stresses study by high resolution neutron diffraction method in nickel base superalloy,
Proc. of the 10th International Symposium on Metallography, April 1998, High Tatras, Slovakia, p. 252